Fisheries and Oceans Canada | Pêches et Océans Canada
Ecosystems and Oceans Science | Sciences des écosystèmes et des océans

Canadian Science Advisory Secretariat (CSAS)

Research Document 2025/055

Pacific Region

Pacific Spiny Dogfish (*Squalus suckleyi*) Population Modelling for Outside Waters of British Columbia in 2024

Sean C. Anderson[1], Quang C. Huynh[2], Lindsay N.K. Davidson[1], Jacquelynne R. King[1]

[1]Pacific Biological Station
Fisheries and Oceans Canada, 3190 Hammond Bay Road
Nanaimo, British Columbia, V9T 6N7, Canada

[2]Blue Matter Science
2150 Bridgman Ave,
North Vancouver, V7P 2T9, Canada

February 2026

Canada

Foreword

This series documents the scientific basis for the evaluation of aquatic resources and ecosystems in Canada. As such, it addresses the issues of the day in the time frames required and the documents it contains are not intended as definitive statements on the subjects addressed but rather as progress reports on ongoing investigations.

Published by:

Fisheries and Oceans Canada
Canadian Science Advisory Secretariat
200 Kent Street
Ottawa ON K1A 0E6

http://www.dfo-mpo.gc.ca/csas-sccs/
DFO.CSAS-SCAS.MPO@dfo-mpo.gc.ca

ISSN 1919-5044
ISBN 978-0-660-78438-0 Cat. No. Fs70-6/2025-055E-PDF

Correct citation for this publication:

Anderson, S.C., Huynh, Q.C., Davidson, L.N.K., and King, J.R. 2026. Pacific Spiny Dogfish (*Squalus suckleyi*) Population Modelling for Outside Waters of British Columbia in 2024. DFO Can. Sci. Advis. Sec. Res. Doc. 2025/055. iv + 164 p.

Aussi disponible en français :

*Anderson, S.C., Huynh, Q.C., Davidson, L.N.K., et King, J.R. 2026. Modélisation de la population d'aiguillats du Pacifique (*Squalus suckleyi*) pour les eaux extérieures de la Colombie-Britannique en 2024. Secr. can. des avis sci. du MPO. Doc. de rech. 2025/055. iv + 185 p.*

TABLE OF CONTENTS

ABSTRACT

Pacific Spiny Dogfish (*Squalus suckleyi*) is a long-lived shark with late maturation and low fecundity, distributed from Alaska to southern Baja California. In British Columbia (BC), Canada, two stocks are assessed: an inside stock in the Strait of Georgia and Johnstone Strait, and an outside stock in remaining coastal areas. This assessment focuses on the outside stock. This stock has been commercially fished since the 1870s with a large vitamin A liver fishery in the 1940s and no targeted fishery since 2011. Discards have exceeded landings over the past decade.

This assessment updates the 2010 analysis using a two-sex, age-structured population dynamics model fitted to fishery and survey catch, indices of abundance, and length composition data. Due to the species' life history, spawning output (number of pups) is used to characterize stock status. This assessment uses literature-informed discard mortality rates under low, base, and high assumptions. The model explores uncertainties in natural mortality (M), discard mortality, index representativeness, stock-recruit curve shape, and potential increases in M. One base model, 15 sensitivity models with constant M, and five increasing-M models were evaluated.

All models estimated a steep decline in spawning output in the 1940s due to the vitamin A fishery, followed by recovery driven by maturation of juvenile cohorts, and a slower decline through 2010 due to fishing and senescence. Estimated 2023 depletion (S/S_0) was robust across most assumptions. Some increasing-M models fit steep recent declines in the Synoptic trawl index but implied a stock that would be unable to replace itself if the higher M were to persist. An increase in M is plausible, but how this change is captured in the model requires future research.

A Limit Reference Point (LRP) of 0.2 S/S_0 and candidate Upper Stock Reference (USR) of 0.4 S/S_0 are proposed, with $F/F_{0.4S0}$ proposed as a Removal Reference. All models estimated the stock to be below the LRP in 2023 with high probability (>0.95), placing it in the Critical Zone. Projected spawning output remains below the LRP through 2028, even under zero catch. Across scenarios, dead catch levels (landed Dogfish plus those assumed to die from discard mortality) associated with $\geq$ 95% probability of $F < F_{0.4S0}$ ranged from 0 to 250 t. Average recent dead catch ranged from 160 to 423 t depending on discard mortality assumption. The known limited productivity of Dogfish, the estimated population size, and steep declines in two of three survey indices suggest that catches need to be lower than the current total allowable catch of 12,000 t to increase the spawning output and achieve a high probability of $F < F_{0.4S0}$. Reassessment is recommended within five years, with monitoring of survey indices in the interim.

1. INTRODUCTION

Pacific Spiny Dogfish (*Squalus suckleyi*; "Dogfish") are a wide-ranging, long-lived shark species. Tagging data suggest that in the northeast Pacific the species exists as one offshore stock that extends from Baja California to Alaska (Ketchen 1986) and two coastal stocks: one in the Strait of Georgia and another in Puget Sound (McFarlane and King 2003, 2009). Because of this, the Dogfish population in British Columbia (BC) is assessed as two stocks: an inside stock inhabiting the Johnstone Strait and Strait of Georgia and an outside stock inhabiting remaining coastal areas. This document focuses on the outside stock.

Dogfish in Pacific waters were originally described as *Squalus suckleyi* and separate from the Atlantic species *Squalus acanthias*. However, from the 1950s to 1970s, several papers suggested *S. suckleyi* may be a subspecies or the same species as *S. acanthias* (e.g., Jones and Geen 1976, Shmidt 1950) and Hart et al. (1973) adopted the name *S. acanthias* for the Pacific species. In 2010, the scientific name was reverted to *S. suckleyi* (Ebert et al. 2010) based on DNA evidence (Veríssimo et al. 2010, Ward et al. 2007). Furthermore, the American Fisheries Society now recommends the common name "Pacific Spiny Dogfish" (Page et al. 2013) over the name "North Pacific Spiny Dogfish" used in the last BC stock assessment (DFO 2010).

Dogfish have long been fished on the BC coast. They are thought to have been fished by First Nations in what is now BC as long as 5,000 years ago for their skin, meat, and oil (Ketchen 1986). Commercial fishing for Dogfish in BC dates back to the 1870s (Anderson 1878). From 1870–1916 Dogfish were pursued for their liver oil to support the industrial lubricant and lighting industries (Ketchen 1986). Peak exploitation occurred from the late 1930s until 1950 as part of a fishery targeting Dogfish for their livers to supplement soldiers with vitamin A (Ketchen 1986). A move to synthetic vitamin A, combined with declines in Dogfish abundance, ended this fishery (Ketchen 1986); several smaller directed fisheries have occurred since. Currently, there is no directed fishery for Dogfish in BC, although they are regularly caught incidentally in groundfish fisheries.

The last stock assessment for Dogfish was completed in 2010 (DFO 2010, 2012, Gallucci et al. 2011); however, there was "no consensus reached on a scientifically valid approach on which to base yield recommendations" (DFO 2010). Model output suggested there was insufficient contrast in the stock index data to provide productivity and scale information given the surplus production model assumptions and concluded there was no immediate conservation concern given the perceptions on stock status and lack of a directed fishery. As a result, quota for the outside stock remained at 12,000 t total (8,160 t for the Dogfish Sector and 3,840 t for the Trawl Sector; DFO 2024) with catches well below this quota. It was recommended that the assessment be revisited within five years (DFO 2010).

In 2010, Dogfish were categorized as Special Concern by the Committee on the Status of Endangered Wildlife in Canada (COSEWIC) due to "low fecundity, long generation time, uncertainty regarding trends in abundance of mature individuals, reduction in size composition, and demonstrated vulnerability to overfishing" (COSEWIC 2011). While a decision by the Governor in Council to list Dogfish species under the *Species at Risk Act* (SARA) is still pending, COSEWIC is required to review the classification of each species at risk every 10 years (s.24 of SARA).

DFO Fisheries Management (Groundfish Management Unit; GMU) has requested DFO Science Branch provide advice regarding the outside Dogfish stock status relative to reference points that are consistent with DFO's Precautionary Approach (DFO 2009).

1.1. OBJECTIVES

The objectives for this document are to

1. Develop and assess a suite of age-structured population dynamics models for Dogfish in outside BC waters and describe the uncertainties the models are meant to address;
2. Document and discuss challenges and uncertainties regarding model assumptions and data that affect (1) reconstructing stock dynamics, (2) developing reference points consistent with the DFO Precautionary Approach (PA) Policy (DFO 2009), and (3) evaluating status with respect to those reference points;
3. Present time series of S/S_{MSY} (spawning output over spawning output at maximum sustainable yield) and S/S_0 (spawning output over unfished spawning output) conditional on the fitted models. Provide an upper bound on potential removal reference rates based on possible stock productivities and models;
4. Calculate probabilities of population decline relevant to COSEWIC status assessment;
5. Consider environmental conditions that may affect the stock as presented in the Guidelines for Implementing the Fish Stocks provisions in the *Fisheries Act*;
6. Recommend an appropriate path forward including recommended data collection and research, a recommended timeline to revisit the assessment, and indicators before then that may trigger an earlier than scheduled assessment. Provide a rationale if indicators and triggers cannot be identified.

1.2. STOCK STRUCTURE

Dogfish are found throughout the Northeast Pacific, mainly in continental shelf and slope waters from Baja California up to the Aleutian Islands and into the Bering Sea (Ketchen 1986). Southern BC has some of the highest biomass densities of Dogfish across the northeast Pacific (Orlov et al. 2012). Dogfish abundance declines moving towards the southern and northern ends of their distributional range; they are uncommon off California and in the western Gulf of Alaska and Bering Sea (Ketchen 1986, Orlov et al. 2012). However, between 1990 and 2008, increases in Dogfish abundance in the Bering Sea have been noted (Orlov et al. 2012).

Within British Columbia, tagging studies suggest there are two distinct stocks: an inside stock in the Johnstone Strait and Strait of Georgia and an outside stock (McFarlane and King 2003, 2009). Over 70,000 Dogfish were tagged between 1978 and 1988 in the Strait of Georgia, the west coast of Vancouver Island and Hecate Strait, with 2,940 recaptured fish by 2000 (McFarlane and King 2003, 2009). Generally, tagged Dogfish were captured in the same region as released, but migrations between the inside and outside stocks did occur (10–14% of recaptured fish); migrations between south and northern outside BC regions were more common (49–80% of recaptured fish) (McFarlane and King 2003, 2009). This assessment covers the outside stock only—Pacific Fisheries Management Area (PFMA) areas 3CD5ABCDE. A portion of DFO Statistical Area 12 (Northern Johnstone Strait) resides in Pacific States Marine Fisheries Commission (PSMFC) areas 3CD5ABCDE. We exlude all of DFO Statistical Area 12 (Northern Johnstone Strait) to reflect the PFMA 3CD5ABCDE.

Movement of Dogfish between Canadian and US waters occurs for both the inside and outside stocks but at low rates. A small proportion ($<$ 5%) of Canadian tagged Dogfish (McFarlane and King 2003) were recaptured in Puget Sound, western US states, and Alaska but since tag reporting could not be standardized to relative fishing effort, annual movement rates were not estimated. Historical tagging data off Washington and in Puget Sound were included in a spatial population dynamics model (Taylor 2008) and annual movement rates in the outside stock between Washington and Vancouver Island were estimated to be only 5%. The estimated annual movement rates between the Puget Sound and Washington were even lower (1%).

Seasonal migrations in both the outside and inside stocks have also been noted. Holland (1957) reported that Dogfish tagged off Washington and Vancouver Island tend to migrate south in fall/winter and north in spring/summer. A more recent tagging study deployed acoustic telemetry tags on Dogfish in Puget Sound and used coastal receivers to elucidate seasonal migration of Dogfish (Andrews and Harvey 2013). All Dogfish tagged within Puget Sound (n=14) migrated out into the Juan de Fuca during winter.

1.3. LIFE HISTORY AND ECOLOGY

Dogfish are long-lived, with maximum estimated age reported as high as 100 years (Beamish et al. 2006); however, data records for this estimate cannot be found and a more reliable maximum estimated age is 80–85 years (with a maximum possible age of 95 years at the upper bound of aging error) (McFarlane and King 2009). Dogfish are slow-growing, reaching a maximum recorded total length of 160 cm (Mecklenburg et al. 2002). They exhibit late maturation with females maturing at 35 years (95 cm) and males maturing at 20 years at a size of 70 cm (McFarlane et al. 2010).

Dogfish reproduction is aplacental viviparous, that is embryos develop with a yolk sac within the female and full-term pups are released at an average size of 26–27 cm (Ketchen 1986). The gestation period is nearly two years (Holden 1977)—one of the longest periods in the animal kingdom (McFarlane and King 2020). Fecundity in Dogfish ranges from two to 16 pups, dependent on the size of female; the average litter size is six to seven pups (Ketchen 1986). The slow-growth, late maturation and low fecundity of Dogfish translates into a very low intrinsic rate of population increase, even among other Pacific shark species (Smith et al. 1998).

Dogfish demographics have been noted to be impacted by environmental conditions and fishing pressure. From the 1940s to 2000, Taylor and Gallucci (2009) observed an increase in growth leading to smaller sizes, along with a decline in age of maturation and an increase in average litter size for Dogfish in the Puget Sound population. The greatest change in these parameters occurred between the 1940 and 1970s, a period of relatively high fishery exploitation and prior to observed increases in sea surface temperature (Taylor and Gallucci 2009). Taylor and Gallucci (2009) imply that if these demographic changes are reflective of density dependence, then the rebuilding potential for Dogfish given fishery reductions is low.

The ecology of Dogfish is well outlined in McFarlane and King (2020). Dogfish are found as aggregations at depths ranging from surface waters to over 1,000 m. Dogfish occupy both pelagic and benthic habitats, with older Dogfish more associated with bottom waters. There are seasonal changes in habitat depths occupied by Dogfish, with movement into shallower waters in summer presumably a reflection of prey distribution. Additionally, adults segregate by sex, with males occupying shallower depths than females.

Dogfish are opportunistic feeders, preying on invertebrates (squid, jellyfish, crabs, and euphausiids) and fish (Pacific herring, Pacific salmon, flatfish, and eulachon). Dogfish have a low metabolism and slow digestion time (Ketchen 1986) and the estimated time between feeding events is as long as 16 days (Jones and Geen 1977). Dogfish predators include large fish such as Lingcod (*Ophiodon elongatus*), other sharks such as Bluntnose Sixgill Shark (*Hexanchus griseus*), and marine mammals such as offshore killer whales (*Orcinus orca*), and Steller and California sea lions (*Eumetopias jubatus* and *Zalophus californianus*).

1.4. COMMERCIAL FISHERY HISTORY

1.4.1. 1870–1916

Although Dogfish are thought to have been caught commercially in the 1860s (Ketchen 1986), their catch statistics first appeared in government reports for BC in the mid 1870s

(Anderson 1878). At that time, Dogfish were fished primarily for their livers and body oil for use as industrial lubricants and lighting oil for lighthouses, vessels, and even head lamps for miners (Ketchen 1986). The Canadian fishery quickly spread to areas around Haida Gwaii in northern British Columbia within a few years (King et al. 2017). In the 1870s, Dogfish were second only to canned salmon in value for BC fisheries (Anderson 1878). For all of BC, from 1876 to 1900, catches ranged from about 2000 to 4000 t, producing from 200,000 to 1,100,000 L of oil (King et al. 2017). By 1917, Dogfish-fueled lights were frequently being replaced by safer carbide lamps and demand for Dogfish declined (Ketchen 1986).

1.4.2. 1917–1936

In this time period, a market opened for using Dogfish oil as an additive for livestock and poultry feed (King et al. 2017); however, fishing was concentrated in the Strait of Georgia and there was no commercial fishing in outside waters (Ketchen 1986). The economic crash in 1929 caused a sharp decrease in production and by the late 1930s only two processing plants remained (Ketchen 1986).

1.4.3. 1937–1950

Dogfish livers were discovered to be a potent source of vitamin A and combined with rising demand due to supplementing soldiers during war, a major commercial Dogfish fishery developed. At its peak in 1944, at 31,000 t and 3000 licenses, Dogfish in BC was the fourth most valuable fishery in Canada and the most valuable fishery in BC (Ketchen 1986) with much of the production by that time coming from Hecate Strait (King et al. 2017). After 1945, the fishery experienced a steep decline due to an assumed decline in the stock from overfishing, a shift to synthetic vitamin A, and markets shifting to Japanese imports; the fishery had nearly collapsed by 1950 (Ketchen 1986).

1.4.4. 1951–1974

From 1951 to 1974, Dogfish are thought to have gradually increased in abundance in BC (Ketchen 1969, 1986, Wood et al. 1979). Eventually, Dogfish became a nuisance to other commercial and recreational fishers and options for controlling the population through subsidy programs, poisoning, or even parasite release programs were considered (Alverson et al. 1963, Ketchen 1969). Despite the resurgence in the marketable stock (i.e., large fish), little commercial fishing developed and government control programs were generally ineffective at reducing the population (Ketchen 1986, King et al. 2017). In 1962, the Canadian eradication programs were stopped and the federal government began again to encourage the development of the Dogfish fishery with a subsidy program for food products (King et al. 2017). This program was unsuccessful for a decade until declines in Dogfish in Europe and Japan opened up new import markets in Europe and Asia (Ketchen 1986), which eventually brought about the revival of the Dogfish fisheries.

1.4.5. 1975–2005

By 1977, a food fishery had been established in BC, although mostly in the Strait of Georgia (Ketchen 1986). Later, trawl fishing for Dogfish shifted to the west coast of Vancouver Island (Ketchen 1986). In this era, Dogfish catches in outside waters of BC peaked in 1988 and then again from 2000 to 2009—mainly caught by longline gear with bottom trawl catch typically discarded (Figures 1–4).

1.4.6. 2006–present

In 2006, large changes to the management of the groundfish fishery had an impact on the dynamics of the Dogfish fishery. Fishers were required to account for bycatch with the application of discard mortality for species, including Dogfish, in annual quota limits. This requirement was coupled with the introduction of transferable Individual Vessel Quotas (IVQs), which allowed fishers to acquire needed quota to account for any discard mortality for a given species. In the Strait of Georgia, severe restrictions on rockfish (*Sebastes* spp.) landings and the high price for rockfish quota to account for bycatch made it financially difficult for fishers to execute a targeted Dogfish fishery. Conversely, in outside waters where these severe restrictions on rockfish bycatch did not exist, Dogfish fishers could then acquire quotas they previously did not have access to (e.g., rockfish), and thereby land more valuable fish. For either case, the result was that targeting of Dogfish declined dramatically throughout BC and landings dropped by 2010 (Figure 2).

By 2012, there were nine active commercial vessels in the BC Dogfish Sector, by 2016 there were three, and there were none from 2017 onwards with the exception of a single license in 2019 (DFO 2024). The TAC (Total Allowable Catch) is currently set at 8,160 t for this Dogfish Sector and 3,840 t for the Trawl Sector (DFO 2024) although catches have been well below these quotas (Figure 2).

1.5. ASSESSMENT HISTORY

1.5.1. 1979

Dogfish was first assessed in 1979 as a trans-boundary population spanning the entire coast of British Columbia, Canada through Washington and Oregon, United States, including the Strait of Georgia and Puget Sound (Wood et al. 1979). Through age-structured matrix modelling, the natural mortality value was estimated to be 0.094 per year. The value generated an equilibrium age structure in an unfished population based on a fecundity-at-age schedule and the assumption that all age classes experience density-independent survival.

From an estimate of an unfished vulnerable biomass of 200,000 t in BC, including inside waters and consisting of market-sized Dogfish older than 16–20 years, the maximum sustainable yield was estimated to be 8,000–10,000 t, where F_{MSY} (fishing mortality at maximum sustainable yield) is 0.5 M (natural mortality). Several density-dependent mechanisms for the stock were proposed.

Compensatory natural mortality was determined to be the most plausible mechanism, where M would need to be reduced to 40–50% of the unfished value to achieve MSY (maximum sustainable yield). In contrast, the increase in compensatory somatic growth and fecundity needed to achieve the estimated MSY were found to be biologically implausible. Using the historical catch trend from 1937–1978, the stock was estimated to be 55% of unfished levels by 1949, but recovered to near unfished levels by 1960 with compensatory mortality.

1.5.2. 1980s

The Wood et al. (1979) model was updated by Saunders in 1985, 1986, and 1987 (Saunders 1989). Saunders (1989) modified the Wood et al. (1979) model to account for unequal sex ratios in the Dogfish catch after noting that only 8.6% of port samples were male due to the time of year the fishery was usually conducted. Accounting for removing more females than males decreased the sustainable yield recommendations (Saunders 1989). Saunders (1989) determined that catches up to 9,000 t were “low risk” and from 9,000–14,000 t were “high risk” assuming continued sex selective bias in the BC fisheries. However, these numbers were for the entire outside stock—Alaska to California. At the time, Saunders (1989) assumed the BC

outside stock was one half to two-thirds of the Alaska-to-California stock, therefore suggesting a "high risk" of declines in female abundance beyond catches of 4,5000–9,333 t (9,000 t $\times$ 0.5–14,000 t $\times$ 2/3)for the BC outside Dogfish stock. We note these numbers in the context of the current combined TAC of 12,000 t (DFO 2024) and in the context of catches in late 1980s and mid 2000s, which climbed into this "high risk" zone several times (Figure 3).

1.5.3. 2010

Pacific Spiny Dogfish were last assessed in BC in 2010 in an assessment that fit models to and presented results for both the inside and outside stocks (DFO 2010, 2012, Gallucci et al. 2011). The assessment used Pella-Tomlinson surplus production models (Pella and Tomlinson 1969) fit by maximum likelihood to CPUE (catch per unit effort) data from longline and trawl fisheries as well as the IPHC FISS (International Pacific Halibut Commission Fisheries Independent Setline Survey), the NMFS (National Marine Fisheries Service) Triennial trawl survey, and the HS MSA (Hecate Strait Multispecies Assemblage) survey. At the time, the time series from the Hard Bottom Long Line (HBLL) survey and the Synoptic bottom trawl surveys, which are now routinely used in BC groundfish assessments, were too short to be included.

The outside stock was determined to likely be in the "Healthy" zone of DFO's Precautionary Approach Framework (DFO 2009), but due to challenges with parameter estimation (parameters tending to hit bounds without priors), model output was not used for formal science advice to management. The Science Advisory Report noted that "there was no consensus reached on a scientifically valid approach on which to base yield recommendations" (DFO 2010). The assessment, however, noted a reduction in the size distribution of Dogfish in the HS MSA survey (DFO 2010, Gallucci et al. 2011). This reduction in the size distribution (see Figure 16 in COSEWIC 2011), combined with a long generation time, low fecundity, uncertainty in population trends for mature Dogfish, and known vulnerability to overfishing for Dogfish in other parts of the world led to a designation of "Special Concern" by COSEWIC (the Committee on the Status of Endangered Wildlife in Canada) in 2011 (COSEWIC 2011).

1.6. NEARBY ASSESSMENTS

1.6.1. Gulf of Alaska

Dogfish are not targeted in the Bering Sea/Aleutian Islands or the Gulf of Alaska but are frequently encountered as bycatch. Nearly all incidental catch is discarded (Tribuzio et al. 2022). The last assessment (Tribuzio et al. 2022) assumed 100% mortality of these discards based on a tagging study of Pacific sleeper sharks with trawl vessels. Overfishing limits were set in the Bering Sea/Aleutian Islands based on maximum catch in a historical time period (2003–2015). Science advice for the Gulf of Alaska was provided based on a demographic model and risk analysis as described in Tribuzio and Kruse (2011) and Tribuzio et al. (2022). Both the Bering Sea/Aleutian Islands and Gulf of Alaska Dogfish were last assessed as not overfished (Tribuzio et al. 2022).

1.6.2. US West Coast

Dogfish have not been targeted on the US West Coast since the vitamin A fishery but have been a landed bycatch species for meat and cartilage during several time periods (Gertseva et al. 2021). On the US West Coast, Dogfish were last assessed with an age-structured Stock Synthesis 3 (SS3) model fit to survey indices, length composition data, and age composition data (with age composition data available from one survey in one year) (Gertseva et al. 2021). Growth was estimated internally in the assessment using one year of combined length and age samples. The assessment estimated the stock to be at 34% of unfished spawning output (S/S_0), which is above an overfishing threshold of 25% but below a management target of 40%.

Overfishing, if defined based on a 50% spawning potential ratio (SPR50%), was estimated to have been occurring with the 1940s vitamin A fishery and in the 1980s through early 1990s. Over the past decade, fishing was estimated to be below this threshold in the base model. Major uncertainties included estimating catchability for the West Coast Groundfish Bottom Trawl survey, whether SPR50% is a sufficiently conservative reference point for a stock with such low productivity, an inability to estimate two key stock-recruit parameters, an inability to fit the extent of the decline in the main trawl survey index, and transboundary concerns with high densities of Dogfish close to the US-Canada border (Gertseva et al. 2021).

2. DATA SOURCES

2.1. CATCH DATA

We used the same reconstructed historical catch as in Gallucci et al. (2011), which is based on reconstructions in Ketchen (1986). We combine these catches with modern catches available in the GFFOS (Groundfish Fisheries Operations System) database `MERGED_CATCH` table from 1996 onward for trawl and for 2006 onward for longline and trap (Figures 1, 2). Following Gallucci et al. (2011), we start the historical catch time series in 1937. Catch statistics are available starting in 1879 (Ketchen 1986), but these catches were much smaller (1,000–4,000 t per year) than in the vitamin A fishery of the 1940s and this early period was followed by a period of little to no fishing for Dogfish in outside waters from 1917 to 1937 (Ketchen 1986).

Longline and trap discards are primarily recorded as counts. In the version of this report presented at the Regional Peer Review meeting, we inadvertently used longline and trap discard weights, which are incomplete. In this revised version, we have included longline and trap discards as counts in the assessment models. For the purposes of visualization, we multiply these counts by an average Dogfish weight of 3.07 kg based on length measurements taken from unsorted longline commercial samples in 2009, 2010, 2012, 2013 after converting these lengths to weight with the length-weight relationships used in this assessment. We chose to exclude assumed discard weights from 1996 to 2005 that were included in the last assessment (Gallucci et al. 2011). These were small values ($<$ 3% of overall catches in those years) and adding them at a late modelling stage (after the regional peer review meeting) would be complicated given the longline discard fleet is now modelled as count data.

Annual catch of dogfish in the recreational fishery is estimated from the Internet Recreational Effort and Catch reporting program (iRec). In 2012, DFO established a coast-wide, internet-based survey of tidal water licence holders, which collects recreational data for the entire Outside region (DFO 2015). The iRec survey includes catch estimates reported by anglers, with catch rate expansions by year and area to account for non-respondent license holders. Dogfish is also incidentally caught in the salmon fishery although the data had only been digitized up to 2010 as of this assessment. In both the recreational fishery and salmon fishery, a high proportion, i.e., 85–95% annually, of dogfish catch is discarded (Figure 4).

Stock assessments for Dogfish have made a wide range of assumptions about mortality after discarding. Gallucci et al. (2011) applied a rule based on the Integrated Fisheries Management Plan (IFMP) (DFO 2024) that applied a 6% discard mortality for longline gear and 5% mortality for the first two hours of a trawl tow and an additional 5% mortality for each subsequent hour. However, it is unclear the origin of these values and whether they were based on biological research; they were criticized as being too low by both reviewers in the last assessment review meeting (DFO 2012). The Alaskan assessment assumes 100% discard mortality based on a tagging study with Pacific sleeper sharks (Tribuzio et al. 2022). The US West Coast assessment assumes 100% mortality for trawl and 50% for longline but also considers sensitivity to other lower levels of discard mortality (Gertseva et al. 2021). The 2007 *S. acanthias*

Spiny Dogfish assessment in Atlantic Canada used 25% discard mortality for trawl catches $>$ 200 kg and 0% for trawl catches $<$ 200 kg, 55% for gillnet catches, 10% for longline catches, and 25% for purse seine catches (DFO 2007). The 2006 Atlantic Spiny Dogfish assessment in New England used 50% discard mortality from trawls, 10% from hook and line, and 30% from gillnets (NEFSC 2006).

For *S. acanthias* and Smooth Dogfish (*Mustelus spp.*), a recent review of post-release live-discard mortality for mortality occurring shortly following the fishing event, (e.g., up 72 hours) derived values ranging from 8–36% for longline, 5–15% for hook and line, 27–36% for gillnet, and 19–36% for trawl (Courtney 2014). These values; however, *do not* include immediate/acute (e.g., at vessel) mortality to our understanding. Table 3 (p. 27) of Courtney (2014) includes a summary of known literature documenting immediate mortality for *S. acanthias* and *Mustelus spp.*: several values are available for gillnets (ranging from 3% to 60%), but gillnets only impact BC Dogfish through bycatch in the salmon fisheries. Values of 0% (n = 24) immediate mortality for Smooth Dogfish from longline gear and 7.5% (n = 41) immediate mortality for Smooth Dogfish from trawl gear are noted in Courtney (2014) with citations of Frick et al. (2010*a*) and Frick et al. (2010*b*), respectively. However, these are small sample sizes and we were unable to verify the source of the 7.5% mortality value in Frick et al. (2010*b*) (their Figure 2).

With the above in mind, we included the following scenarios (Table 2) to bound possible discard mortality values and test model sensitivity:

- Low discard mortality—use the “low” values from Courtney (2014) (Table 1) for each gear type and assume no initial mortality. This results in longline: 8%, hook and line: 5%, gillnet: 27% (salmon fishery), trawl: 19%.
- Base discard mortality—use the “base” values from Courtney (2014) (Table 1) for each gear type and add 10% initial trawl mortality (near the value cited in Courtney (2014)) and 50% initial gillnet mortality (approximate average of the three commercial sources in Table 3 and row C in Courtney (2014)). This results in longline: 27% (0% + 27%), hook and line: 10% (0% + 27%), gillnet: 81% (30% + 51%), trawl: 37% (10% + 27%), where values in parentheses are initial + post-release live-discard mortality.
- High discard mortality—use the “high” values from Courtney (2014) (Table 1) for each gear type and add 20% initial trawl mortality, and 50% initial gillnet mortality. This results in longline: 36% (0% + 36%), hook and line: 15% (0% + 15%), gillnet: 86% (50% + 36%), trawl: 56% (20% + 36%).
- 100% discard mortality—we include this scenario not because we deem it plausible but to assess model sensitivity. We do not include it when calculating reference points or making projections.

Table 1. Post-release live-discard mortality values from Courtney (2014).

Level	Longline	Hook and line	Gillnet	Trawl
Low	8%	5%	27%	19%
Base	27%	10%	31%	27%
High	36%	15%	36%	36%

Table 2. Discard mortality rates (including initial and post-release live-discard mortality) under low, base, and high assumptions in this assessment.

Level	Longline	Hook and line	Gillnet	Trawl
Low	8%	5%	27%	19%
Base	27%	10%	81%	37%
High	36%	15%	86%	56%

We apply these same discard mortality values to the gear types used in recreational (hook and line), commercial, and survey settings acknowledging that in reality the rates may differ. Lethal sampling of Dogfish has not been conducted in large quantities in the modern surveys with catch included in this assessment, and, even in recent years, survey catches make up a small component of overall catches. Dogfish used as bait are coded as discards in the DFO databases since they are not landed. That means this portion of the catch will be assigned the same discard mortality as other discards although in reality these Dogfish would experience 100% mortality. This corresponds to a very small percentage of the overall catch and so should not qualitatively affect the assessment models.

Throughout the rest of this document, we refer to “catch” as the total of all landings and discards (i.e., before any discard mortality is applied) and we refer to “dead catch” as the total of all landings and discards after a discard mortality rate has been applied. Visualizations of raw data such as Figures 1–4 show “catch”. Visualizations of outputs such as removal references and projections show “dead catch” since this aligns with the intent of TAC, which intends to account for Dogfish that experience mortality, i.e. dead catch.

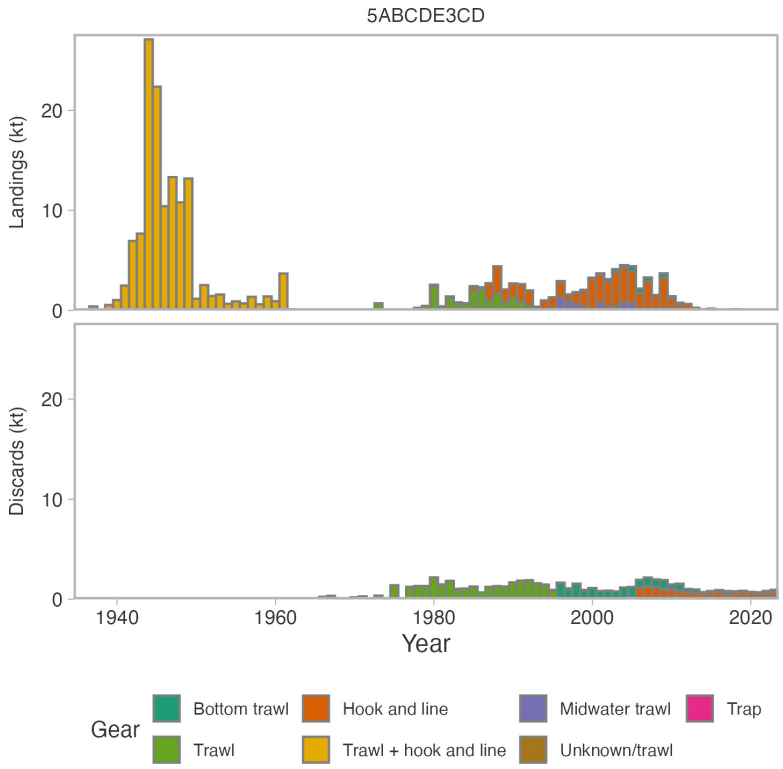

Figure 1. Reconstructed catches (discards and landings) of outside Dogfish. See Figure 2 for a version that better illustrates the 1980–2023 data. Longline discards 2006 onwards are illustrated here as weight based on an assumed average weight of 3.07 kg/Dogfish but were modelled as counts. Longline discard data prior to 2006 were not recorded and are therefore not shown.

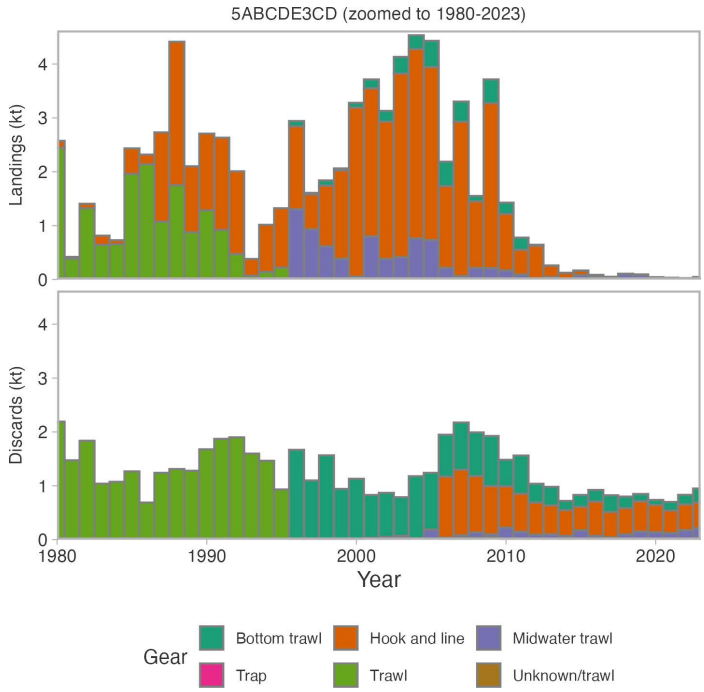

Figure 2. Reconstructed catches (discards and landings) of outside Dogfish. Same as Figure 1 but zoomed in to 1980–2023 so the recent catches can be seen. Note the y-axis scale compared to Figure 1. Longline discards 2006 onwards are illustrated here as weight based on an assumed average weight of 3.07 kg/Dogfish but were modelled as counts. Longline discard data prior to 2006 were not recorded and are therefore not shown.

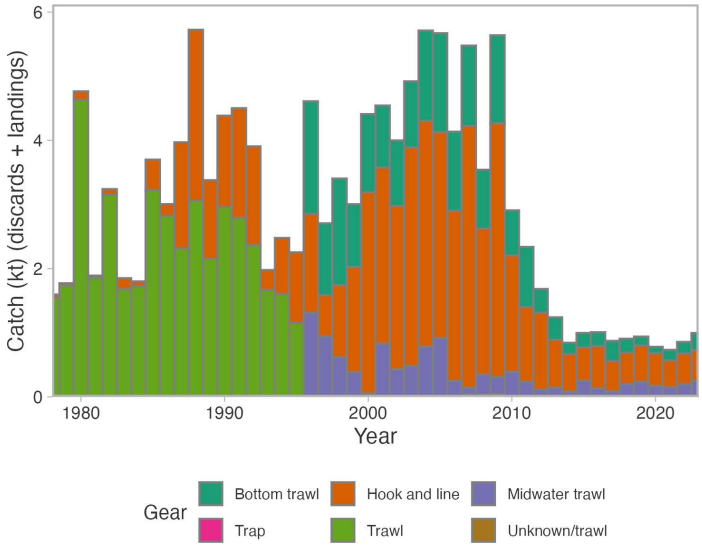

Figure 3. Reconstructed catches (discards and landings) of outside Dogfish. Same as Figure 2 but starting in 1978 and with landings and discards combined. Longline discards 2006 onwards are illustrated here as weight based on an assumed average weight of 3.07 kg/Dogfish but were modelled as counts. Longline discard data prior to 2006 were not recorded and are therefore not shown

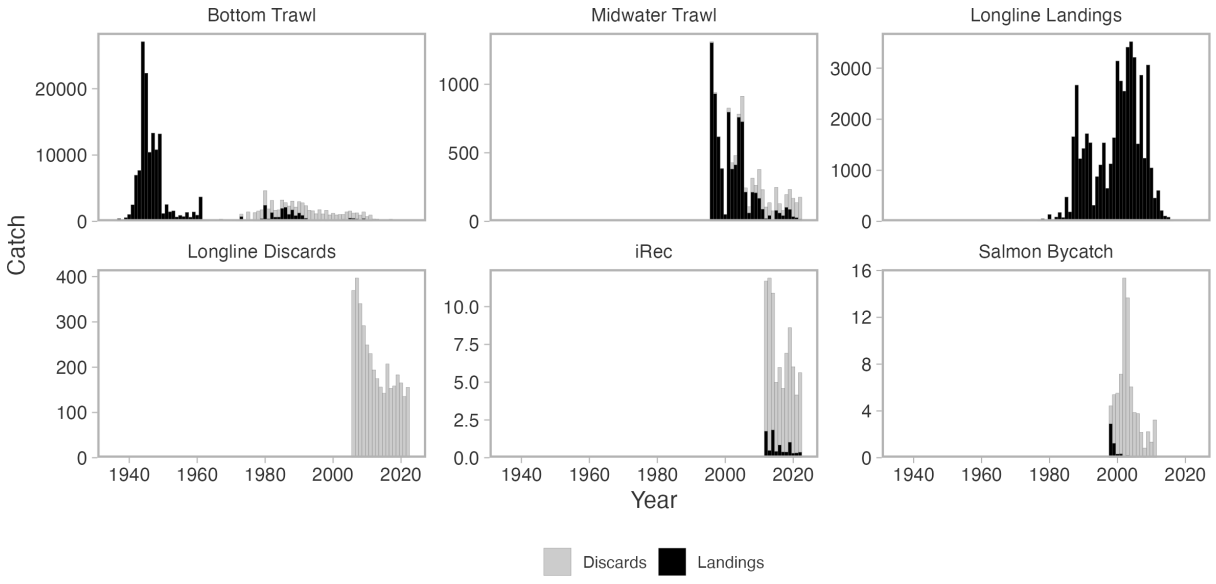

Figure 4. Landed and discarded catch in the commercial fishery (by gear) and the recreational fishery (iRec). The units of catch are tonnes for the top row and thousands of pieces for the bottom row. Discards are shown before any discard mortality rate is applied. Dogfish catch values from the "salmon bycatch" fleet were not available after 2011 at the time of writing.

2.2. INDICES OF ABUNDANCE

We summarize the survey design, data, survey domain grids, fitted spatiotemporal models, and spatiotemporal predictions from the models in the following appendix sections:

- Outside Hard Bottom Long Line (HBLL OUT) survey: Section A.2;
- International Pacific Halibut Commission (IPHC) Fishery-Independent Setline Survey: Section A.3;
- Synoptic trawl survey: Section A.4; and
- Hecate Strait Multispecies Assemblage survey (HS MSA): Section A.5.

The number of survey sets per year for a given survey ranged from 88 and 297 across surveys (Figure A.1). The longline surveys monitor the number of Dogfish caught. In the IPHC survey, nearly all sets catch at least one Dogfish. The trawl surveys monitor the catch weight of Dogfish and sometimes also record counts. The proportion of sets per year with positive catch weight for Dogfish in the Synoptic trawl survey ranged from 5% to 85%; this encounter probability was lowest in the SYN WCHG survey. Dogfish were regularly (43%–88% of sets positive for Dogfish) caught in the HS MSA survey.

All surveys take place in the summer or early fall (Figure A.2). The IPHC survey has the broadest range of dates fished. The SYN WCVI and SYN HS surveys are fished in May and/or June whereas the SYN QCS is fished in July/August and the SYN WCHG survey is usually conducted in August/September. The HBLL OUT N and S surveys are usually conducted in August/September.

We developed spatiotemporal-model-based area-weighted indices of abundance and biomass using the R (R Core Team 2024) package sdmTMB (Anderson et al. 2024*c*) (Appendix A.1). The resulting standardized indices are summarized in Figure 5. Comparing the spatiotemporal-model-based indexes of abundance to design-based estimators, the patterns were largely the same with the exception of some extreme (and uncertain) years for the design-based estimators (Figure A.22). By splitting the predicted biomass from the Synoptic trawl survey by subregion, we observed that the majority of predicted biomass was in the WCVI subregion (Figure A.23).

We constructed a standardized bottom trawl catch per unit effort (CPUE) index from a similar spatiotemporal model used with the survey data (Section B.3). The model differed mainly in that it introduced a random intercept for fishing vessels to account for differences in catchability, it assumed a different spatiotemporal random effect structure, and it introduced a covariate for month (Section B.3). Such an approach has shown to be promising for commercial CPUE data (e.g., Babcock et al. 2023, Grüss et al. 2019). With this commerical CPUE model, we investigated trends in CPUE at different depths (Figure B.12) and months (Figures B.13, B.14) of the year. Declines were steepest in the shallow waters (Figure B.12). CPUE was highest from May to November, but overall trends were similar across months with the exception of a steeper decline in August (Figures B.13–B.15).

2.3. BIOLOGICAL DATA

There are considerable length, weight, and maturity samples from the Synoptic trawl surveys (Figure A.1). The historical HS MSA survey and the IPHC survey only have length samples. We have no biological samples for Dogfish from the HBLL OUT survey. Length composition data in the Synoptic trawl survey does not show any clear trend with time, although there is considerable variability from year-to-year and from subregion-to-subregion (Figure 7). Length composition data within the IPHC setline survey were relatively stable (Figure 7). Although Dogfish have historically been aged in BC for research projects (Beamish and McFarlane 1985, McFarlane and Beamish 1987, McFarlane and King 2009), we were unable to link

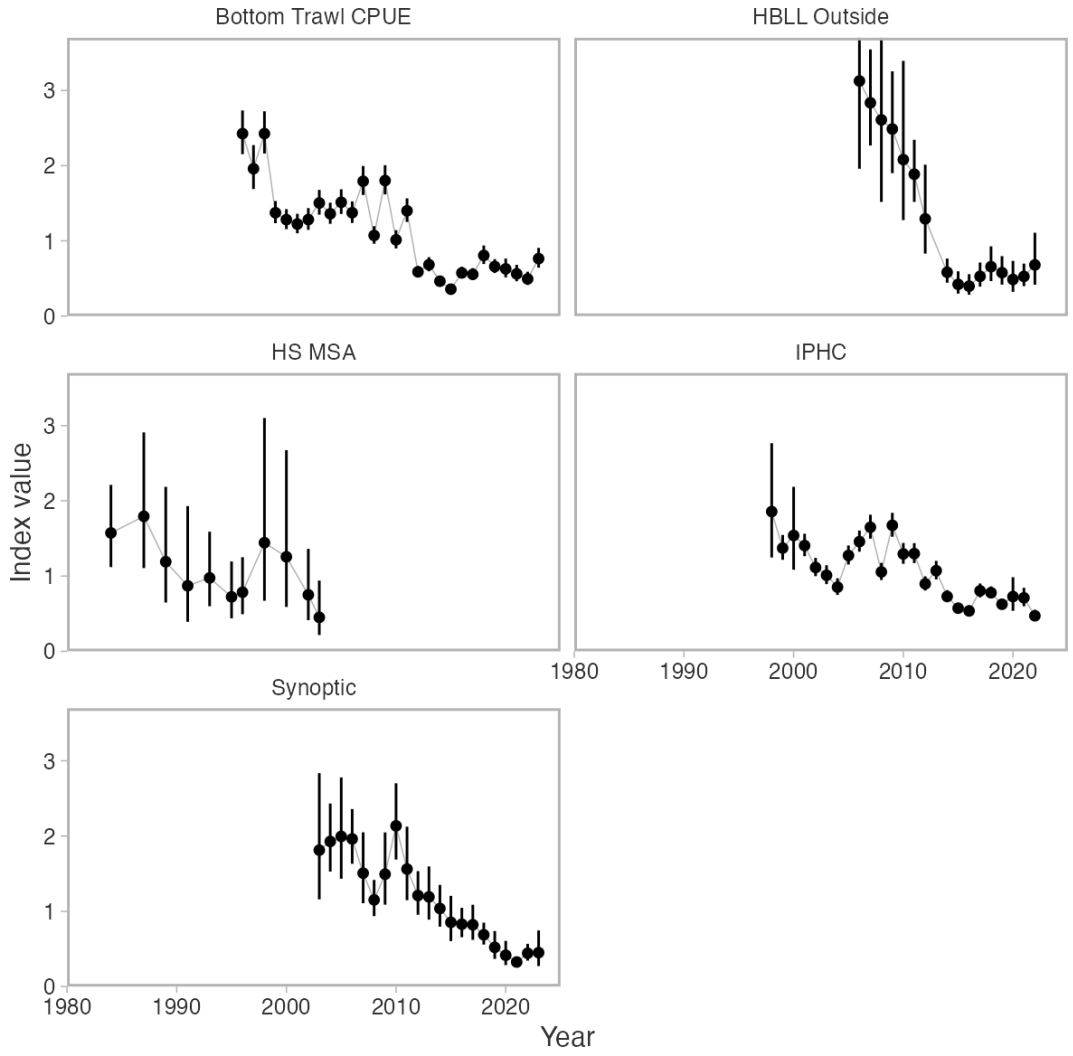

Figure 5. Standardized indices of abundance or biomass density for outside Dogfish. Dots represent mean estimates and vertical line segments represent 95% confidence intervals derived from spatiotemporal modelling. The indices are based on area-weighted expansions of predicted density on respective survey domain grids. All indices have been scaled to have the same geometric mean.

these samples to specific survey-year combinations (or commercial fishing events) for use as composition data and the samples were collected before the “modern” surveys of the last two decades. We do, however use these age data to characterize a growth curve, which we describe later in Section 3.1.

Commercial biological samples are available as a mix of sampling types (Figure B.2). However, the available sampled Dogfish come from a relatively small number of independent fishing events and no samples are available after 2019 (Figure B.2). Within the commercial fleets, length composition data are available for “unsorted” samples (Figure 9), “retained” samples (Figure 10), and “discarded” samples (Figure 11) with the type of sample corresponding to the timing and type of fish sampling with respect to a fishing event.

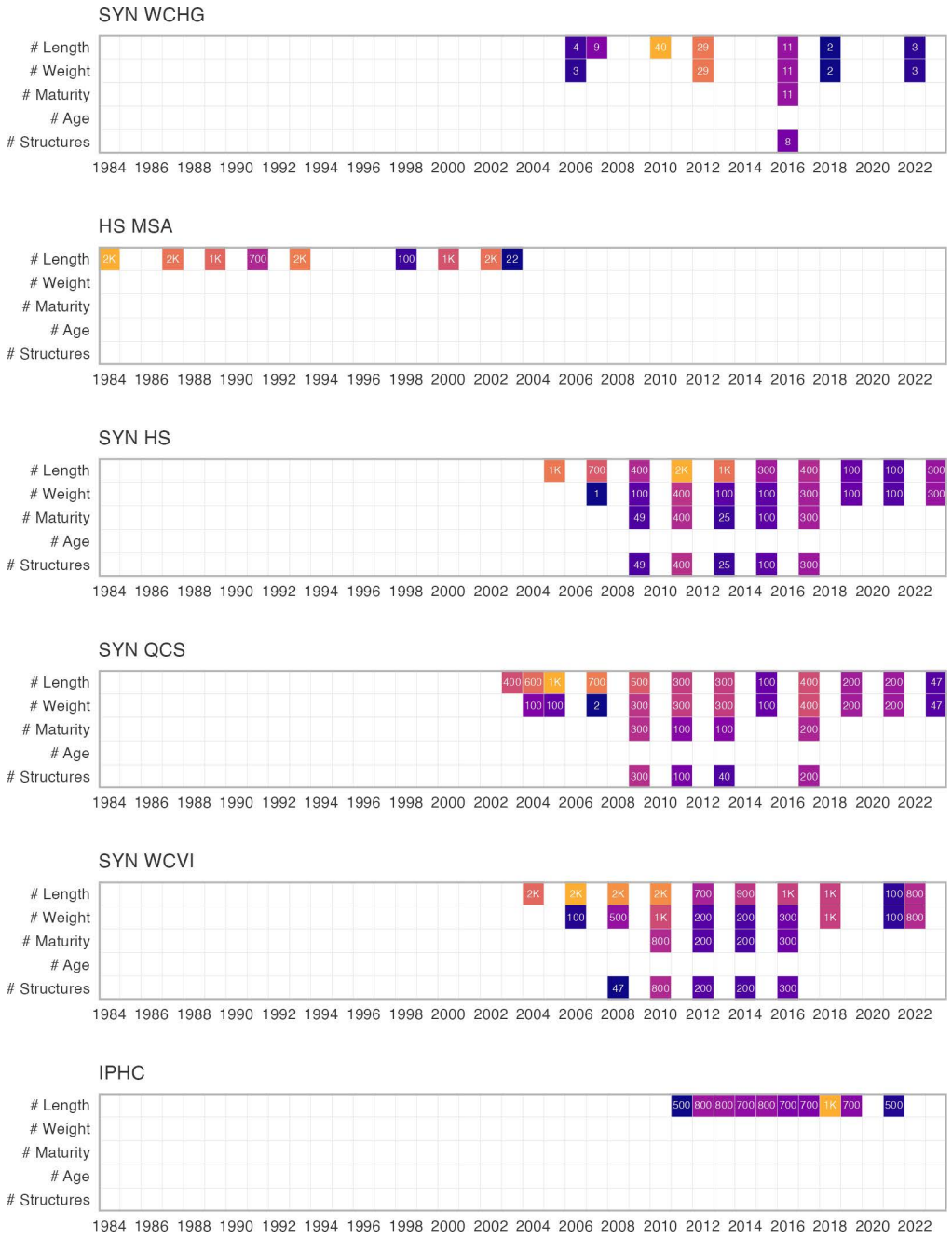

Figure 6. Biological samples available from survey sources by year. HS MSA is the Hecate Strait Multispecies Assemblage Survey. Synoptic trawl surveys include bottom trawl surveys in Hecate Strait (SYN HS), Queen Charlotte Sound (SYN QCS), and West Coast Vancouver Island (SYN WCVI).

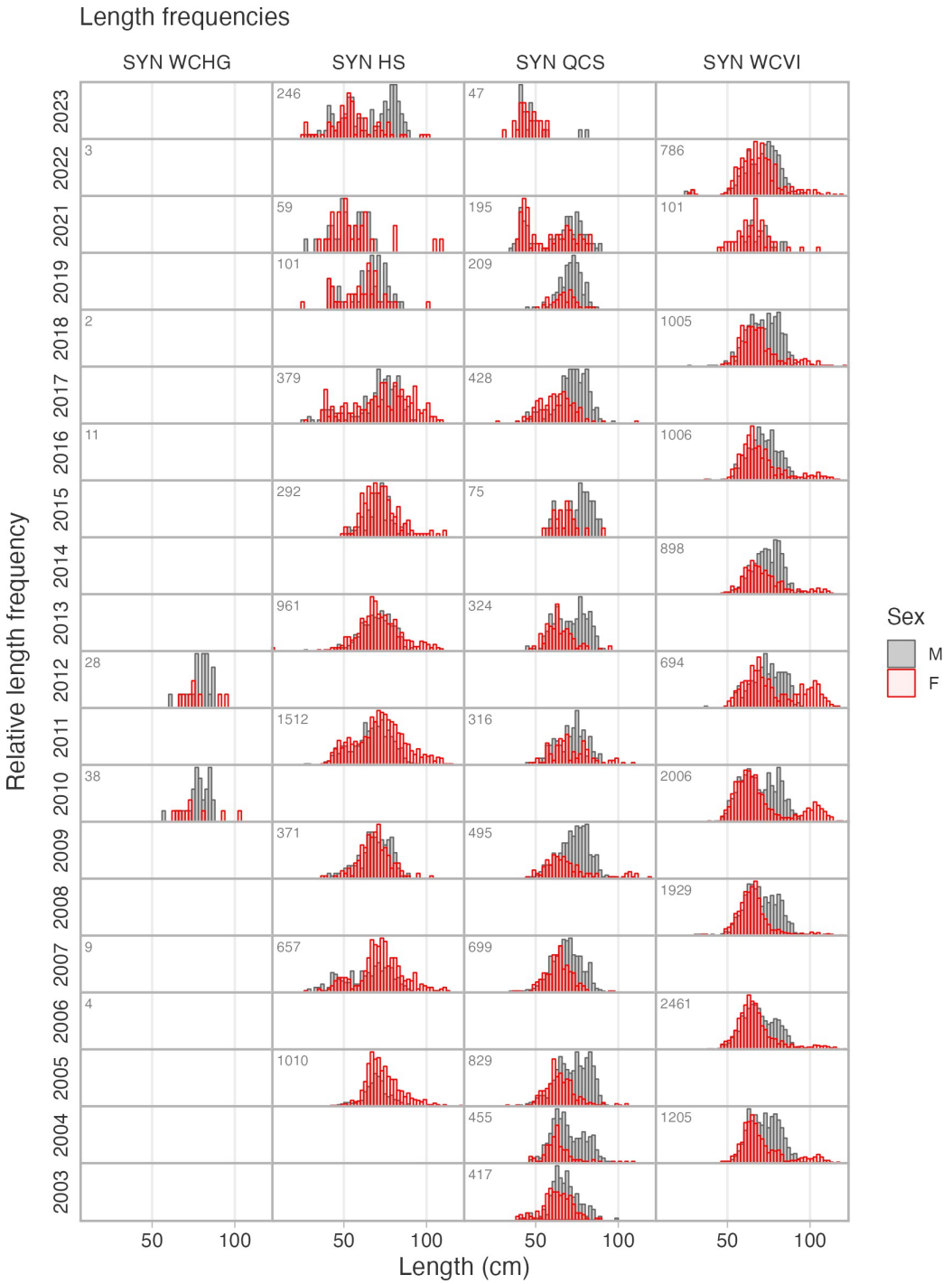

Figure 7. Dogfish length composition by sex from the Synoptic trawl surveys. Numbers in top left of panels are number of specimens.

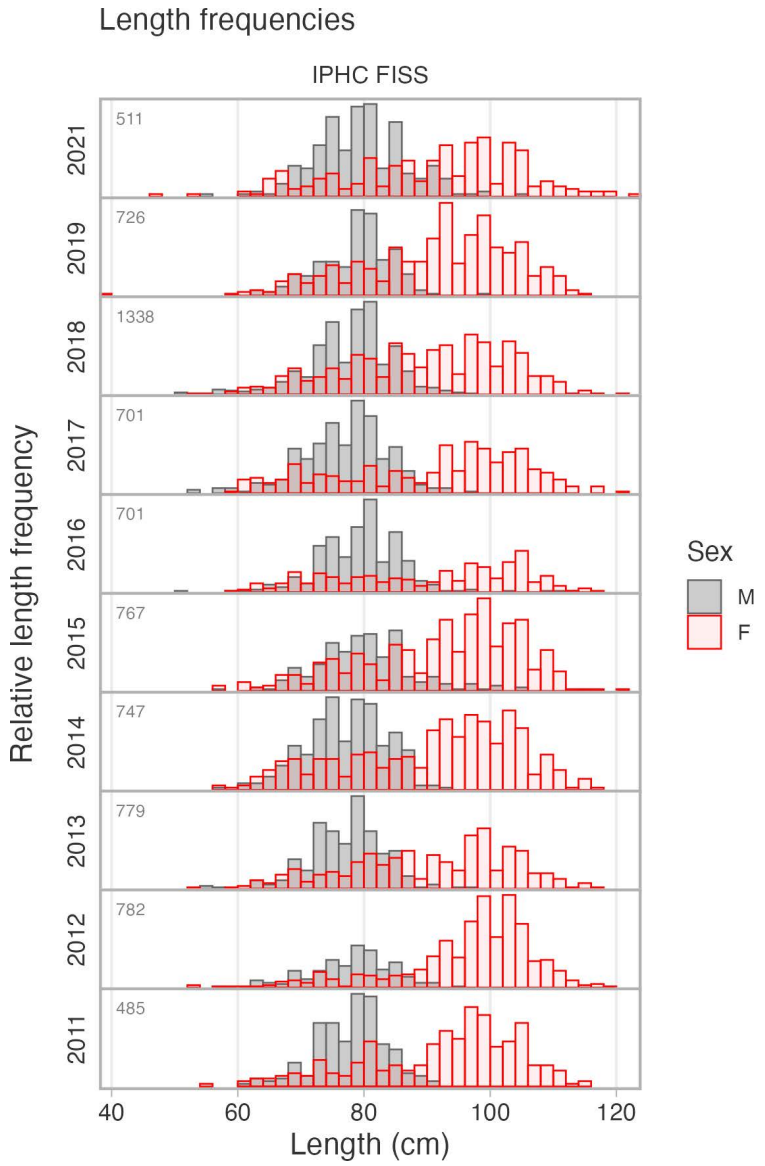

Figure 8. Dogfish length composition by sex from the IPHC setline survey. Numbers in top left of panels are number of specimens.

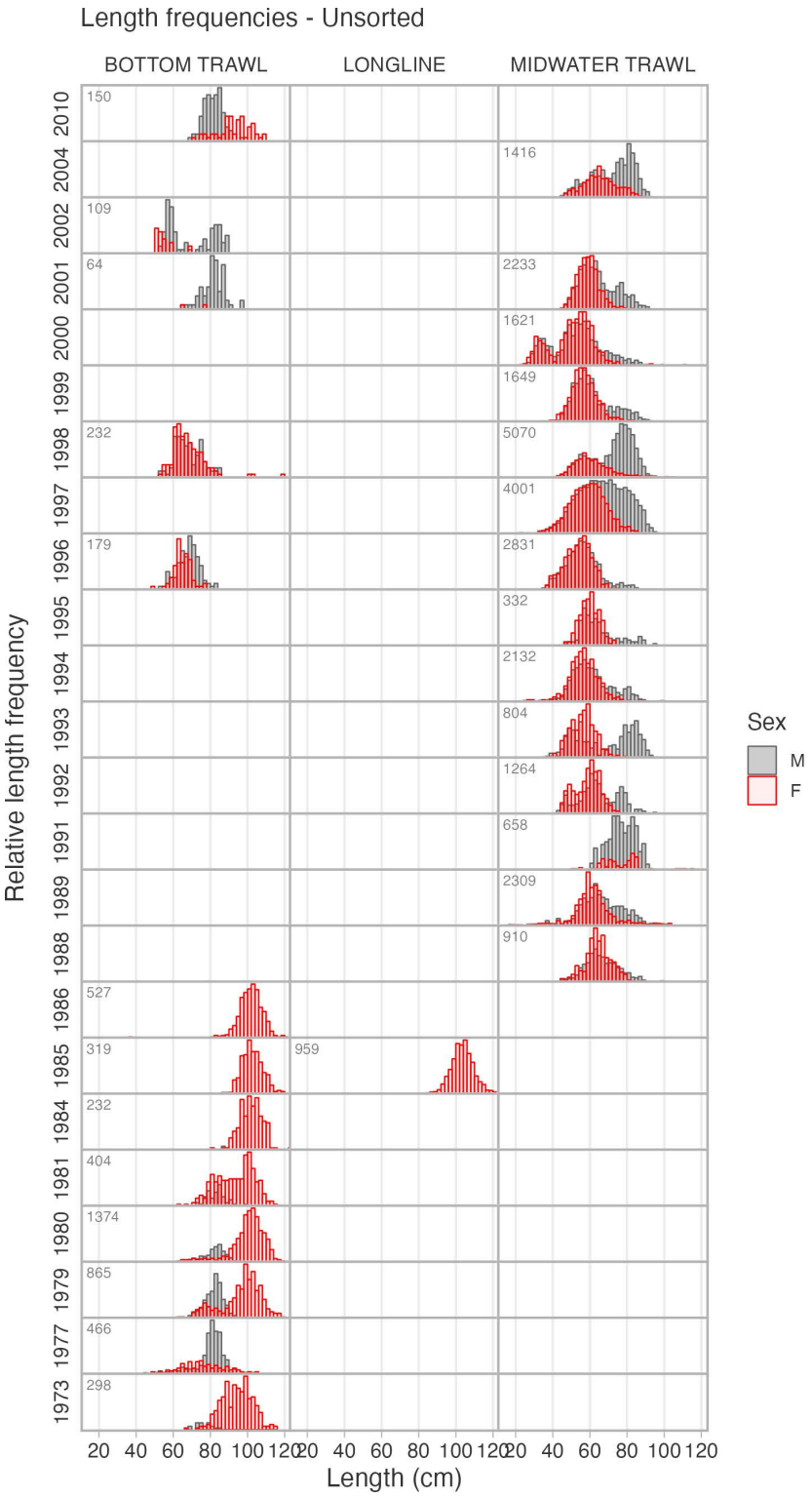

Figure 9. Unsorted length frequency in the commercial fishery by fishing gear.

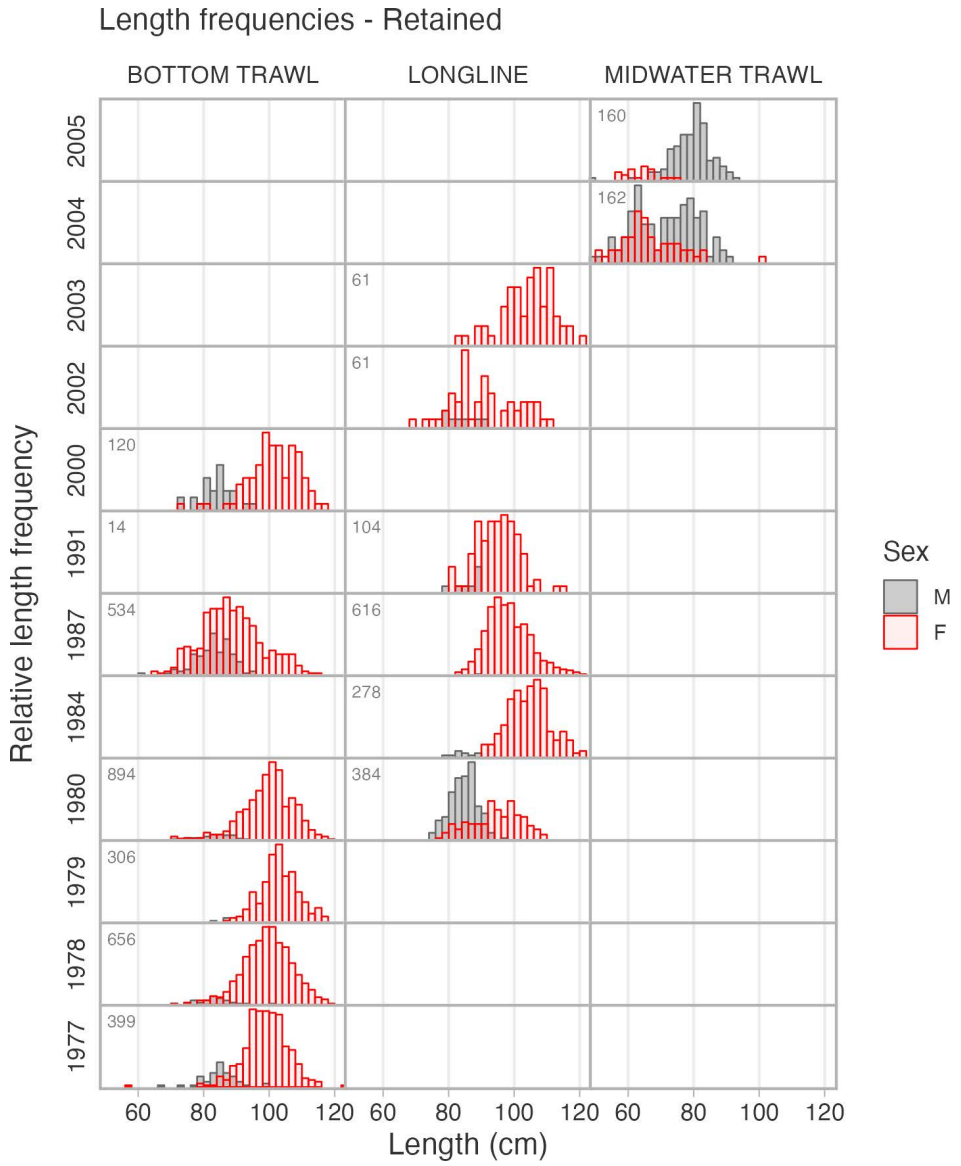

Figure 10. Length frequency in the commercial fishery by fishing gear of retained dogfish.

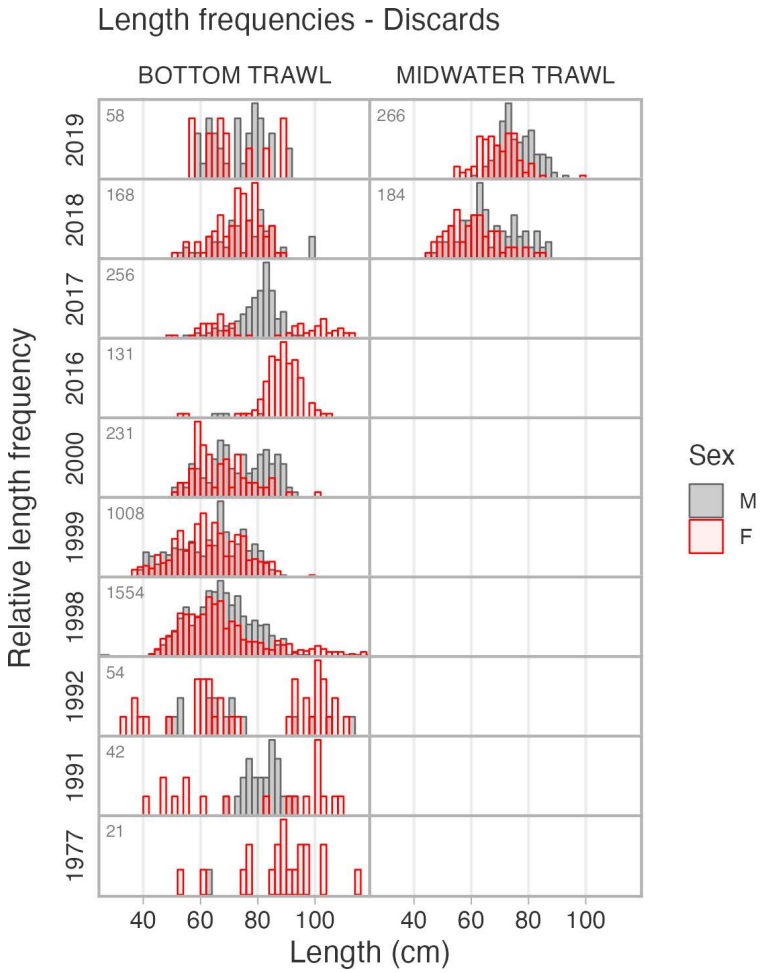

Figure 11. Length frequency in the commercial fishery by fishing gear of discarded dogfish.

3. POPULATION DYNAMICS MODEL

We reconstructed the historical abundance of outside Dogfish through Stock Synthesis 3 (SS3), version 3.30.21 (Methot and Wetzel 2013). We fit two-sex, age-structured population models to fishery and survey catch, indices of abundance, and length composition from both fisheries and surveys.

3.1. BIOLOGICAL PARAMETERS

Sex-specific biological parameters were estimated from biological samples and fixed in the population model. Estimates from biological samples are presented in Appendix C, and the values imported into the SS3 control file are presented in Table 3.

As described above in Section 2.3, age samples were collected for research projects from various surveys, tag returns, and some fisheries, although are not linked to specific surveys are fishing events in our assessment. Growth was described with a von Bertalanffy function, and several growth fits were explored (Figure 12). There was notably high variation around the mean length-age relationship. Several factors likely contribute to this behaviour, including aging error and cessation of annular ring deposition in pregnant females. Further discussion is provided in Appendix C.

Age samples in BC were not collected for the youngest Dogfish, i.e., less than 5 years, resulting in a large negative value for the a_0 parameter, the theoretical age at size zero. When fitted with age samples from both BC (inside and outside waters) and the 2010 Northwest Fisheries Science Center (NWFSC) bottom trawl survey (Gertseva et al. 2021), the growth curve for outside Dogfish had a more appropriate a_0 estimate, such that the size of newborn age-0 Dogfish was approximately 20–30 cm. This is the range of uterine pup sizes observed near the end of the gestational period (Ketchen 1972). This was the primary growth curve used in the population model, termed “BC growth”.

Variability in length-at-age decreased as age increased. Based on the lognormal residual standard deviation by age and sex in the fitted von Bertalanffy model (BC growth curve), the population model was configured so that the coefficient of variation (CV) in length at age linearly decreases from 0.25 to 0.075 for ages 0 to 40, respectively, for females. For males, the CV at age was slightly larger, where the decrease was from 0.25 to 0.1 for ages 0 to 40, respectively. The CV remained constant for ages 40 and above.

An alternative growth curve was also explored from age samples collected in Washington and estimated in the 2021 U.S. assessment, termed “US growth”. Compared to the primary growth curve, the alternative describes a larger but slower growing animal (Figure 13).

Weight-at-length was estimated from survey samples in outside waters (Figure 14).

Maturity-at-age estimates were obtained from the literature (McFarlane and Beamish 1987, Taylor et al. 2013*b*) (Figure 15). Maturity-at-length was also estimated from biological samples in the Synoptic survey (Figure 16, Appendix C). Conversion of maturity at size to maturity-at-age values is dependent on the length-age function (Figure 15). The conversion used a length-age key: a probability matrix, where the probability of length given age follows a Gaussian distribution with the mean from the von Bertalanffy equation and standard deviation from the CV in length-at-age.

Due to uncertainty in the growth curve, and to facilitate sensitivity analyses, maturity was explicitly parameterized with respect to age in the population model. Two ogives were considered in the sensitivity analyses. The maturity-at-age ogive from Taylor and Gallucci (2009) with early maturity (samples in the 2000s) was used as the base scenario, where the ages of 50 and 95% female maturity were 31.5 and 55.8 years, respectively. This ogive defines mature as females that are pregnant or between pregnancies and it most closely resembles the maturity-at-length

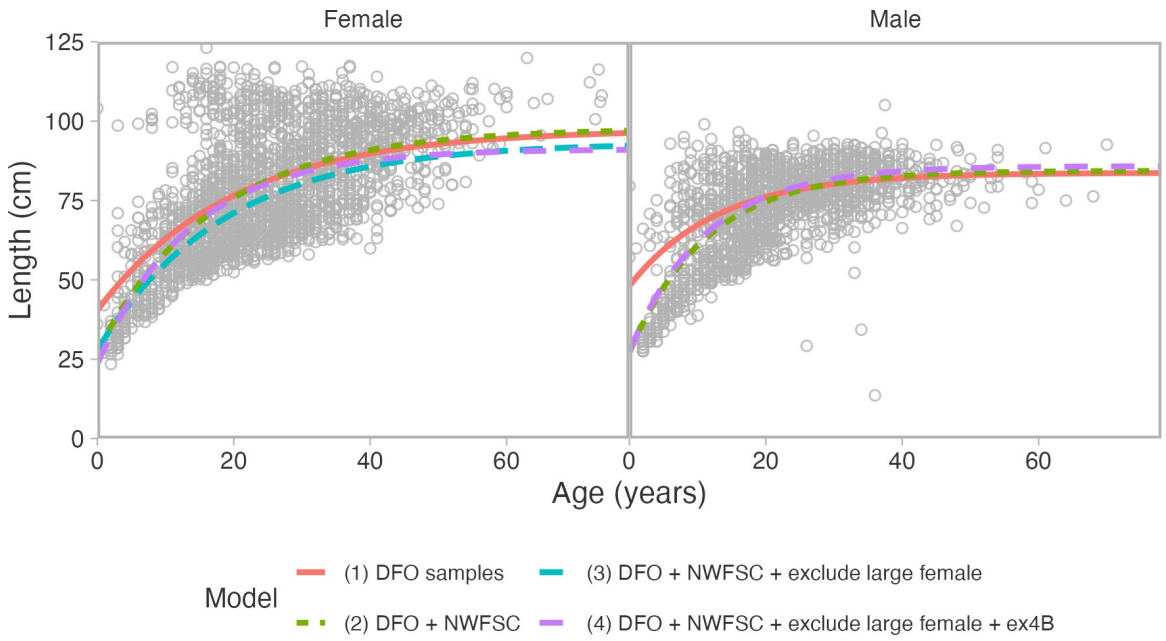

Figure 12. A comparison of four von Bertalanffy growth curves (coloured lines) considered in this study. Points show all length-at-age samples used to fit Model 2. However, a subset were used to fit the other three models. See Appendix C for details. The cluster of points towards the top left of the left panel is likely due to difficulty aging larger, and presumably older, Dogfish. The "exclude large female" scenarios exclude these points.

ogive from the Synoptic survey (Figure 15). The second maturity-at-age ogive considered in the population models was from McFarlane and Beamish (1987), which sampled Dogfish in the Strait of Georgia. For this ogive, females were considered mature if uterine eggs or yolksac pups were present in the uteri and/or large yellow ova were present in the ovaries (Saunders and McFarlane 1993). This maturity schedule consists of slightly older females, where the ages of 50% and 95% female maturity were 35.5 and 45 years, respectively. Male maturity was not modelled because it is assumed that female abundance is the limiting factor in the spawning output of the population.

To accommodate the two-year gestation period for Dogfish pups, the maturity ogive input into the model was set to half of their original values, i.e., with a maximum of 0.5 for any age class. In this manner, half of the mature population on average is calculated to produce young in a given year.

Fecundity estimates f were obtained from Ketchen (1972), where the number of pups is a linear function of length ℓ, with $f_\ell = 0.20\ell - 13.24$ (Figure 17). On average, females produce 6–7 young per litter. No fecundity-at-age estimates are available, so the model internally converts values from the fecundity-at-length schedule through the length-age key.

Natural mortality M was indirectly estimated to be 0.064 year^{-1} based on a maximum age of ≈85 years using the meta-analytic estimator in Hamel and Cope (2022): $M = 5.4/a_{\max}$. This is nearly identical to the estimated value of 0.065^{-1} in Smith et al. (1998), which is the value used in the US West Coast assessment (Gertseva et al. 2021). We proceed with 0.065 year^{-1} as our base value and explore sensitivity to other values (described below). A maximum age of ≈85 years is based on reports of "80+" year-old aged Dogfish in BC in studies from the 1980s (e.g., McFarlane and Beamish 1987) along with personal communication with G.A. McFarlane who recalled aging BC Dogfish up to 84 years old. Given similar longevity between sexes, natural mortality was set as sex-invariant in the model.

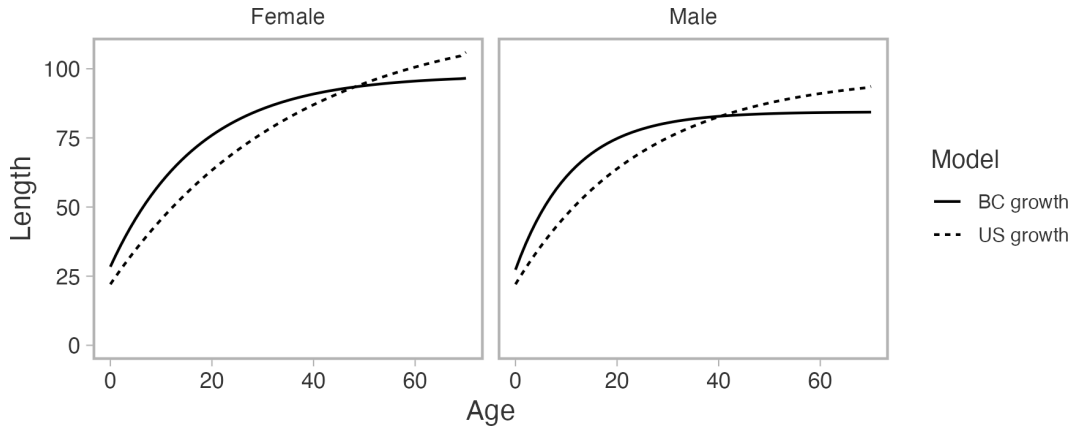

Figure 13. Comparison of two growth curves, estimated from either samples in BC + US ("BC growth") or solely from US samples ("US growth"). The US growth curve has a larger asymptotic length with slower growth to the asymptote. For the BC growth curve, the asymptotic length $L_\infty = 97.7, 84.4$ cm and the growth coefficient $k = 0.058, 0.089$ for females and males, respectively. For the US growth curve, the asymptotic length $L_\infty = 119.0, 98.0$ cm and the growth coefficient $k = 0.028, 0.040$ for females and males, respectively (Gertseva et al. 2021).

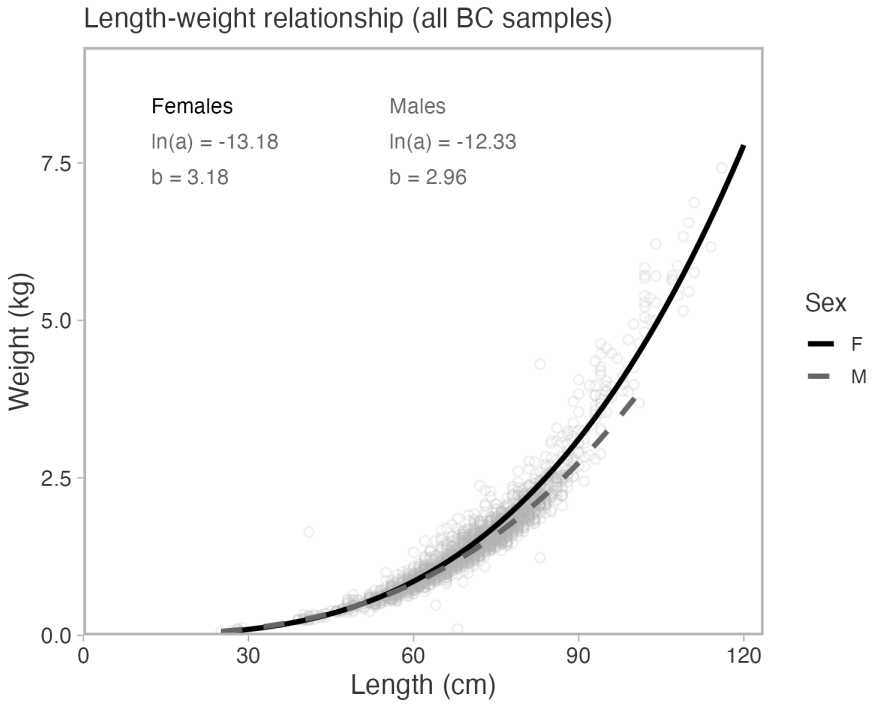

Figure 14. Weight-at-length by sex estimated from biological samples collected in British Columbia surveys in British Columbia (including samples from inside and outside waters).

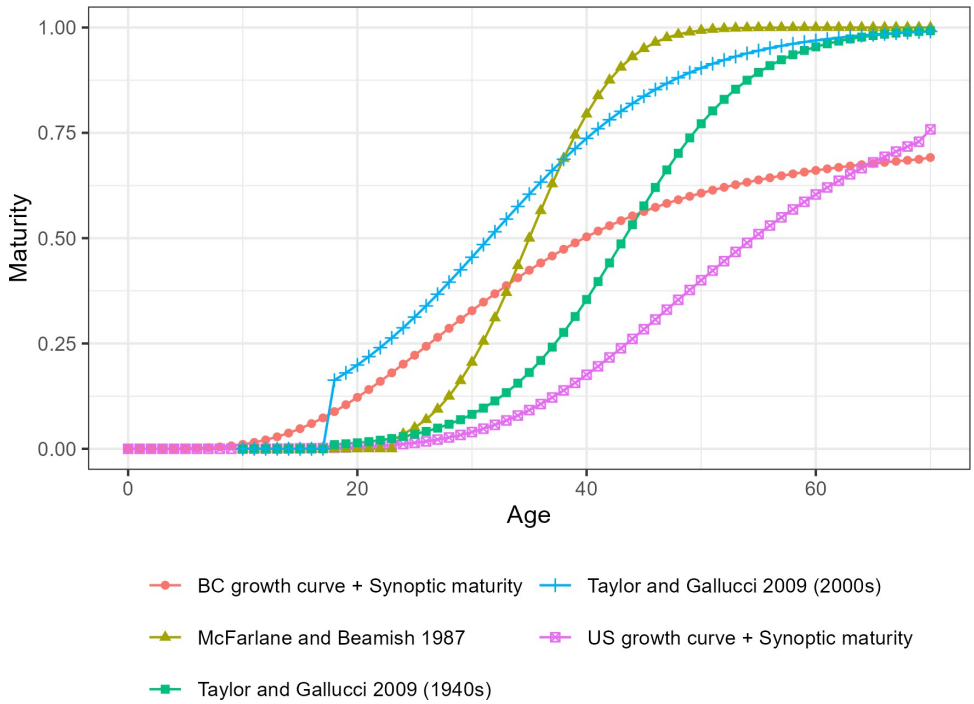

Figure 15. Estimates of female maturity-at-age, either from the literature or converted from maturity-at-length from biological samples in the Synoptic survey and then converted to maturity-at-age in SS3 using the specified growth curve. Taylor and Gallucci (2009) estimated two maturity ogives based on biological samples collected in Puget Sound in either the 1940s or 2000s, and the minimum age of a mature female was 18 years (maturity defined as pregnant females and females between pregnancies). McFarlane and Beamish (1987) estimate age-at-maturity for SOG Dogfish during the early 1980s (maturity defined as uterine eggs or yolksac pups present in the uteri and/or large yellow ova present in ovaries). For the Synoptic survey, maturity-at-age (pregnant females and females between pregnancies) was converted from maturity-at-length in conjunction with either a BC growth curve or the US growth curve (Figure 13).

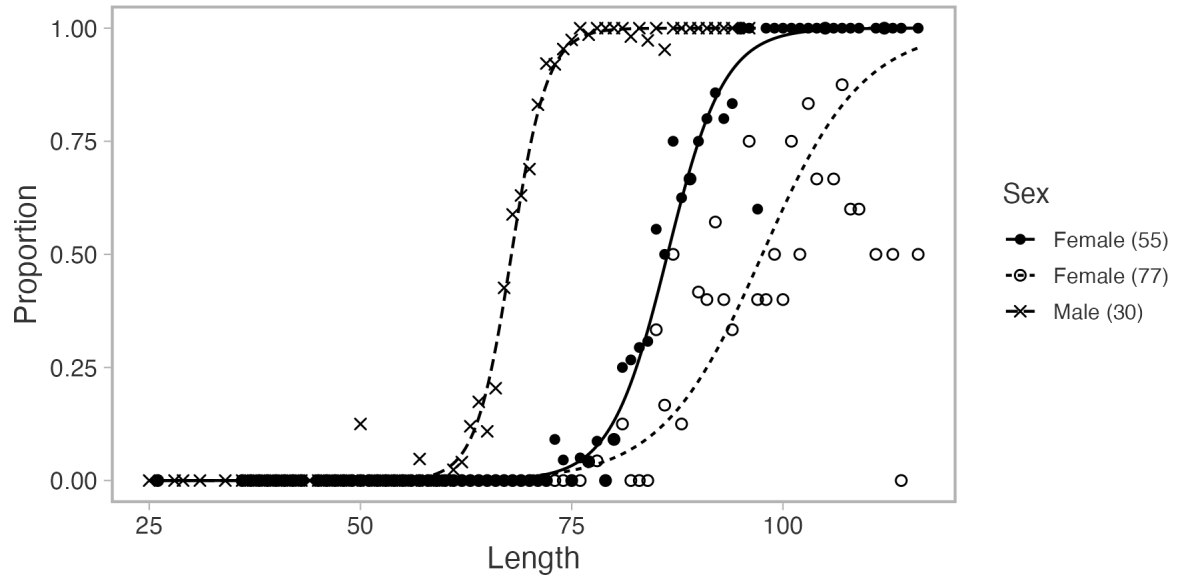

Figure 16. Maturity ogives estimated from biological samples collected in the Synoptic trawl surveys in outside waters. Maturity status is classified based on macroscopic evaluation of gonads. Female (55) indicates maturing females based on ova size 5–10 mm and thickened uterii (>10 mm). Female (77) indicates mature females as defined by the presence of yolk sac pups. Male (30) describes maturing and mature males (i.e., claspers extend past the posterior margin of the pelvic fin and are either calcified or not). Lines and points indicate the estimated and observed proportions. Figure 15 uses the curve with code 77 shown here for female maturity.

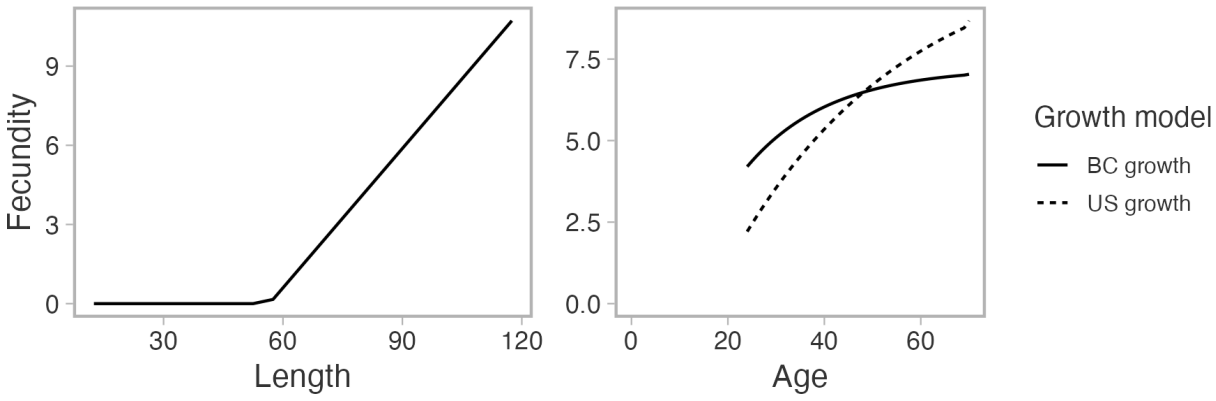

Figure 17. Fecundity at length relationship from Ketchen (1972) (left) and the corresponding fecundity at age is converted in conjunction with two growth curves (right, Figure 13). The minimum age of a mature female in the population model was set to 18 years.

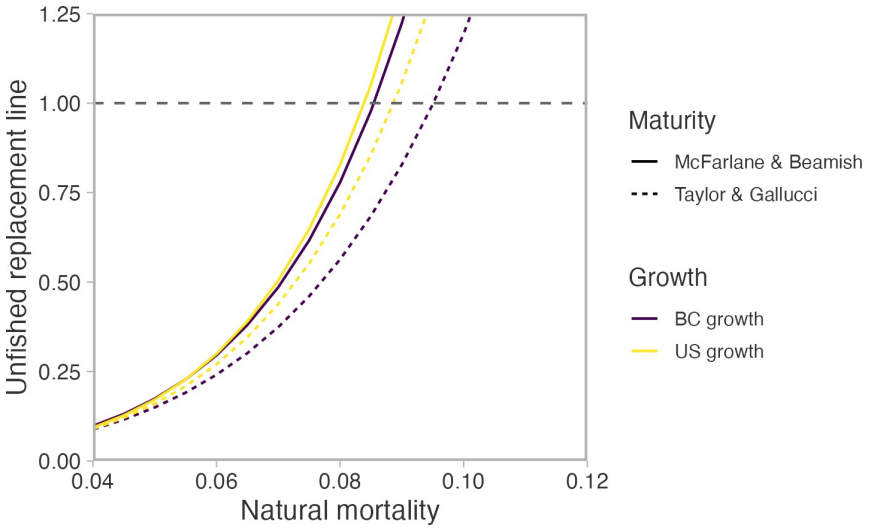

Figure 18. The slope of the unfished replacement line as a function of natural mortality, conditional on a combination of growth curve (colour) or maturity ogive (linetype). These biological parameters determine the fecundity-at-age schedule in the population model. Low fecundity implies an upper bound on natural mortality. The slope of the unfished replacement line cannot exceed 1, which implies that the survival of newborn offspring is greater than 1 and is impossible for a closed population. Natural mortality above this limit indicates that a female on average cannot replace herself over the course of her lifetime.

3.2. MODEL STRUCTURE

The base model estimated the unfished recruitment in log-space $\log(R_0)$, the productivity parameter z_{frac} (fixed in all but one model), and selectivity parameters for the various fisheries and surveys (Table 3). No recruitment deviations were estimated as no information about cohort strength was evident in the size composition data. The US West Coast assessment came to the same conclusion for their stock (Gertseva et al. 2021). Gertseva et al. (2021) further argues that the large size of Dogfish pups at birth (20–30 cm) suggests that recruitment variability would be lower than for a species with a larval stage that experiences higher mortality. Preliminary models estimated recruitment deviates that were deemed to be spurious because they did not change the fit and stock estimates compared to those in simpler models without deviates.

The start year of the model was 1937, when it was assumed that the stock was in an unfished state (after the oil fishery of the late 1800s but before the vitamin A fishery began), and the terminal year was 2023. The maximum age in the model was 70 years.

Model equations are provided in Table 4.

3.2.1. Stock-recruit relationship

An explicit survival-based stock-recruit relationship (SRR) was used in the model, where recruitment R in year y is

$$R_y = S_y \times \exp\left(-z_0 + (z_0 - z_{\min})\left(1 - \frac{S_y}{S_0}\right)^{\beta}\right), \tag{1}$$

where S_y is the spawning output in year y, $S_0 = R_0 \times \phi_0$ is the unfished spawning output as the product of unfished recruitment R_0 and spawning output per recruit ϕ_0, $z_{\min} = z_0(1 - z_{\text{frac}})$, and $z_0 = -\log(1/\phi_0)$ (Taylor et al. 2013*b*).

Mechanistically, the recruitment is simply the product of the spawning output of the population S_y and its survival over some time interval, defined by the exponent term. The term in the exponent is the corresponding instantaneous mortality rate (exponentiation converts the instantaneous rate to a survival term between 0–1). Since this term describes the density-dependent mechanism in the population, the pup-recruit mortality rate decreases as the stock declines.

The inverse of spawning output per recruit $(1/\phi_0)$ is the unfished replacement line and can be interpreted as the survival of pups to the recruit life stage when the stock is at unfished levels. The symbol z_0 is the instantaneous rate when the stock is at S_0. The symbol $z_{\min}$ is the mortality rate as the stock approaches zero, and is parameterized as a z_{frac} proportion of z_0, i.e., $z_{\min} = z_0(1 - z_{\text{frac}})$. When $\beta = 1$, the decline in the density-dependent mortality rate is linear with stock size. As z_{frac} approaches zero, the mortality rate is independent of stock size, i.e., there is no density-dependence. As z_{frac} approaches one, the pup mortality rate approaches zero (survival is one) as the stock approaches zero.

Steepness, the recruitment relative to R_0 when the stock is at $0.2S_0$, is calculated as

$$h = 0.2\exp(z_0 z_{\text{frac}}(1 - 0.2^{\beta})). \tag{2}$$

Due to the longevity and low fecundity of Dogfish, and many elasmobranch species in general, there are upper bounds to the maximum per-capita rate of recruitment in a closed population. The spawning output is measured in the number of pups, and the recruitment after density-dependence cannot exceed the pup production (De Oliveira et al. 2013, Forrest and Walters 2009, Taylor et al. 2013*b*). As a result, there is an implied upper bound to steepness, where steepness cannot exceed $1/(5\phi_0)$ (Taylor et al. 2013*b*).

This upper bound can be illustrated with a simple example. If the unfished population is 100 females that each produce 10 pups, then $S_0 = 1000$. If pup survival is 0.6 ($1/\phi_0 = 0.6$), then the corresponding recruitment R_0 is 600. At a state of $S/S_0 = 0.2$, the population of 20 females produces 200 pups, which is also the maximum recruitment if pup survival were to increase to one. We use 0.2 because of the definition of steepness: the fraction of recruitment obtained at a 20% unfished state compared to an unfished state. In this case, the maximum possible steepness would be 0.33 (200/600).

The unfished spawning output per recruit ϕ_0 is calculated from natural mortality, maturity, and fecundity. Low fecundity also implies an upper limit to natural mortality because ϕ_0 must remain above one. With high natural mortality, it is possible to calculate $\phi_0 < 1$. In other words, the unfished replacement line $1/\phi_0 > 1$. Such as situation implies that a female cannot produce enough offspring over the course of her lifetime to replace herself. The upper bound on natural mortality implied from the various combinations of growth curves and maturity ogives considered here are presented in Figure 18. The range in the upper bound is between 0.083–0.095. The upper bound marginally increases with either earlier maturity or faster growth.

3.2.2. Selectivity

Selectivity at length was modelled using a double Gaussian formulation. If female selectivity is dome shaped, then selectivity was parameterized with three parameters that control the size of full selectivity (μ^{Female}), the width of the ascending limb ($\Delta^{\text{Female,asc}}$), and the width of the descending limb ($\Delta^{\text{Female,dsc}}$). If female selectivity is flat-topped, then the descending limb parameter was fixed to $\Delta^{\text{Female,dsc}} = 15$ which set selectivity to be effectively 1 at lengths greater than μ^{Female}.

Female selectivity at length v_ℓ was parameterized as

$$v_\ell^{\text{Female}} = \begin{cases} \exp\left(\dfrac{-(\ell - \mu^{\text{Female}})^2}{\exp(\Delta^{\text{Female,asc}})}\right) & \ell \leq \mu^{\text{Female}} \\ \exp\left(\dfrac{-(\ell - \mu^{\text{Female}})^2}{\exp(\Delta^{\text{Female,dsc}})}\right) & \text{otherwise} \end{cases} \tag{3}$$

Four additional selectivity parameters were estimated for males, with three parameters controlling the shape of the selectivity curve (μ^{Male}, $\Delta^{\text{Male,asc}}$, $\Delta^{\text{Male,dsc}}$), as an offset from the corresponding female parameter, and a fourth parameter (A^{Male}) that specifies the apical selectivity of males relative to females (between 0-1).

Male selectivity at length, all presumed to be dome-shaped, was

$$v_\ell^{\text{Male}} = A^{\text{Male}} \times \begin{cases} \exp\left(\dfrac{-(\ell - [\mu^{\text{Female}} + \mu^{\text{Male}}])^2}{\exp(\Delta^{\text{Female,asc}} + \Delta^{\text{Male,asc}})}\right) & \ell \leq \mu^{\text{Female}} + \mu^{\text{Male}} \\ \exp\left(\dfrac{-(\ell - \mu^{\text{Female}})^2}{\exp(\Delta^{\text{Female,dsc}} + \Delta^{\text{Male,dsc}})}\right) & \text{otherwise} \end{cases} \tag{4}$$

The corresponding selectivity at age is obtained through the length-age key (Table 4).

3.3. MODEL FITTING

The estimated parameters for the stock-recruit relationship are $\log(R_0)$ and z_{frac}. A uniform prior was used for $\log(R_0)$ with a lower bound of 9 and upper bound of 15. A beta prior was used for z_{frac} with mean of 0.5 and standard deviation of 0.287, corresponding to a symmetrical, weakly informative prior with slightly lower prior density at the bounds of 0 and 1. The mean and standard deviation correspond to beta distribution parameters $\alpha = 1.01$ and $\beta = 1.01$.

For fisheries and/or surveys with length composition, six parameters were estimated if the female selectivity was assumed to be flat-topped or seven parameters if dome-shaped. From the length composition (summed across all years), the modal length L_{mode} was used as the prior mean for the female length of full selectivity μ^{Female}. The prior mean for the male length of full selectivity μ^{Male} was the difference between the modal lengths in the female and male length composition. For both sexes, the standard deviation of the prior was set to 30% of the mean (15% for the longline landings fleet to improve convergence). A normal distribution was used for both parameters.

The apical male selectivity A^{Male} parameter was estimated with a weakly informative prior with a mean and standard deviation of 0.5 and 0.287, respectively. The mean and standard deviation correspond to beta distribution parameters $\alpha = 1.01$ and $\beta = 1.01$.

The Δ control the selectivity limbs and are estimated in logspace. They were estimated assuming a normal prior distribution with a prior standard deviation of 0.3. The length at the 5$^{\text{th}}$ percentile $L_{5\%}$ of the length composition, i.e., from the empirical cumulative distribution function, was used to calculate the prior mean of $\Delta^{\mathrm{Female,asc}}$ was set to $\log(L_{\mathrm{mode}} - L_{5\%})$. Δ are logspace parameters, estimated with a prior standard deviation of 0.3. If dome selectivity was assumed, then the prior mean of $\Delta^{\mathrm{Female,dsc}}$ was set to $\log(L_{95\%} - L_{\mathrm{mode}})$, where $L_{95\%}$ is the size at the 95$^{\text{th}}$ percentile of the length composition. The process was repeated for the male parameters, where the difference in female and male values was used as the prior mean for the males, since these parameters are estimated as offsets.

For fisheries and surveys without length data, selectivity was mirrored, i.e., borrowed from other fisheries and surveys in the model. The fleet structure of the fisheries in the model was broadly organized in terms of fishing gear and retention behaviour (landings vs. discards), due to the differences in length composition upon visual inspection. For example, trawl landings were comprised primarily of large females while trawl discards were comprised of smaller Dogfish with an even sex ratio.

Dome-shaped selectivity was estimated for the bottom trawl discard, midwater trawl, and the Synoptic trawl survey fleets (thereby also affecting selectivity for fleets that mirrored these fleets). Similarly to the US assessment, we observed that non-trawl landings and the IPHC survey caught the largest individuals. Furthermore, the Synoptic trawl survey avoids rocky habitat and thereby does not have complete spatial coverage of Dogfish habitat within the assessment area. For these reasons, we assumed dome-shaped selectivity for these fleets. The US assessment came to a similar conclusion and also estimated dome-shaped selectivity for fleets other than non-trawl landings and the IPHC survey (Gertseva et al. 2021).

The following fleets were defined:

1. Bottom Trawl Landings. Female selectivity is flat-topped.
2. Bottom Trawl Discards. Female selectivity is dome-shaped. Several other fleets mirror the selectivity of this fleet since it is the only discard fleet with length composition data.
3. Midwater Trawl, where catches included both landings and dead discards, the latter calculated according to the presumed discard mortality rate, since the length composition for retained and discarded catch were similar. Female selectivity is dome-shaped.
4. Longline Landings. Female selectivity is flat-topped.
5. Longline Discards, where the selectivity was mirrored to Bottom Trawl Discards since there were no size samples collected.
6. IPHC Survey. Female selectivity is flat-topped.
7. HBLL Outside Survey, where the selectivity was mirrored to the IPHC survey.
8. Synoptic Survey. Female selectivity is dome-shaped.

9. Recreational catch as recorded in the iREC survey (Internet Recreational Effort and Catch reporting program), selectivity was mirrored to Bottom Trawl Discards.
10. Salmon Bycatch, selectivity was mirrored to Bottom Trawl Discards.
11. HS MSA Survey, where selectivity was mirrored to the Synoptic survey.
12. Bottom Trawl CPUE, used as an index of abundance with selectivity mirrored to Bottom Trawl Discards.

Survey catch was also included in the model since it constituted a small but notable proportion of the total removals in recent years. For each index series, catchability is an implicit parameter, which is calculated internally from the observed values and state variables in the model. The US West Coast assessment took a similar approach—they attempted to estimate catchability for their main current bottom trawl survey but were forced to fix it due to estimation issues (Gertseva et al. 2021).

The model likelihood included a component for the indices of abundance from the surveys and fishery CPUE, using a lognormal distribution with the standard deviation calculated from the standardization method.

The multinomial likelihood was used for the length composition. The annual sample size specified in the model was the number of specimens (i.e., Dogfish) measured. Following a preliminary fit of the base model, the sample sizes were adjusted, i.e., downweighted, using the McAllister and Ianelli (1997) method in order to balance the variance between the length composition and the indices of abundance. These weighting factors were identical in all models.

The base model (labelled "**A0**") was fitted with the following structure:

- two sexes modelled (but with shared natural mortality) with length-at-age specified using the BC growth curve;
- maturity-at-age following the Taylor and Gallucci (2009) ogive for the 2000s;
- discard mortality following the "base" level described in Section 2.1;
- natural mortality fixed at 0.065;
- z_{frac} fixed at 0.4 and β fixed at 1 following Gertseva et al. (2021); and
- all indices of abundance included.

We assessed the fitting of the models as being consistent with convergence if the maximum absolute value of the log-likelihood gradient with respect to parameters was < 0.0001 and the Hessian matrix was invertible. Furthermore, we sampled from selected models with MCMC (Markov chain Monte Carlo) to ensure our models were identifiable with a more robust sampling approach (Section 3.3.2).

3.3.1. Sensitivity models

Additional sensitivity runs (relative to the base model) explored the impact of various modelling assumptions, particularly in the choice of biological parameters (maturity, growth, natural mortality), discard mortality rates, and most representative index, on the estimated stock biomass and fishing mortality rates.

The model names with the "A" prefix denote time-invariant natural mortality.

- **A1**: Same as A0 but attempt to estimate z_{frac}. The parameter z_{frac} hits the lower bound of 0. We therefore focus on the base model A0, which has z_{frac} fixed at 0.4 as in Gertseva et al. (2021). We do, however, sample from model A1 with MCMC as described in Section 3.3.2 and Appendix E.

- **A2**: Length-at-age specified with the growth curve estimated in the US assessment (Gertseva et al. 2021).
- **A3**: Older maturity at age, specified by the McFarlane and Beamish (1987) ogive.
- **A4**: Use both the US growth curve and the older maturity ogive.
- **A14**: Assume the low discard mortality rates described in Section 2.1.
- **A5**: Assume the high discard mortality rates described in Section 2.1.
- **A15**: Assume 100% discard mortality to investigate the sensitivity to the assumed discard mortality rate. We subsequently exclude this scenario from reference point calculations because we deem it less plausible than the other discard rate scenarios.
- **A6**: Fit to only the IPHC index and fishery bycatch CPUE. These indices were grouped together since they describe a steady decline in the population over time.
- **A7**: Fit to only the Synoptic index.
- **A8**: Fit to only the HBLL Outside index. This model had convergence issues we could not resolve (the HBLL Outside survey lacks length composition data and has a steeper decline than the other indices); it is therefore not shown.
- **A13**: Estimate an additional error term on the IPHC survey index. This index had the smallest standard errors, was the most influential in the likelihood of the base model, and has a less steep decline than the other two major modern surveys. We therefore tried estimating additional error on this index to down-weight it. We could not successfully fit a model with additional error estimated on all survey indexes.
- **A9**: Fix natural mortality at a lower value of 0.057, which is based on a maximum age of approximately 95 years from Figure 7 in McFarlane and King (2009) and the approach in Hamel and Cope (2022): $5.4/95 = 0.057$. Approximately 95 years old was the maximum age when the maximum observed inter-reader error absolute difference was added.
- **A10**: Fix natural mortality at a higher value of 0.074, which is based on a maximum age of 73 years from samples used to fit the growth curves in this assessment and the Hamel and Cope (2022) approach: $5.4/73 = 0.074$.
- **A11**: Assume a lower productivity stock: set $z_{\text{frac}} = 0.2$ and $\beta = 0.6$. This is the lower productivity scenario explored in Gertseva et al. (2021).
- **A12**: Assume a higher productivity stock: set $z_{\text{frac}} = 0.6$ and $\beta = 2$. This is the upper productivity scenario explored in Gertseva et al. (2021).

The model names with the "B" prefix denote time-varying natural mortality. Several models were fitted in an attempt to attribute the recent decrease in the indices to changes in non-fishery mortality:

- **B1**: Estimate an increase in natural mortality starting in 1990 around when Steller sea lion abundance began to increase exponentially in BC, eventually returning to historical levels (DFO 2021, 2023, Olesiuk 2018). The increase in M is linear year-over-year. A single additional parameter representing the slope of the increase is estimated.
- **B2**: Estimate an increase in natural mortality starting in 2010 as a stepwise change. A single additional parameter, a multiplicative factor on the base mortality value, is estimated. This starting year was chosen to test if changes in natural mortality could explain the steep declines starting around 2010 in the Synoptic trawl survey.
- **B3**: Estimate an increase in natural mortality starting in 2005 as a stepwise change. A single additional parameter is estimated as a multiplicative effect. This start year was chosen to align approximately with the period of steepest decline in the HBLL Outside longline survey.

- **B4**: Same as B1, but the natural mortality prior to 1990 is 0.057 (instead of 0.065).
- **B5**: Same as B2, but the natural mortality prior to 1990 is 0.057 (instead of 0.065).

Although we only explore time-varying M in this assessment, Taylor and Gallucci (2009) observed an increase in growth to smaller sizes, along with a decline in age of maturation and an increase in average litter size, which was most pronounced between the 40s and 70s. Future versions of the assessment could consider allowing for time-varying growth.

3.3.2. MCMC

After fitting the models by minimizing the negative log posterior, a subset of models were sampled with Bayesian MCMC (Markov Chain Monte Carlo) for general diagnostics purposes, for example, evidence of over-parameterization. We used the No U-Turn Sampling (NUTS) algorithm (Hoffman and Gelman 2014) from the adnuts R package (Monnahan and Kristensen 2018). We sampled with 800 iterations on each of 4 chains with a warm-up period of 300 iterations per chain. We proceeded with the MCMC for models A1 (our base model with an estimated z_{frac} parameter) and B2.

Table 3. Parameters reported from SS3 for model A0, including the parameter name in the report file, value, and standard error (if estimated) calculated from inverting the Hessian matrix. Male biological parameters are parameterized as offsets from the female parameter in logspace. For example, the male natural mortality value y is equal to the female parameter x, the offset in the control and report files should be $\log(y/x) = 0$. Parameters labelled as `_Mult` act as multipliers relating dead catch to observed catch. I.e., they are the reciprocal of the discard mortality rates from Table 1.

Parameter	Estimated?	Value	Standard Error	Description
NatM_uniform_Fem_GP_1	Fixed	0.065	NA	Female natural mortality, derived from literature
L_at_Amin_Fem_GP_1	Fixed	28.400	NA	Female mean length at age 0, estimated from data
L_at_Amax_Fem_GP_1	Fixed	90.870	NA	Female mean length at age 40, estimated from data
VonBert_K_Fem_GP_1	Fixed	0.058	NA	Female von Bertalanffy K parameter, estimated from data
CV_young_Fem_GP_1	Fixed	0.250	NA	Female variability in length at age 0, estimated from data
CV_old_Fem_GP_1	Fixed	0.075	NA	Female variability in length at age 40, estimated from data
Wtlen_1_Fem_GP_1	Fixed	0.000	NA	Female length-weight scalar (a), estimated from data
Wtlen_2_Fem_GP_1	Fixed	3.190	NA	Female length-weight exponent (b), estimated from data
Mat50Mat_slope_Fem_GP_1	Fixed	-0.168	NA	Not used - female maturity at age (from literature) directly specified in control file
Eggs_intercept_Fem_GP_1	Fixed	-9.960	NA	Female fecundity intercept term, from literature
Eggs_slope_len_Fem_GP_1	Fixed	0.176	NA	Female fecundity slope term, from literature
NatM_uniform_Mal_GP_1	Fixed	0.000	NA	Male offset for natural mortality, derived from literature
L_at_Amin_Mal_GP_1	Fixed	-0.039	NA	Male offset for mean length at age 0, estimated from data
L_at_Amax_Mal_GP_1	Fixed	-0.093	NA	Male offset for mean length at age 40, estimated from data
VonBert_K_Mal_GP_1	Fixed	0.428	NA	Male offset for von Bertalanffy K parameter, estimated from data
CV_young_Mal_GP_1	Fixed	0.000	NA	Male offset for variability in length at age 0, estimated from data
CV_old_Mal_GP_1	Fixed	0.287	NA	Male offset for variability in length at age 40, estimated from data
Wtlen_1_Mal_GP_1	Fixed	0.000	NA	Male length-weight scalar (a), estimated from data

Parameter	Estimated?	Value	Standard Error	Description
Wtlen_2_Mal_GP_1	Fixed	3.030	NA	Male length-weight exponent (b), estimated from data
CohortGrowDev	Fixed	1.000	NA	Internal SS3 parameter
Catch_Mult:_1_Bottom_Trawl_Landings	Fixed	1.000	NA	Catch multiplier
Catch_Mult:_2_Bottom_Trawl_Discards	Fixed	2.703	NA	Catch multiplier - accounts for discard mortality
Catch_Mult:_3_MidwaterTrawl	Fixed	1.000	NA	Catch multiplier
Catch_Mult:_4_HookLine_Landings	Fixed	1.000	NA	Catch multiplier
Catch_Mult:_5_HookLine_Discards	Fixed	3.704	NA	Catch multiplier - accounts for discard mortality
Catch_Mult:_6_IPHC	Fixed	3.704	NA	Catch multiplier
Catch_Mult:_7_HBLL	Fixed	3.704	NA	Catch multiplier
Catch_Mult:_8_SYN	Fixed	2.703	NA	Catch multiplier
Catch_Mult:_9_iRec	Fixed	10.000	NA	Catch multiplier - accounts for discard mortality
Catch_Mult:_10_Salmon_Bycatch	Fixed	1.235	NA	Catch multiplier - accounts for discard mortality
FracFemale_GP_1	Fixed	0.500	NA	Proportion of recruitment that is female
SR_LN(R0)	Yes	9.386	0.031	Unfished recruitment
SR_surv_zfrac	Fixed	0.400	NA	Stock-recruit productivity parameter
SR_surv_Beta	Fixed	1.000	NA	Stock-recruit beta parameter
SR_sigmaR	Fixed	0.400	NA	Not used - no recruitment deviations
SR_regime	Fixed	0.000	NA	Not used
SR_autocorr	Fixed	0.000	NA	Not used
LnQ_base_IPHC(6)	Fixed	-1.380	NA	Not used - index catchability calculated internally
LnQ_base_HBLL(7)	Fixed	1.011	NA	Not used - index catchability calculated internally
LnQ_base_SYN(8)	Fixed	-9.721	NA	Not used - index catchability calculated internally
LnQ_base_HS_MSA(11)	Fixed	-2.366	NA	Not used - index catchability calculated internally
LnQ_base_Bottom_Trawl_CPUE(12)	Fixed	4.282	NA	Not used - index catchability calculated internally
Size_DblN_peak_Bottom_Trawl_Landings(1)	Yes	110.127	1.904	Selectivity parameter μ^{Female}
Size_DblN_top_logit_Bottom_Trawl_Landings(1)	Fixed	-10.000	NA	Not used
Size_DblN_ascend_se_Bottom_Trawl_Landings(1)	Yes	5.479	0.178	Selectivity parameter $\Delta^{\text{Female, asc}}$
Size_DblN_descend_se_Bottom_Trawl_Landings(1)	Fixed	15.000	NA	Not used, flat-top selectivity
Size_DblN_start_logit_Bottom_Trawl_Landings(1)	Fixed	-999.000	NA	Not used
Size_DblN_end_logit_Bottom_Trawl_Landings(1)	Fixed	-999.000	NA	Not used
SzSel_Male_Peak_Bottom_Trawl_Landings(1)	Yes	-4.538	10.952	Selectivity parameter μ^{Male}
SzSel_Male_Ascend_Bottom_Trawl_Landings(1)	Yes	0.912	0.291	Selectivity parameter $\Delta^{\text{Male, asc}}$
SzSel_Male_Descend_Bottom_Trawl_Landings(1)	Yes	-11.800	0.300	Selectivity parameter $\Delta^{\text{Male, dsc}}$
SzSel_Male_Final_Bottom_Trawl_Landings(1)	Fixed	-999.000	NA	Not used
SzSel_Male_Scale_Bottom_Trawl_Landings(1)	Yes	0.037	0.028	Selectivity parameter A^{Male}
Size_DblN_peak_Bottom_Trawl_Discards(2)	Yes	50.608	2.042	Selectivity parameter μ^{Female}
Size_DblN_top_logit_Bottom_Trawl_Discards(2)	Fixed	-10.000	NA	Not used
Size_DblN_ascend_se_Bottom_Trawl_Discards(2)	Yes	4.473	0.263	Selectivity parameter $\Delta^{\text{Female, asc}}$
Size_DblN_descend_se_Bottom_Trawl_Discards(2)	Yes	6.422	0.180	Selectivity parameter $\Delta^{\text{Female, dsc}}$
Size_DblN_start_logit_Bottom_Trawl_Discards(2)	Fixed	-999.000	NA	Not used
Size_DblN_end_logit_Bottom_Trawl_Discards(2)	Fixed	-999.000	NA	Not used
SzSel_Male_Peak_Bottom_Trawl_Discards(2)	Yes	6.953	2.719	Selectivity parameter μ^{Male}
SzSel_Male_Ascend_Bottom_Trawl_Discards(2)	Yes	0.489	0.278	Selectivity parameter $\Delta^{\text{Male, asc}}$
SzSel_Male_Descend_Bottom_Trawl_Discards(2)	Yes	-0.820	0.230	Selectivity parameter $\Delta^{\text{Male, dsc}}$
SzSel_Male_Final_Bottom_Trawl_Discards(2)	Fixed	-999.000	NA	Not used
SzSel_Male_Scale_Bottom_Trawl_Discards(2)	Yes	0.560	0.125	Selectivity parameter A^{Male}
Size_DblN_peak_MidwaterTrawl(3)	Yes	55.157	1.085	Selectivity parameter μ^{Female}
Size_DblN_top_logit_MidwaterTrawl(3)	Fixed	-10.000	NA	Not used
Size_DblN_ascend_se_MidwaterTrawl(3)	Yes	4.797	0.178	Selectivity parameter $\Delta^{\text{Female, asc}}$
Size_DblN_descend_se_MidwaterTrawl(3)	Yes	4.884	0.165	Selectivity parameter $\Delta^{\text{Female, dsc}}$
Size_DblN_start_logit_MidwaterTrawl(3)	Fixed	-999.000	NA	Not used
Size_DblN_end_logit_MidwaterTrawl(3)	Fixed	-999.000	NA	Not used
SzSel_Male_Peak_MidwaterTrawl(3)	Yes	-2.308	1.694	Selectivity parameter μ^{Male}
SzSel_Male_Ascend_MidwaterTrawl(3)	Yes	-0.279	0.243	Selectivity parameter $\Delta^{\text{Male, asc}}$
SzSel_Male_Descend_MidwaterTrawl(3)	Yes	1.835	0.202	Selectivity parameter $\Delta^{\text{Male, dsc}}$

Parameter	Estimated?	Value	Standard Error	Description
SzSel_Male_Final_MidwaterTrawl(3)	Fixed	-999.000	NA	Not used
SzSel_Male_Scale_MidwaterTrawl(3)	Yes	0.703	0.076	Selectivity parameter A^{Male}
Size_DblN_peak_HookLine_Landings(4)	Yes	105.892	1.457	Selectivity parameter μ^{Female}
Size_DblN_top_logit_HookLine_Landings(4)	Fixed	-10.000	NA	Not used
Size_DblN_ascend_se_HookLine_Landings(4)	Yes	4.651	0.201	Selectivity parameter $\Delta^{\mathrm{Female,\ asc}}$
Size_DblN_descend_se_HookLine_Landings(4)	Fixed	15.000	NA	Not used, flat-top selectivity
Size_DblN_start_logit_HookLine_Landings(4)	Fixed	-999.000	NA	Not used
Size_DblN_end_logit_HookLine_Landings(4)	Fixed	-999.000	NA	Not used
SzSel_Male_Peak_HookLine_Landings(4)	Yes	-16.040	2.304	Selectivity parameter μ^{Male}
SzSel_Male_Ascend_HookLine_Landings(4)	Yes	-0.107	0.271	Selectivity parameter $\Delta^{\mathrm{Male,\ asc}}$
SzSel_Male_Descend_HookLine_Landings(4)	Yes	-13.211	0.299	Selectivity parameter $\Delta^{\mathrm{Male,\ dsc}}$
SzSel_Male_Final_HookLine_Landings(4)	Fixed	-999.000	NA	Not used
SzSel_Male_Scale_HookLine_Landings(4)	Yes	0.028	0.007	Selectivity parameter A^{Male}
Size_DblN_peak_IPHC(6)	Yes	164.417	8.677	Selectivity parameter μ^{Female}
Size_DblN_top_logit_IPHC(6)	Fixed	-10.000	NA	Not used
Size_DblN_ascend_se_IPHC(6)	Yes	7.129	0.112	Selectivity parameter $\Delta^{\mathrm{Female,\ asc}}$
Size_DblN_descend_se_IPHC(6)	Fixed	15.000	NA	Not used, flat-top selectivity
Size_DblN_start_logit_IPHC(6)	Fixed	-999.000	NA	Not used
Size_DblN_end_logit_IPHC(6)	Fixed	-999.000	NA	Not used
SzSel_Male_Peak_IPHC(6)	Yes	-85.317	8.624	Selectivity parameter μ^{Male}
SzSel_Male_Ascend_IPHC(6)	Yes	-1.922	0.179	Selectivity parameter $\Delta^{\mathrm{Male,\ asc}}$
SzSel_Male_Descend_IPHC(6)	Yes	-11.351	0.226	Selectivity parameter $\Delta^{\mathrm{Male,\ dsc}}$
SzSel_Male_Final_IPHC(6)	Fixed	-999.000	NA	Not used
SzSel_Male_Scale_IPHC(6)	Yes	0.005	0.003	Selectivity parameter A^{Male}
Size_DblN_peak_SYN(8)	Yes	63.738	1.102	Selectivity parameter μ^{Female}
Size_DblN_top_logit_SYN(8)	Fixed	-10.000	NA	Not used
Size_DblN_ascend_se_SYN(8)	Yes	5.305	0.136	Selectivity parameter $\Delta^{\mathrm{Female,\ asc}}$
Size_DblN_descend_se_SYN(8)	Yes	6.739	0.180	Not used, flat-top selectivity
Size_DblN_start_logit_SYN(8)	Fixed	-999.000	NA	Not used
Size_DblN_end_logit_SYN(8)	Fixed	-999.000	NA	Not used
SzSel_Male_Peak_SYN(8)	Yes	18.592	1.099	Selectivity parameter μ^{Male}
SzSel_Male_Ascend_SYN(8)	Yes	1.466	0.150	Selectivity parameter $\Delta^{\mathrm{Male,\ asc}}$
SzSel_Male_Descend_SYN(8)	Yes	-10.383	0.301	Selectivity parameter $\Delta^{\mathrm{Male,\ dsc}}$
SzSel_Male_Final_SYN(8)	Fixed	-999.000	NA	Not used
SzSel_Male_Scale_SYN(8)	Yes	0.921	0.070	Selectivity parameter A^{Male}

Table 4. Summary of SS3 model equations for outside Dogfish. Variables $a = 0, 1, ..., A$ ($A = 70$) indexes age, $y = 1937, 1938, \ldots, 2023$ indexes year, f indexes fishery, i indexes survey, $s = 1, 2$ indexes sex (1 = females, 2 = males), j indexes size bin, ℓ_j is the corresponding length, L_a is the mean length at age a, σ_a is the variability in length at age, $g()$ is the normal cumulative probability density function, f_ℓ is female fecundity at length, m_a is female maturity at age, $w_{a,s}$ is weight at age, and R_0 is unfished recruitment.

Variable	Equation	Number
Length-age key	$P(\ell_j \vert a)_s = \begin{cases} g(\ell_j; L_a, \sigma_a) & j = 1 \\ g(\ell_j; L_a, \sigma_a) - g(\ell_{j-1}; L_a, \sigma_a) & j = 2, \ldots, J-1 \\ 1 - g(\ell_j; L_a, \sigma_a) & j = J \end{cases}$	1
Fecundity at age	$f_a = \sum_j f_\ell \times P(\ell_j \vert a)_{s=1}$	2
Unfished survival (equilibrium)	$l_a = \begin{cases} \exp(-Ma) & a = 0, 1, \ldots, A-1 \\ \exp(-Ma)/(1-\exp(-M)) & a = A \end{cases}$	3
Spawning output	$S_y = \sum_a N_{y,a,s=1} m_a f_a$	4
Recruitment	$R_y = S_y \times \exp\left(-z_0 + (z_0 - z_{\min})\left(1 - \frac{S_y}{S_0}\right)^\beta\right)$	5
Unfished spawning output per recruit	$\phi_0 = 0.5 \sum_a l_a m_a w_a$	6
Female selectivity at length	$v_{\ell,f,s=1} = \begin{cases} \exp\left(\frac{-(\ell - \mu^{\text{Female}})^2}{\exp(\Delta^{\text{Female,asc}})}\right) & \ell \leq \mu^{\text{Female}} \\ \exp\left(\frac{-(\ell - \mu^{\text{Female}})^2}{\exp(\Delta^{\text{Female,dsc}})}\right) & \text{otherwise} \end{cases}$	7
Male selectivity at length	$v_{\ell,f,s=2} = A_f^{\text{Male}} \times \begin{cases} \exp\left(\frac{-(\ell - [\mu_f^{\text{Female}} + \mu_f^{\text{Male}}])^2}{\exp(\Delta_f^{\text{Female,asc}} + \Delta_f^{\text{Male,asc}})}\right) & \ell \leq \mu_f^{\text{Female}} + \mu_f^{\text{Male}} \\ \exp\left(\frac{-(\ell - \mu_f^{\text{Female}})^2}{\exp(\Delta_f^{\text{Female,dsc}} + \Delta_f^{\text{Male,dsc}})}\right) & \text{otherwise} \end{cases}$	8
Selectivity at age	$v_{a,f,s} = \sum_\ell s_{\ell,f,s} \times P(\ell \vert a)_s$	9
Fishing mortality	$F_{y,a,s} = \sum_f v_{a,f,s} F_{y,f}$	10
Total mortality	$Z_{y,a,s} = F_{y,a,s} + M$	11
Initial stock abundance (in 1937)	$N_{y,a,s} = 0.5 R_0 l_a$	12
Stock abundance	$N_{y,a,s} = \begin{cases} 0.5 R_y & a = 0 \\ N_{y-1,a-1,s} \exp(-Z_{y-1,a-1,s}) & a = 1, 2, \ldots, A-1 \\ N_{y-1,a-1,s} \exp(-Z_{y-1,a-1,s}) + N_{y-1,A,s} \exp(-Z_{y-1,A,s}) & a = A \end{cases}$	13
Fishery catch at age (abundance)	$C_{y,a,f,s} = v_{a,f,s} F_{y,f} N_{y,a,s} (1 - \exp(-Z_{y,a,s}))/Z_{y,a,s}$	14
Total fishery catch (abundance)	$Y_{y,f}^N = \sum_s \sum_a C_{y,a,f,s}$	15
Total fishery catch (weight)	$Y_{y,f}^W = \sum_s \sum_a C_{y,a,f,s} w_{a,s}$	16
Fishery catch at length	$C_{y,\ell,f,s} = \sum_a C_{y,a,f,s} P(\ell \vert a)_s$	17
Annual catch at length proportion	$p_{y,\ell,f,s} = C_{y,\ell,f,s} / \sum_s \sum_\ell C_{y,\ell,f,s}$	18
Index (units of abundance)	$I_{y,i}^N = q_i^N \sum_s \sum_a N_{y,a,s} v_{a,i,s}$	19
Index (units of weight)	$I_{y,i}^W = q_i^W \sum_s \sum_a N_{y,a,s} v_{a,i,s} w_{a,s}$	20

Table 5. Summary of SS3 likelihood and prior equations. Variables a indexes age, y indexes year, f indexes fishery, i indexes survey, s indexes sex, k indexes selectivity parameters. m is the prior mean, SD is the prior standard deviation, I is the observed index, N is the sample size of the length composition, p is the proportion by length and sex, A^{Male} is the male apical selectivity, x is the estimated selectivity parameter. For the beta distribution, $\alpha = (1-m)(\frac{m(1-m)}{\mathrm{SD}^2} - 1)$ and $\beta = m(\frac{m(1-m)}{\mathrm{SD}^2} - 1)$. Set $\mathcal{K} = \{\mu^{\mathrm{Female}}, \mu^{\mathrm{Male}}, \Delta^{\mathrm{Female,asc}}, \Delta^{\mathrm{Female,dsc}}, \Delta^{\mathrm{Male,asc}}, \Delta^{\mathrm{Male,dsc}}\}$ denotes the set of selectivity parameters, excluding A. The circumflex symbol denotes an estimate.

Component	Distribution	Equation	Number
Index likelihood	Lognormal	$\mathcal{L}_1 = -\sum_i \sum_y 0.5 \left(\frac{\log(I_{y,i}/\hat{I}_{y,i})}{\sigma^I_{y,i}} \right)^2$	1
Fishery length composition likelihood	Multinomial	$\mathcal{L}_2 = \sum_y \sum_f \sum_\ell \sum_s N_{y,f} p_{y,\ell,f,s} \log(\hat{p}_{y,\ell,f,s})$	2
Prior, z_{frac}	Beta	$\mathcal{P}_{z\mathrm{frac}} = (1-\beta_z)\log(z_{\mathrm{frac}}) + (1-\alpha_z)\log(z_{\mathrm{frac}})$	3
Prior, selectivity parameter A^{Male}	Beta	$\mathcal{P}_A = \sum_f \left((1-\beta_{A_f})\log(A_f) + (1-\alpha_{A_f})\log(A_f) \right)$	4
Prior, other selectivity parameters	Normal	$\mathcal{P}_\mathcal{K} = -\sum_f \sum_k 0.5 \left(\frac{\hat{x}_{k,f} - m_{k,f}}{\mathrm{SD}_{k,f}} \right)^2$	5
Log-posterior function	NA	$f = \mathcal{L}_1 + \mathcal{L}_2 + \mathcal{P}_{z\mathrm{frac}} + \mathcal{P}_A + \mathcal{P}_\mathcal{K}$	6

4. MODEL RESULTS

4.1. BASE MODEL

The base model estimated a large, fast decline in the spawning output of the population in the 1940s as a result of the vitamin A fishery (Figures 19, 20). In the following decades, through the mid 1970s, the spawning output increased and then declined again, albeit at a slower rate, through to 2010. Since 2010, the spawning output has been relatively constant at low levels. In contrast to the spawning output, the total stock biomass gradually declined at different rates since the 1930s (Figure 21).

Total biomass (e.g., Figure 21) does not reveal delayed effects of fishing on the age structure (Figure 22). However, the lagged effects on age structure are readily apparent—particularly for males—where the decline in recruitment (age zero) then cascades towards older age classes moving forward in time. I.e., the lack of pups born during and shortly after the vitamin A fishery results in a low-abundance cohort that progresses through time (Figures 22, 23). The vitamin A fishery quickly decreased the abundance of older-aged females (30+ years) in the 1950s, although the abundance of younger fish in the population (age 20) was less impacted. Young cohorts that were invulnerable to the early fishery rebuilt the abundance of older females in the 1970s–1980s. However, low recruitment during the 1940s (due to fewer older-aged females) contributed to the second decline in the older age classes into recent years. This can also be illustrated by running the model from 1950 onwards with estimated parameters but with catches set to zero and looking at spawning output (Berger 2019) (Figure 24).

The selectivity curve of the bottom trawl landings was estimated such that the respective catch consisted predominantly of large females (Figure 25). When converted to selectivity-at-age, the selectivity ogive was to the right of the base maturity curve (Figures 26) and 27). On the other hand, the selectivity of the bottom trawl discards, along with discards in other fishing fleets and in the midwater trawl fleet, was comprised of younger, immature fish.

The model fit the declines in some indices of abundance, which reflect stock trends in more recent decades, reasonably well for the fishery CPUE, IPHC survey, and HS MSA survey (Figure 28). Overall, these indices show a slower decline year-over-year than the other indices of abundance. The model did not fit the HBLL Outside or Synoptic trawl indices well (Figure 28). The HBLL index had a marked decline after 2014 while the trend in the Synoptic survey index had a downwards concavity in the 2010s that was not matched in the fit.

The model appeared to have some difficulty estimating the selectivity of the IPHC survey, as the inflection point of the selectivity ogive was greater than the largest observed size class (Figure 25). Since the size composition in the Synoptic trawl survey was smaller than in the IPHC survey, selectivity for the former was estimated to be dome-shaped.

Fits to the length composition are shown in Figures 29–34. The corresponding mean length calculated from the observed and predicted proportions are shown in Figure 35. The mean length from the bottom trawl discards was the most erratic—possibly as a result of opportunistic sampling, while the trend in the other fleets and surveys were more consistent through time.

The length composition data do not appear to be informative about stock depletion. This can be demonstrated through the predicted length composition produced by the model in 1937, in unfished conditions, and in the most recent years of data (Figure 36). Despite depletion estimates of less than 0.4 during the 2000s, the shape of the length composition, and the corresponding mean lengths, change little compared to those in 1937. In contrast, age composition data would be more likely to reveal a truncated age structure as the population (and survival) declines. Length composition are uninformative here likely due to the low M/K ratio and the high variability in the length-at-age relationship. With the low M/K ratio, fish near

the asymptotic length are comprised of many age classes, and the length composition data are less sensitive to the loss of the oldest fish compared to a high M/K stock (Hordyk et al. 2015).

The effective selectivity is calculated annually from the fishing mortality at age, with $v^{\text{eff}}_{y,a,s} = F_{y,a,s}/\max_a F_{y,a,s}$, and shows the relative mortality experienced by age class for all fishery removals. The age of apical effective selectivity has oscillated several times (Figure 37). Whereas the apical selectivity was initially on the oldest age classes, the age of apical selectivity shifted to younger, immature age classes when fishery removals were primarily discards—for example, in the 1970s and 2020s.

The estimate of the productivity parameter z_{frac} hit the lower bound of zero in model A1, inferring that there is no density-dependence in the population, i.e., steepness is 0.2 and there are no MSY-based reference points. The likelihood profile showed that the z_{frac} estimate was influenced by both the indices of abundance and length composition (Figure 38). In light of the low catches since the 1980s (relative to the early 20$^{\text{th}}$ century), the model estimates that the stock must be as unproductive as possible to produce the observed declines in the index. However, the fit to the indices (Figure 39) and the estimated selectivity curves (Figure 40) were only minimally affected by changes to the value of z_{frac} in the likelihood profiling. Future analyses could consider a joint profile of z_{frac} and β.

The z_{frac} profile is strongly influenced by the likelihood for the IPHC index, which has relatively small standard deviations on the order of 0.05. The profile was repeated in a model that estimated an additional standard deviation term to downweight the IPHC index (model A13). That model increased the IPHC index error to approximately 0.35 but did not substantially change the results of the profile (results not shown).

Alternative assumptions of z_{frac} affect the size of the population, with lower stock sizes implied from higher z_{frac}, although the depletion to 2023 appears relatively robust to the productivity parameter (Figure 41). When fit across the range of possible productivity parameter values in the base model, fishing mortality has exceeded F_{MSY} for much of the stock history (Figure 41).

The yield curve was calculated with the z_{frac} profile using the effective selectivity in 2023, reflecting current exploitation patterns, where the age of apical selectivity is 10 years. The shape and skew of the yield curve does not appear to vary with respect to z_{frac} (Figure 42), although the height, i.e., MSY, and the corresponding fishing mortality (F_{MSY}) increases with z_{frac} (Figure 43). The shape and skew of the yield curve also it does not appear to vary with respect to the stock-recruit parameter β (Figure 44). Lines drawn at the provisional DFO limit and upper stock reference points of $0.4S/S_{\text{MSY}}$ and $0.8S/S_{\text{MSY}}$ (DFO 2009) align approximately with 0.2 and 0.4 S/S_0 across the profiled values of z_{frac} and β (Figures 42, 44).

The unfished replacement line, i.e., pup survival, is $1/\phi_0 = 0.30$ and the maximum steepness is 0.66. In comparison, the survival implied from the adult natural mortality rate is $\exp(-M) = 0.94$.

4.2. SENSITIVITY MODELS

4.2.1. Sensitivity to growth, maturity, and discard mortality assumptions

The first set of sensitivity analyses explored alternative growth parameters, maturity parameters, and discard mortality rates in the fishery. Estimates of spawning output and biomass were slightly higher with either the US growth curve (compared to the BC growth curve) or the higher discard mortality rate assumption (Figure 19–21). With the later maturity ogive, the spawning output is lower but the biomass is higher than with the base maturity at age. Estimates of depletion in 2023 do not significantly differ among these models (Figure 20). No significant change in the fit to the indices were observed (Figure 28).

There were erratic selectivity estimates for longline landings when the US growth curve was used (A2 and A4), where the fleet selected for small fish despite the presence of only larger fish in the length composition (Figure 25). This behaviour could not be sufficiently addressed at the time of writing. The fit to the survey indices and length composition improved in model A2 with the US growth curve compared to model A0 with the BC growth curve at the cost of the fit to the longline length composition data, based on a comparison of likelihood values (values not shown). Attempts to increase the likelihood weighting component of the longline length composition improved the fit and the selectivity estimate, but the estimate of the unfished recruitment hit the upper bound. As a result, the $S/S0$ ratio was effectively one for all years, implying a large, unfished population. We deemed this implausible. We exclude these models when calculating reference points in Section 5.

4.2.2. Sensitivity to indexes of abundance included

The second set of sensitivity analyses explored alternative hypotheses on recent stock trends by index. The base model fit to the IPHC and fishery CPUE the best, as there was little to no difference in the index fit and spawning estimates between models (A0) and (A6) (Figures 48, 49). The model still could not fit the Synoptic survey index even when it was the sole index in the model (A6) (Figure 48). This behaviour indicated that the model structure could not explain the trend in this index.

4.2.3. Sensitivity to assumptions about natural mortality

The third set of sensitivity analyses explored alternative assumptions on natural mortality. Compared to the base model, a lower or high, constant natural mortality of 0.05 or 0.074 did not significantly change either the fit to the index or the historical stock trajectory (Figures 51 and 52).

Models with a change in natural mortality estimated an increase to 0.13–0.16 by 2023 (Figure 50). For example, model B2 estimated an increase in natural mortality from 0.065 to 0.14. Models with a change in M had a much better fit to the Synoptic index compared to the base model, along with reasonably good fits to the Bottom Trawl CPUE, IPHC index, and HS MSA index (Figure 51). A notable bend in the predicted index occurred in the year of the M change. No model could suitably fit the HBLL Outside index (Figure 51).

A lower constant M had little effect on stock depletion (Figure 52). Large impacts on the stock depletion were observed depending on the timing of the M change. With M increases in 2010 (B2 and B5), the stock followed a similar trajectory as the base model, but was less depleted for much of the 20th century, i.e., higher S/S_0, until 2010 when a sizable decrease occurred.

Models with earlier increases in M around 1990, i.e., in models B1 and B4, did not produce plausible stock trends, even though this was when pinniped populations started increasing (Figure 52). Similar behaviour was seen in model B3 with the M increase in 2005 (Figure 52). In these models, the stock was estimated to be lightly fished through most of the 20th century and the only stock decline occurred as a result of the M increase. This trend is not corroborated by historical observations of declining Dogfish abundance following periods of high catches. Thus, these models were not considered credible.

4.2.4. Sensitivity to assumptions about the stock-recruit relationship

The last set of sensitivity analyses explored alternative assumptions about productivity in the stock-recruit relationship. The alternative assumptions of a less- or more-productive stock adjust the stock-recruit curve shape but mostly at the higher end of the curve where data were only available early in the time series and when no indexes of abundance were available (Figure 53). The alternative models had little impact on fitting to the indexes of abundance

(Figure 54) and resulted in similar levels of spawning depletion by the end of the time series (Figure 55).

4.3. RETROSPECTIVE PATTERNS

No substantial retrospective patterns were observed in spawning output from the base model when removing up to 7 years of data (Figure 45). There was a slight retrospective pattern at the end of the time series where estimates of spawning output would get shifted down as each new year's data was added—this is likely due to the steeply declining survey trends. Time-varying natural mortality models were able to eliminate the upward curved retrospective patterns (e.g., Figure 47). This is likely because they were better able to capture declines in the indexes of abundance over the last two decades. However, this time-varying M example exhibits a slight retrospective bias in the opposite direction to model A0 where the last decade of spawning output declines slightly less steeply with each additional year of data (Figure 47).

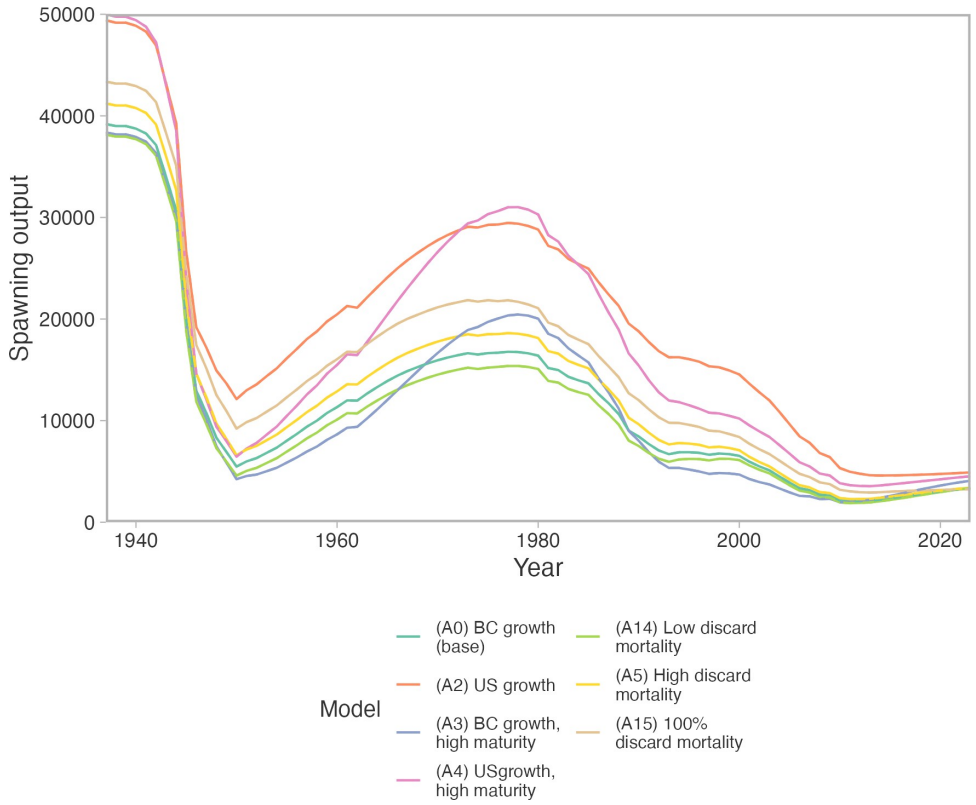

Figure 19. Estimates of spawning output (pup production) for outside Dogfish from the base model and sensitivity models exploring growth, maturity, and discard mortality.

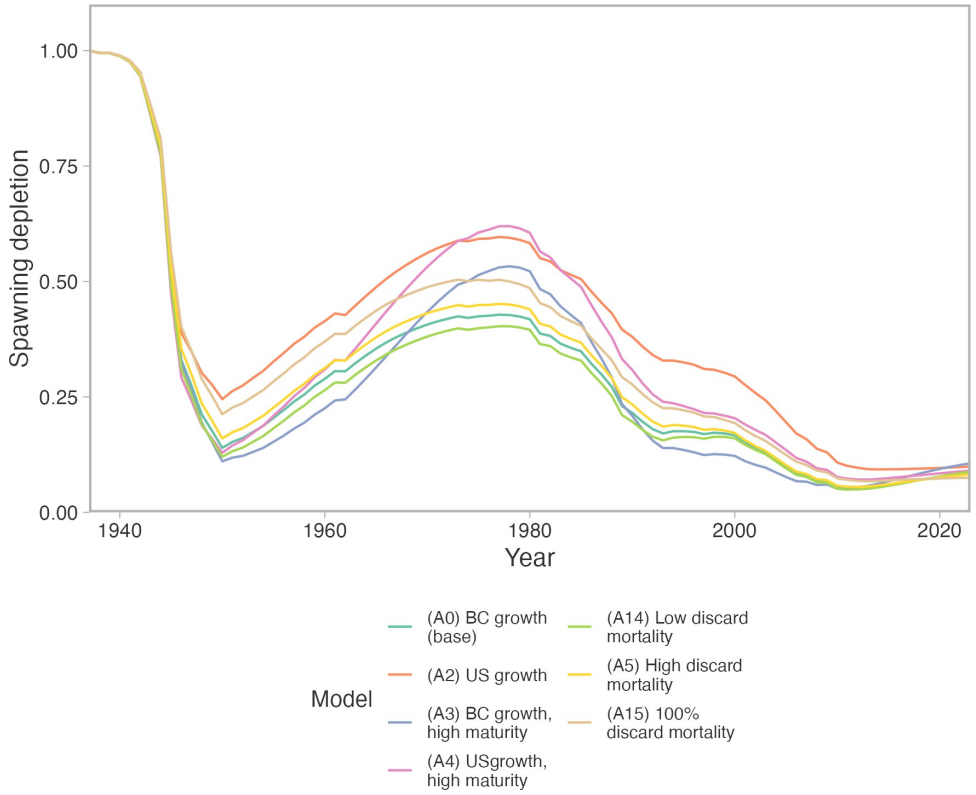

Figure 20. Estimates of the spawning depletion (S/S_0) from the base model and sensitivity models exploring growth, maturity, and discard mortality.

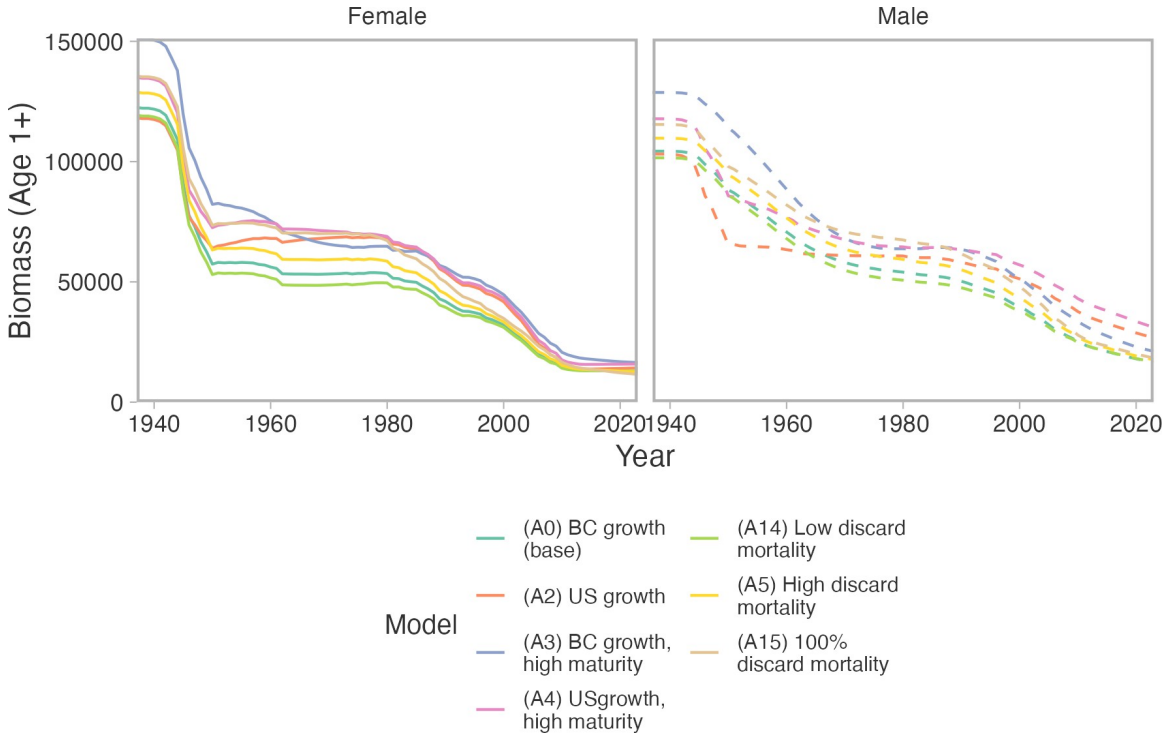

Figure 21. Estimates of stock biomass by sex from the base model and sensitivity models exploring growth, maturity, and discard mortality.

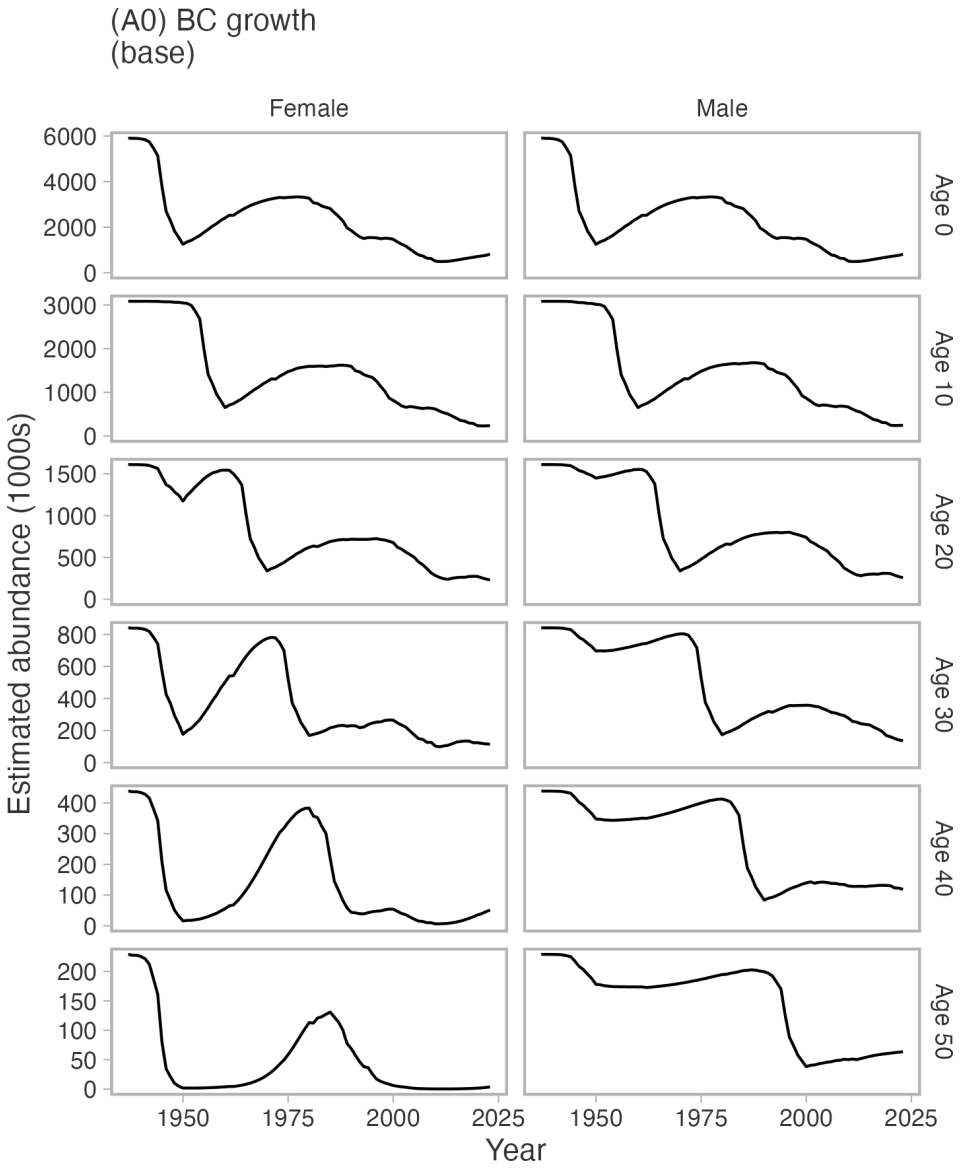

Figure 22. Estimates of abundance at age for six age classes from the base model. This figure illustrates the lagged effects of fishing on the age structure of the population.

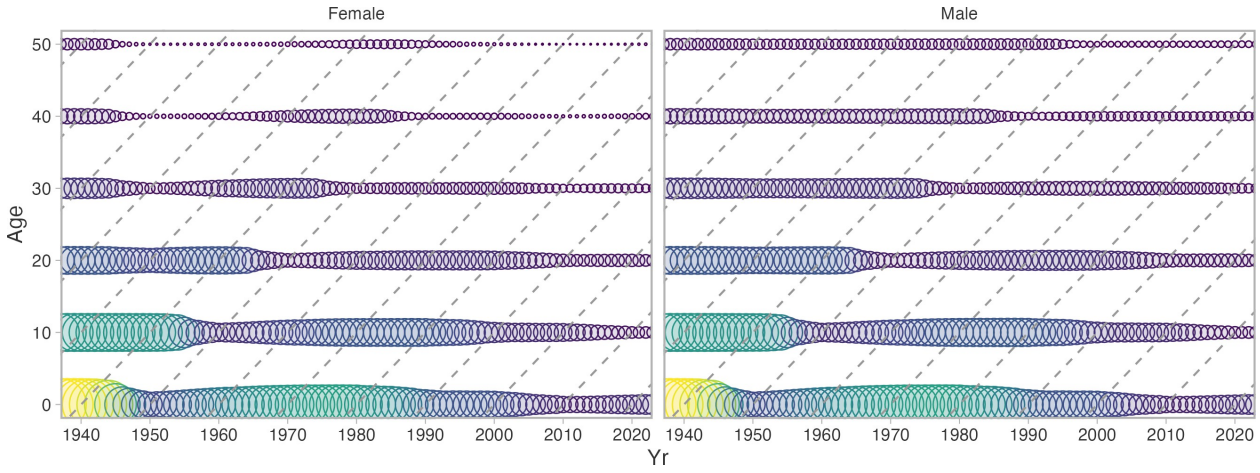

Figure 23. Estimates of abundance at age for six age classes from the base model. This figure the same data as Figure 22 but represented as a bubble plot where the area (and colour) of circles reflects estimated abundance of Dogfish for a given age and year.

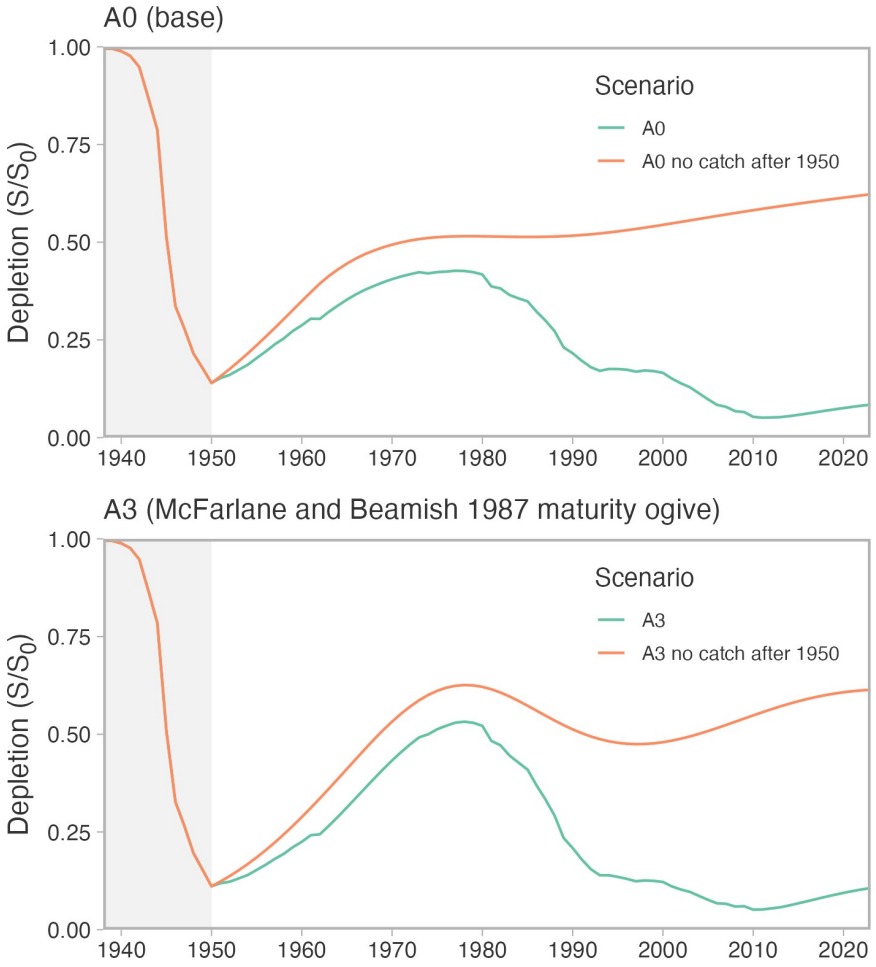

Figure 24. Visualization of spawning output depletion under the fitted models (green) and the models run forward under their population dynamics and estimated parameters with no catch removed after 1950 (orange). This "dynamic B0" (Berger 2019) approach illustrates the expected stock trajectory had fishing ceased in 1950. The lack of pups born around 1950 from heavy fishing in the 1940s results in a downward oscillation in the 1980s to 1990s. The effect is stronger in model A3 where the maturity ogive is steeper.

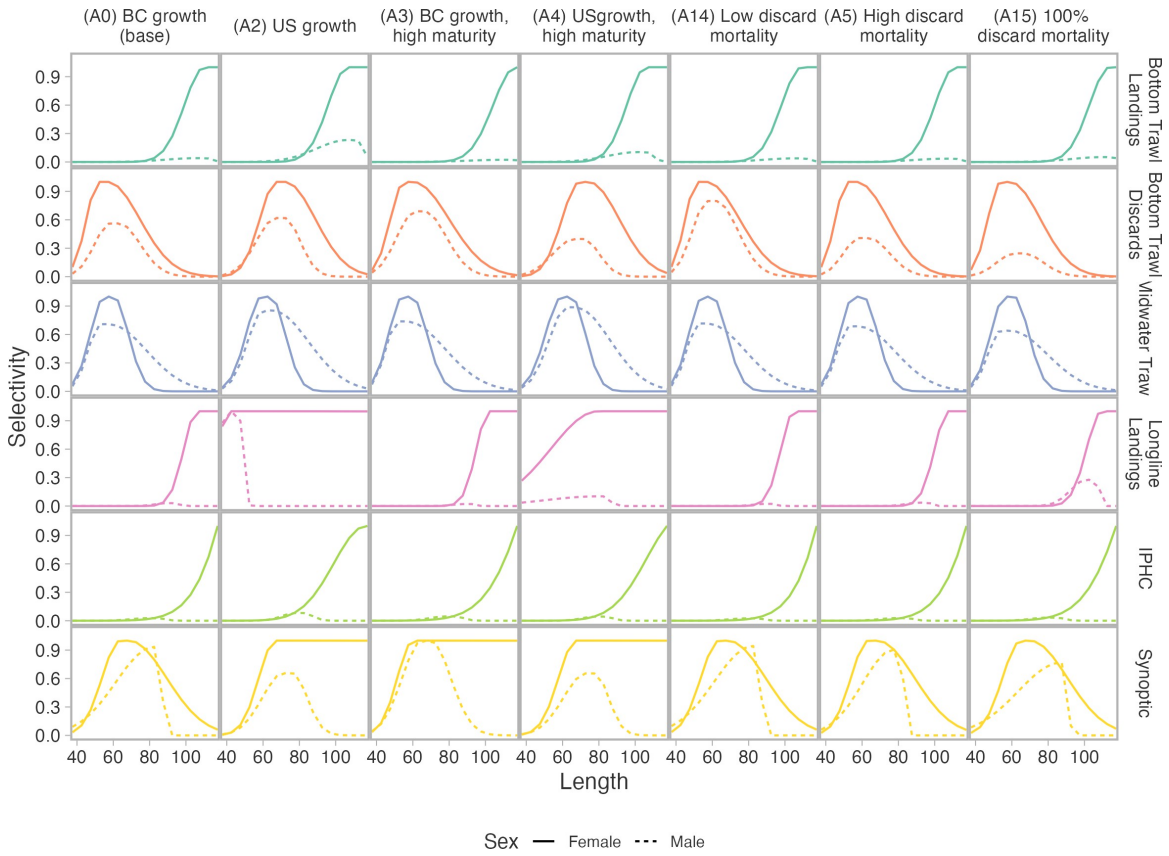

Figure 25. Estimates of selectivity at length by sex for fleets and surveys with length composition data from the base model and sensitivity models exploring growth, maturity, and discard mortality. For other fleets and surveys, the selectivity was mirrored to one of these selectivity ogives (see Modelling section 3).

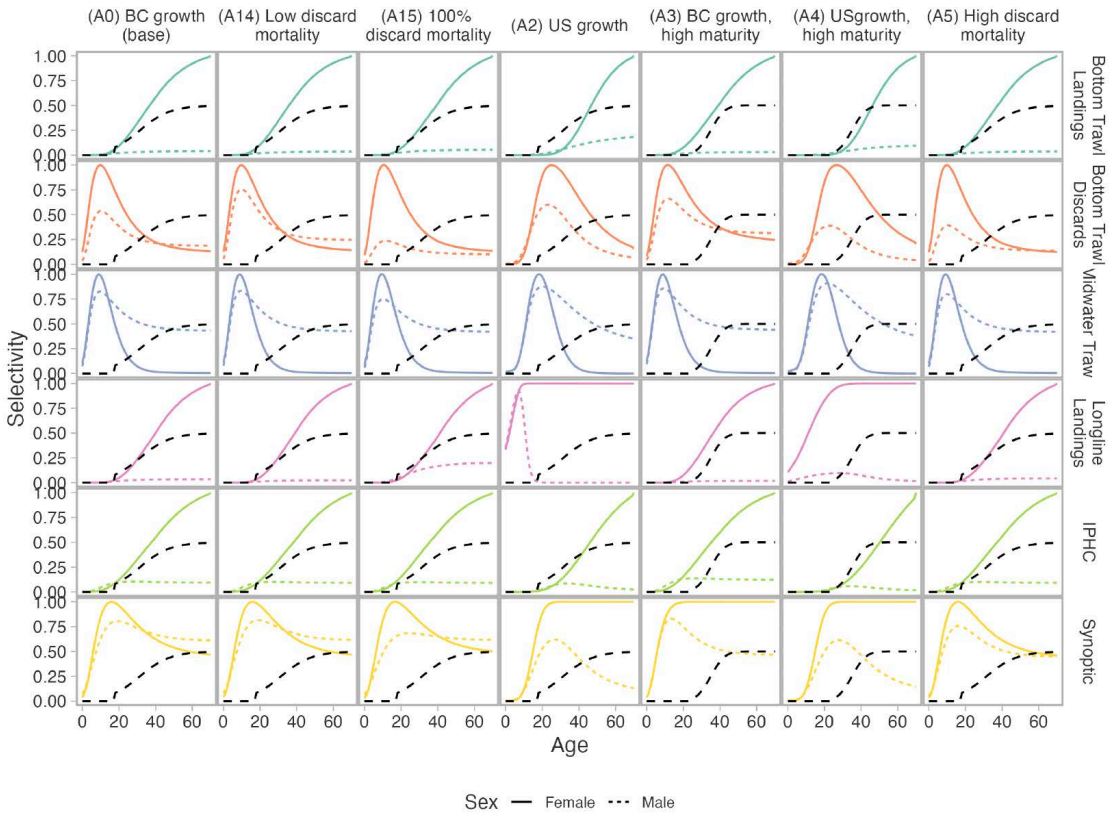

Figure 26. Estimates of selectivity at age by sex for fleets and surveys with length composition data from the base model and sensitivity models exploring growth, maturity, and discard mortality. For other fleets and surveys, the selectivity was mirrored to one of these selectivity ogives (see Modeling section 3). Selectivity at age is converted from selectivity at length (Figure 25) using the growth curve in the model. For fleets with apical value less than one, year-specific apical fishing mortality should calculated from the F-at-age vector. The black, dotted line denotes the female maturity at age ogive. The maximum proportion mature is 0.5 to account for a two year gestation period, such that half the mature population spawns annually.

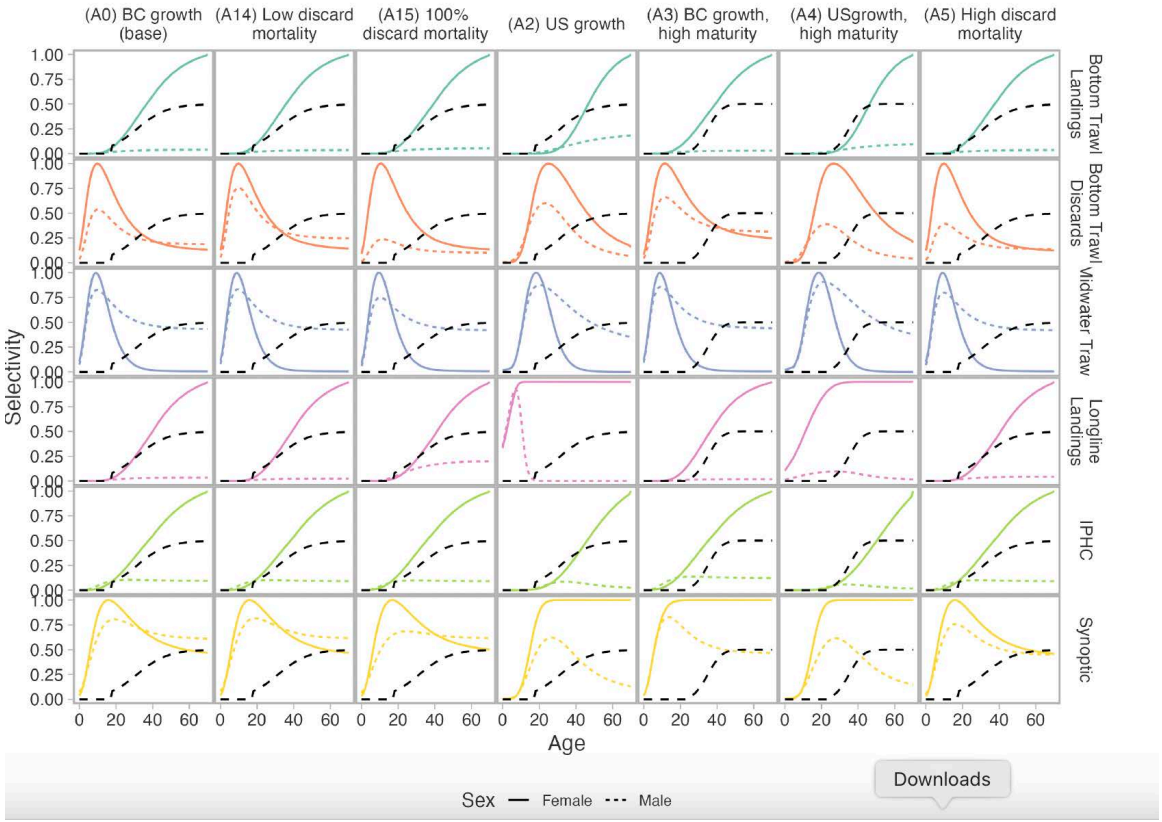

Figure 27. Estimates of selectivity at age re-scaled where the apical value for females is 1. The black, dotted line denotes the female maturity at age ogive. The maximum proportion mature is 0.5 to account for a two year gestation period, such that half the mature population spawns annually.

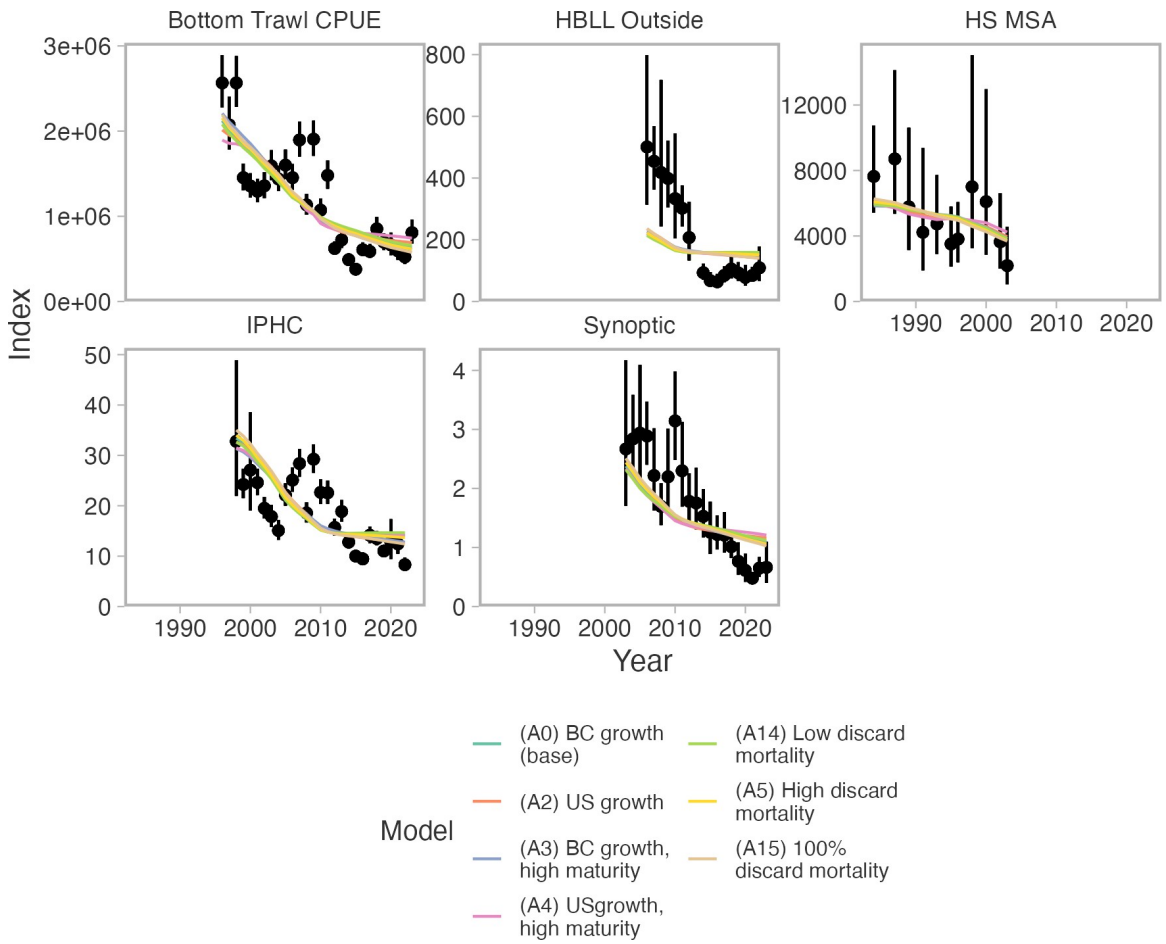

Figure 28. Observed indices of abundance (black points with 95% confidence intervals) and predicted values (coloured lines) from the base model and sensitivity models exploring growth, maturity, and discard mortality.

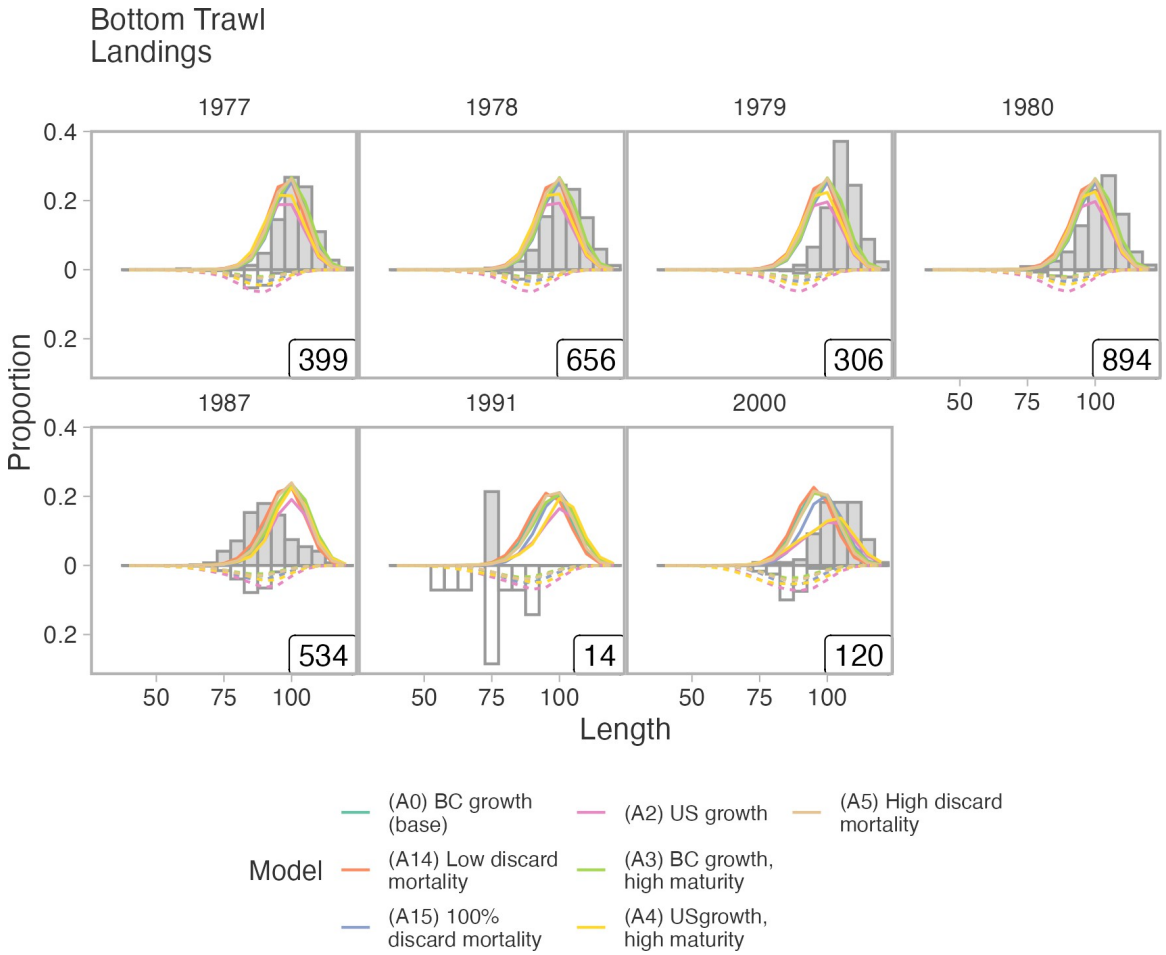

Figure 29. Observed length proportions (bars) and predicted values (coloured lines) for Bottom Trawl Landings from the base model and sensitivity models exploring growth, maturity, and discard mortality. Grey bars and solid lines correspond to females while white bars and dotted lines correspond to males. Proportions sum to one when combined across both sexes. Numbers in the lower right corners of the panels are the annual sample sizes and are downweighted in the likelihood.

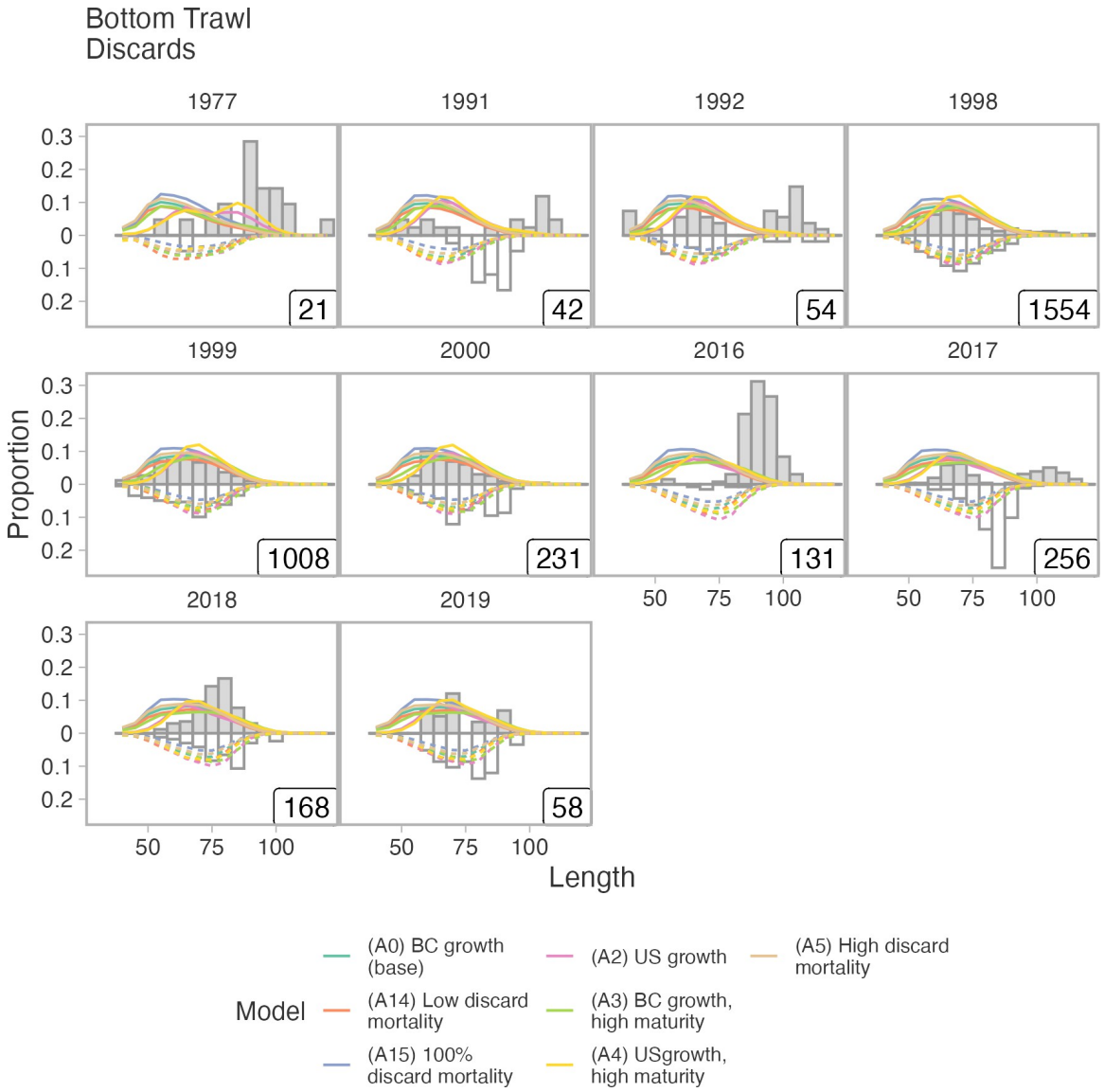

Figure 30. Observed length proportions (bars) and predicted values (coloured lines) for Bottom Trawl Discards from the base model and sensitivity models exploring growth, maturity, and discard mortality. Grey bars and solid lines correspond to females while white bars and dotted lines correspond to males. Proportions sum to one when combined across both sexes. Numbers in the lower right corners of the panels are the annual sample sizes and are downweighted in the likelihood.

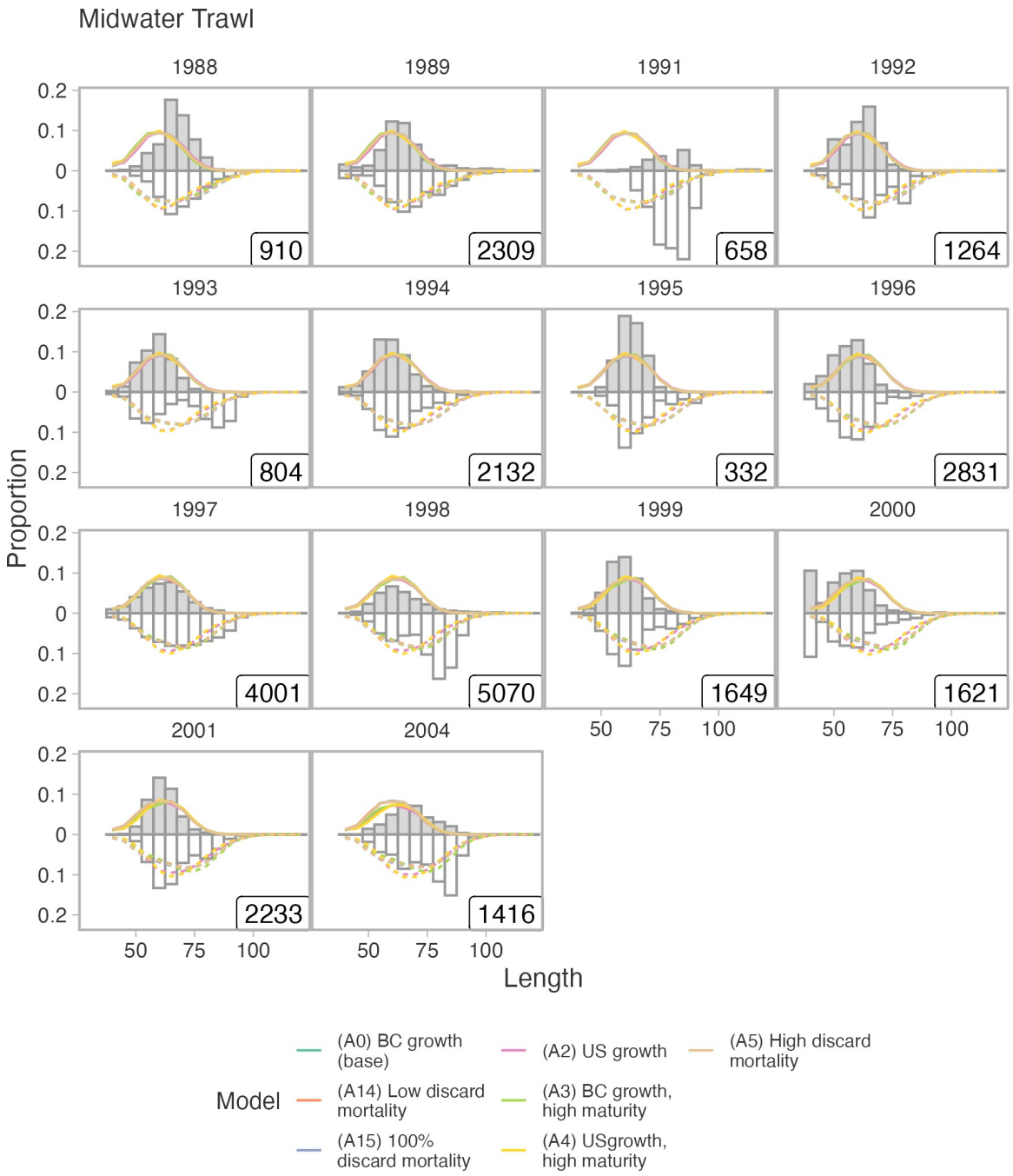

Figure 31. Observed length proportions (bars) and predicted values (coloured lines) for Midwater Trawl from the base model and sensitivity models exploring growth, maturity, and discard mortality. Grey bars and solid lines correspond to females while white bars and dotted lines correspond to males. Proportions sum to one when combined across both sexes. Numbers in the lower right corners of the panels are the annual sample sizes and are downweighted in the likelihood.

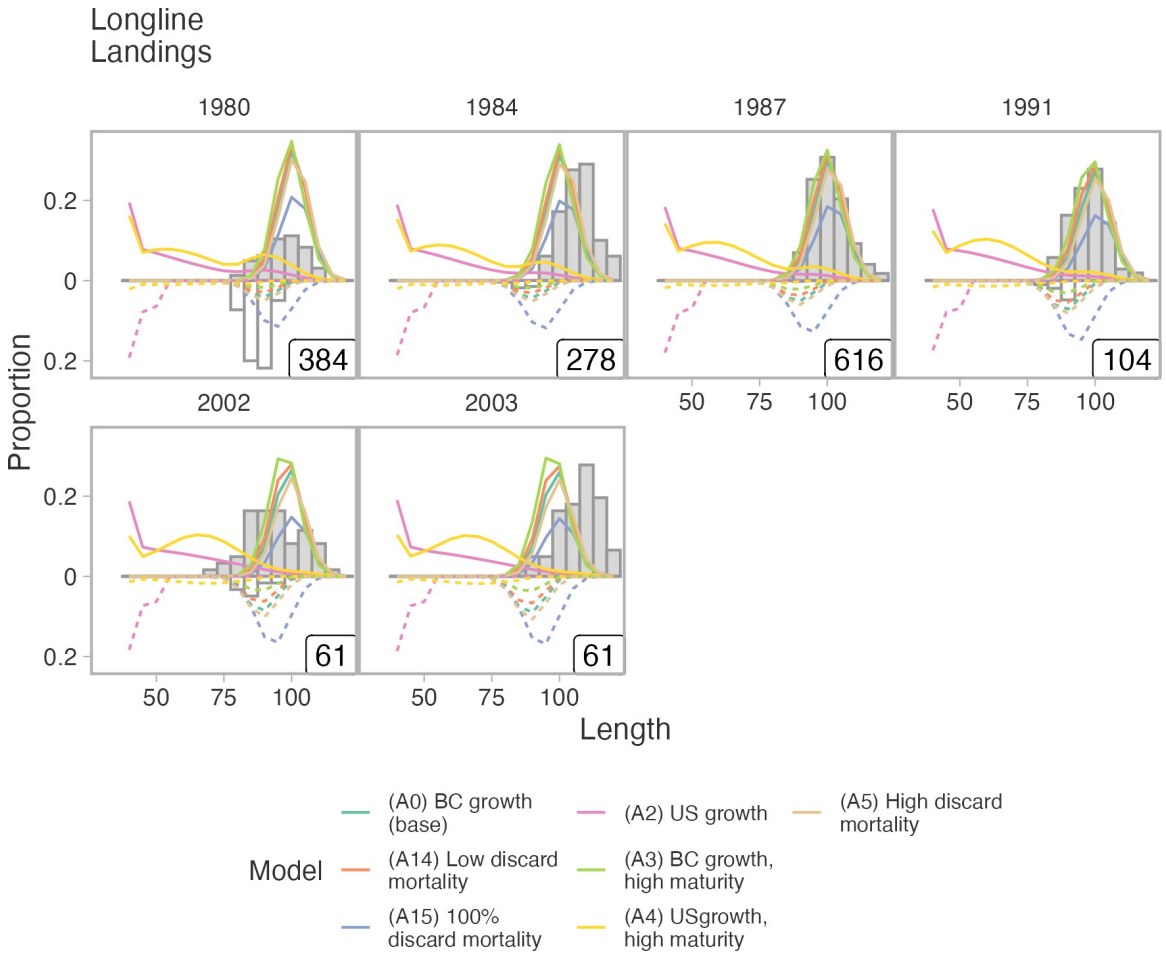

Figure 32. Observed length proportions (bars) and predicted values (coloured lines) for longline landings from the base model and sensitivity models exploring growth, maturity, and discard mortality. Grey bars and solid lines correspond to females while white bars and dotted lines correspond to males. Proportions sum to one when combined across both sexes. Numbers in the lower right corners of the panels are the annual sample sizes and are downweighted in the likelihood. Models with US growth (A2 and A4) had erratic selectivity parameter estimates for the longline landings fleet and were subsequently excluded from reference point calculations.

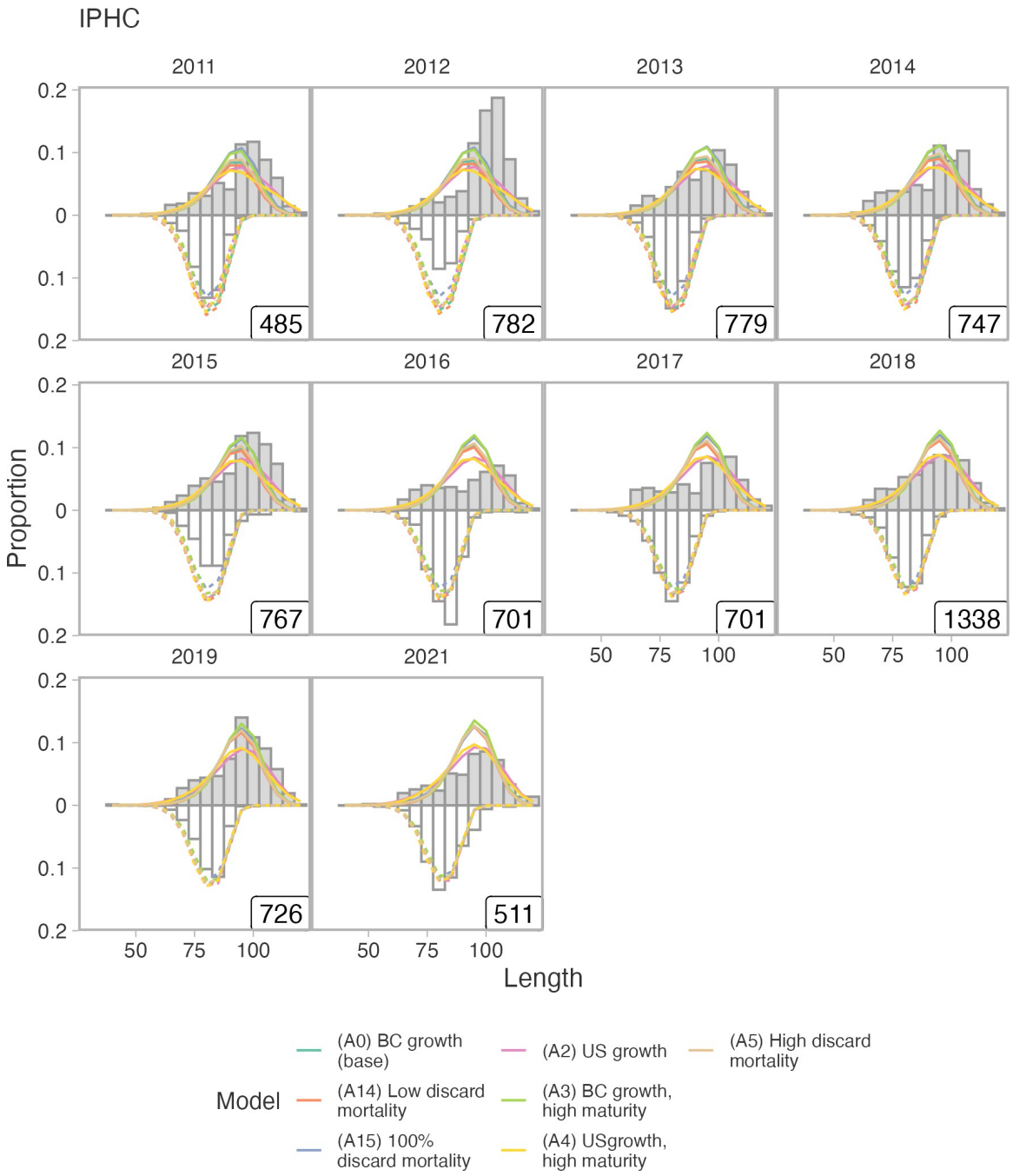

Figure 33. Observed length proportions (bars) and predicted values (coloured lines) for the IPHC survey from the base model and sensitivity models exploring growth, maturity, and discard mortality. Grey bars and solid lines correspond to females while white bars and dotted lines correspond to males. Proportions sum to one when combined across both sexes. Numbers in the lower right corners of the panels are the annual sample sizes and are downweighted in the likelihood.

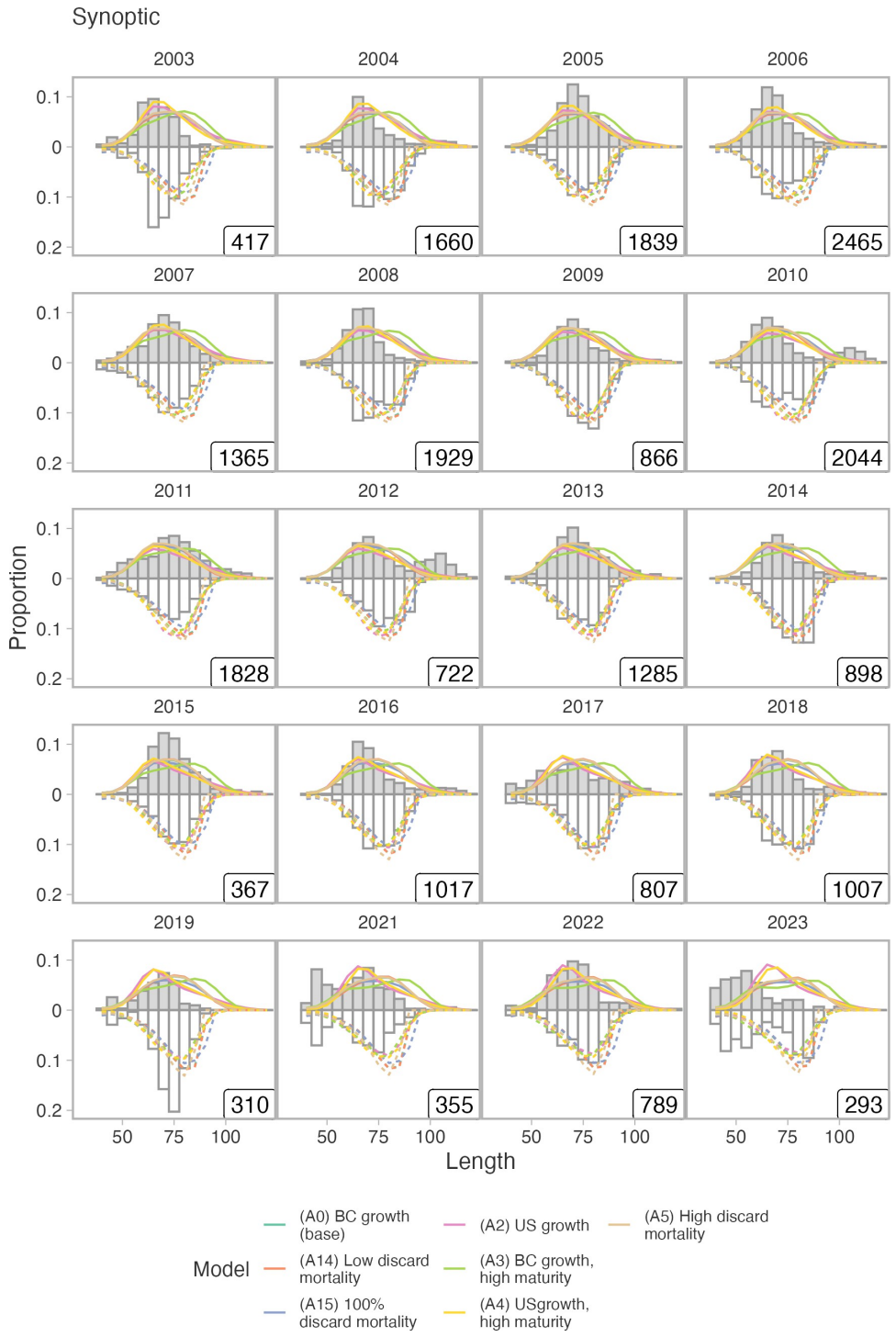

Figure 34. Observed length proportions (bars) and predicted values (coloured lines) for the Synoptic survey from the base model and sensitivity models exploring growth, maturity, and discard mortality. Grey bars and solid lines correspond to females while white bars and dotted lines correspond to males. Proportions sum to one when combined across both sexes. Numbers in the lower right corners of the panels are the annual sample sizes and are downweighted in the likelihood.

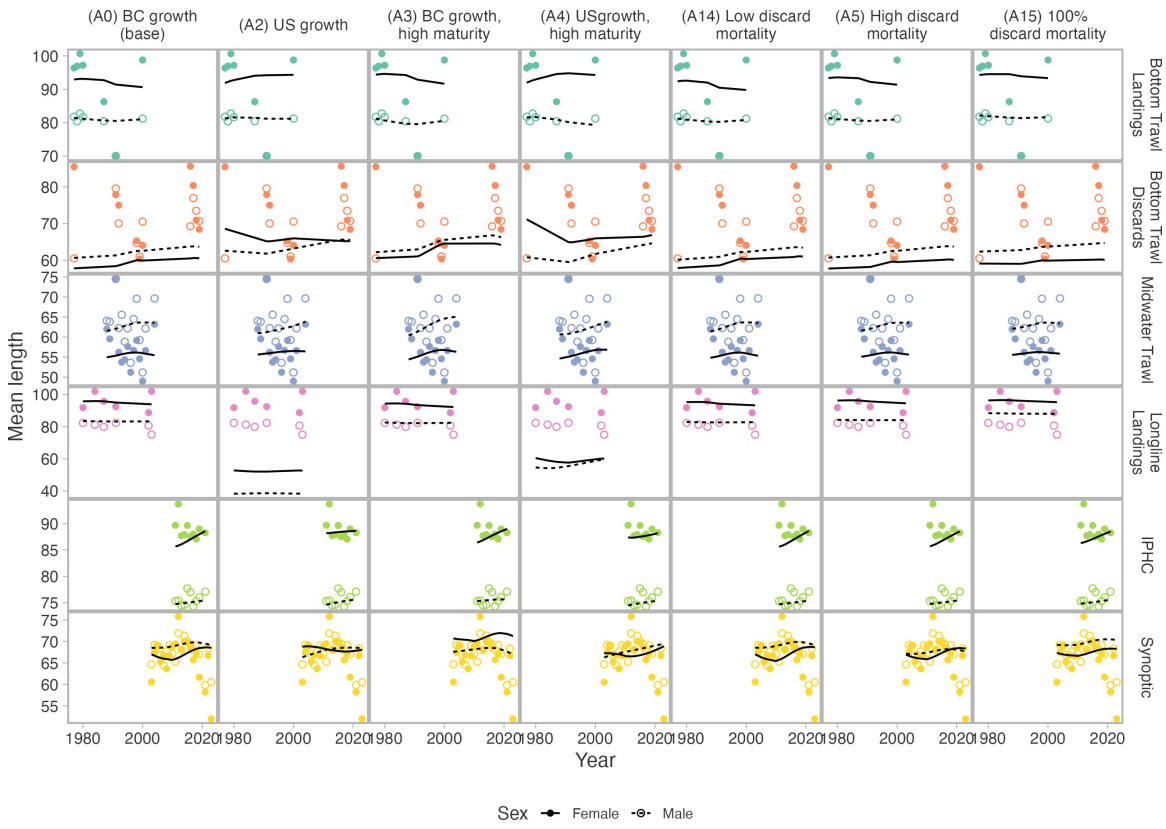

Figure 35. Observed (points) and predicted (lines) mean lengths calculated from the length composition from the base model and sensitivity models exploring growth, maturity, and discard mortality. Filled points and lines correspond to females while open points and dotted lines correspond to males. The models using US growth curves (A2 and A4) had erratic length selectivity parameter estimates that could not be resolved and were excluded from reference points calculations.

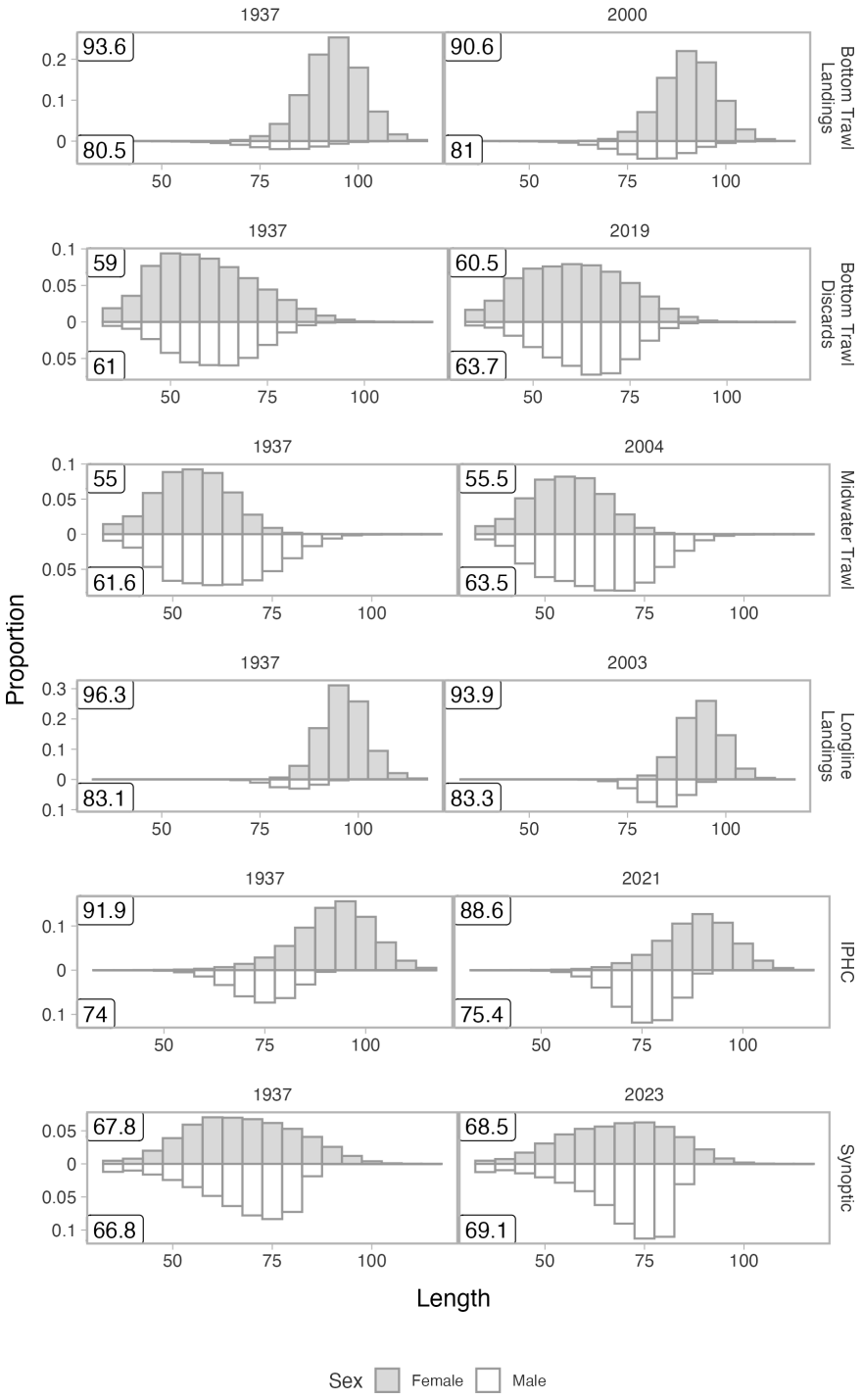

Figure 36. Comparison of the predicted length proportions in 1937 (first year of model, assumed unfished conditions) and in the 2000s, corresponding to the last year of length data for the various fleets and surveys from the base model. In each panel the upper and lower numbers report the mean length for females and males, respectively. This figure is intended to illustrate the insensitivity of the length data to changes in stock depletion across time.

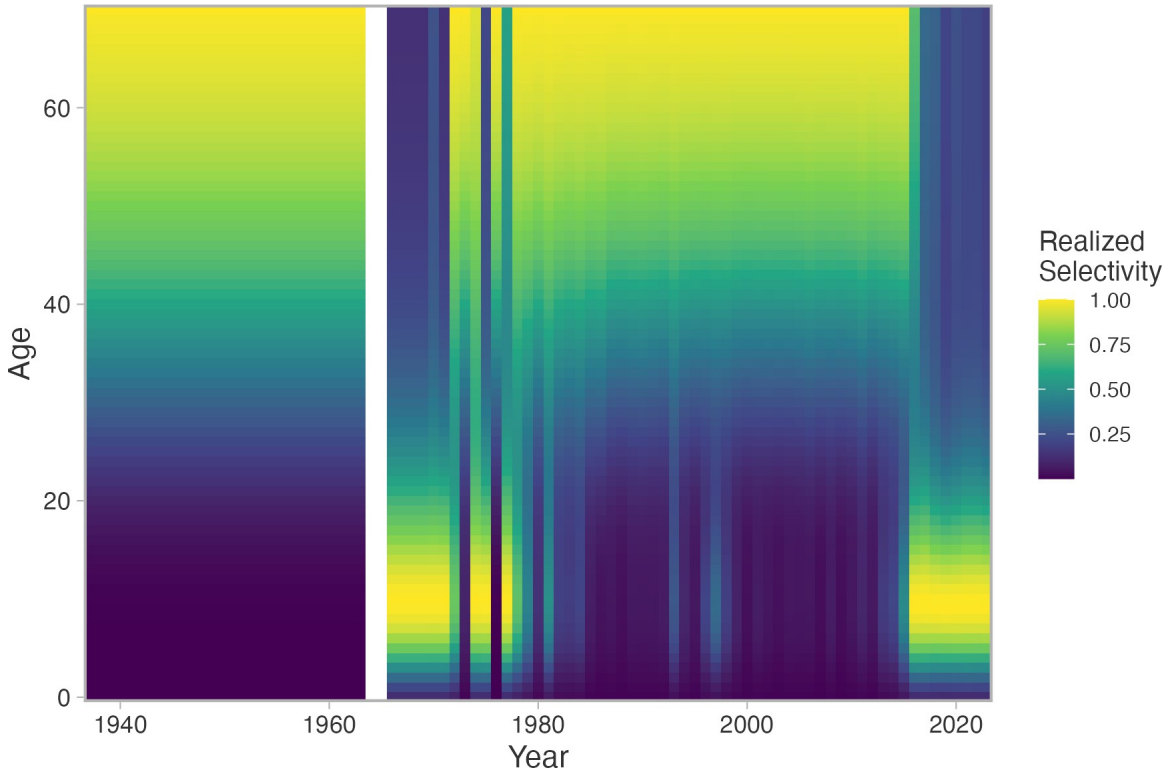

Figure 37. Annual effective selectivity for females calculated from the F-at-age vector in base model A1. The age class with a value of one experiences the highest (apical) fishing mortality but does not infer that 100% of that age class are selected.

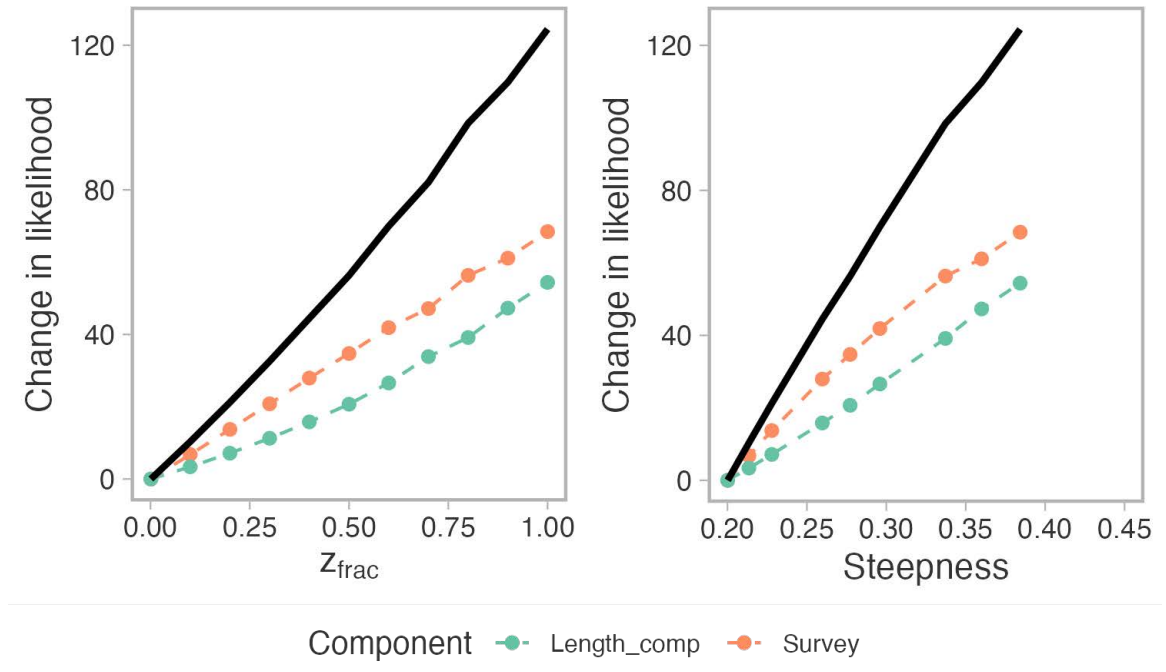

Figure 38. Left: Likelihood profile of z_{frac} in the base model (A0). The solid black line is the total negative log-likelihood and the coloured lines correspond to individual data components. Right: Likelihood profile where values of z_{frac} is converted to the steepness.

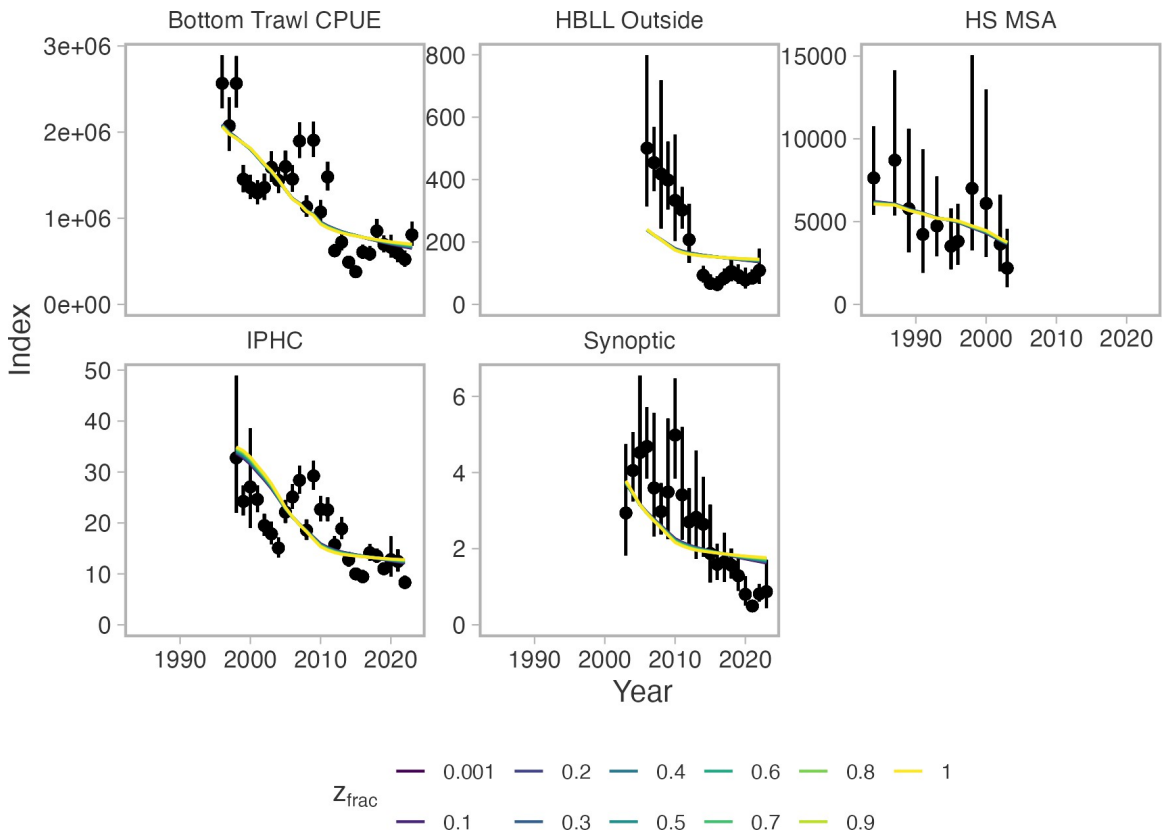

Figure 39. Fits to the indices of abundance in the likelihood profile of z_{frac} in the base model (A0).

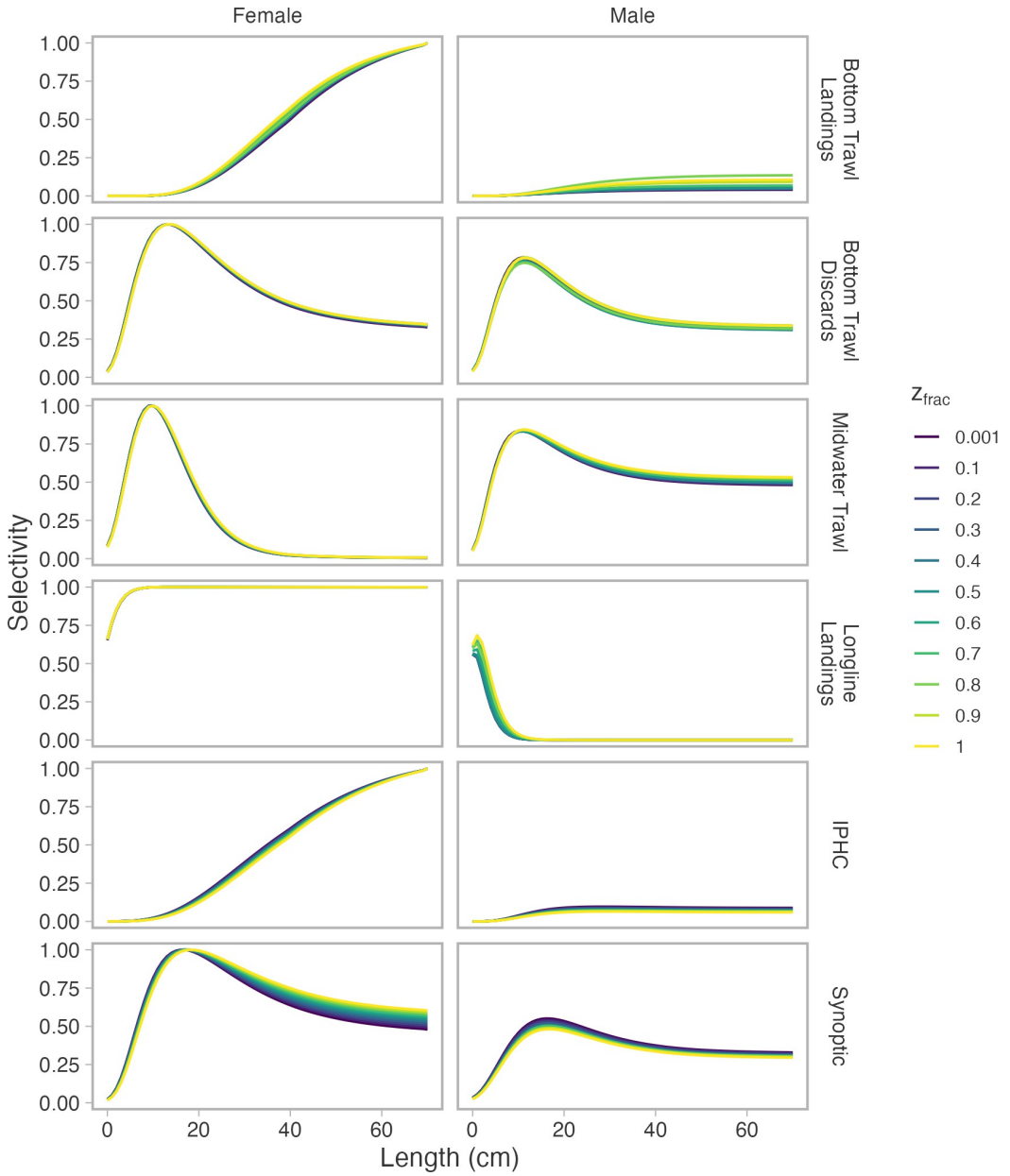

Figure 40. Selectivity curves in the likelihood profile of z_{frac} in the base model (A0). Curves are scaled such that apical selectivity is 1 for females for all fleets.

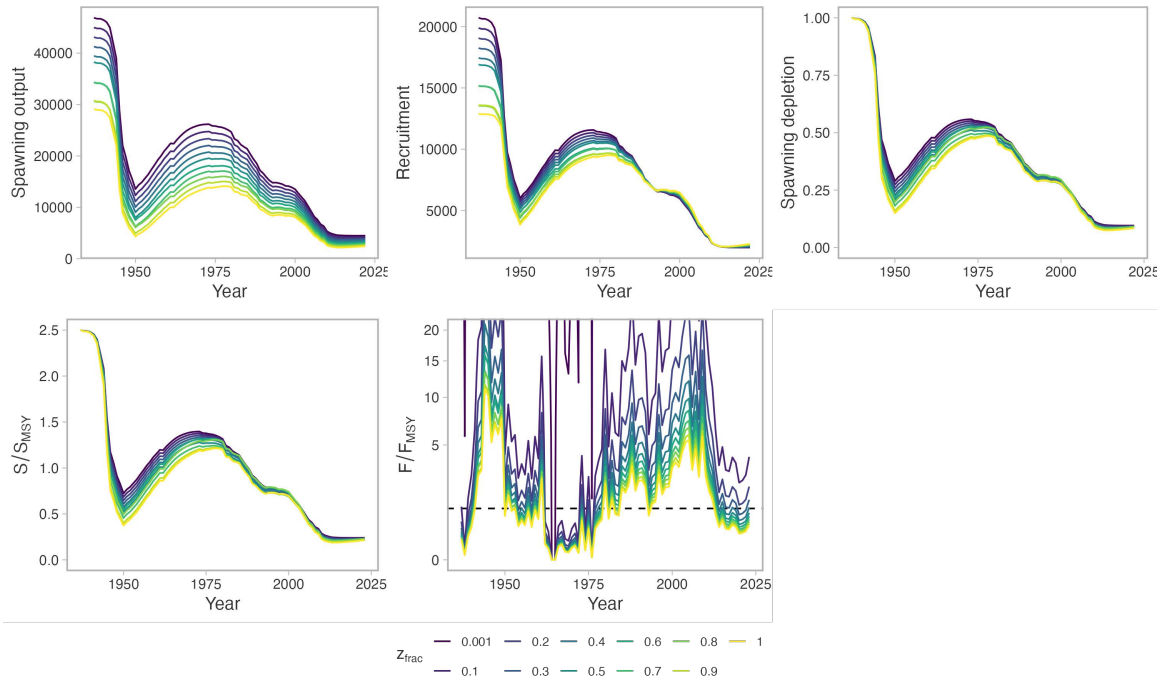

Figure 41. Time series of state variables in base model (A0) to the range of values of z_{frac} evaluated in the likelihood profile. Symbol S/S_{MSY} and F/F_{MSY} is the spawning output and fishing mortality, respectively, relative to values at maximum sustainable yield. Note that z_{frac} could not be estimated off the lower bound of 0 in this base model. This figure is included to illustrate the issues with MSY given an inestimable z_{frac}.

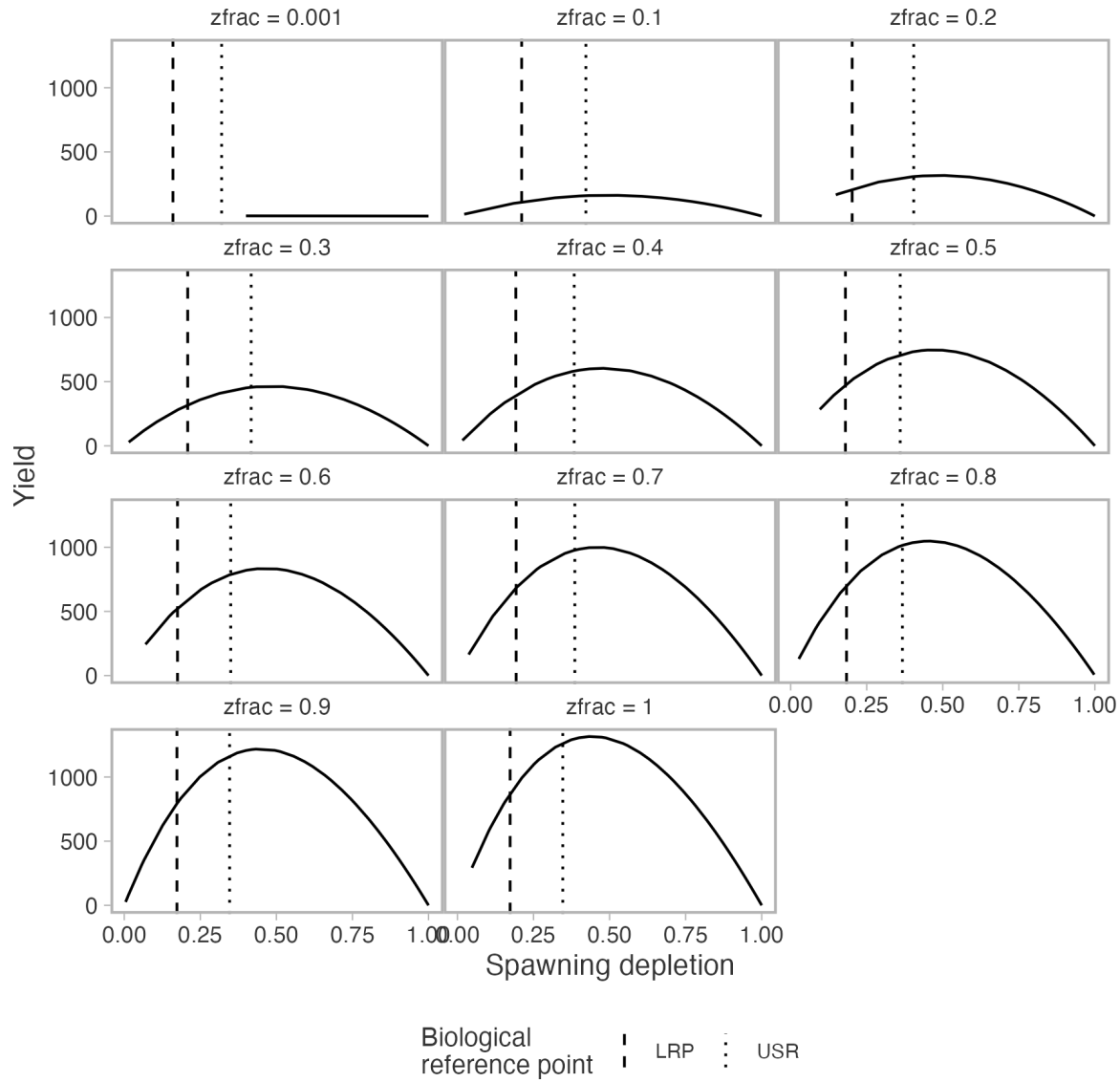

Figure 42. Yield curves calculated for the range of values of z_{frac} evaluated in the likelihood profile. The effective selectivity in 2023 was used to calculate the total yield. The vertical dashed and dotted lines correspond to 40% and 80% S_{MSY}, values of the provisional limit reference point (LRP) and upper stock reference (USR), respectively, identified in DFO's Precautionary Approach (PA) policy (DFO 2009).

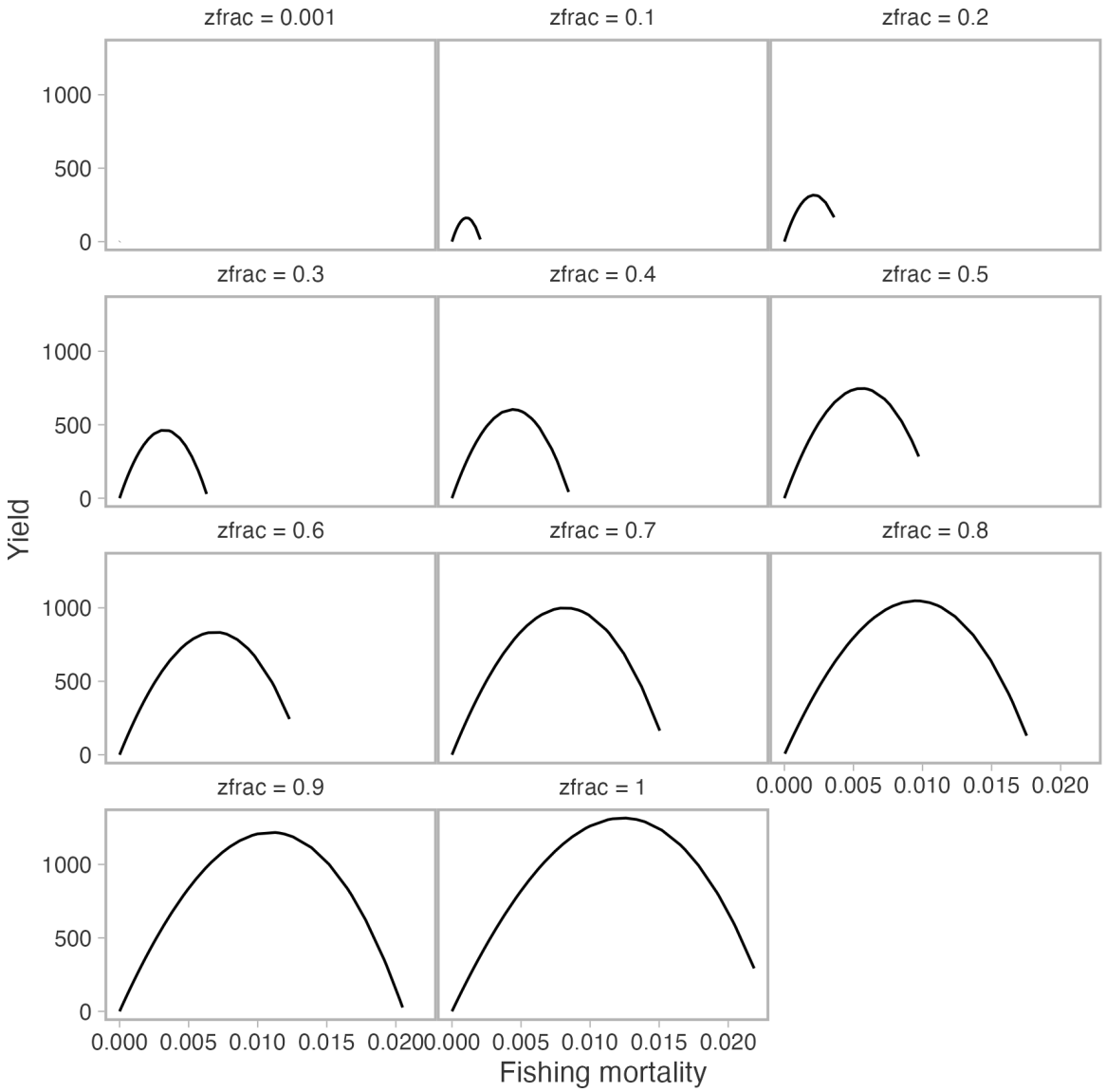

Figure 43. Yield curves as a function of fishing mortality calculated for the range of values of z_{frac} evaluated in the likelihood profile. The effective selectivity in 2023 was used to calculate the total yield.

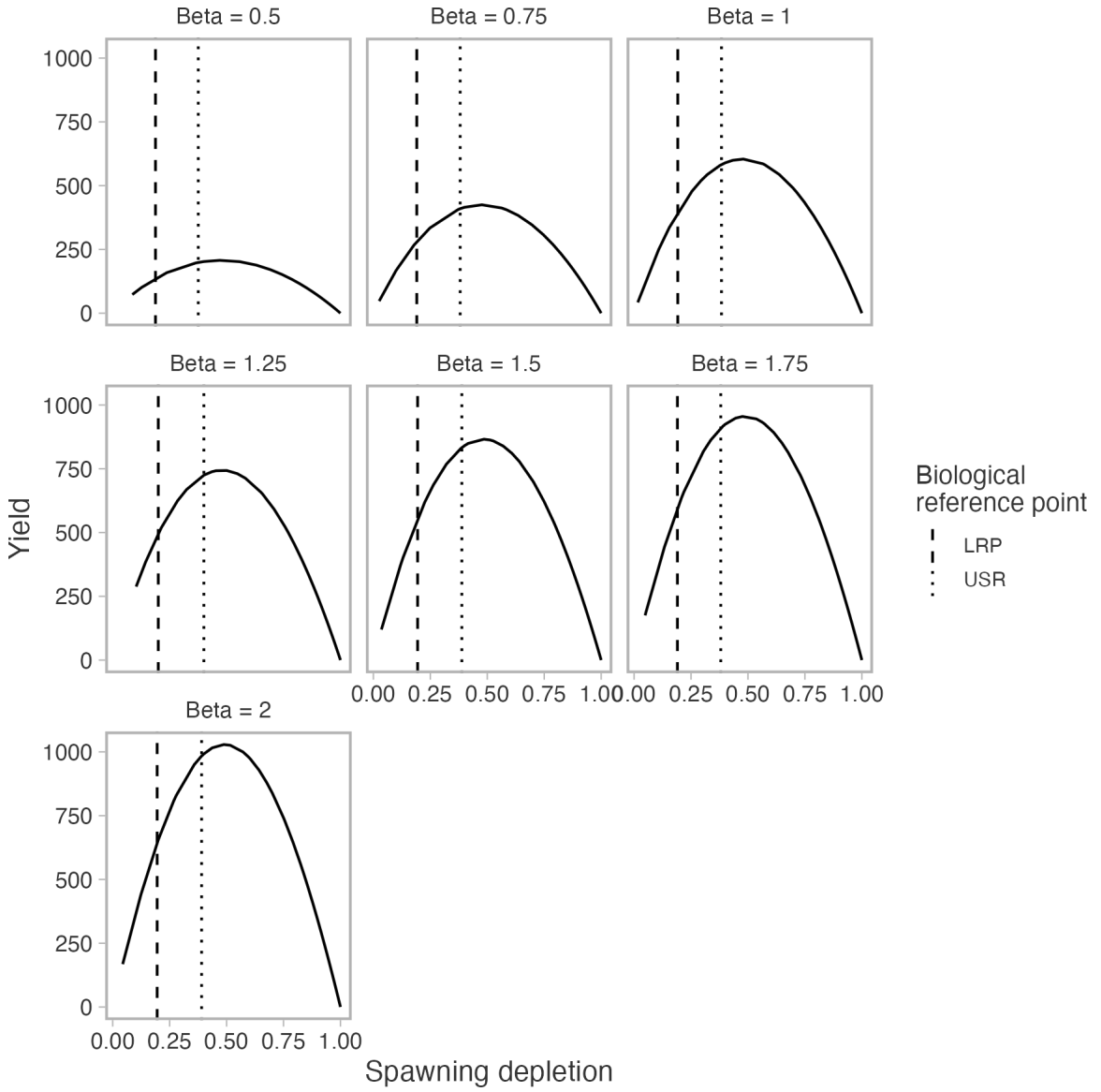

Figure 44. Yield curves calculated for the range of values of β values (a parameter in the stock-recruit curve) evaluated in the likelihood profile. The effective selectivity in 2023 was used to calculate the total yield. The vertical dashed and dotted lines correspond to 40% and 80% S_{MSY}, values of the provisional limit reference point (LRP) and upper stock reference (USR), respectively, identified in DFO's Precautionary Approach (PA) policy (DFO 2009).

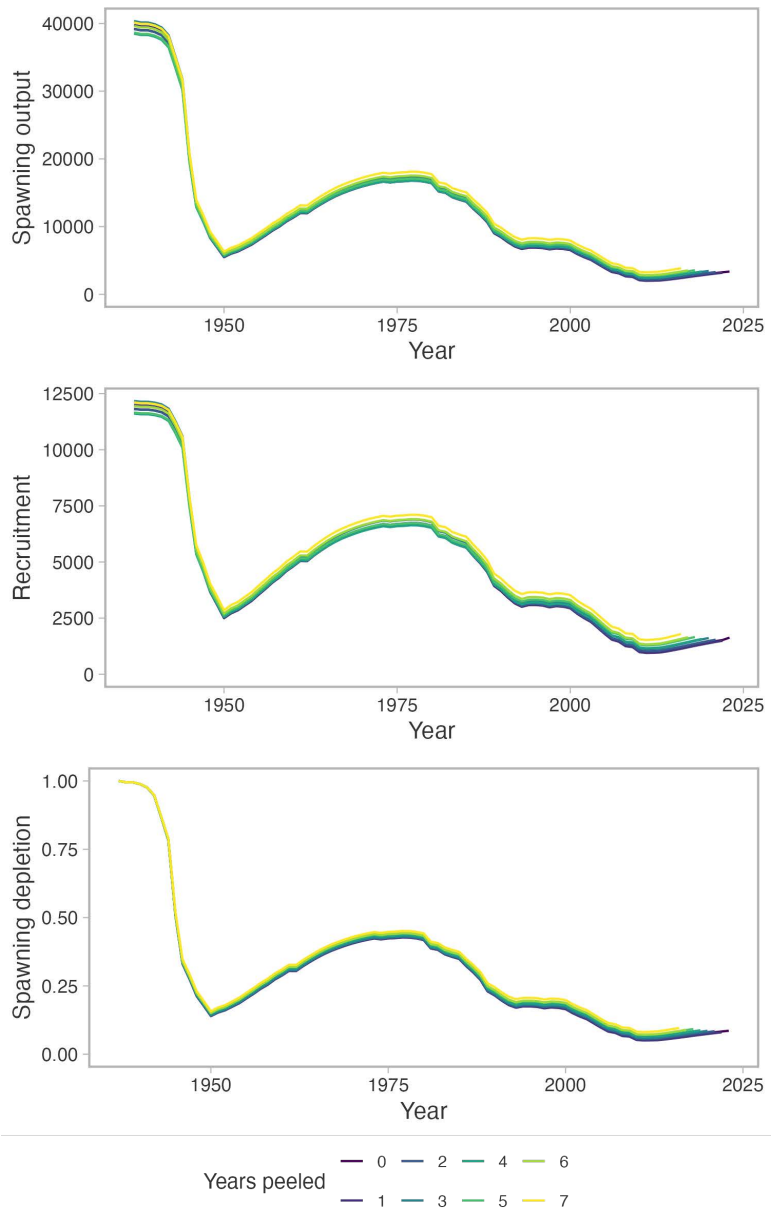

Figure 45. Spawning output, recruitment, and depletion time series in a retrospective analysis of the base model (A0). Colours indicate the number of recent years for which data are removed from the model. A value of zero corresponds to the original model fitted to all years of data.

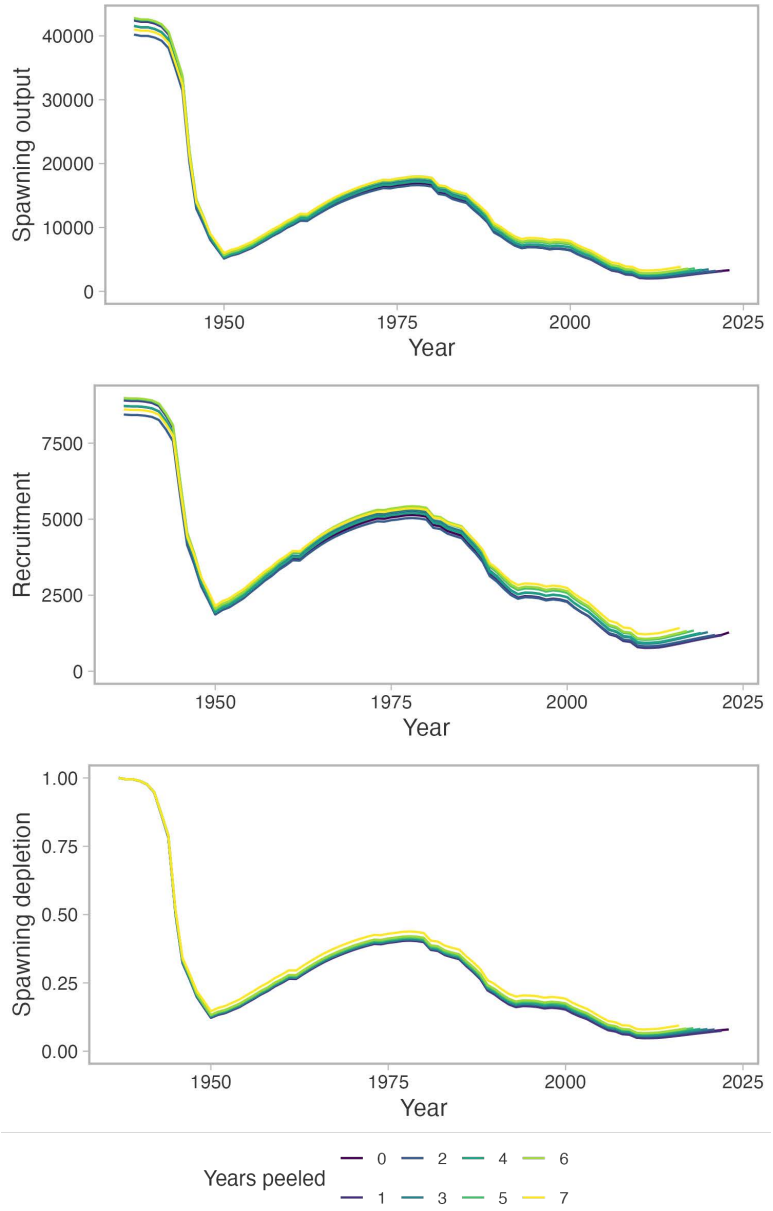

Figure 46. Spawning output, recruitment, and depletion time series in a retrospective analysis of the model with low M (A9). Colours indicate the number of recent years for which data are removed from the model. A value of zero corresponds to the original model fitted to all years of data.

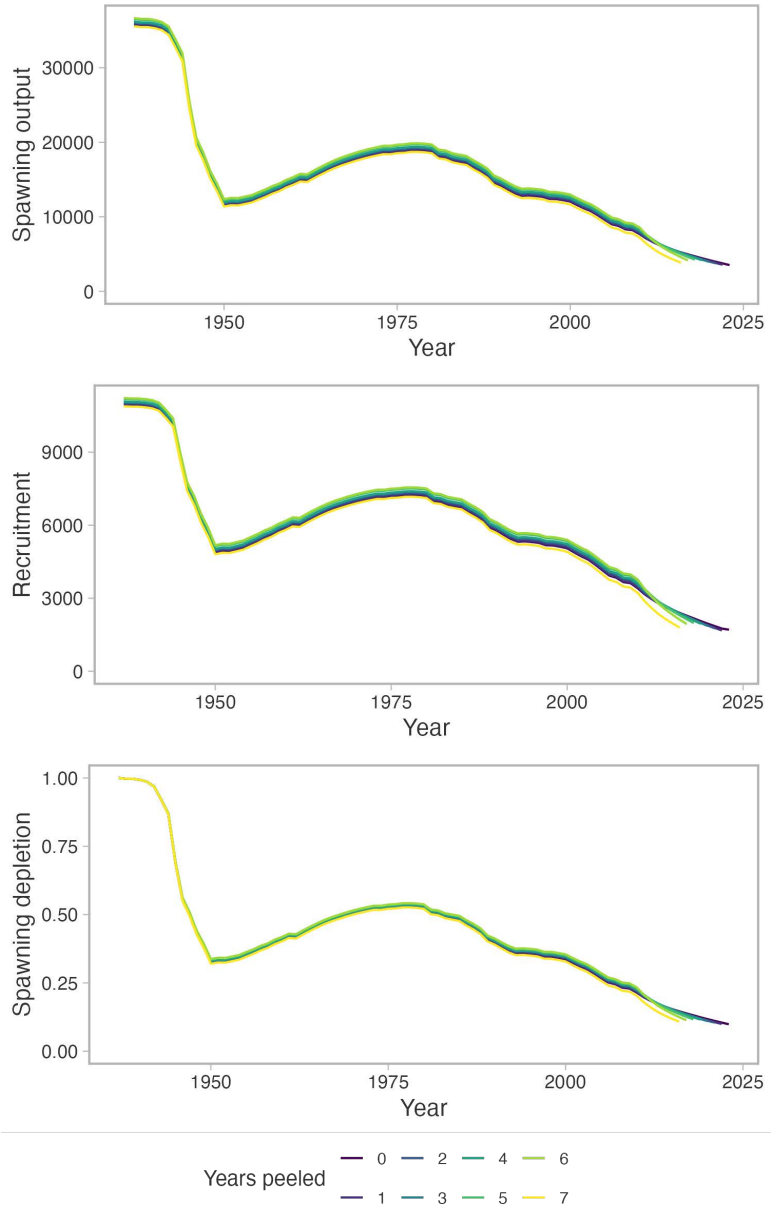

Figure 47. Spawning output, recruitment, and depletion time series in a retrospective analysis of a model with time-varying M (B2). Colours indicate the number of recent years for which data are removed from the model. A value of zero corresponds to the original model fitted to all years of data.

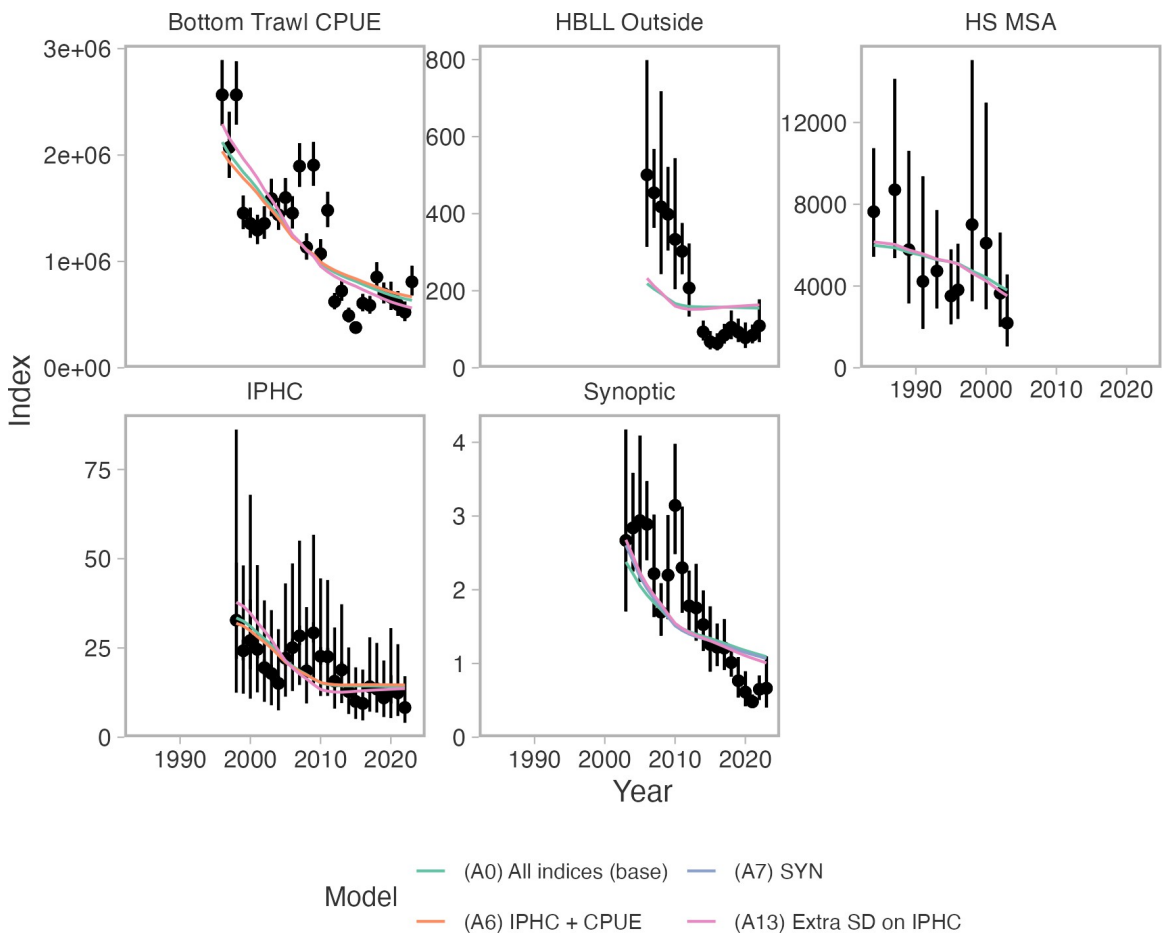

Figure 48. Fits to the indices of abundance in the sensitivity analyses to which indices of abundance were in the model or extra variance estimated on the IPHC survey. The IPHC panel illustrates the additional estimated variance.

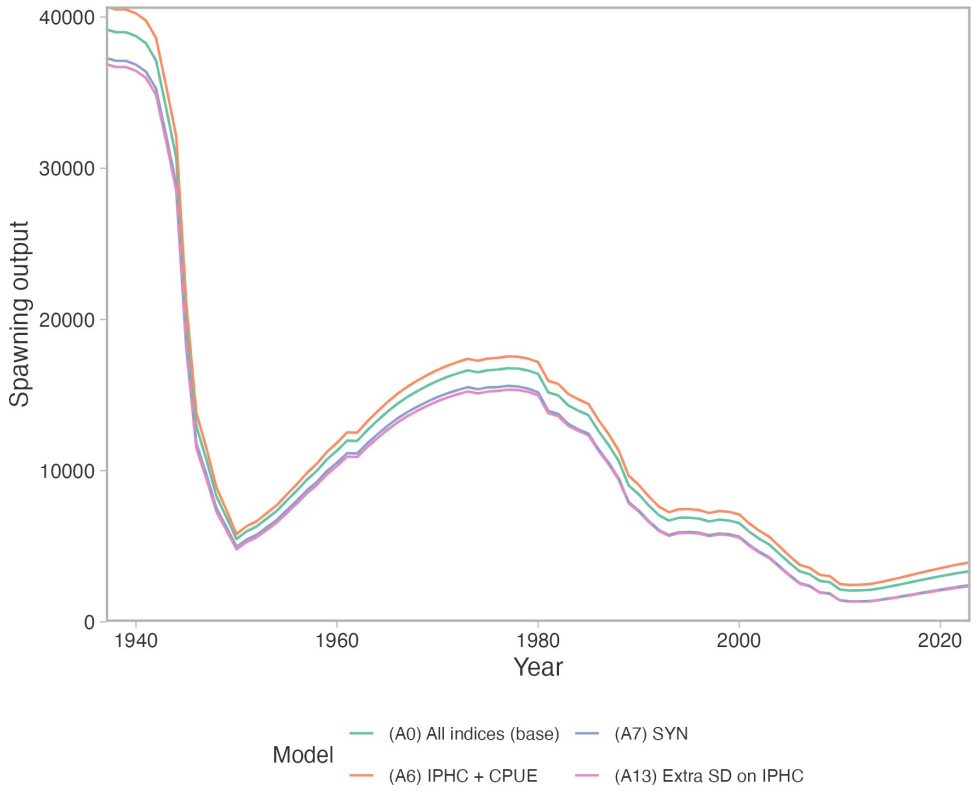

Figure 49. Comparison of historical estimates of spawning output in the sensitivity analyses from jackknifing survey series.

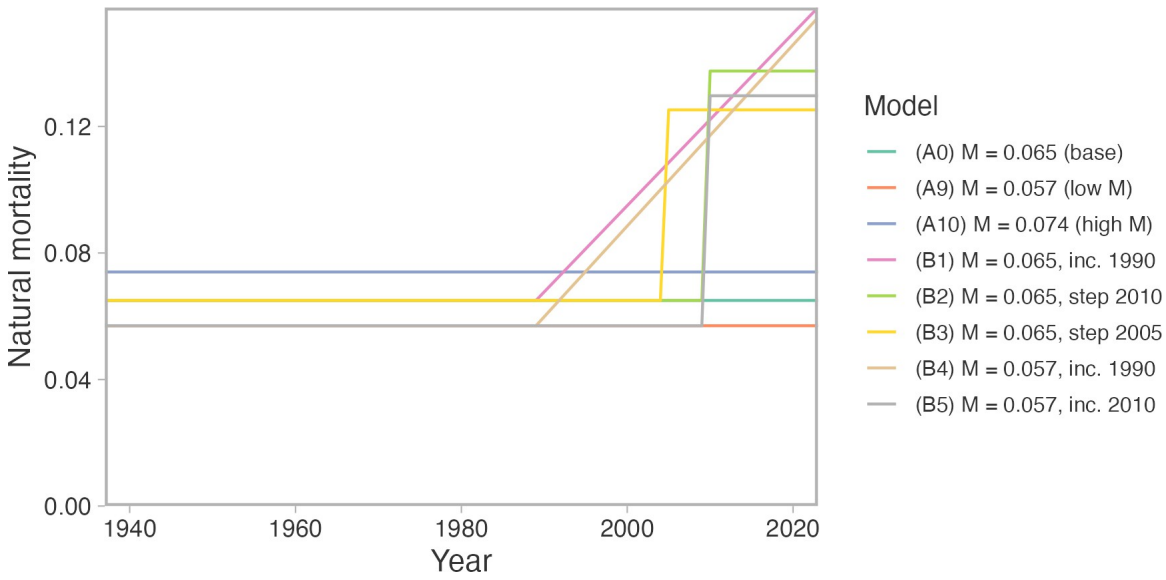

Figure 50. Time series of natural mortality among the sensitivity models.

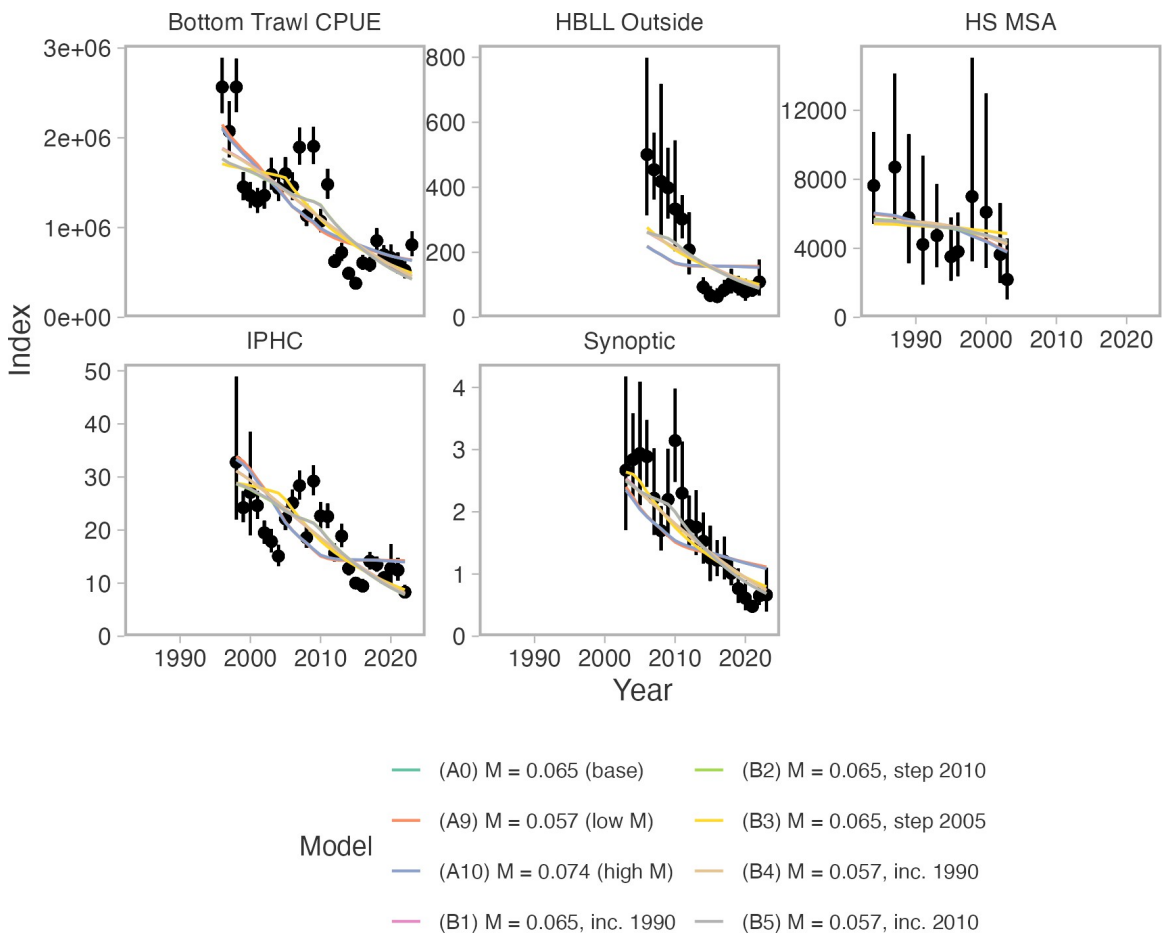

Figure 51. Fits to the indices of abundance in the sensitivity analyses of alternative natural mortality assumptions.

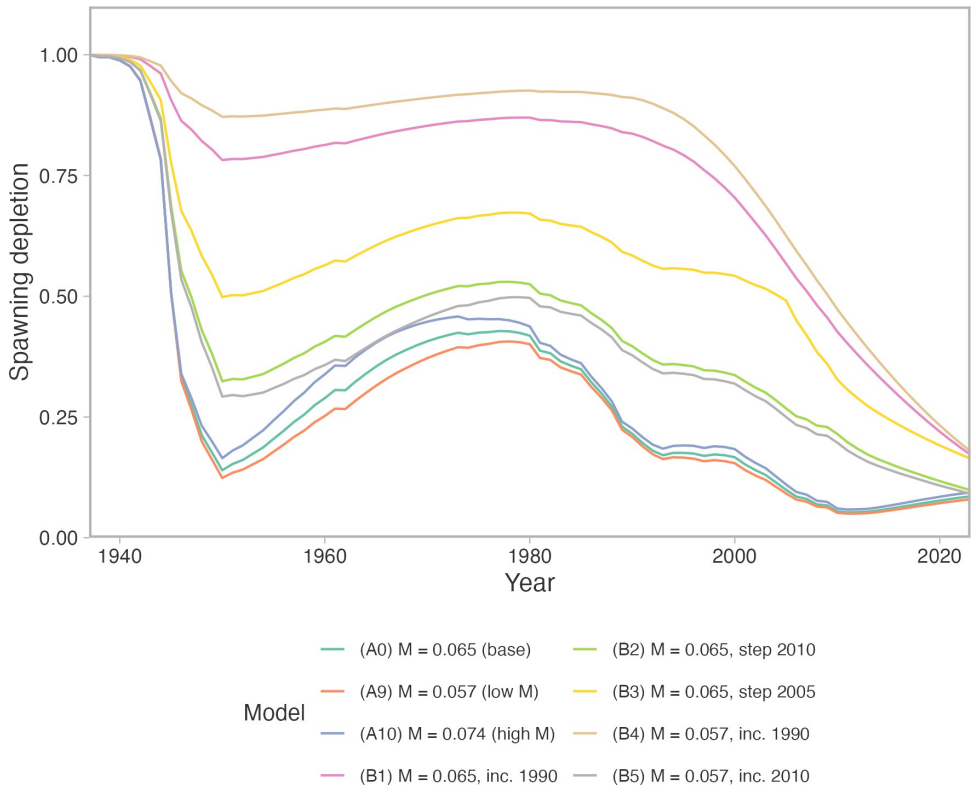

Figure 52. Comparison of depletion estimates in the sensitivity analyses of alternative natural mortality assumptions.

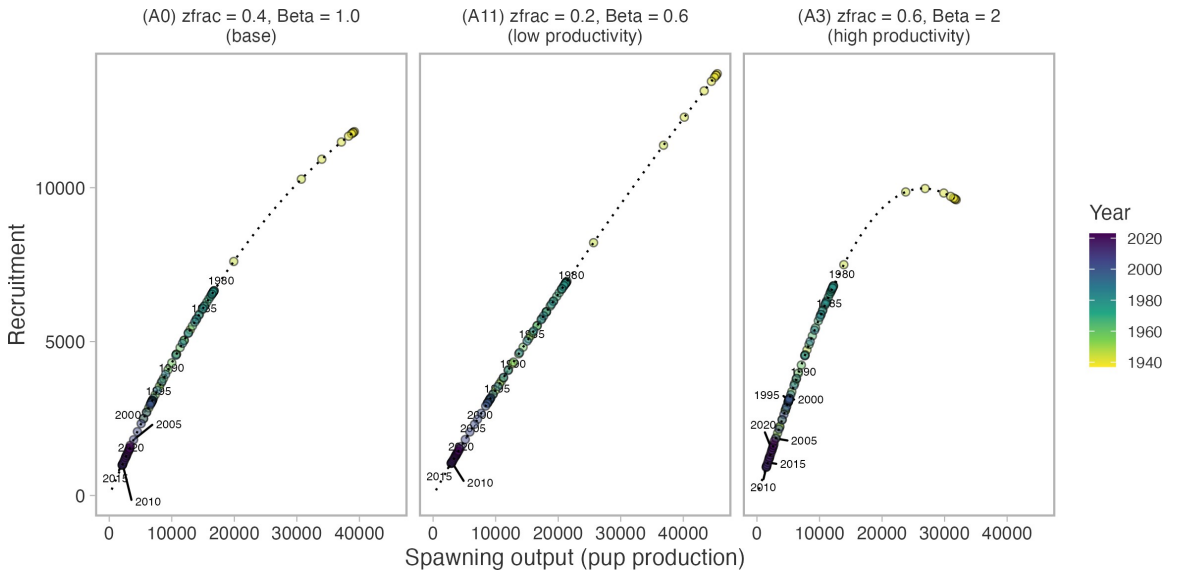

Figure 53. Stock-recruit relationships in the sensitivity analyses of alternative stock-recruit parameters.

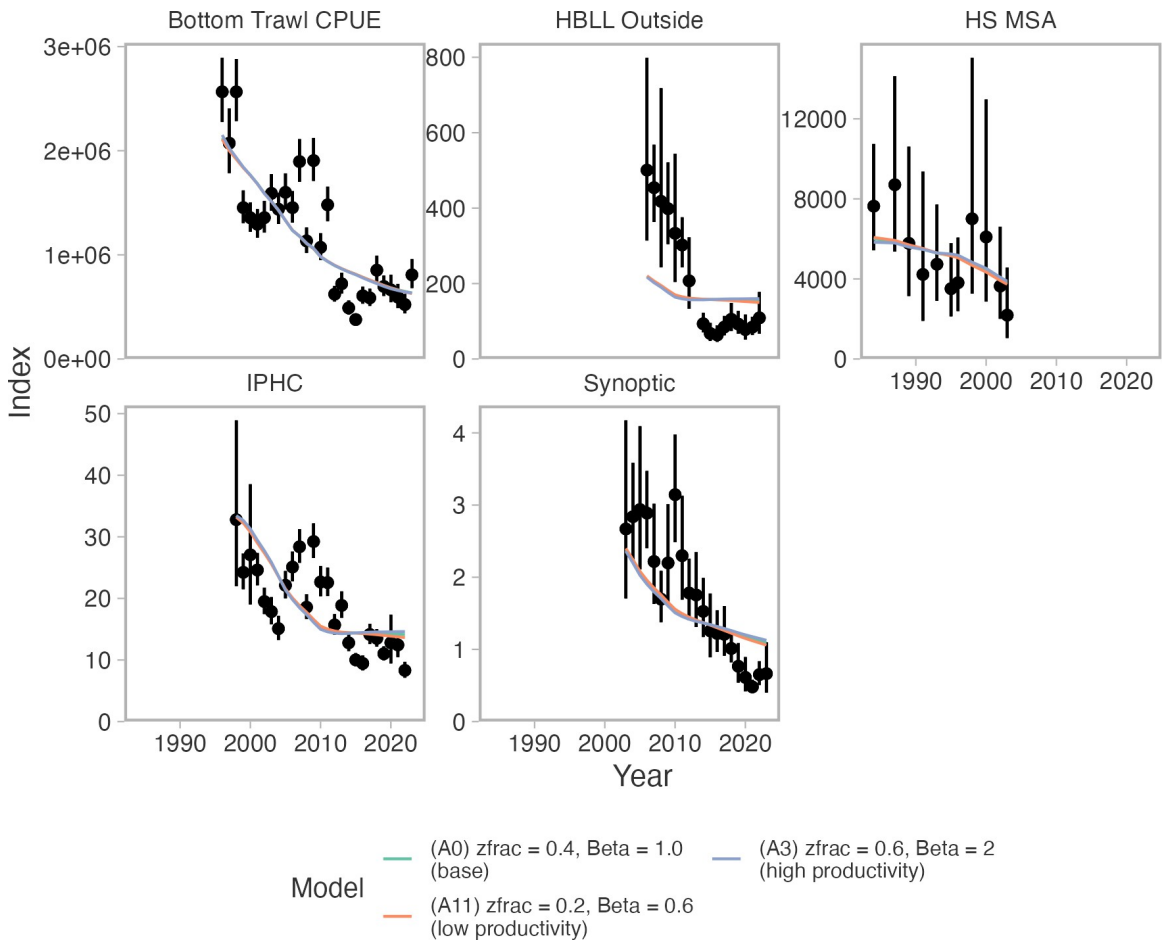

Figure 54. Fits to the indices of abundance in the sensitivity analyses of alternative stock-recruit parameters.

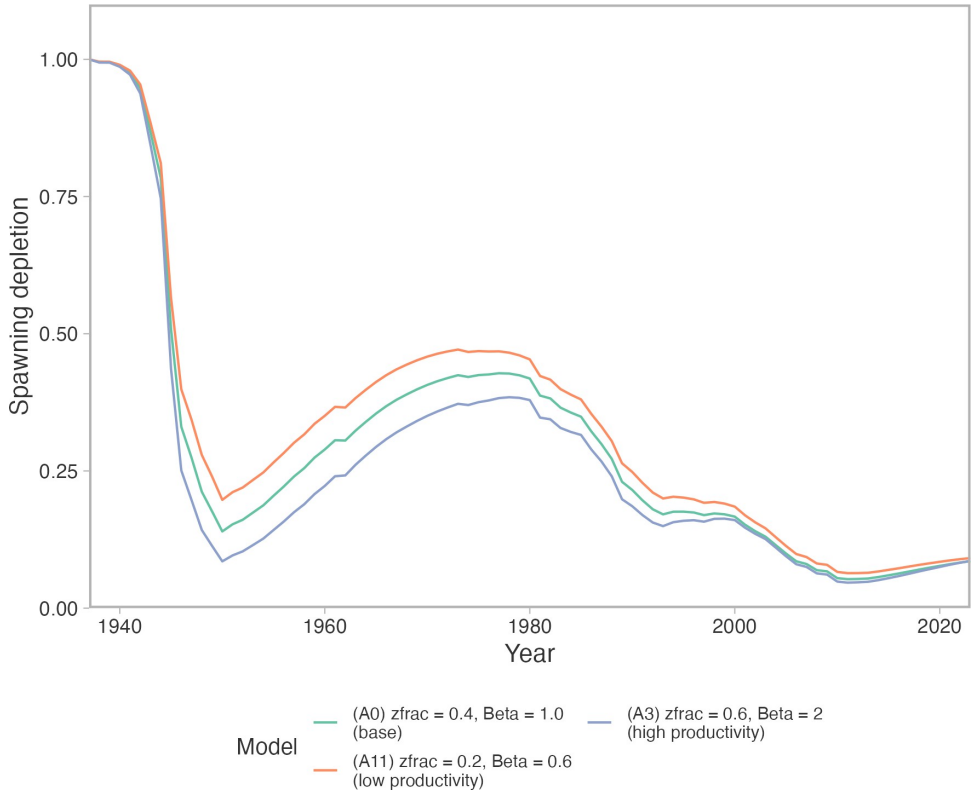

Figure 55. Comparison of depletion estimates in the sensitivity analyses of alternative stock-recruit parameters.

5. REFERENCE POINTS

Here, we provide a rationale for a set of biological and fisheries reference points and calculate status with respect to those reference points throughout the fitted time period and for a projection period conditional on the model assumptions.

There were challenges with using MSY- (maximum sustainable yield) based reference points in this assessment—we therefore provide a rationale for depletion-based reference points. The height of the yield curve and hence maximum sustainable yield (MSY) was sensitive to the stock-recruit parameters z_{frac} and β, neither of which could be estimated from the data; however, a maximally productive stock at $z_{\text{frac}} = 1$ with β fixed at 1—although implausible from the likelihood profile—provides an upper bound on MSY conditional on the fitted models (Figure 42–44). The ratio F/F_{MSY} was highly sensitive to the value of z_{frac} (Figure 41). However, the shape of yield curve with respect to depletion across values of z_{frac} and β was relatively constant (Figure 42). If we draw lines at 0.4 and 0.8 S/S_{MSY}, which correspond to the provisional DFO LRP and USR (DFO 2009), these align to approximately 0.2 and 0.4 S/S_0. We propose these depletion-based values as potential biological reference points. We note that these approximately align with the US West Coast Dogfish overfished and target reference points of 0.25 and 0.4 S/S_0 (Gertseva et al. 2021). We propose a corresponding removal reference of F at $0.4S_0$, i.e., the fishing mortality rate that would take the spawning output to 40% of unfished spawning output at equilibrium.

We can also view these proposed depletion-based biological reference points from a historical-based perspective. An LRP at $0.2S/S_0$ corresponds approximately to the low point of modelled S after the vitamin A fishery (Figure 56), which is a time when the fishery is presumed to have closed partially due to a lack of Dogfish (Ketchen 1986), but from which the stock was capable of recovering from (Gallucci et al. 2011, Wood et al. 1979, this assessment)—albeit slowly and with long-term consequences to age structure (Figure 22). We can therefore also view $0.2S/S_0$ as a historical reference point (sensu Forrest et al. 2020, for Pacific Cod in BC)—a low stock point that one likely does not wish to return to but from which the stock could recover. Spawning output above $0.4S/S_0$ (up to $\approx 0.6S/S_0$ in some models) corresponds to the time period in the 1960s to 1970s that triggered efforts to reduce a "nuisance" Dogfish "problem" (Ketchen 1969) (Figure 56).

We propose basing reference points for outside Dogfish on spawning output instead of spawning biomass. Spawning output is commonly used for reference points for long-lived low fecundity species such as sharks (e.g., Gertseva et al. 2021, Rice et al. 2013, Taylor et al. 2013*b*). In the most comparable example, the US West Coast dogfish assessment also uses spawning output for reference points (Gertseva et al. 2021). In stock assessment, mature female biomass is usually used as a proxy for spawning output (egg production) in teleost fish, since more direct information about fecundity is unavailable. Spawning output is the most direct measure of productivity—the ability for population replacement—and therefore we think best aligns with the PA Framework (DFO 2009). The PA Framework states: "the limit reference point is the stock level below which productivity is sufficiently impaired to cause serious harm. The PA framework would normally be described using units that relate directly to stock productivity. For stocks with age-structured analytical assessments, the most direct measurement of stock productivity is usually spawning biomass or egg production." Here, we can directly use spawning output, which is analogous to egg production in teleost fish. For management, there are likely advantages to measuring productivity with respect to spawning output over biomass as well. Spawning output can be more responsive to changes in exploitation than biomass, as demonstrated in historical estimates of biomass or spawning output over time in our models (e.g., compare total biomass in Figure 21 to spawning output in Figure 20).

Across all models considered, the upper asymptotic 95% confidence interval on S/S_0 in 2023 was below an LRP of 0.2 S/S_0 (Figure 56). The base model estimated S/S_0 in 2023 to be 0.09 (0.08–0.09 asymptotic 95% confidence interval, CI). Across all models without time-varying M, the average S/S_0 was 0.09 and the range of upper and lower 95% CIs across all models without time-varying M was 0.06–0.12. Lower catches starting around 2010 substantially reduced F to be below the proposed reference removal rate of $F_{0.4S0}$ (Figure 57) for many of the models considered. F is estimated to have been above this level from the mid 1980s until around 2010. The base model estimated $F/F_{0.4S0}$ in 2023 to be 1.5 (1.3–1.6 95% CI). Across all models without time-varying M, the average $F/F_{0.4S0}$ was 2.4 and the lower and upper 95% CIs across all models without time-varying M were 0.7–12.8. The low productivity scenario had the highest F compared to the proposed reference removal rate (Figure 57). Excluding this low productivity scenario from this ensemble, the average $F/F_{0.4S0}$ was 1.5 and the upper and lower 95% CIs were 0.7–2.4. Examining "Kobe" plots of fishing mortality against depletion shows the estimated paths of the stock trajectory (Figure 58).

If time-varying M was included, M increased to a degree where the stock would not be able to replace itself. Therefore, calculating reference points based on M in 2023 was not feasible (no amount of catch could be sustained) (Figures 59, 60). Instead, we illustrate S/S_0 and $F/F_{0.4S0}$ with M set to the initial historical value. In this case, spawning output would be expected to continue to decline despite F being set to the historical $F_{0.4S0}$ (Figure 60).

5.1. PROJECTIONS

We can project from the models under a range of fixed dead catch scenarios to illustrate expected trajectories conditional on model assumptions (Figures 61, 62). We illustrate these projections for 10 years—not because we think the models can reasonably predict 10 years (or further) into the future, but because given the slow life-history dynamics, we need a sufficient window of time to illustrate expected trajectories conditional on model assumptions. The low productivity scenario (A11)—and especially the time-varying natural mortality scenarios (B2–B5)—show little to no room for catch reductions to prevent further declines in spawning output. I.e., these models project spawning output to continue declining even with dead catch levels under $\approx$ 300 t (A11) or even at 0 t (time-varying natural mortality scenarios) (Figures 61, F.1).

We can summarize the probability that $B > 0.2B_0$, $B > 0.4B_0$, and $F < F_{0.4S0}$ across models and dead catch levels for a given year (Figures 65, 67). Although similar summaries are often based on Bayesian MCMC sampling in BC groundfish stock assessments, we present probabilities based on asymptotic confidence intervals from the maximum likelihood fits. We argue that in this assessment, structural and across-model uncertainty dominates parametric uncertainty within any one model and therefore precisely quantifying probabilities for a given model is not worth the computational cost.

To distribute dead catch among the fleets we employed the following algorithm:

1. Calculate average dead catch from the last five years for each fleet within the model in weight.
2. Assign that average dead catch to each of the surveys since we assume multispecies surveys would continue for monitoring.
3. If the remaining dead catch to assign is less than or equal to zero, assign zero catch to the remaining fleets.
4. If the remaining dead catch to assign is greater than zero, assign the remaining dead catch to fleets in proportion to average dead catch from the last five years in the model.

Given these projections under fixed levels of dead catch, spawning output S is expected to remain below both $0.2S_0$ and $0.4S_0$ with very high likelihood in 2024–2028 regardless of dead catch level across all models considered (Figures 65, 66). The pattern of how F remains below $F_{0.4S0}$ depends on the model (Figure 67). High vs. low productivity assumptions (A11 vs. A12) have the strongest contrast for a given discard mortality assumption. The assumed discard mortality level has a strong contrast when considered in the context of how this impacts the assumed current dead catch levels are (vertical dashed lines in Figure 67).

The maximum dead catch where there was $\geq$ 95% probability of $F < F_{0.4S0}$ ranged from 0 t for the low productivity scenario to 250 t for the high productivity scenario (Figure 67). The base scenario resulted in 150 t of dead catch corresponding to a $\geq$ 0.95 probability that $F < F_{0.4S0}$, whereas 200 t surpassed $F_{0.4S0}$ with high probability (Figure 67) When the low, base, and high discard mortality rates used in the assessment were applied to average reported catch over the last five years, they resulted in 160 t, 315 t, and 423 t of dead catch per year.

5.2. COSEWIC AND REBUILDING CONSIDERATIONS

We provide information relevant to COSEWIC status assessment on the probability of population decline in Appendix E. Furthermore, although a full rebuilding plan is beyond the scope of this report, we provide information relevant to a potential rebuilding plan in Appendix F.

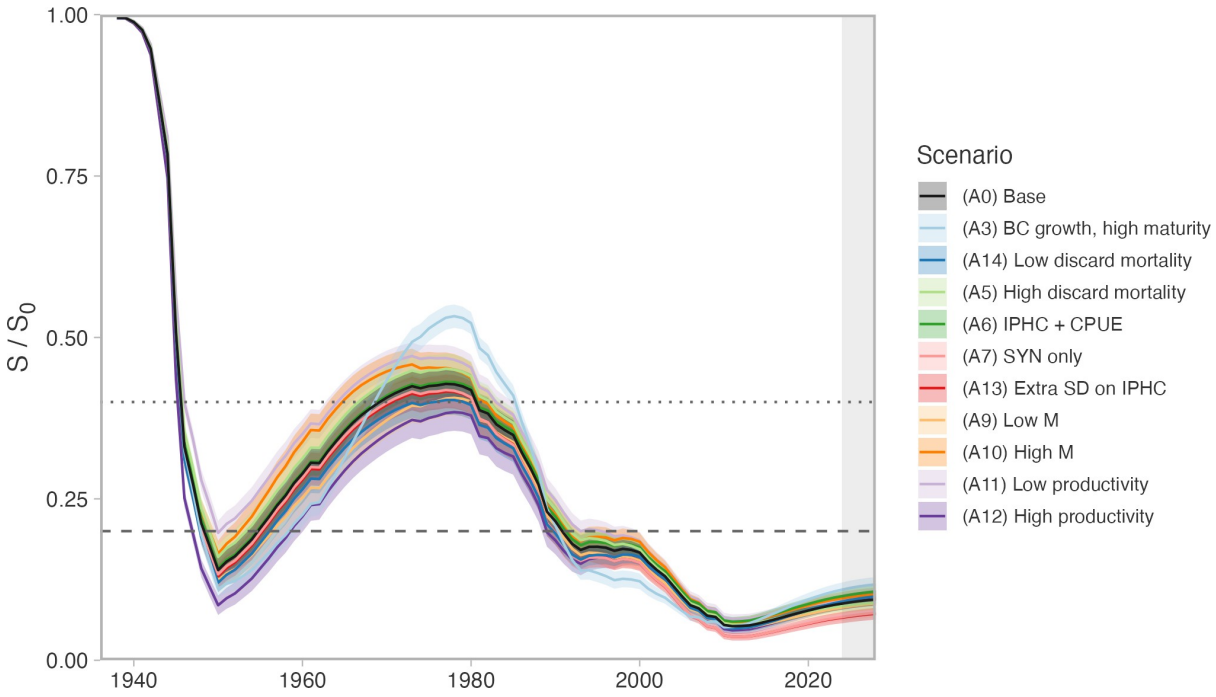

Figure 56. Depletion (S/S_0) over time across models. Lines represent means and ribbons represent 95% confidence intervals. The dotted line indicates 0.4 S/S_0 (a proposed USR) and the dashed line indicates 0.2 S/S_0 (a proposed LRP). The grey shaded rectangle at the right represents a 5-year projection (2024–2028) at $F_{0.4S0}$.

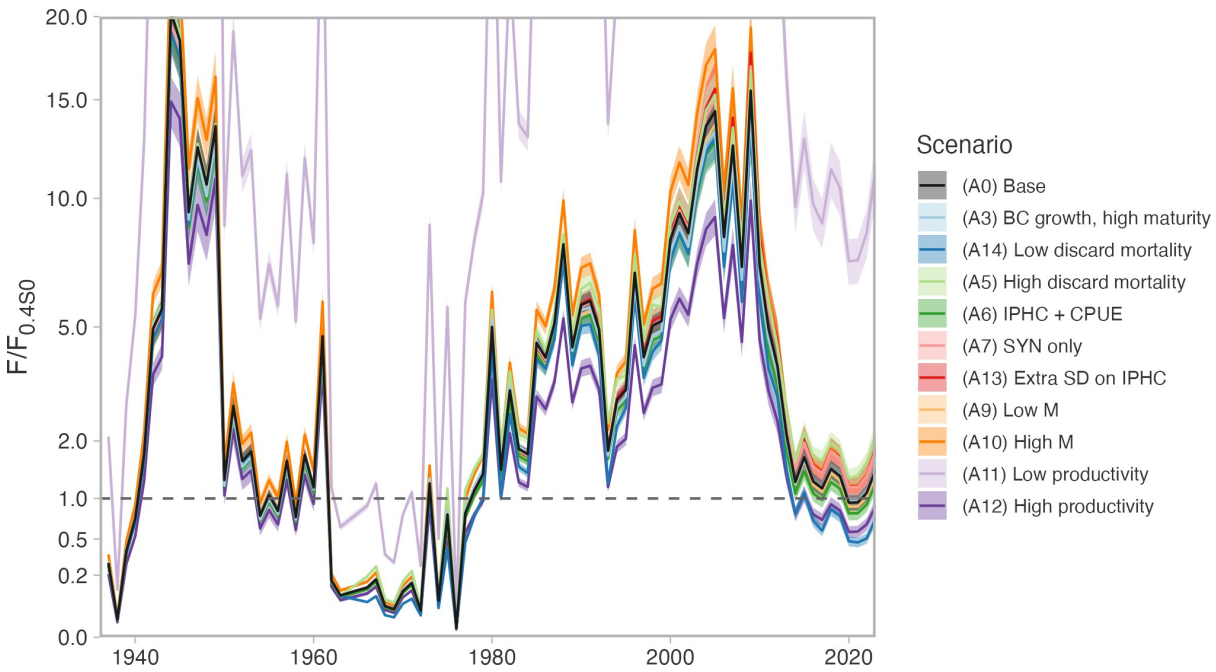

Figure 57. Fishing mortality over fishing mortality at $F_{0.4S0}$ (the fishing mortality that would be expected to achieve $0.4S_0$ at equilibrium) across models. Lines represent means and ribbons represent 95% confidence intervals. $F_{0.4S0}$ is a proposed removal reference rate. A value of 1 (dashed line) represents values at this removal reference rate.

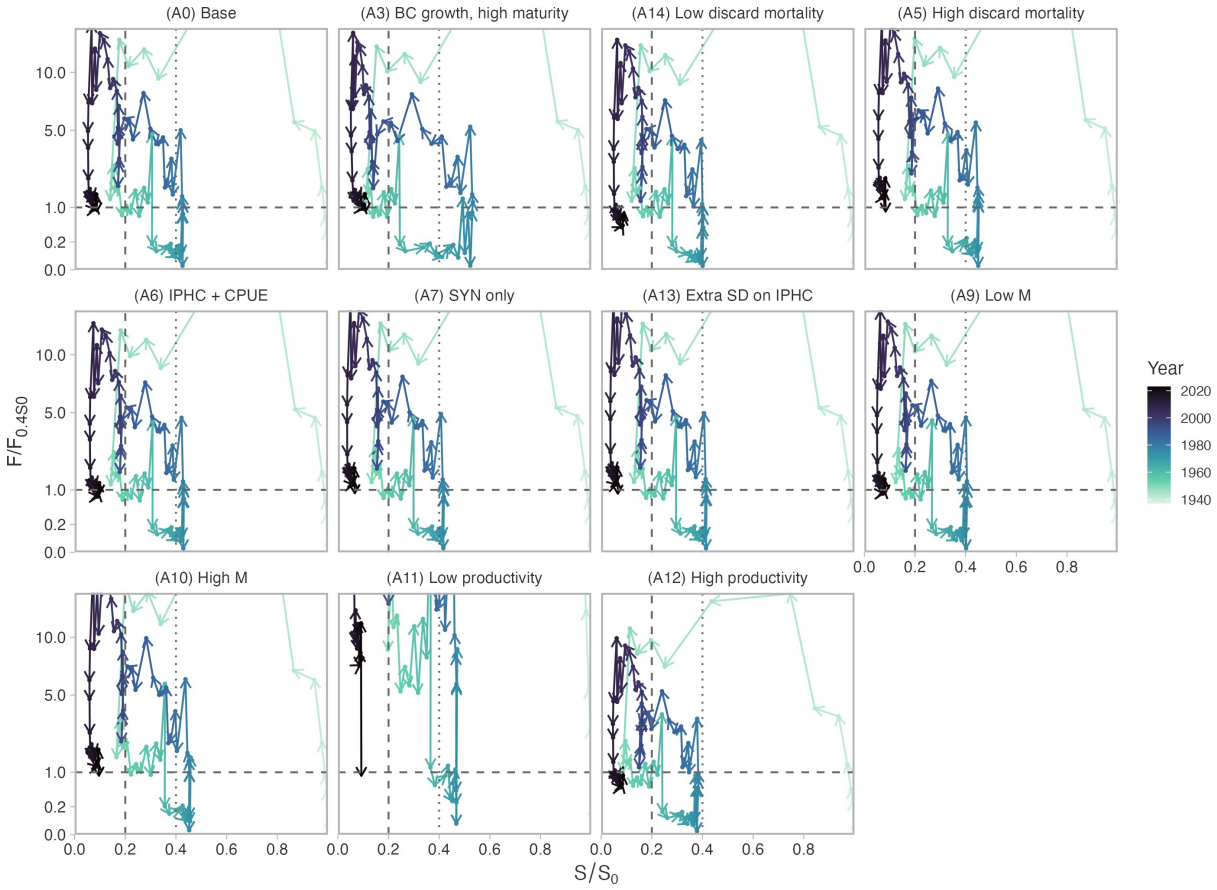

Figure 58. "Kobe" plot showing fishing mortality over fishing mortality at $F_{0.4S0}$ (y axis) and spawning output over unfished spawning output (S/S_0) (x axis). Individual years are connected in order by arrows. A horizontal dashed line at 1 represents F at the proposed removal reference rate. Vertical dashed and dotted lines represent proposed LRP and USR reference points.

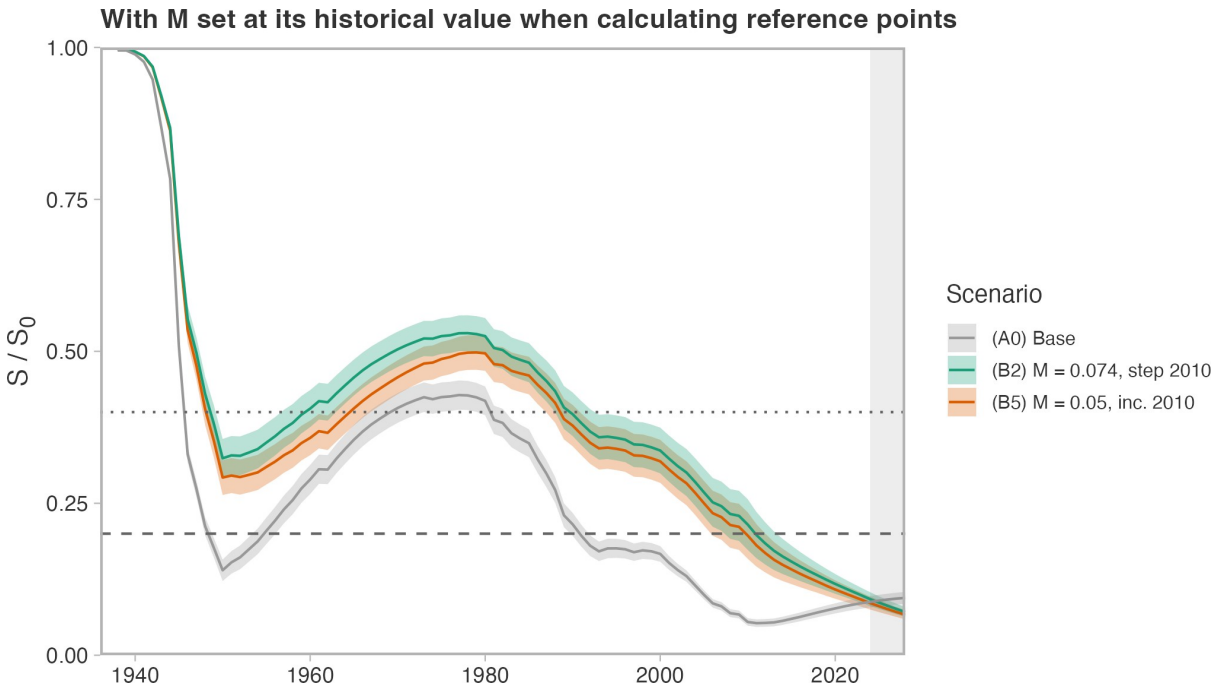

Figure 59. Same as Figure 56 but for two of the time-varying M scenarios. Note that in the calculation of S_0, and in the reference catch used in the projection, M has been set to the historical level before an increase was modelled in order to calculate reference points. This is because M ends up estimated at a level where the stock cannot replace itself.

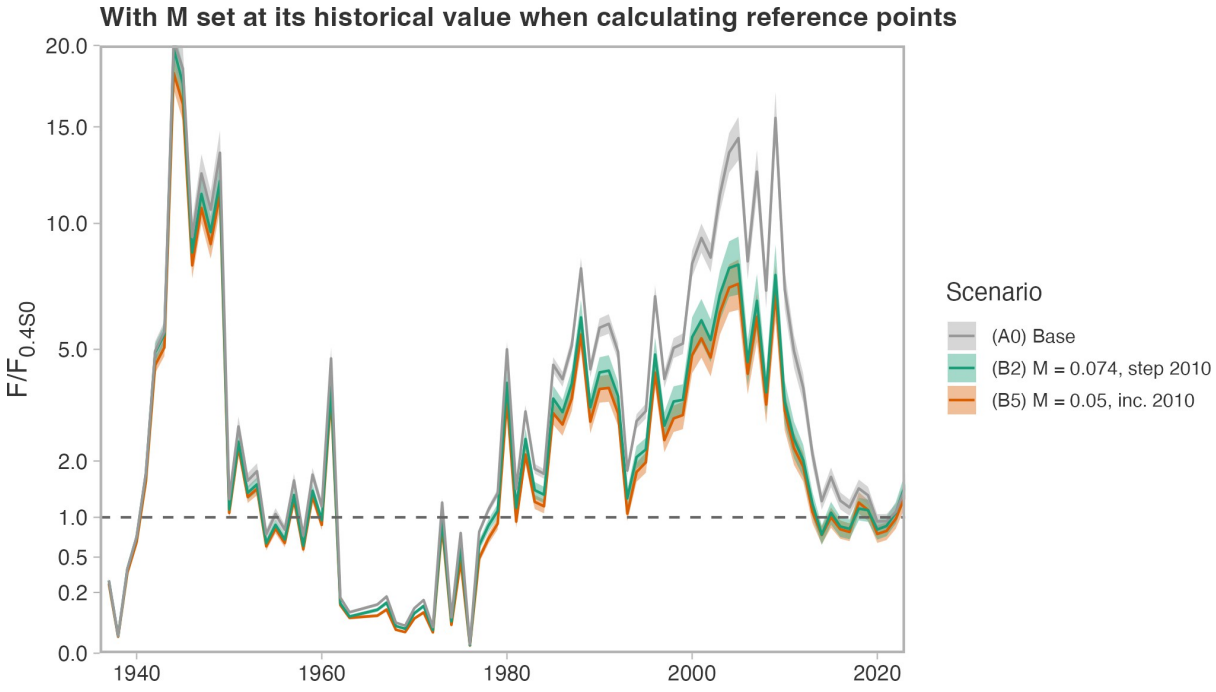

Figure 60. Same as Figure 57 but for two of the time-varying M scenarios. Note that in the calculation of $F_{0.4S0}$, M has been set to the historical level before an increase was modelled in order to calculate reference points. This is because M ends up estimated at a level where the stock cannot replace itself. Spawning output continues to decline in the projection period despite F being set at the historical $F_{0.4S0}$.

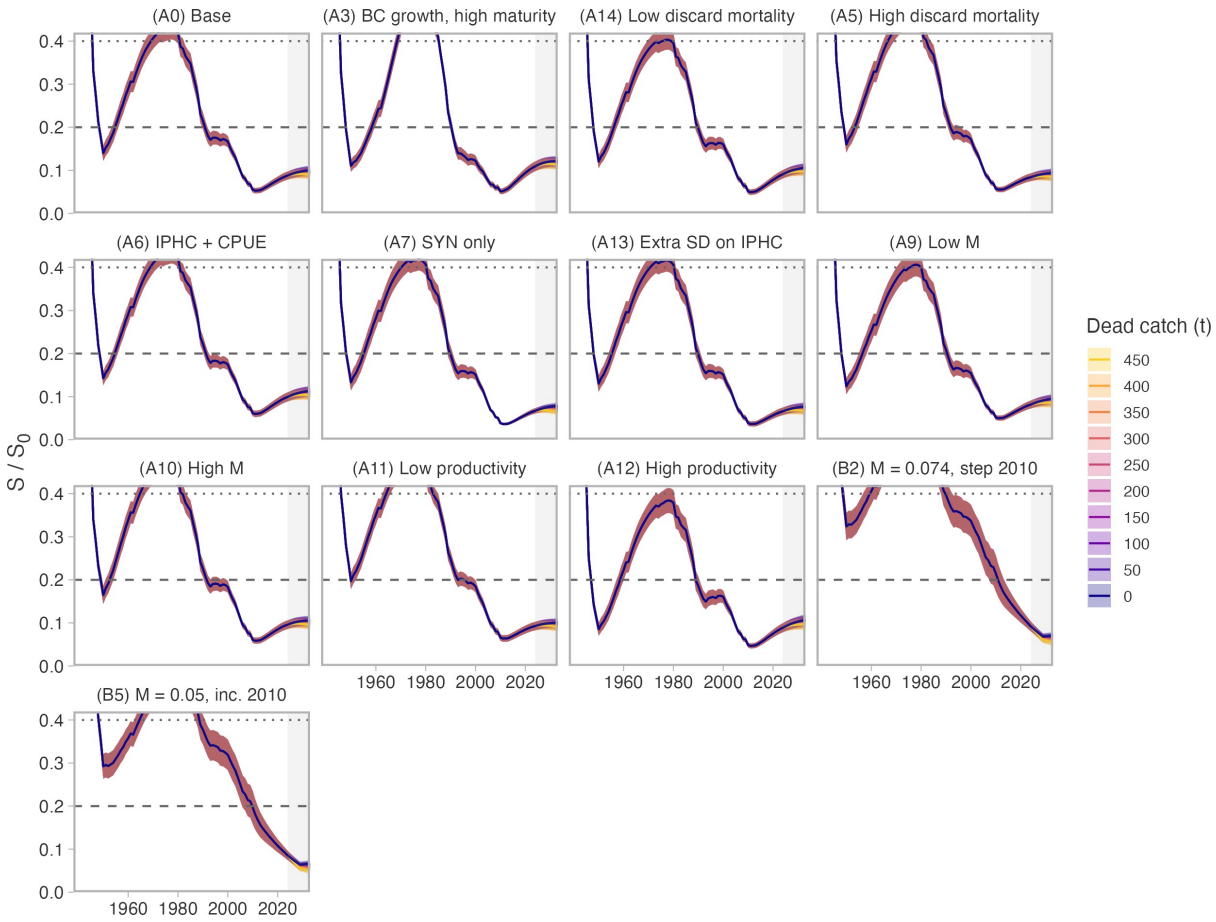

Figure 61. Illustrative projections conditional on model fits for 10 years at different dead catch levels. Note that the y-axis is truncated near 0.4 S/S_0 to make it easier to differentiate the projections. The dotted line is a proposed USR of 0.4 S/S_0 and the dashed line is a proposed LRP of 0.2 S/S_0. The "B" models allow for an increase in natural mortality but do not fully align with our understanding of plausible timing of changes to M. Lines represent means and ribbons represent 95% asymptotic confidence intervals. The shaded rectangle represents the projection period.

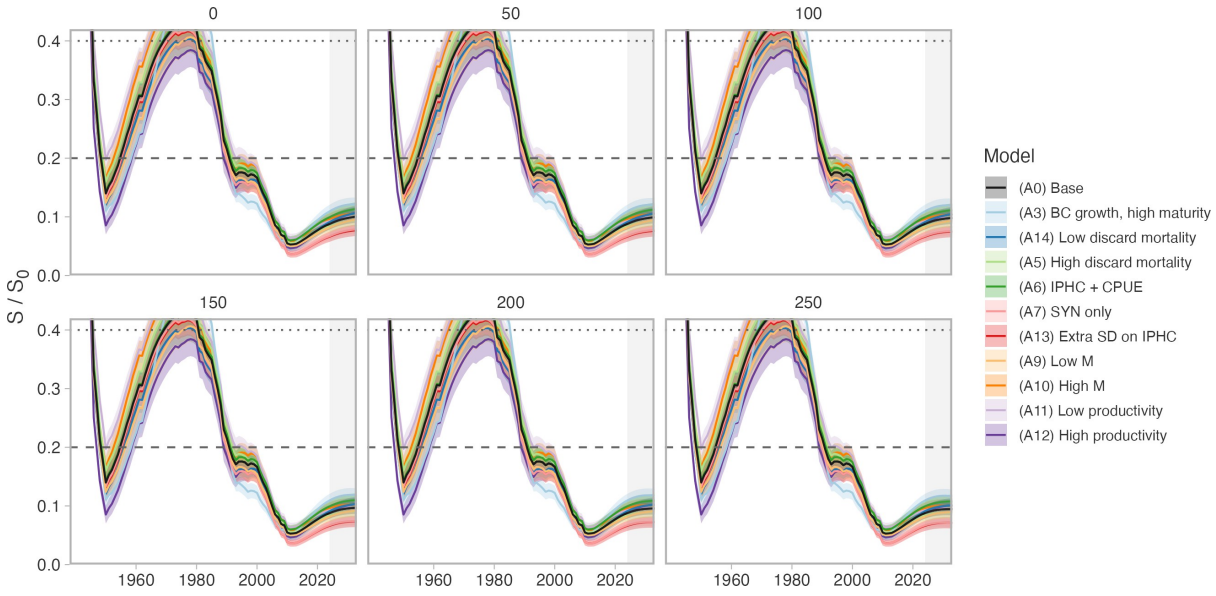

Figure 62. Same as Figure 61 but with panels for dead catch levels (in tonnes) and with the models shown with different colours. The "B" models are omitted here.

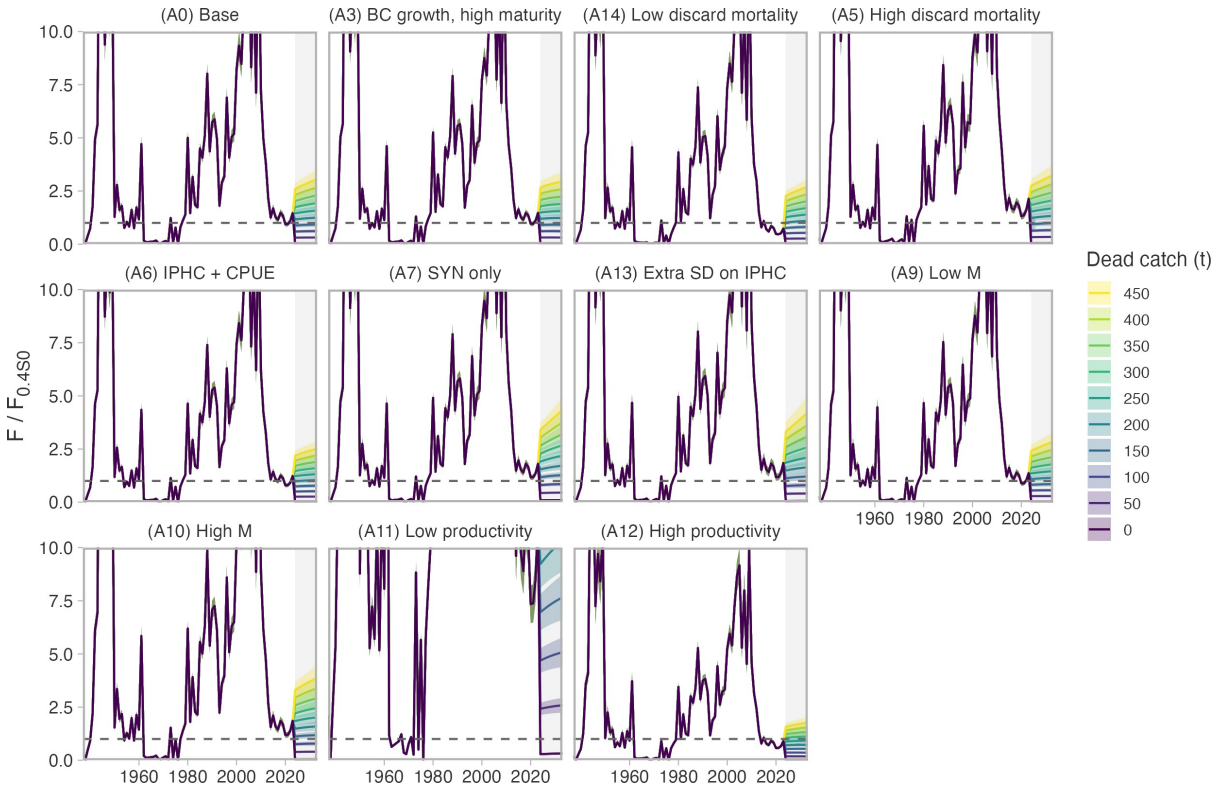

Figure 63. Illustrative projections conditional on model fits for 10 years at different dead catch levels. The dashed line at a value of F corresponding to a proposed removal reference of $F_{0.4S0}$. The "B" models are omitted here. Lines represent means and ribbons represent 95% asymptotic confidence intervals. The shaded rectangle represents the projection period.

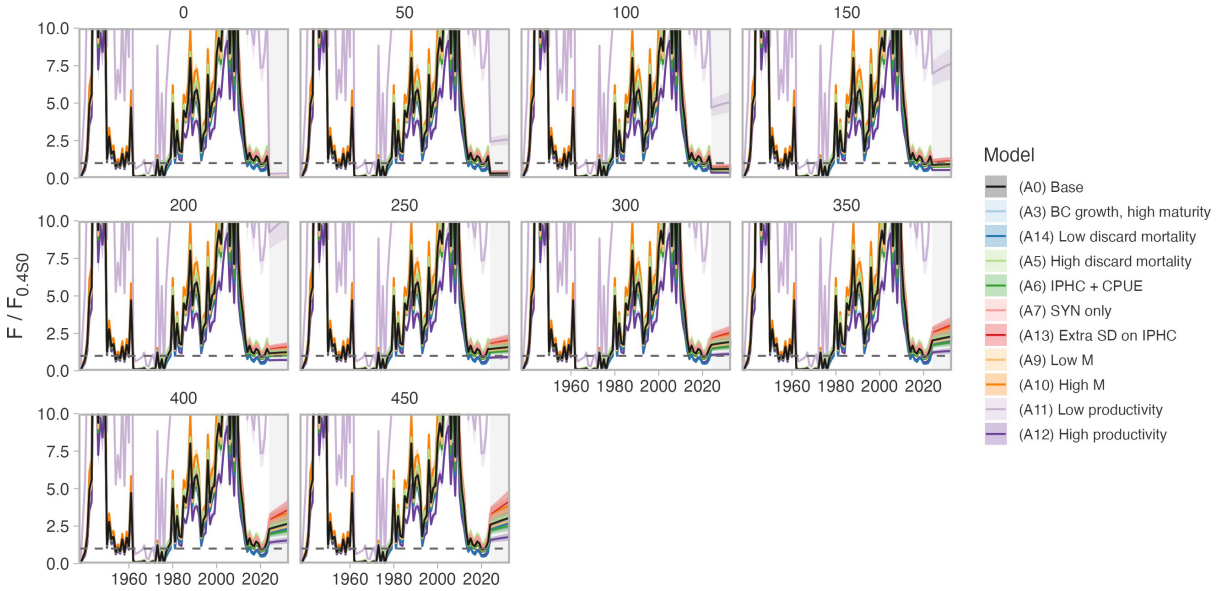

Figure 64. Same as Figure 63 but with panels for dead catch levels (in tonnes) and with the models shown with different colours. The "B" models are omitted here.

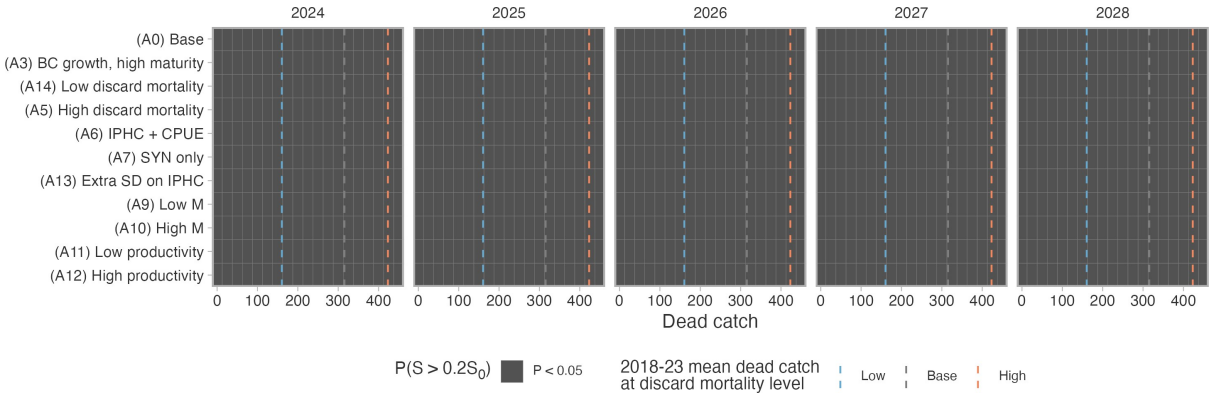

Figure 65. Illustration of probability that $S > 0.2S_0$ across models and dead catch levels. Probabilities are based on asymptotic confidence intervals. The dashed vertical lines indicate average total dead catch over the last five years under low, base, and high discard mortality scenarios. All models and all dead catch levels result in $P < 0.05$ that $S > 0.2S_0$.

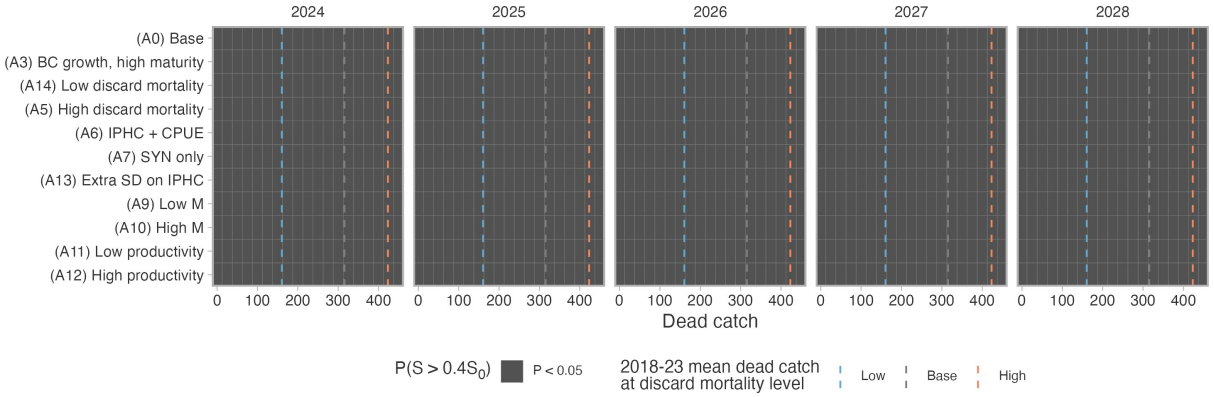

Figure 66. Illustration of probability that $S > 0.4S_0$ across models and dead catch levels. Probabilities are based on asymptotic confidence intervals. The dashed vertical lines indicate average total dead catch over the last five years under low, base, and high discard mortality scenarios. All models and all dead catch levels result in $P < 0.05$ that $S > 0.4S_0$.

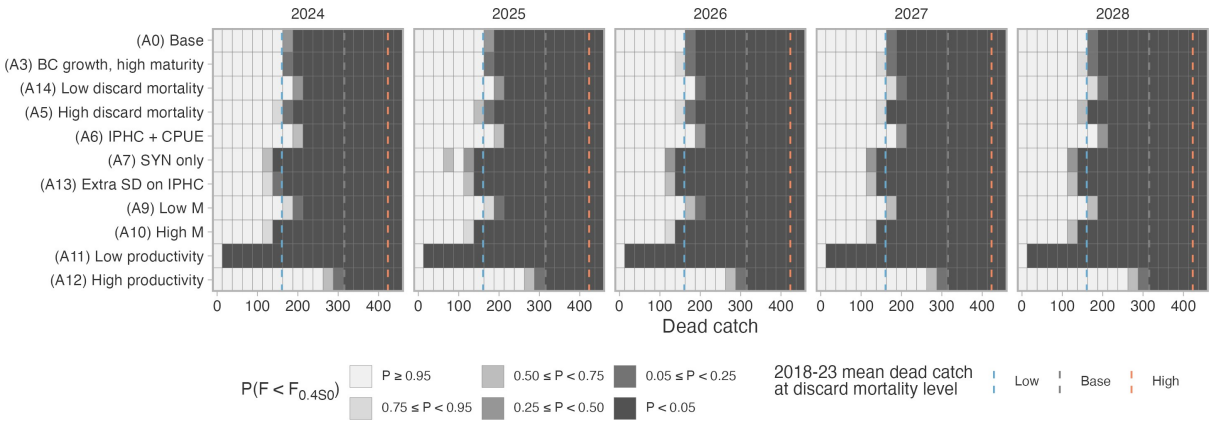

Figure 67. Illustration of probability that $F < F_{0.4S0}$ (with $F_{0.4S0}$ being a possible removal reference rate) across models and dead catch levels. Probabilities are based on asymptotic confidence intervals. The dashed vertical lines indicate average total dead catch over the last five years under low, base, and high discard mortality scenarios.

6. DISCUSSION

We developed two-sex age-structured population dynamics models fit to fishery and survey catch, indices of abundance, and length composition data for outside BC Dogfish. We explored a range of parametric and structural uncertainty through 20 alternative models. All models estimated the stock to be at a low level of spawning output compared to unfished spawning output. Based on a proposed LRP of 0.2 S/S_0, all models estimated the stock to be below this threshold with very high likelihood, conditional on their assumptions. We proposed a potential removal reference rate and explored the catches implied by this rate across the range of assumptions considered in the models.

In this discussion section, we discuss improvements to the methods in this assessment compared to the previous assessment, challenges fitting to the survey indices, evidence for time-varying natural mortality, challenges estimating density-dependent dynamics, and why—despite these challenges—our models and the data are informative with regards to stock status and provide information regarding catch advice. We then discuss environmental considerations, research recommendations, a suggested timeline to revisit the assessment, and note specifically how this document has met the Terms of Reference objectives.

We transitioned from a surplus production model used in the previous assessment in 2010 (DFO 2010, Gallucci et al. 2011) to an age-structured assessment fit to length composition data, catches, and indexes of abundance. This transition was made possible by the availability of substantial new survey index and length composition data. An age-structured model has several advantages over a simpler surplus production model, primarily in the biological realism that can be modelled. Our age-structured model let us evaluate population trajectories that are consistent with our understanding of Dogfish growth, maturity, fecundity, and stock-recruit productivity while also fitting the length composition and index data. Mechanistically, age-structured models incorporate lags in the response of the population due to late maturity and low fecundity. Similar to the previous BC Dogfish assessment (Gallucci et al. 2011), and the previous US West Coast Dogfish assessment (Gertseva et al. 2021), we were unable to estimate a productivity parameter without that parameter hitting a lower bound. However, we were able to bound predictions of recruitment with a stock-recruit curve (Taylor et al. 2013*b*) designed explicitly for Dogfish and other low-fecundity species.

Currently, three major surveys catch Dogfish in outside waters, each of which have declining, but somewhat different trends over time. Since all three have significant coverage over Dogfish habitat, it is difficult to exclude any index of abundance series. The population models developed in this paper had difficulty fitting to the Synoptic survey, which was presumably a representative survey since it samples predominantly Dogfish habitat, i.e., muddy habitat. Fast declines in the Synoptic index could not be explained from the catch history alone. The best fit to the Synoptic index occurred when an increase in natural mortality was modelled. No model could capture the rate of decline in the HBLL index. The HBLL survey explicitly covers hard bottom (rocky) habitat, i.e. less preferred Dogfish habitat. Although we do not have additional data to support the hypothesis, one possibility is that the HBLL survey generates a hyperdepletive index due to Dogfish straying less from their preferred muddy habitat when at lower population densities. Another possibility is that declines have been steepest in shallower waters (Figure B.12) and the HBLL survey has a shallower and more narrow depth range than the other surveys.

The models were sensitive to the assumptions of time-varying natural mortality. The only plausible time-varying natural mortality models had increases in natural mortality in 2010, and followed the decline in the Synoptic index. There is some support for the timing of the increase in natural mortality if these models incorporate the hypothesis of predation mortality by pinnipeds. A threefold increase in over-wintering populations of California sea lions has been estimated since the beginning of the time series (2010), with no significant increase since

2017 (DFO 2023). On the other hand, the number of overwintering Steller sea lions in BC has increased approximately 3.8% per year since the 1970s (DFO 2021, Olesiuk 2018), recovering from control programs and commercial harvests and surpassing peak historical levels (Olesiuk 2018). However, models with earlier increases in natural mortality for Dogfish, were deemed implausible because of lack of depletion from the vitamin A fishery in their dynamics. We note that M could also increase as the Dogfish population decreases even given a constant predator population since the number of individuals that are preyed upon does not necessarily decrease proportionally with decreasing population size.

Low fecundity limits the density-dependent dynamics, i.e., steepness, of the population given the survival-based stock-recruit function (Taylor et al. 2013*b*). This is in contrast to a BevertonHolt stockrecruitment relationship, for example, that has no such limit on productivity (Taylor et al. 2013*b*). The likelihood profile indicated there was little to no density-dependence, precluding calculation of MSY-based fishery reference points. On the other hand, there was little discernible difference in the index fits between all steepness values up to the maximum value. This is likely because the survey indices do not appear in the data until a time when the stock is already estimated to be low on the stock-recruit curve where there is little difference in the shape across stock-recruit parameters. We therefore chose to fix the steepness at a range of possible values, following the lead of Gertseva et al. (2021).

Sensitivity analyses to evaluate uncertainties in other biological parameters did not substantially alter the perception of historical stock abundance. The population trajectory was considerably constrained by low fecundity. However, this behaviour could be indicative of robustness or it could reflect missing some additional major structural difference between reality and assumed system dynamics. As an example, the population dynamics model could be modified to allow for additional density-dependent dynamics, such as the natural survival of adults, to account for historical rebounds in the population (Wood et al. 1979). However, density-dependent M is not currently likely to be the most important factor affecting Dogfish abundance since the declines we are observing are on a stock at depletion levels already 0.4 or lower.

The estimated current status is inferred from the decline in indices in light of low catches relative to historical levels. While length data are likely not informative about stock depletion in this model, they do indicate that there is discard mortality on immature females—from the bottom and midwater trawl fleets. Vulnerability of immature females reduces survival to mature ages. Therefore, it is expected that any reduction of this mortality on juvenile Dogfish would have disproportionate effects on the ability for the stock to recover compared to overall reductions in fishing mortality. However, the exact extent to which discarding of juvenile Dogfish affects population status is clouded by uncertainties in steepness and the discard mortality rate.

In light of the challenges documented above in reconstructing outside Dogfish population dynamics, decision tables are not explicitly presented in this report. However, this assessment is the best population reconstruction currently possible with the data at hand and provides a consistent perspective on outside Dogfish for several reasons:

- The commercial length composition data are variable from year-to-year, possibly due to sampling issues. Regardless of the reason, no population model for such a long-lived species will be able to reconcile their variability.
- We were unable to estimate the parameters defining density-dependence in the stock-recruit curve; however, the US West Coast assessment faced the same challenge (Gertseva et al. 2021) as did the original paper defining this stock-recruit curve despite fixing the selectivity parameters (Taylor et al. 2013*b*). We therefore bounded a range of plausible density-dependence shapes and show results under the extreme scenario of maximum possible pup survival as the stock approaches zero ($z_{\text{frac}} = 1$).

- Assessment models perform best when supporting data, e.g., fishery CPUE or survey indices, inform how much the stock declined in the period of highest catches. These data are not available when the largest fishery catches were observed in the early 20th century; however, these data will never exist.
- We were unable to fit two of the steepest survey index declines in most of our models (the US West Coast assessment had similar challenges; Gertseva et al. 2021), but if we had fit those indexes, the model would have inferred steeper declines in stock size. Even with missing the decline in these indices, the stock is already estimated to have crossed a level of depletion that is beyond what we propose as a reasonable definition of an LRP across even the most optimistic of the models considered. Therefore, the expected bias is in a direction that would further increase the conservation concern but place the stock in the same place from a policy perspective—below the LRP.
- We were unable to address all major sources of uncertainty in any one model; however, this is not uncommon in stock assessment. Through the approximately 20 alternative models, we bounded a wide range of possible parametric and structural uncertainties.
- Stock depletion estimates were fairly consistent across the models considered; however, this is plausible because Dogfish population dynamics are heavily constrained by life span (and therefore natural mortality), late maturity, fecundity, and a two-year gestation period. There is therefore a tighter band of plausible population dynamics we can fit to data than for most teleost fish where the dynamics may not be bounded by fecundity.
- There is considerable variability across the models about how changes to catches would be expected to affect the stock trajectory. However, even the most optimistic models considered here, i.e., with high productivity and low discard mortality, suggest that catch levels well below the current total allowable catch would be required to have a reasonable probability of the stock rebuilding.
- The limited productivity of Dogfish, the estimated population size, and steep declines over the last two decades in several survey-based population indices suggest that catches would need to be considerably lower than the current total allowable catch and not higher than recent catches to be consistent with a precautionary approach to stock management. This result is independent of the choice of reference points.

6.1. ENVIRONMENTAL CONSIDERATIONS

Although we did not consider environmental conditions directly in population dynamics modelling beyond time-varying natural mortality scenarios, other recent research has examined possible climate drivers of outside Dogfish distribution in BC. Perhaps most relevant, in a paper looking at 38 groundfish species, English et al. (2021) did not find any strong patterns in changes to Dogfish distribution correlated with local changes to bottom temperature or dissolved oxygen. In US West Coast waters, Taylor and Gallucci (2009) considered whether climate might explain declines in length-and-age at maturity but were unable to come to a conclusion on the topic. They noted the challenges of attributing population or demography to environmental conditions for a long-lived species such as Dogfish that serves as an extreme “biological integrator” of conditions over time.

It has been hypothesized that Dogfish may have shifted their range north, potentially due to climate change (Conrath and Foy 2009, Orlov et al. 2012, Shiffman et al. 2022). However, ongoing work (Davidson et al. 2025) has found coastwide declines in bottom trawl and longline survey data over the last two decades from California to the Gulf of Alaska. The rate of decline was similar along the US West Coast and BC coast. Although overall rate of decline was less steep in the Gulf of Alaska, population densities were found to have declined throughout the Gulf of Alaska as well over the same time period.

Another possibility is that Dogfish have moved further offshore (or inshore) outside of the fishery and survey domains—perhaps in response to changes in temperature, oxygen, or to evade predation in shallower waters. Indeed, the bottom trawl CPUE decline was strongest in shallower ($<$ 100 m) waters and weakest (although still present) in deep ($>$ 200 m) waters (Figure B.12) and the steepest survey decline was in the HBLL OUT survey, which is the shallowest of the surveys included. However, the Synoptic trawl survey regularly has sets below 400 m, below which Dogfish are only encountered in minor densities (Figure A.17), so the survey should be deep enough to encompass a shift from the current peak depth ($\approx$ 100 m). Furthermore, the Sablefish *Anoplopoma fimbria* offshore BC trap survey shows a stable trend for Dogfish (Figure A.29). With regards to inside Vancouver Island waters, the inside HBLL survey index for Dogfish has been declining over the last two decades (Anderson et al. 2024*a*), which suggests Dogfish have not moved out of the survey domain to these waters. Regarding environmental drivers of such movement, as noted above, English et al. (2021) failed to find any strong relationships between local changes in bottom temperature or dissolved oxygen and changes to Dogfish distribution within BC.

A third hypothesis is that shifts in seasonal distribution have caused a decline in catchability for the surveys that are typically conducted in the summer (Figure A.2). However, the commercial bottom trawl CPUE time series is standardized based on year-round data. Furthermore, when we re-calculated the CPUE index for individual months, we found declines typically ranging from $\approx$ 30% to $\approx$ 50% per decade with no clear seasonal trend (Figure B.14). August had the steepest decline at $\approx$ 60% and the shallowest decline was in November at $\approx$ 20% (Figure B.14). The HBLL OUT survey is typically conducted in August to September, so a steeper August decline may explain some of the divergence of this survey from the others. However, the Synoptic WCVI survey, where the bulk of the biomass for the coastwide Synoptic index comes from (Figure A.23), is conducted in May to June when the decline in the commercial CPUE by month appears typical.

Taken together, we do not observe compelling evidence of northward, offshore, or seasonal shifts in distribution that would explain the majority of the declines in the indices of Dogfish biomass or abundance. Regardless of the cause of the observed declines—whether it is natural mortality, fishing mortality, or movement—the population indices and the population reconstruction suggest there are far fewer Dogfish in BC than there were when the surveys began, and catches would need to be adjusted accordingly to remain consistent with a precautionary approach to management.

6.2. RESEARCH RECOMMENDATIONS

Although it is critical to continue collection of the current fishing and survey data, it is not likely that current data streams will substantially improve this stock assessment model in the near future. In this section we suggest recommendations for future research that may improve future Dogfish assessments.

Exchange between the US West Coast, BC, and Alaskan Dogfish populations is thought to be low based on previous tagging studies (see review in Section 1.2). However, some degree of exchange occurs and the nearby stocks may be experiencing shared ecosystem pressures. It would be valuable to investigate the degree to which trends in survey indices along the entire northeast Pacific coast are consistent. Some hotspots of Dogfish population density (e.g., along the southern portion of west coast Vancouver island) border on neighbouring region waters (Washington State). There is ongoing work on this topic through a collaboration with AFSC (Alaska Fisheries Science Center), NWFSC (Northwest Fisheries Science Center), and PBS (Pacific Biological Station) scientists. Early results (not shown) indicate declines along the entire coast, but with rates of decline steepest on the US West Coast and BC vs. Alaska and rates of decline steepest in the trawl surveys vs. the IPHC survey.

The time-varying natural mortality scenarios could be better justified (or excluded) and better parameterized with knowledge about current and historical diet patterns of Dogfish predators. Predators include marine mammals such as sea lions, orcas, and northern elephant seals (*Mirounga angustirostris*). However, data on predation rates are currently limited. Existing diet data for Alaskan Steller sea lion populations, (e.g., Trites and Calkins 2008, Winship and Trites 2003) suggest Dogfish were not a major diet component (1993–1999). In California, Dogfish were found to comprise $\approx$ 8% of California sea lion diets (*Zalophus californianus*) (1997–1999) through an analysis of hard parts of scat. It is possible that the hard parts analysis of scat underestimated Dogfish consumption as many predators of sharks exclusively consume the lipid rich liver (e.g., Fallows et al. 2015, Ford et al. 2011). There is ongoing research at Pacific Biological Station analyzing Steller and California sea lion scat data to assess trends in their diet by region within BC. Early results suggest Dogfish could comprise a notable percentage of Steller and California sea lion diet in BC outside waters (K. Trzcinski, personal communication). Aside from increased predation by sea lions, there is also a potential for non-lethal effects of sea lions on Dogfish (e.g., changes in the fear landscape that affect availability of Dogfish to the fishery and survey).

Another predator, offshore killer whales (*Orcinus orca*), consume sharks as their main prey items (Dahlheim et al. 2008, Ford et al. 2011). With the loss of Basking sharks (*Cetorhinus maximus*) from BC's waters (DFO 2009), increased reliance on Dogfish may be possible. There is also ongoing work at Pacific Biological Station to understand diets of transient killer whales (*Orcinus orca rectipinnus*); Dogfish form a portion of their diet (T. Doniol-Valcroze, personal communication).

Although there are historical aging data available for outside BC Dogfish, they are currently not linked to specific surveys, fleets, or years and they are primarily from before the era of modern surveys. Newly collected age composition data may be beneficial to population modelling efforts—especially given the lack of informativeness of the length composition data to depletion and challenges estimating growth parameters from the existing historical data. In addition to lacking a robust age dataset, there are inherent challenges with aging sharks in general. While techniques for aging Dogfish via their dorsal spine have been validated (McFarlane and King 2009) aging Dogfish spines is time consuming and wear on the dorsal spine presents challenges to accurate estimation (Taylor et al. 2013*a*). A potential opportunity is to age Dogfish from vertebrae (e.g., Bubley et al. 2012). DFO is currently collaborating with Washington State's Department of Fish and Wildlife researchers who are leading the development of this for Dogfish.

Length data were not available for the HBLL OUT survey, which had the steepest decline of the survey indices. Due to the lack of sampled length data, the selectivity had to be mirrored to the IPHC fleet. It would be valuable to be able to estimate a separate selectivity curve for the HBLL OUT survey. It is possible that artificial intelligence approaches could be used to pull length data from historical video footage from this survey. This would be a valuable avenue to explore before the next assessment.

Discard mortality rates remain an area of high uncertainty in this assessment. Furthermore, the discard mortality rates assumed in the IFMP for both trawl and longline differ substantially from the literature-based values used in this assessment. First, we recommend revisiting the IFMP discard mortality rates in light of the literature reviewed in the document. Second, better determination of post-release discard mortality for Pacific Dogfish using the commercial gear used by the fleets in this assessment would be challenging, but valuable. However, it may be possible to better determine immediate (i.e., at-vessel) mortality by recording this data from surveys using similar gear or from reviewing at-sea video monitoring footage of the commercial fleet.

Close-kin mark-recapture (CKMR) (Bravington et al. 2016) is a relatively new approach that could potentially inform our perception of key population parameters such as unfished abundance and natural mortality. CKMR is a modification of traditional mark recapture techniques that introduces genetic sampling to transition from needing to recapture the same individuals to allowing for recapturing closely related kin to estimate the absolute abundance of mature individuals (Bravington et al. 2016). Recently, the approach was successfully applied to Thornback Ray (*Raja clavata*) in European waters (Bay of Biscay) (Trenkel et al. 2022). However, CKMR requires assumptions of a closed population and random sampling. Thus, any CKMR program would be complicated by the extent to which there is immigration or emigration from BC waters to nearby regions and schooling of siblings.

6.3. TIMELINE TO REVISIT ASSESSMENT

We recommend this assessment be revisited within approximately five years. The stock is estimated to be below its LRP with very high likelihood and several population indices show steeper declines over the last one to two decades than our population models could fit. One basis for revisiting the assessment in a timely manner are recent length composition data from the Synoptic trawl survey, which shows some evidence of increases in small Dogfish in the last two years—possibly indicative of incoming recruitment. These increases, however, are small compared to the declines over the last 20 years. Given the slow life history of Dogfish, the long history of catches that are much higher than current catches, and challenges fitting several of the modern population indices, advice from this population model is unlikely to change markedly over a short (e.g., less than five year) time span.

There is no formal trigger we can recommend that would suggest an earlier than anticipated reassessment. However, it will be important to monitor population indices and length distributions in the annual updates to the groundfish data synopsis report (Anderson et al. 2019, 2020, 2024*a*, DFO 2022*a*). The population models presented here differ slightly in the predicted recent index trend. With constant natural mortality, the index is predicted to be somewhat constant or with a slower rate of decline in recent years, compared to faster declines in models with increasing natural mortality. Thus, it will be important to revisit the model quickly if there are signs of faster than expected recovery in the survey indices or commercial CPUE. Rapid changes in the index trend or size distribution would warrant an evaluation of whether the data are representative of population trends or if there may be behavioural changes that affect survey catchability.

6.4. OBJECTIVES SUMMARY

This stock assessment document provides scientific advice and recommendations as outlined by the Terms of Reference objectives:

1. *Develop and assess a suite of age-structured population dynamics models for Dogfish in outside BC waters and describe the uncertainties the models are meant to address.*

   In Section 3 we described a two-sex age-structured population dynamics model fit to fishery and survey catch, indices of abundance, and length composition from both fisheries and surveys for Dogfish in outside BC waters. Biological parameters related to growth and maturity were estimated outside of the population dynamics model, but uncertainty was captured through several alternative sets of parameters (Section 3.1). In Section 3.2 we described uncertainty captured through parameter estimation in terms of unfished recruitment, productivity, and selectivity parameters. We explored uncertainties related to maturity, growth, natural mortality, discard mortality assumptions, the representativeness of various indexes, the shape of the stock-recruit curve, and possible time-varying changes to natural mortality through sensitivity analyses (Section 3.3.1). We further explored model

estimability and confirmed the maximum likelihood estimates were consistent with MCMC sampling from selected models' posterior distributions (Section 3.3.2, Appendix D).

2. *Document and discuss challenges and uncertainties regarding model assumptions and data that affect (1) reconstructing stock dynamics, (2) developing reference points consistent with the DFO Precautionary Approach (PA) Policy (DFO 2009), and (3) evaluating status with respect to those reference points.*

   In the Discussion section (Section 6) and through the results, we summarized challenges and uncertainties regarding model assumptions and data that affected our ability to reconstruct stock dynamics, develop reference points, and evaluate status with respect to those reference points. These challenges included:

   a. Differing rates of decline in the three major survey indexes could not be reconciled with selectivity alone (e.g., Figures 28, 48). We have no reason to reject any of these surveys, but the model cannot fit all three simultaneously.

   b. A need for some external factor beyond the base population dynamics models to reconcile the data with the steep declines seen in the HBLL and Synoptic survey indexes. We explored an increase in natural mortality (Figure 50–52), potentially due to increased pinniped predation, but the model was highly sensitive to the timing of this change in natural mortality (Figure 52) and the best fit to survey indexes did not match our current understanding of the timing of changes to pinniped populations in outside BC waters. Furthermore, we have little data at this point indicating Dogfish are a major prey item for pinnipeds in BC.

   c. The models tended to estimate steepness at its lower bound (Figure 38), i.e., they assumed a population with no density-dependence, which is likely a result of the model attempting to reconcile recent declines in population indexes with low catches compared to historical levels rather than biological plausibility.

   d. We did not have age composition data linked to specific fleets or years and the length data we did have were at times highly variable (e.g., the commercial "discard" fleets; Figure 11) and were only weakly informative about depletion (Figure 36).

3. *Present time series of S/S_{MSY} and S/S_0 conditional on the fitted assessment models. Provide an upper bound on potential removal reference rates based on possible stock productivities and models.*

   We presented time series of S/S_0 conditional on the fitted assessment models (e.g., Figures 20, 41, D.9, 56, 59). Final year depletion (S/S_0) was relatively insensitive to model assumptions (e.g., Figures 20, 41, 52, 55). We showed that F/F_{MSY} was highly sensitive to the value of z_{frac} (Figure 41), which could not be estimated well from the data (Figure 38). In that same time-series plot, we showed S/S_{MSY} across a range of possible z_{frac} values (Figure 41). We proposed $F_{0.4S0}$ as a potential removal reference and we showed time series of $F/F_{0.4S0}$ across the models considered (Figures 57, 60). We forecasted with the models at a sequence of potential catch levels and calculated the probability that given catch levels will result in biomass being above the LRP or proposed USR and $F < F_{0.4S0}$ for each model (Figures 65–67).

4. *Calculate probabilities of population decline relevant to COSEWIC status assessment.*

   We documented probabilities of decline relevant to COSEWIC status assessments in Appendix E.

5. *Consider environmental conditions that may affect the stock as presented in the Guidelines for Implementing the Fish Stocks provisions in the Fisheries Act.*

   The primary environmental condition that may affect the stock we presented was an increase in predation via several time-varying natural mortality scenarios (Figure 50–52),

i.e., a change in ecosystem condition. We presented this change in natural mortality as potentially being due to increased predation, although the mechanism could be other environmental conditions affecting survival. In the discussion (Section 6.1), we reviewed other recent literature that has evaluated how environmental conditions (bottom temperature and sometimes oxygen) may be influencing the distribution of Dogfish in BC and nearby waters.

6. *Recommend an appropriate path forward including recommended data collection and research, a recommended timeline to revisit the assessment, and indicators before then that may trigger an earlier than scheduled assessment. Provide a rationale if indicators and triggers cannot be identified.*

   In Section 6.2, we considered data collection and research that may help reconcile BC Dogfish population dynamics in outside waters. In Section 6.3, we provided a suggested timeline for revisiting the assessment and discussed possible triggers of an earlier than scheduled assessment.

7. ACKNOWLEDGMENTS

We thank members of the Technical Working Group: T.R. Carruthers, D. Edwards, P.A. English, D. Finn, N.C. Fisch, E. Fisher, R.E. Forrest, D.R. Haggarty, G. Mason, L.A. Rogers, C. Sporer, and B. Turris. We thank G.A. McFarlane for advice on maximum Dogfish age and I.G. Taylor for advice on the Dogfish stock-recruit function. We thank D.L. Courtney and S.A. Pardo for providing constructive reviews of this report. We thank participants of the Regional Review Meeting for providing constructive feedback and suggestions that improved this report. We thank M.E. Greenlaw for chairing the Centre for Science Advice, Pacific Regional Peer Review process.

8. COMPUTATIONAL ENVIRONMENT AND REPRODUCIBILITY

The analyses for this report were conducted with R 4.4.2 (R Core Team 2024), Stock Synthesis 3.30.22.1 (Methot and Wetzel 2013), and sdmTMB 0.6.0.9004 (Anderson et al. 2024*c*). The input data, source code, and SS3 configuration files are available in a GitHub repository. The document was produced using the csasdown R package and templates.

REFERENCES CITED

Aitchison, J. 1955. On the distribution of a positive random variable having a discrete probability mass at the origin. Journal of the American Statistical Association 50(271). 901.

Alverson, D., Stansby, M., Fish, U., Service, W. and Service, U.S.N.M.F. 1963. The Spiny Dogfish (*Squalusacanthias*) in the Northeastern Pacific. Special Scientific Report–Fisheries. U.S. Department of Interior, Fish and Wildlife Service.

Anderson, A.C. 1878. Report of the Inspector of Fisheries for British Columbia for the year 1877. In Tenth Annual Report of the Minister of Marine and Fisheries for the Year, 1877, Supplement No. 5., 287–309. Department of Marine and Fisheries, Ottawa.

Anderson, S., Keppel, E. and Edwards, A. 2019. A reproducible data synopsis for over 100 species of British Columbia groundfish. DFO Can. Sci. Advis. Sec. Res. Doc. 2019/041. vii + 321 p.

Anderson, S.C., Keppel, E.A. and Edwards, A.M. 2020. Reproducible visualization of raw fisheries data for 113 species improves transparency, assessment efficiency, and monitoring. Fisheries 45. 535–543.

Anderson, S.C., Dunic, J.C., Keppel, E.A. and Edwards, A.M. 2024*a*. A data synopsis for British Columbia groundfish: 2022 data update. Can. Tech. Rep. Fish. Aquat. Sci. 3624, Fisheries and Oceans Canada.

Anderson, S.C., English, P.A., Gale, K.S.P., Haggarty, D.R., Robb, C.K., Rubidge, E.M. and Thompson, P.L. 2024*b*. Impacts on population indices if scientific surveys are excluded from marine protected areas. ICES Journal of Marine Science fsae009.

Anderson, S.C., Ward, E.J., English, P.A., Barnett, L.A.K. and Thorson, J.T. 2024*c*. sdmTMB: An R package for fast, flexible, and user-friendly generalized linear mixed effects models with spatial and spatiotemporal random fields. bioRxiv 10.1101/2022.03.24.485545.

Andrews, K. and Harvey, C. 2013. Ecosystem-level consequences of movement: Seasonal variation in the trophic impact of a top predator. Marine Ecology Progress Series 473. 247–260.

Babcock, E.A., Harford, W.J., Gedamke, T., Anderson, S C and Goodyear, C.P. 2023. Simulation-testing model-based and design-based bycatch estimators. Collect. Vol. Sci. Pap. ICCAT 80(6). 51–79.

Beamish, R.J. and McFarlane, G.A. 1985. Annulus development on the second dorsal spine of the Spiny Dogfish (*Squalus acanthias*) and its validity for age determination. Canadian Journal of Fisheries and Aquatic Sciences 42(11). 1799–1805.

Beamish, R., McFarlane, G. and Benson, A. 2006. Longevity overfishing. Progress in Oceanography 68. 289–302.

Berger, A.M. 2019. Character of temporal variability in stock productivity influences the utility of dynamic reference points. Fisheries Research 217. 185–197.

Bravington, M.V., Skaug, H.J. and Anderson, E.C. 2016. Close-Kin Mark-Recapture. Statistical Science 31(2). 259–274.

Bubley, W.J., Kneebone, J., Sulikowski, J.A. and Tsang, P.C. 2012. Reassessment of spiny dogfish Squalus acanthias age and growth using vertebrae and dorsal-fin spines. Journal of Fish Biology 80(5). 1300–1319.

Choromanski, E.M., Fargo, J., Workman, G.D. and Mathias, K. 2004. Multispecies trawl survey of Hecate Strait, F/V Viking Storm, June 10 – 28, 2002. DFO Can. Data Rep. Fish. Aquat. Sci. 2004/1124. 81 p.

Conrath, C.L. and Foy, R.J. 2009. A History of the Distribution and Abundance of Spiny Dogfish in Alaska Waters. In G. G. Gallucci, Vincent F., McFarlane, G.A., Bargmann, ed., Biology and Management of Dogfish Sharks, 119–126. American Fisheries Society, Bethesda, Maryland.

COSEWIC. 2011. COSEWIC assessment and status report on the North Pacific Spiny Dogfish *Squalus suckleyi* in Canada. COSEWIC x + 45 p.

COSEWIC. 2015. COSEWIC assessment process, categories and guidelines. Committee on the Status of Endangered Wildlife in Canada. .

Courtney, D. 2014. A preliminary review of post-release live-discard mortality rate estimates in sharks for use in SEDAR 39. Tech. Rep. SEDAR39-DW-21, North Charleston, SC, North Charleston, SC.

Dahlheim, M.E., Schulman-Janiger, A., Black, N., Ternullo, R., Ellifrit, D. and Balcomb, K.C. 2008. Eastern temperate North Pacific offshore killer whales (*Orcinus orca*): Occurrence, movements, and insights into feeding ecology. Marine Mammal Science 24(3). 719–729.

Davidson, L.N.K., English, P.A., King, J.R., Grant, P., Taylor, I.G., Barnett, L., Gertseva, V., Tribuzio, C.A. and Anderson, S.C. 2025. Rapid widespread declines of an abundant coastal shark. EcoEvoRxiv. DOI: 10.32942/X2V64Z .

De Oliveira, J., Ellis, J. and Dobby, H. 2013. Incorporating density dependence in pup production in a stock assessment of NE Atlantic spurdog *Squalus acanthias*. ICES J. Mar. Sci. 70. 1341–1353.

DFO. 2007. Assessment of Spiny Dogfish in Atlantic Canada. DFO Can. Sci. Advis. Sec. Sci. Advis. Rep. 2007/0046.

DFO. 2009. A Fishery Decision-Making Framework Incorporating the Precautionary Approach.

DFO. 2009. Recovery Potential Assessment for Basking Sharks in Canadian Pacific Waters. Tech. rep., DFO Can. Sci. Advis. Sec. Sci. Advis. Rep. 2009/046.

DFO. 2010. Assessment of Spiny Dogfish (*Squalus acanthias*) in British Columbia in 2010. DFO Can. Sci. Advis. Sec. Sci. Advis. Rep. 2010/057.

DFO. 2012. Proceedings of the Pacific Region Science Advisory Process for Spiny Dogfish (*Squalus acanthius*) in British Columbia, Canada. DFO Can. Sci. Advis. Sec. Proceed. Ser. 2011/071.

DFO. 2015. Evaluation of the Internet Recreational Effort and Catch (iREC) survey methods. DFO Can. Sci. Advis. Sec. Sci. Advis. Rep. 2015/059.

DFO. 2021. Trends in Abundance and Distribution of Steller Sea Lions (*Eumetopias jubatus*) in Canada. Can. Sci. Advis. Sec. Sci. Advis. Rep. 2021/035(August). 8.

DFO. 2022*a*. A data synopsis for British Columbia groundfish: 2021 data update. Canadian Science Advisory Secretariat Science Response 2022/020.

DFO. 2022*b*. Guidelines for writing rebuilding plans per the Fish Stocks Provisions and A Fishery Decision-making Framework Incorporating the Precautionary Approach.

DFO. 2023. California sea lion abundance estimation in Canada 2020–21. DFO Can. Sci. Advis. Sec. Sci. Advis. Rep. 2023/016.

DFO. 2024. Groundfish Integrated Fisheries Management Plan 2024/25. Tech. Rep. 23-2317.

Doherty, B., Benson, A. and Cox, S. 2019. Data summary and review of the PHMA hard bottom longline survey in British Columbia after the first 10 years (2006-2016). Canadian Technical Report of Fisheries and Aquatic Sciences 3276.

Dunn, P.K. and Smyth, G.K. 1996. Randomized quantile residuals. Journal of Computational and Graphical Statistics 5(3). 236–244.

Ebert, D.A., White, W.T., Goldman, K.J., Compagno, L.J.V., Daly–Engel, T.S. and Ward, R.D. 2010. Resurrection and redescription of *Squalus suckleyi* (Girard, 1854) from the North Pacific, with comments on the *Squalus acanthias* subgroup (Squaliformes: Squalidae). Zootaxa 2612(1).

English, P.A., Ward, E.J., Rooper, C.N., Forrest, R.E., Rogers, L.A., Hunter, K.L., Edwards, A.M., Connors, B.M. and Anderson, S.C. 2021. Contrasting climate velocity impacts in warm and cool locations show that effects of marine warming are worse in already warmer temperate waters. Fish and Fisheries 23(1). 239–255.

Fallows, C., Benoît, H.P. and Hammerschlag, N. 2015. Intraguild predation and partial consumption of blue sharks Prionace glauca by Cape fur seals Arctocephalus pusillus pusillus. African Journal of Marine Science 37(1). 125–128.

Ford, J.K., Ellis, G.M., Matkin, C.O., Wetklo, M.H., Barrett-Lennard, L.G. and Withler, R.E. 2011. Shark predation and tooth wear in a population of northeastern pacific killer whales. Aquatic Biology 11(3). 213–224.

Forrest, R.E., Anderson, S.C., Grandin, C.J. and J., S.P. 2020. Assessment of Pacific Cod (*Gadus macrocephalus*) for Hecate Strait and Queen Charlotte Sound (Area 5ABCD), and West Coast Vancouver Island (Area 3CD) in 2018. DFO Can. Sci. Advis. Sec. Res. Doc. 2020/070. v + 215 p.

Forrest, R. and Walters, C. 2009. Estimating thresholds to optimal harvest rate for long-lived, low-fecundity sharks accounting for selectivity and density dependence in recruitment. Can. J. Fish. Aquat. Sci. 66. 2062–2080.

Freshwater, C., Anderson, S.C. and King, J. 2024. Model-based indices of juvenile Pacific salmon abundance highlight species-specific seasonal distributions and impacts of changes to survey design. Fisheries Research 277. 107,063.

Frick, L.H., Reina, R.D. and Walker, T.I. 2010*a*. Stress related physiological changes and post-release survival of Port Jackson sharks (*Heterodontus portusjacksoni*) and gummy sharks (*Mustelus antarcticus*) following gill-net and longline capture in captivity. Journal of Experimental Marine Biology and Ecology 385(1). 29–37.

Frick, L.H., Walker, T.I. and Reina, R.D. 2010*b*. Trawl capture of Port Jackson sharks, *Heterodontus Portusjacksoni*, and gummy sharks, *Mustelus antarcticus*, in a controlled setting: Effects of tow duration, air exposure and crowding. Fisheries Research 106(3). 344–350.

Gallucci, V., Taylor, I., King, J., McFarlane, G.A. and McPhie, R. 2011. Spiny Dogfish (*Squalus acanthias*) assessment and catch recommendations for 2010. DFO Can. Sci. Advis. Sec. Res. Doc. 2011/034. xii + 69 p.

Gay, D.M. 1990. Usage summary for selected optimization routines. Computing science technical report 153. 1–21.

Gertseva, V., Taylor, I.G., Wallace, J. and Matson, S.E. 2021. Status of the Pacific Spiny Dogfish shark resource off the continental U.S. Pacific Coast in 2022. Tech. rep., Pacific Fishery Management Council, Portland, OR.

Grüss, A., Walter, J.F., Babcock, E.A., Forrestal, F.C., Thorson, J.T., Lauretta, M.V. and Schirripa, M.J. 2019. Evaluation of the impacts of different treatments of spatio-temporal variation in catch-per-unit-effort standardization models. Fisheries Research 213. 75–93.

Hamel, O. and Cope, J. 2022. Development and considerations for application of a longevity-based prior for the natural mortality rate. Fish. Res. 256. 106,477.

Hardy, S.M., Lacko, L.C. and Holt, K.R. 2024. Summary of the 2022 British Columbia Sablefish (*Anoplopoma fimbria*) trap survey, October 3–November 19, 2022. Can. Tech. Rep. Fish. Aquat. Sci. 3625, Fisheries and Oceans Canada.

Hart, J.L., Clemens, W.A. and Fisheries Research Board of Canada. 1973. Pacific Fishes of Canada. Fisheries Research Board of Canada.

Hartig, F. 2022. DHARMa: Residual Diagnostics for Hierarchical (Multi-Level / Mixed) Regression Models. R package version 0.4.6.

Haskard, K.A. 2007. An Anisotropic Matern Spatial Covariance Model: REML Estimation and Properties. Thesis.

Hilbe, J.M. 2011. Negative Binomial Regression. Cambridge University Press.

Hoffman, M.D. and Gelman, A. 2014. The No-U-Turn Sampler: adaptively setting path lengths in Hamiltonian Monte Carlo. Journal of Machine Learning Research 15. 1593–1623.

Holden, M. 1977. Elasmobranchs. In Fish Population Dynamics, 187–215. Wiley and Sons, New York.

Holland, G.A. 1957. Migration and growth of the dogfish shark, *Squalus acanthias* (Linnaeus), of the eastern North Pacific. Wash. Dept. Fish. Fish. Res. Pap. 2(1). 43–59.

Hordyk, A., Ono, K., Sainsbury, K., Loneragan, N. and Prince, J. 2015. Some explorations of the life history ratios to describe length composition, spawning-per-recruit, and the spawning potential ratio. ICES J. Mar. Sci. 72. 204–216.

Huynh, Q., Siegle, M. and Haggarty, D. 2024. Application of the management procedure framework for Outside Quillback Rockfish (*Sebastes maliger*) in British Columbia in 2021. DFO Can. Sci. Advis. Sec. Res. Doc. In press.

Jones, B.C. and Geen, G.H. 1976. Taxonomic reevaluation of the Spiny Dogfish (*Squalus acanthias* L.) in the Northeastern Pacific Ocean. Journal of the Fisheries Research Board of Canada 33(11). 2500–2506.

Jones, B. and Geen, G. 1977. Food and feeding of spiny dogfish (*Squalus acanthias*) in british columbia waters. Journal of the Fisheries Research Board of Canada 34. 2067–2078.

Ketchen, K.S. 1969. A review of the dogfish problem off the West Coast of Canada. Tech. Rep. 1048, Fisheries Research Board of Canada, Nanaimo, BC, Canada.

Ketchen, K.S. 1986. The Spiny Dogfish (*Squalus Acanthias*) in the Northeast Pacific and a History of Its Utilization. No. 88 in Canadian Special Publication of Fisheries and Aquatic Sciences. Dept. of Fisheries and Oceans, Ottawa.

Ketchen, K. 1972. Size at Maturity, Fecundity, and Embryonic Growth of the Spiny Dogfish (*Squalus acanthia*) in British Columbia Waters. J. Fish. Res. Bd. Can. 29. 1717–1723.

Ketchen, K. 1975. Age and growth of dogfish *Squalus acanthias* in British Columbia waters. J. Fish. Res. Bd. Can. 32. 43–59.

King, J., McFarlane, G.A., Gertseva, V., Gasper, J., Matson, S. and Tribuzio, C.A. 2017. Shark Interactions With Directed and Incidental Fisheries in the Northeast Pacific Ocean: Historic and Current Encounters , and Challenges for Shark Conservation. In Advances in Marine Biology, vol. 78, 9–44. Elsevier.

Kristensen, K., Nielsen, A., Berg, C.W., Skaug, H. and Bell, B.M. 2016. TMB: Automatic differentiation and Laplace approximation. Journal of Statistical Software 70(5). 1–21.

Kuriyama, P.T., Branch, T.A., Hicks, A.C., Harms, J.H. and Hamel, O.S. 2019. Investigating three sources of bias in hook-and-line surveys: Survey design, gear saturation, and multispecies interactions. Canadian Journal of Fisheries and Aquatic Sciences 76(2). 192–207.

Lindgren, F. 2024. fmesher: Triangle Meshes and Related Geometry Tools. R package version 0.1.7.

Lindgren, F., Rue, H. and Lindström, J. 2011. An explicit link between Gaussian fields and Gaussian Markov random fields: The stochastic partial differential equation approach. Journal of the Royal Statistical Society: Series B (Statistical Methodology) 73(4). 423–498.

Matérn, B. 1960. Spatial Variation. Springer, New York.

McAllister, M.K. and Ianelli, J.N. 1997. Bayesian stock assessment using catch-age data and the sampling - importance resampling algorithm. Canadian Journal of Fisheries and Aquatic Sciences 54(2). 284–300.

McCullagh, P. and Nelder, J.A. 1989. Generalized linear models. Chapman & Hall, New York.

McFarlane, G.A. and Beamish, R.J. 1987. Validation of the dorsal spine method of age determination for spiny dogfish. In R. C. Summerfelt and G. E. Hall, eds., The Age and Growth of Fish, 287–300. Iowa State University Press, Ames, Iowa.

McFarlane, G. and King, J. 2003. Migration patterns of spiny dogfish (*Squalus acanthias*) in the North Pacific Ocean. Fish. Bull. 101. 358–367.

McFarlane, G. and King, J. 2009. Re-evaluating the Age Determination of Spiny Dogfish Using Oxytetracycline and Fish at Liberty Up to 20 Years. In V. Gallucci, G. McFarlane and G. Bargmann, eds., Biology and management of dogfish sharks, chap. 13, 153–160. American Fisheries Society.

McFarlane, G. and King, J. 2020. Sharks, Skates, Rays and Chimeras of British Columbia. Royal BC Museum, Victoria, BC.

McFarlane, G., McPhie, R. and King, J. 2010. Distribution and life history parameters of elasmobranch species in british columbia waters. Can. Tech. Rep. Fish. Aquat. Sci. 2908, Fisheries and Oceans Canada.

Mecklenburg, C., Mecklenburg, T. and Thorsteinson, L. 2002. Fishes of Alaska. American Fisheries Society, Bethsda, Maryland.

Methot, R. and Wetzel, C. 2013. Stock synthesis: A biological and statistical framework for fish stock assessment and fishery management. Fish. Res. 142. 86–99.

Monnahan, C. and Kristensen, K. 2018. No-U-turn sampling for fast Bayesian inference in ADMB and TMB: Introducing the adnuts and tmbstan R packages. PLoS ONE 13(5). e0197,954.

NEFSC. 2006. 43rd Northeast Regional Stock Assessment Workshop (43rd SAW): 43rd SAW assessment summary report. Northeast Fish. Sci. Cent. Ref. Doc. 06-14.

Olesiuk, P. 2018. Recent Trends in Abundance of Steller Sea Lions (*Eumetopias jubatus*) in British Columbia. DFO Can. Sci. Advis. Sec. Res. Doc. 2018/006. v + 67 p.

Orlov, A.M., Savinykh, V.F., Kulish, E.F. and Pelenev, D.V. 2012. New data on the distribution and size composition of the North Pacific spiny dogfish *Squalus suckleyi* (Girard, 1854). Scientia Marina 76(1). 111–122.

Page, L.M., Bemis, K.E., Dowling, T.E., Espinosa-Pérez, H.S., Findley, L.T., Gilbert, C.R., Hartel, K.E., Lea, R.N., Mandrak, N.E., Neighbors, M.A., Schmitter-Soto, J.J. and Walker, H.J., eds. 2013. Common and Scientific Names of Fishes from the United States, Canada, and Mexico, 8th Edition. American Fisheries Society, 8 ed.

Pella, J.J. and Tomlinson, P.K. 1969. A generalized stock production model. Inter-American Tropical Tuna Commission Bulletin 13(3). 416–497.

R Core Team. 2024. R: A Language and Environment for Statistical Computing. R Foundation for Statistical Computing, Vienna, Austria.

Rice, J., Harley, S., Maunder, M. and Da-Silva, A.A. 2013. Stock assessment of blue sharks in the north Pacific Ocean using Stock Synthesis. Tech. Rep. WCPFC-SC9-2013/SA-WP-02, Western and Central Pacific Fisheries Commission.

Rothschild, B.J. 1967. Competition for gear in a multiple-species fishery. ICES Journal of Marine Science 31(1). 102–110.

Rufener, M.C., Kristensen, K., Nielsen, J.R. and Bastardie, F. 2021. Bridging the gap between commercial fisheries and survey data to model the spatiotemporal dynamics of marine species. Ecological Applications 31(8). e02,453.

Saunders, M.W. 1989. Spiny Dogfish *In* groundfish stock assessments for the West Coast of Canada in 1988 and recommended yield options for 1989. Canadian Technical Report of Fisheries and Aquatic Sciences 1646, Department of Fisheries and Oceans.

Saunders, M.W. and McFarlane, G.A. 1993. Age and length at maturity of the female spiny dogfish, *Squalus acanthias*, in the Strait of Georgia, British Columbia, Canada. Environmental Biology of Fishes 38(1-3). 49–57.

Shiffman, D., Bangley, C. and Macdonald, C. 2022. "A prized Pacific shark": the rise and fall (and rise again . . . ?) of the world's first ecolabel certified sustainable shark fishery. Fish Biology 103(3). 623–634.

Shmidt, P.YU. 1950. Fishes of the Sea of Okhotsk. Israel Program for Sci. Translations, Jerusalem, 1965.

Sinclair, A., Schnute, J.T., Haigh, R., Starr, P.J., Stanley, R., Fargo, J. and Workman, G. 2003. Feasibility of multispecies groundfish bottom trawl surveys on the BC coast. Canadian Science Advisory Secretariat Research Document 2003/049.

Smith, S.E., Au, D.W. and Show, C. 1998. Intrinsic rebound potentials of 26 species of Pacific sharks. Marine and Freshwater Research 49(7). 663.

Taylor, I.G. and Gallucci, V.F. 2009. Unconfounding the effects of climate and density dependence using 60 years of data on spiny dogfish (*Squalus Acanthias*). Canadian Journal of Fisheries and Aquatic Sciences 66(3). 351–366.

Taylor, I., Gertseva, V. and Matson, S. 2013*a*. Spine-based ageing methods in the spiny dogfish shark, *Squalus suckleyi*: How they measure up. Fish. Res. 147. 83–92.

Taylor, I., Gertseva, V., Methot, R. and Maunder, M. 2013*b*. A stockrecruitment relationship based on pre-recruit survival, illustrated with application to spiny dogfish shark. Fish. Res. 142. 15–21.

Taylor, T. 2008. Modeling spiny dogfish population dynamics in the Northeast Pacific. Ph.D. thesis, University of Washington.

Thorson, J.T. and Kristensen, K. 2016. Implementing a generic method for bias correction in statistical models using random effects, with spatial and population dynamics examples. Fisheries Research 175. 66–74.

Thorson, J.T. and Kristensen, K. 2024. Spatio-Temporal Models for Ecologists. CRC Press, Boca Raton, FL.

Thorson, J.T., Shelton, A.O., Ward, E.J. and Skaug, H.J. 2015. Geostatistical delta-generalized linear mixed models improve precision for estimated abundance indices for West Coast groundfishes. ICES Journal of Marine Science: Journal du Conseil 72(5). 1297–1310.

Thorson, J.T., Cunningham, C.J., Jorgensen, E., Havron, A., Hulson, P.J.F., Monnahan, C.C. and von Szalay, P. 2021. The surprising sensitivity of index scale to delta-model assumptions: Recommendations for model-based index standardization. Fisheries Research 233. 105,745.

Thorson, J. 2019. Guidance for decisions using the Vector Autoregressive Spatio-Temporal (VAST) package in stock, ecosystem, habitat and climate assessments. Fish. Res. 210. 143–161.

Thygesen, U.H., Albertsen, C.M., Berg, C.W., Kristensen, K. and Nielsen, A. 2017. Validation of ecological state space models using the Laplace approximation. Environmental and Ecological Statistics 24(2). 317–339.

Trenkel, V.M., Charrier, G., Lorance, P. and Bravington, M.V. 2022. Close-kin mark–recapture abundance estimation: Practical insights and lessons learned. ICES Journal of Marine Science 79(2). 413–422.

Tribuzio, C.A. and Kruse, G.H. 2011. Demographic and risk analyses of spiny dogfish (*Squalus Suckleyi*) in the Gulf of Alaska using age- and stage-based population models. Marine and Freshwater Research 62(12). 1395–1406.

Tribuzio, C.A., Matta, M.E., Echave, K.B., Rodgveller, C., Dunne, G. and Fuller, K. 2022. Assessment of the Shark Stock Complex in the Bering Sea/ Aleutian Islands and Gulf of Alaska. Tech. rep., NOAA National Marine Fisheries Service.

Trites, A.W. and Calkins, D.G. 2008. Diets of mature male and female steller sea lions (*Eumetopias jubatus*) differ and cannot be used as proxies for each other. Aquatic Mammals 34(1). 25–34.

Veríssimo, A., Mcdowell, J.R. and Graves, J.E. 2010. Global population structure of the spiny dogfish *Squalus acanthias*, a temperate shark with an antitropical distribution. Molecular Ecology 19(8). 1651–1662.

Waagepetersen, R. 2006. A simulation-based goodness-of-fit test for random effects in generalized linear mixed models. Scandinavian Journal of Statistics 33(4). 721–731.

Ward, R.D., Holmes, B.H., Zemlak, T.S. and Smith, P.J. 2007. DNA barcoding discriminates spurdogs of the genus *Squalus*. CSIRO Marine and Atmospheric Research Paper 014, CSIRO Marine and Atmospheric Research Paper.

Watson, J., Edwards, A. and Auger-Méthé, M. 2023. A statistical censoring approach accounts for hook competition in abundance indices from longline surveys. Canadian Journal of Fisheries and Aquatic Sciences 80(3). 468–486.

Webster, R. and Wilson, D. 2023. 2023-25 FISS design evaluation. IPHC Secretariat IPHC-2023-AM099-10.

Winship, A.J. and Trites, A.W. 2003. Prey consumption of Steller sea lions (*Eumetopias Jubatus*) off Alaska: How much prey do they require? Fishery Bulletin 101. 147–167.

Wood, C., Kethen, K. and Beamish, R. 1979. Population Dynamics of Spiny Dogfish (*Squalus acanthias*) in British Columbia Waters. J. Fish. Res. Board Can. 36. 647–656.

Yalcin, S., Anderson, S.C., Regular, P.M. and English, P.A. 2023. Exploring the limits of spatiotemporal and design-based index standardization under reduced survey coverage. ICES Journal of Marine Science 80(9). 2368–2379.

Zheng, N. and Cadigan, N. 2021. Frequentist delta-variance approximations with mixed-effects models and TMB. Computational Statistics & Data Analysis 160. 107,227.

APPENDIX A. SURVEY DATA

Four surveys were considered for Outside Dogfish for developing indices of abundance: the Outside Hard-Bottom Longline (HBLL) Survey, the IPHC Fishery-Independent Setline Survey, the Synoptic Trawl Survey, and the Hecate Strait Multispecies Assemblage Bottom Trawl Survey. The design and the spatiotemporal modelling of indices, including individual set data, model residuals, effect sizes for covariate data, i.e., depth, and spatial predictions, for each survey are described here. Figure A.1 provides a summary of the annual sets and the proportion of sets with positive catch. Figure A.2 provides the number of sets by month and year. Seasonal timing can be used to evaluate whether behavioural changes, e.g., migration patterns, influence catch rates in the survey.

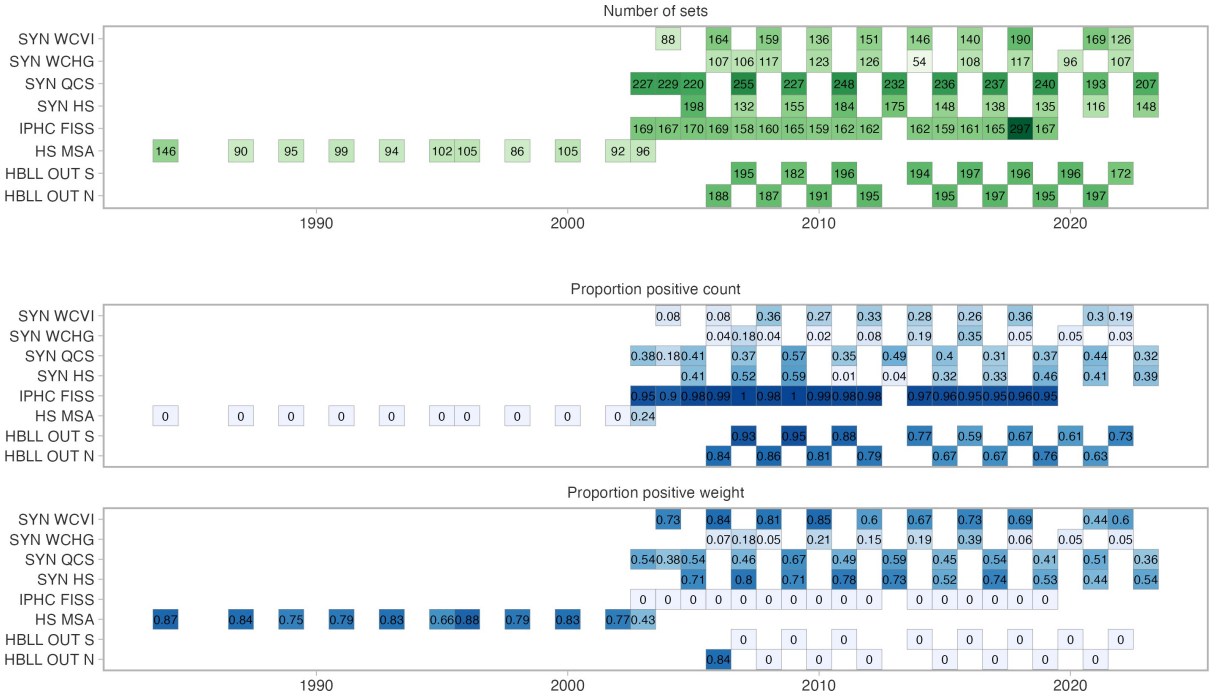

Figure A.1. Summary of survey sets for Outside Dogfish. Sets record the catch in either numbers, weight, or both. Darker colours in cells highlight a larger number of sets (green) and a higher proportion of positive sets (blue). The Synoptic survey (SYN) operates in four major areas, including West Coast Vancouver Island (WCVI), West Coast Haida Gawii (WCHG), Queen Charlotte Sound (QCS), and Hecate Strait (HS). The HBLL survey typically sample a northern (N) and southern (S) region in alternate years.

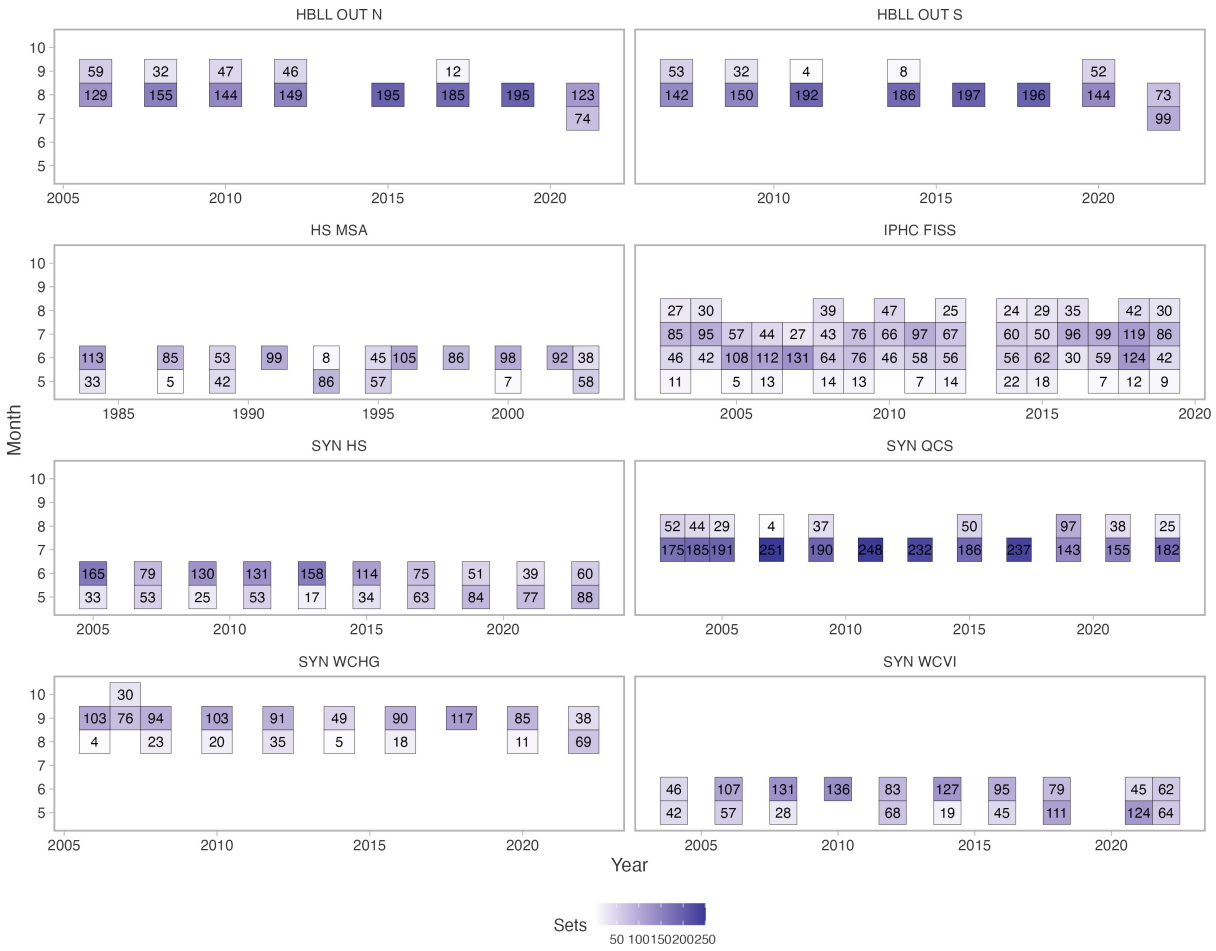

Figure A.2. Timing of survey sets across surveys. Colour shading (and numbers) reflect the number of survey sets in a given year-month combination for a given survey.

A.1. SPATIOTEMPORAL MODELLING OF SURVEY DATA

Our general approach is to fit spatiotemporal geostatistical generalized linear mixed effects models (GLMMs) to survey catch per unit effort with spatial and spatiotemporal random effects representing latent variables causing spatial and spatiotemporal patterns in the data. We can then predict from our models over a grid covering the full survey domain and sum our predictions to generate an area-weighted estimate of total (relative) biomass or abundance for the survey domain. This approach allows us to account for changes to survey design over time (e.g., with the IPHC stations changing) as well as to combine several of the surveys that are conducted with the same gear and protocols but cover alternating areas of the coast on a biennial schedule. This lets us generate a single index that covers the full survey domain instead of generating several indexes covering only part of the survey domains. Furthermore, spatiotemporal model-based estimators have been shown to be capable of generating population indices with proper statistical properties (e.g., appropriate confidence intervals coverage and a lack of bias) and with greater precision than design-based alternatives (e.g., Anderson et al. 2019, 2024*b*,*c*, Thorson et al. 2015, 2021, Thorson 2019, Yalcin et al. 2023).

A.1.1. LONGLINE SURVEY MODELS

We model all surveys that collect catch count data with GLMMs with a single linear predictor and a negative binomial (NB2) (Hilbe 2011) observation likelihood. For these count-data (longline) surveys, we model the expected value of catch y at point in space s and time t ($\mu_{\boldsymbol{s},t}$) as a linear function of fixed and random effects transformed by an inverse link function g^{-1} (here an exponential function):

$$
\begin{aligned}
\mathbb{E}[y_{\boldsymbol{s},t}] &= \mu_{\boldsymbol{s},t}, \\
\mu_{\boldsymbol{s},t} &= \exp\left(\boldsymbol{X}_{\boldsymbol{s},t}\boldsymbol{\beta} + O_{\boldsymbol{s},t} + \omega_{\boldsymbol{s}} + \epsilon_{\boldsymbol{s},t}\right), \\
\boldsymbol{\omega} &\sim \mathrm{MVNormal}\left(\mathbf{0}, \boldsymbol{\Sigma}_{\omega}\right), \\
\boldsymbol{\epsilon}_{t=1} &\sim \mathrm{MVNormal}(\mathbf{0}, \boldsymbol{\Sigma}_{\epsilon}), \\
\boldsymbol{\epsilon}_{t>1} &= \boldsymbol{\epsilon}_{t-1} + \boldsymbol{\delta}_t,\ \boldsymbol{\delta}_t \sim \mathrm{MVNormal}\left(\mathbf{0}, \boldsymbol{\Sigma}_{\epsilon}\right).
\end{aligned}
\tag{A.1}
$$

The symbol $\boldsymbol{X}$ defines a fixed effect model matrix (an intercept and quadratic effects of depth) and β defines an associated vector of coefficients; the symbol $O_{\boldsymbol{s},t}$ defines an offset term (McCullagh and Nelder 1989) accounting for effort—log hook count. The symbols $\omega_{\boldsymbol{s}}$ and $\epsilon_{\boldsymbol{s},t}$ define spatial and spatiotemporal latent variables. The vector of $\omega_{\boldsymbol{s}}$ ($\boldsymbol{\omega}$) are assumed drawn from a Gaussian Markov random field (GMRF): a multivariate normal distribution with mean zero and a covariance matrix (i.e., inverse precision matrix) $\boldsymbol{\Sigma}_{\omega}$. The GFMR is assumed to follow an anisotropic (i.e., directionally dependent) Matérn (Matérn 1960) covariance function (Haskard 2007, Lindgren et al. 2011, Thorson et al. 2015). The $\epsilon_{\boldsymbol{s},t}$ are assumed to follow a spatiotemporal random walk where the innovations from year-to-year are themselves independent draws from a GMRF. We denote these innovations with the symbol $\boldsymbol{\delta}_t$. Effectively, the $\omega_{\boldsymbol{s}}$ represent all missing static spatially correlated variables and the $\epsilon_{\boldsymbol{s},t}$ represent all missing temporally evolving spatially correlated variables. The random walk random field model structure also means that the $\epsilon_{\boldsymbol{s},t}$ account for changes to the mean expectation through time. Ongoing research suggests such a model structure performs well when combining the biennial survey designs featured here (e.g., Freshwater et al. 2024, Huynh et al. 2024).

A.1.2. HOOK COMPETITION

Varying competition for hooks through time due to varying levels of hook saturation from other fish can cause error or bias in longline survey indexes (Anderson et al. 2019, Kuriyama et al. 2019, Rothschild 1967, Watson et al. 2023). Various approaches to handling this hook

competition effect have been proposed (reviewed in Watson et al. 2023). Traditionally, an "instantaneous catch rate" adjustment has been applied (see Appendix G of Anderson et al. 2019). Recently, a model-based approach with a censored Poisson likelihood was proposed in Watson et al. (2023) where they showed it to be superior to the instantaneous catch rate adjustment. However, Watson et al. (2023) showed that Dogfish were an outlier among groundfish in longline surveys (specifically, the IPHC survey) presumably because of their high mobility and high degree of schooling—Dogfish showed an increase in CPUE as the proportion of hooks was saturated nearly to complete saturation (see Figure 6 in Watson et al. 2023). The censored likelihood approach relies on choosing a proportion threshold of hook saturation beyond which CPUE declines. For Dogfish, this limit is so close to 1 so as to not be distinguishable from 1 using the smoother approach proposed in Watson et al. (2023). As a result, the censored hook competition model has no effect on Dogfish CPUE estimates compared to a model without censoring. We therefore did not account for hook competition in our longline survey models for Dogfish. If hook competition were included in some form, it would tend to make the survey declines appear more steep than ignoring it since Dogfish are a major competitor on the HBLL and IPHC surveys and they have been declining in abundance in the surveys.

A.1.3. TRAWL SURVEY MODELS

In contrast to the longline surveys, which collect counts of Dogfish, the trawl surveys collect catch weight data that sometimes includes zeros. For these surveys, we modelled catch weight with delta or hurdle models (Aitchison 1955) that model an encounter probability with one linear predictor and an expected catch density given an encounter with a second linear predictor. Both linear predictors have the same form as Equation A.1, but the first linear predictor is structured with a Bernoulli likelihood and a logit link and the second linear predictor is structured with lognormal likelihood and a log link. Experimentation suggested a lognormal likelihood best accounted for the heavy tails in the biomass observations caused by well-known clustering or schooling of dogfish. The US West Coast assessment came to a similar conclusion (Gertseva et al. 2021). We can represent these two linear predictors as

$$\begin{aligned}
\mu_{1,\boldsymbol{s},t} &= \text{logit}^{-1}\left(\boldsymbol{X}_{1,\boldsymbol{s},t}\boldsymbol{\beta}_1 + \omega_{1,\boldsymbol{s}} + \epsilon_{1,\boldsymbol{s},t}\right), \\
\boldsymbol{\omega}_1 &\sim \text{MVNormal}\left(\mathbf{0}, \boldsymbol{\Sigma}_{1,\omega}\right), \\
\boldsymbol{\epsilon}_{1,t=1} &\sim \text{MVNormal}(\mathbf{0}, \boldsymbol{\Sigma}_{1,\epsilon}), \\
\boldsymbol{\epsilon}_{1,t>1} &= \boldsymbol{\epsilon}_{1,t-1} + \boldsymbol{\delta}_{1,t},\ \boldsymbol{\delta}_{1,t} \sim \text{MVNormal}\left(\mathbf{0}, \boldsymbol{\Sigma}_{1,\epsilon}\right),
\end{aligned} \tag{A.2}$$

and

$$\begin{aligned}
\mu_{2,\boldsymbol{s},t} &= \exp\left(\boldsymbol{X}_{2,\boldsymbol{s},t}\boldsymbol{\beta}_2 + O_{2,\boldsymbol{s},t} + \omega_{2,\boldsymbol{s}} + \epsilon_{2,\boldsymbol{s},t}\right), \\
\boldsymbol{\omega}_2 &\sim \text{MVNormal}\left(\mathbf{0}, \boldsymbol{\Sigma}_{2,\omega}\right), \\
\boldsymbol{\epsilon}_{2,t=1} &\sim \text{MVNormal}(\mathbf{0}, \boldsymbol{\Sigma}_{2,\epsilon}), \\
\boldsymbol{\epsilon}_{2,t>1} &= \boldsymbol{\epsilon}_{2,t-1} + \boldsymbol{\delta}_{1,t},\ \boldsymbol{\delta}_{2,t} \sim \text{MVNormal}\left(\mathbf{0}, \boldsymbol{\Sigma}_{2,\epsilon}\right),
\end{aligned} \tag{A.3}$$

where the symbols the same meaning as in Equation A.1 but with the subscripts 1 and 2 denoting the first and second linear predictors. Here, the offset term is defined as log area swept. The combined expectation is then a product of the expected encounter probability and the expected density conditional on encounter, i.e., $\mu_{\boldsymbol{s},t} = \mu_{1,\boldsymbol{s},t} \times \mu_{2,\boldsymbol{s},t}$.

A.1.4. AREA INTEGRATION

These spatiotemporal models can be used to make predictions on a grid covering the survey domain (e.g., Figures A.4, A.9, A.17, A.25). By summing the predicted biomass or abundance

density multiplied by the area of each grid cell, we can integrate biomass or abundance over the full survey domain. This form of discretized integration is sometimes called Monte Carlo integration (Thorson and Kristensen 2024).

A.1.5. MODEL FITTING

Fitting spatial or spatiotemporal models is often computationally challenging. One computationally efficient approach is to use the the SPDE (stochastic partial differential equation) approach, which links efficient and discreetly indexed GMRFs to continuously indexed Gaussian random fields (Lindgren et al. 2011). We fit these GMRF models with the R (R Core Team 2024) package sdmTMB (Anderson et al. 2024*c*), which is an interface to a TMB (Kristensen et al. 2016) model template that uses input matrices needed to define the precision matrix constructed via the fmesher (Lindgren 2024) R package. We fit the models with maximum marginal likelihood with a non-linear minimizer (`nlminb`) in R (R Core Team 2024). We then applied an additional Newton optimization step (using `optimHess`) to further reduce the absolute marginal log likelihood gradients (Gay 1990, R Core Team 2024). Standard errors were calculated with the generalized delta method (Kristensen et al. 2016, Zheng and Cadigan 2021). We corrected for bias caused by the non-linear (exponential) transformation of random effects when making density predictions with a generic bias adjustment algorithm in TMB (Thorson and Kristensen 2016). We assessed model convergence by checking that the maximum absolute marginal log-likelihood gradient with respect to fixed effects was < 0.001, that the Hessian was positive definite, and that no random field marginal standard deviations were < 0.01 (which would imply they were near a parameter boundary).

A.1.6. MODEL EVALUATION

We evaluated whether the models' distributional assumptions were consistent with the observed data by inspecting randomized quantile residuals (Dunn and Smyth 1996). In the case of the negative binomial count models, we calculated the residuals based on the known theoretical NB2 quantile function. In the case of the delta-lognormal models for biomass data, we calculated the residuals using a simulation approach to derive the quantiles of the observed data with respect to simulated observations (Hartig 2022). In all cases, we derived expected values for the purpose of residual calculation after taking a single draw of the random effects from their approximate (multivariate normal) posterior distribution. This one-sample approach for the random effects (vs. using "empirical Bayes" estimates that are penalized towards the mean) is necessary to generate residuals with the expected distribution (Rufener et al. 2021, Thorson and Kristensen 2024, Thygesen et al. 2017, Waagepetersen 2006).

A.2. OUTSIDE HBLL SURVEY

We adapt the following survey description from recent Outside Quillback Research Document (Huynh et al. 2024):

The Outside HBLL Survey is conducted by DFO in collaboration with the Pacific Halibut Management Association (PHMA) and takes place on several chartered commercial fishing vessels each year since 2006. The HBLL survey covers most of the hard bottom, i.e., untrawlable habitats, of British Columbia coastline, excluding the inlets and protected waters east of Vancouver Island, i.e., excluding Statistical Areas 12-20 and 27–29. The PHMA provides the chartered commercial fishing vessels and field technicians, while DFO provides support for running the surveys, including survey design and equipment. The survey excludes Rockfish Conservation Areas.

The survey has a depth-stratified (shallow: 20–70 m; medium: 71–150 m; deep: 151–260 m), random design consisting of 2 km by 2 km survey blocks. The survey uses size 14/0 circle hooks, baited with frozen squid. Each set has a two-hour soak time. Hook-by-hook data, which has been collected since the start of the survey, is electronically collected and stored in a database. For further details on survey design, see Doherty et al. (2019).

The survey area is divided into northern and southern regions, which are fished in alternating years (Figure A.3). Both regions incorporate some parts of Management Areas 5B and 5C. The survey was not run in 2013. The 2012 survey covered the northern region and the 2014 continued the alternating scheme and sampled the southern region.

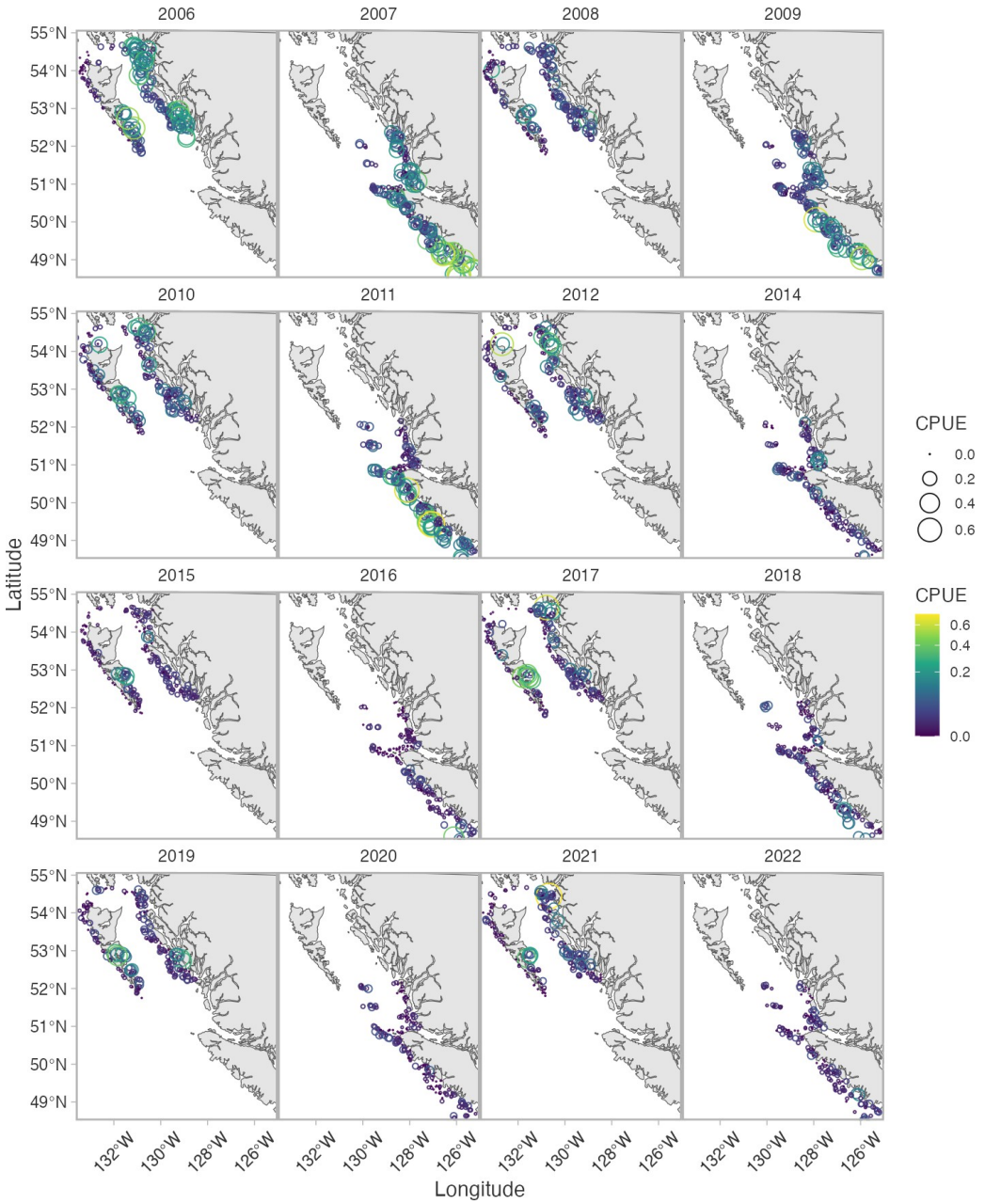

Figure A.3. Catch rates (units of Dogfish count per hook) from the Outside HBLL survey.

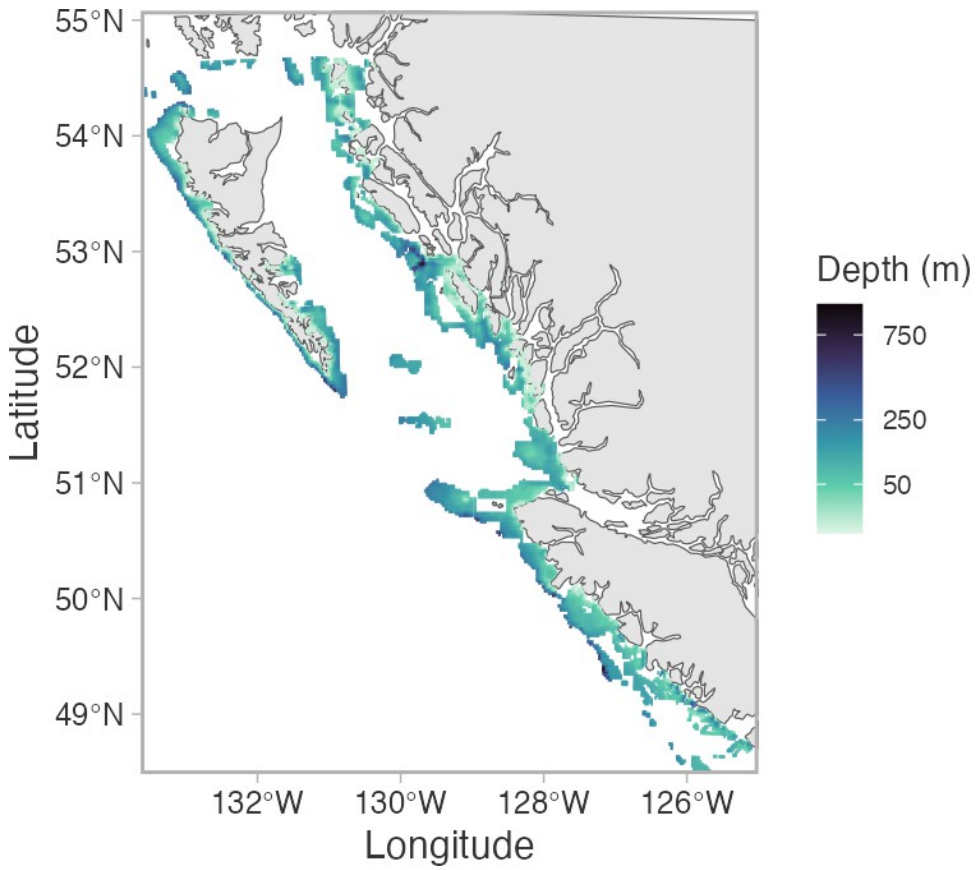

Figure A.4. Depth of the Outside HBLL survey grid.

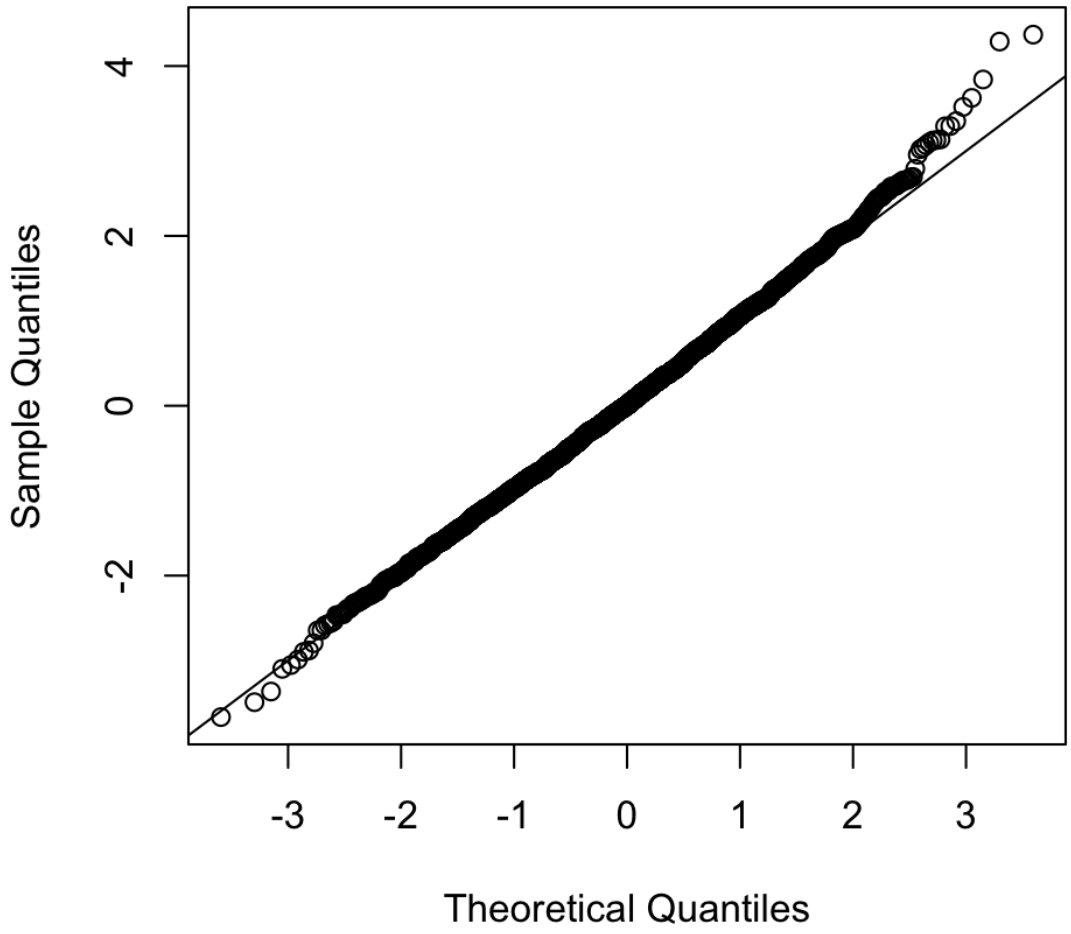

Figure A.5. Randomized quantile residuals for the NB2 spatiotemporal model fit to the Outside HBLL survey catches. The expected distribution in this case is a normal distribution if the observations are consistent with the model.

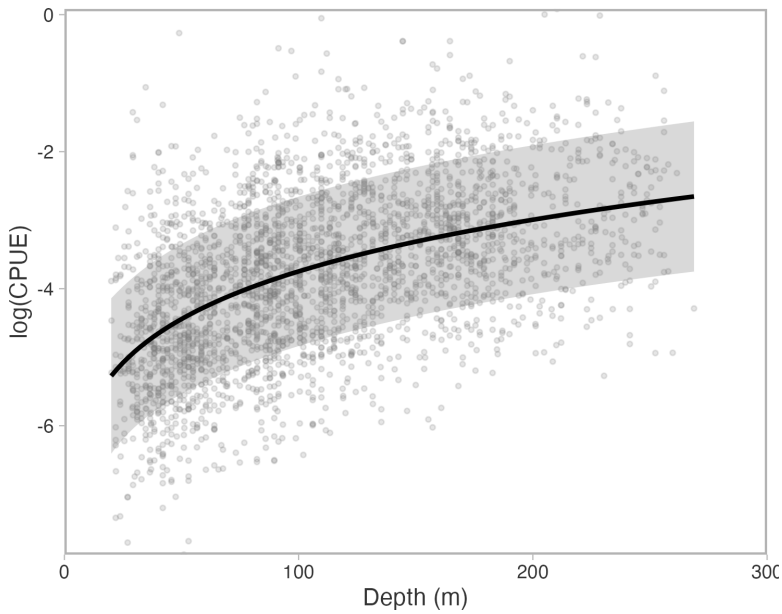

Figure A.6. Log outside HBLL catch rate by depth from individual sets (points) and the conditional depth effect (black line) estimated in the spatiotemporal model. Dots represent partial randomized quantile residuals. The grey ribbon indicates the 95% confidence interval on the mean.

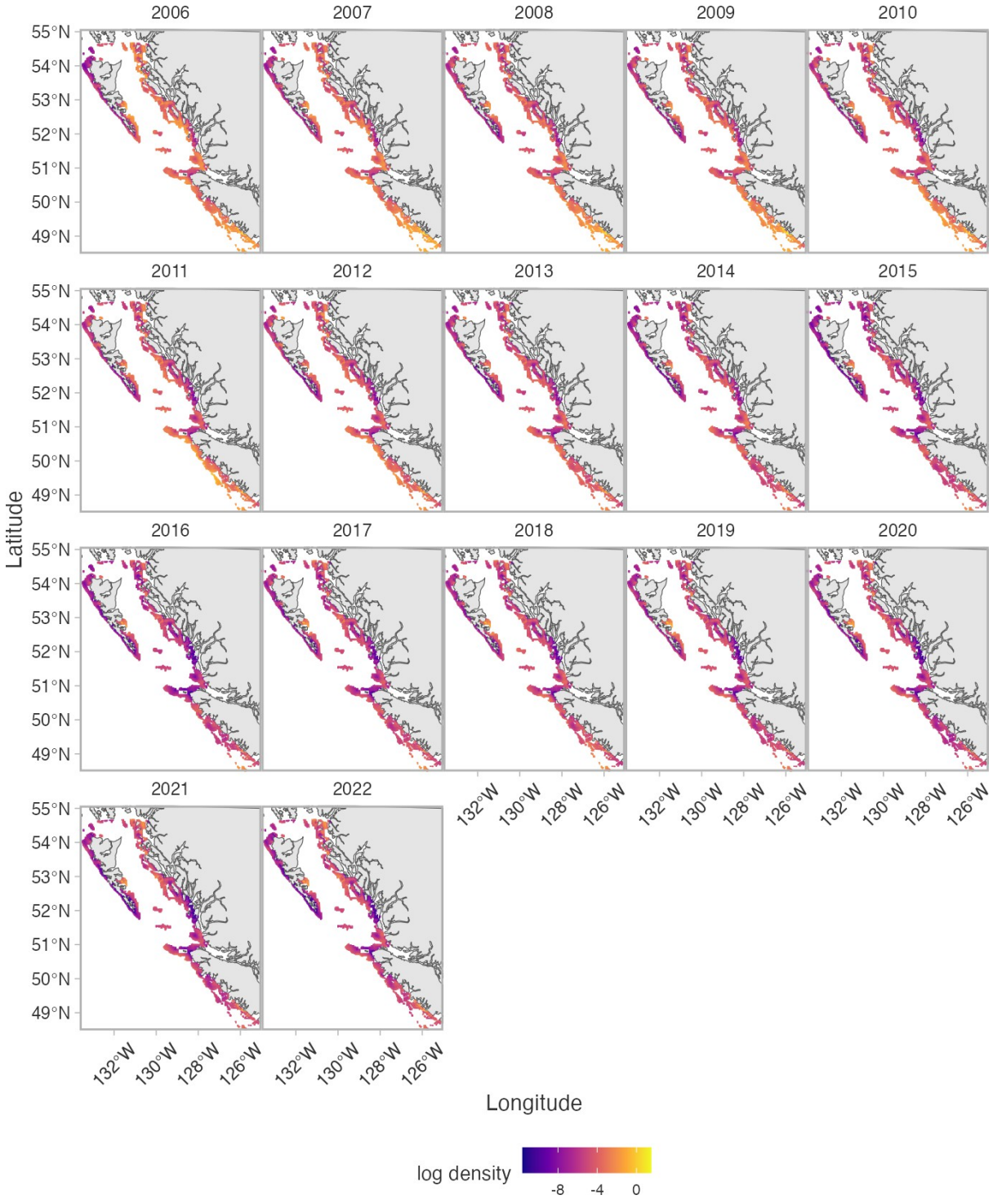

Figure A.7. Predicted log density (log Dogfish count per hook) from the spatiotemporal model for the Outside HBLL survey.

A.3. IPHC FISHERY-INDEPENDENT SETLINE SURVEY

We adapt the following survey description from the recent Outside Quillback Research Document (Huynh et al. 2024):

The International Pacific Halibut Commission (IPHC) has conducted an annual fishery-independent setline survey (FISS) in BC coastal waters since 1995. The survey is intended to index population trends of Pacific halibut but incidentally many other species, including Dogfish. The sampling design of the survey in BC waters has changed over time. Between 1995–1997, the survey had a spatially triangular station design and the data are not made avaialble publicly. In 1998, stations were re-organized and evenly spaced in northern BC (5ABCDE), then expanded down into West Coast Vancouver Island (WCVI, Areas 3CD) in 1999 (Figure A.8). In 2020, only the stations in 5ABCDE (excluding WCVI) were sampled. A random subset of WCVI stations are sampled for 2021–2022, and it is likely that this sampling scheme will continue (Webster and Wilson 2023).

The resolution at which rockfish catch is recorded in the IPHC FISS survey has varied depending on the availability of a third technician. In some years, catch is recorded on a hook-by-hook or set level, whereas in other years, only the catch in the first 20 hooks per skate is recorded (Anderson et al. 2019).

Here, we develop an index from 1998 onwards, excluding the sets that used the previous station design during 1995–1997. Expansion stations introduced since 2018 were also excluded (Figure A.12). We use the unique stations themselves as the survey “grid” rather than overlaying a separate grid onto the survey domain (Figure A.9).

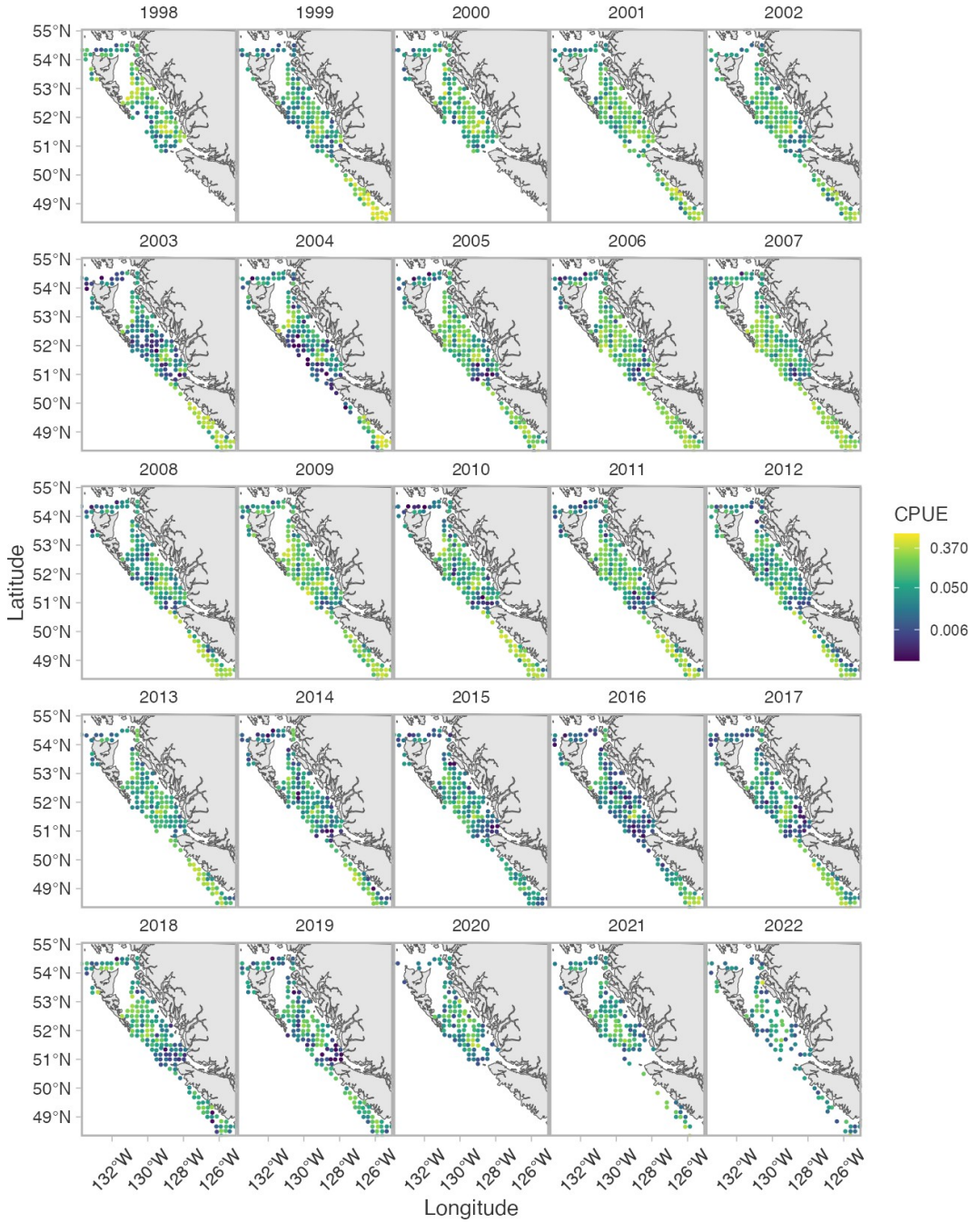

Figure A.8. Catch rate (units of Dogfish per hook) by station from the IPHC survey.

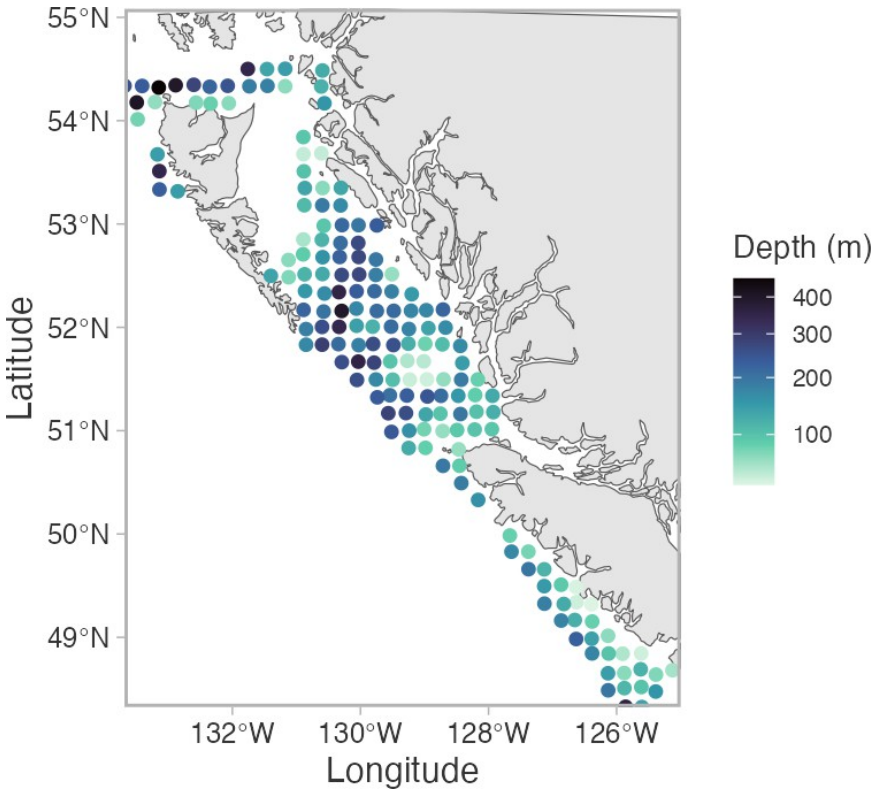

Figure A.9. Bottom depth for the IPHC survey stations.

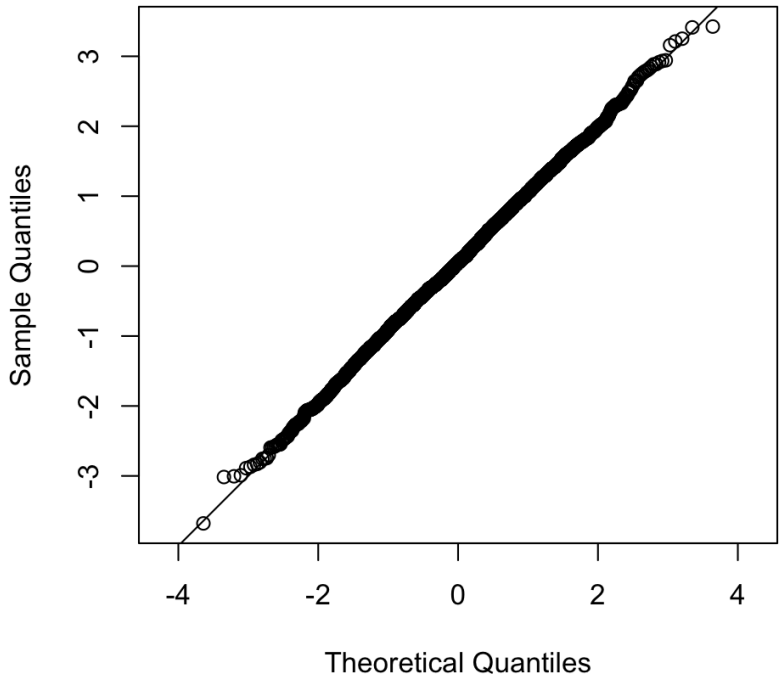

Figure A.10. Randomized quantile residuals for the NB2 spatiotemporal model fit to the IPHC survey catches. The expected distribution in this case is a normal distribution if the observations are consistent with the model.

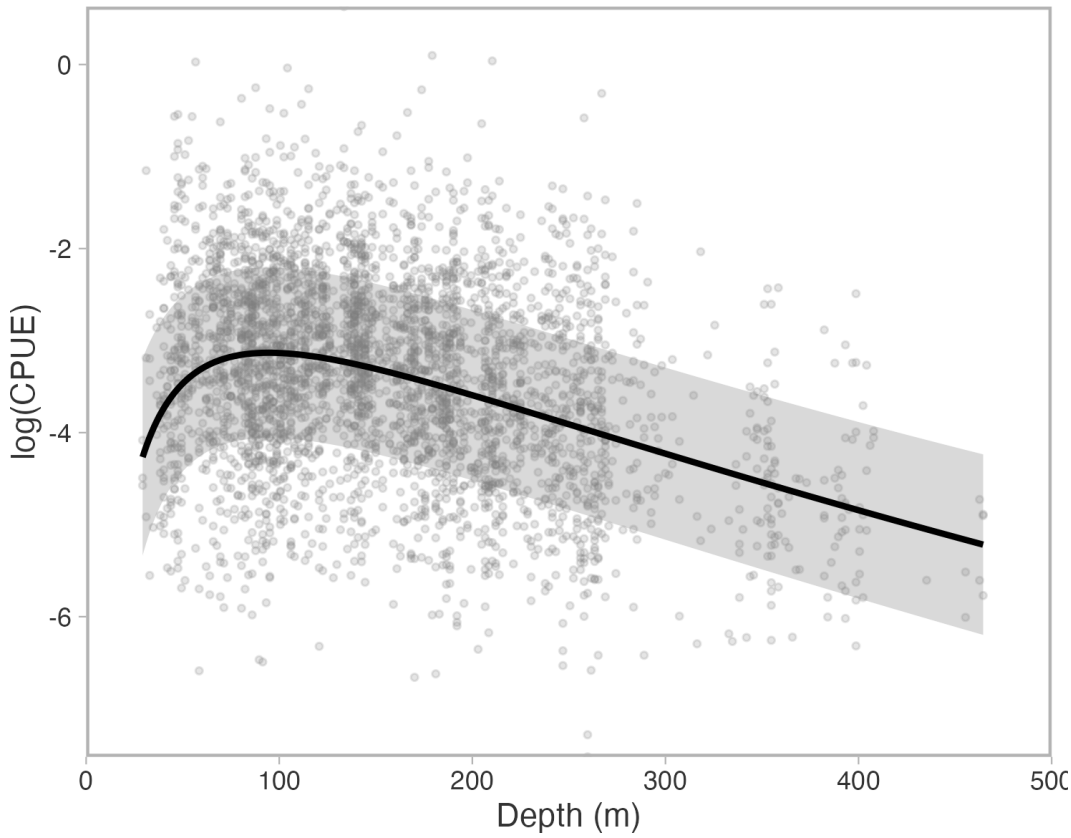

Figure A.11. Log IPHC catch rate by depth from individual sets (points) and the conditional depth effect (black line) estimated in the spatiotemporal model. Dots represent partial randomized quantile residuals. The grey ribbon indicates the 95% confidence interval on the mean.

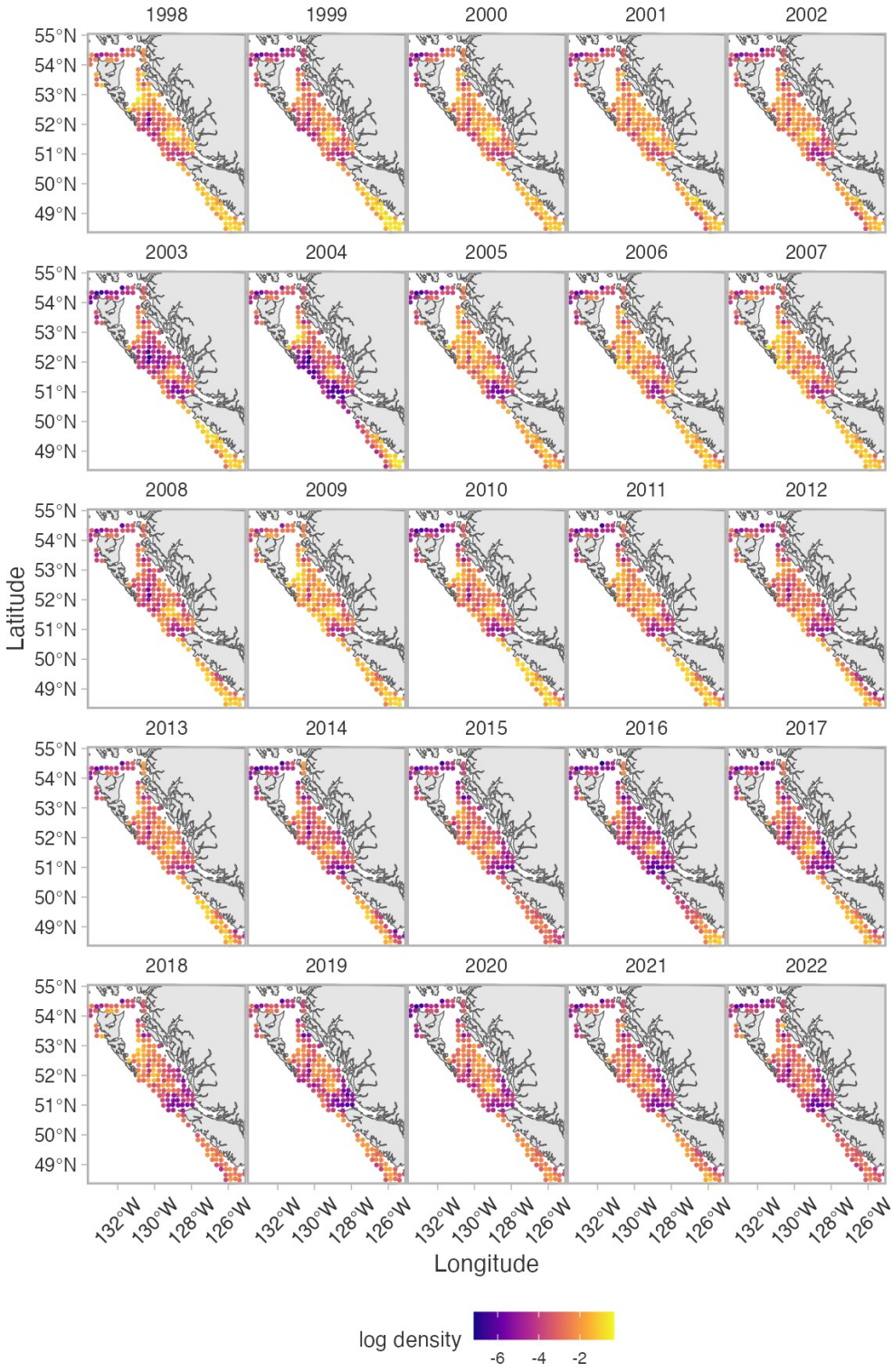

Figure A.12. Predicted log density each year at the full set of IPHC survey stations used in calculating the area-weighted index.

A.4. SYNOPTIC TRAWL SURVEYS

We adapt the following survey description from Anderson et al. (2019).

DFO, together with the Canadian Groundfish Research and Conservation Society, implemented a coordinated set of bottom trawl surveys that together cover the continental shelf and upper slope of most of the BC coast. The surveys follow a random depth stratified design with sampling units of 2 km by 2 km blocks and use the same bottom trawl fishing gear and fishing protocols (Sinclair et al. 2003). The surveys were designed to provide a synopsis of all species available to bottom trawl gear as opposed to focusing on specific species. There are a total of four synoptic (SYN) surveys: Hecate Strait (HS), West Coast Vancouver Island (WCVI), Queen Charlotte Sound (QCS), and West Coast Haida Gwaii (WCHG) (Figures A.13–A.16). Usually, two of the synoptic surveys are conducted each year on an alternating basis so that each survey is conducted every two years. In this report, we refer to these four areas as subregions and we combine them into a single coastwide index using a spatiotemporal model as described in Section A.1.3.

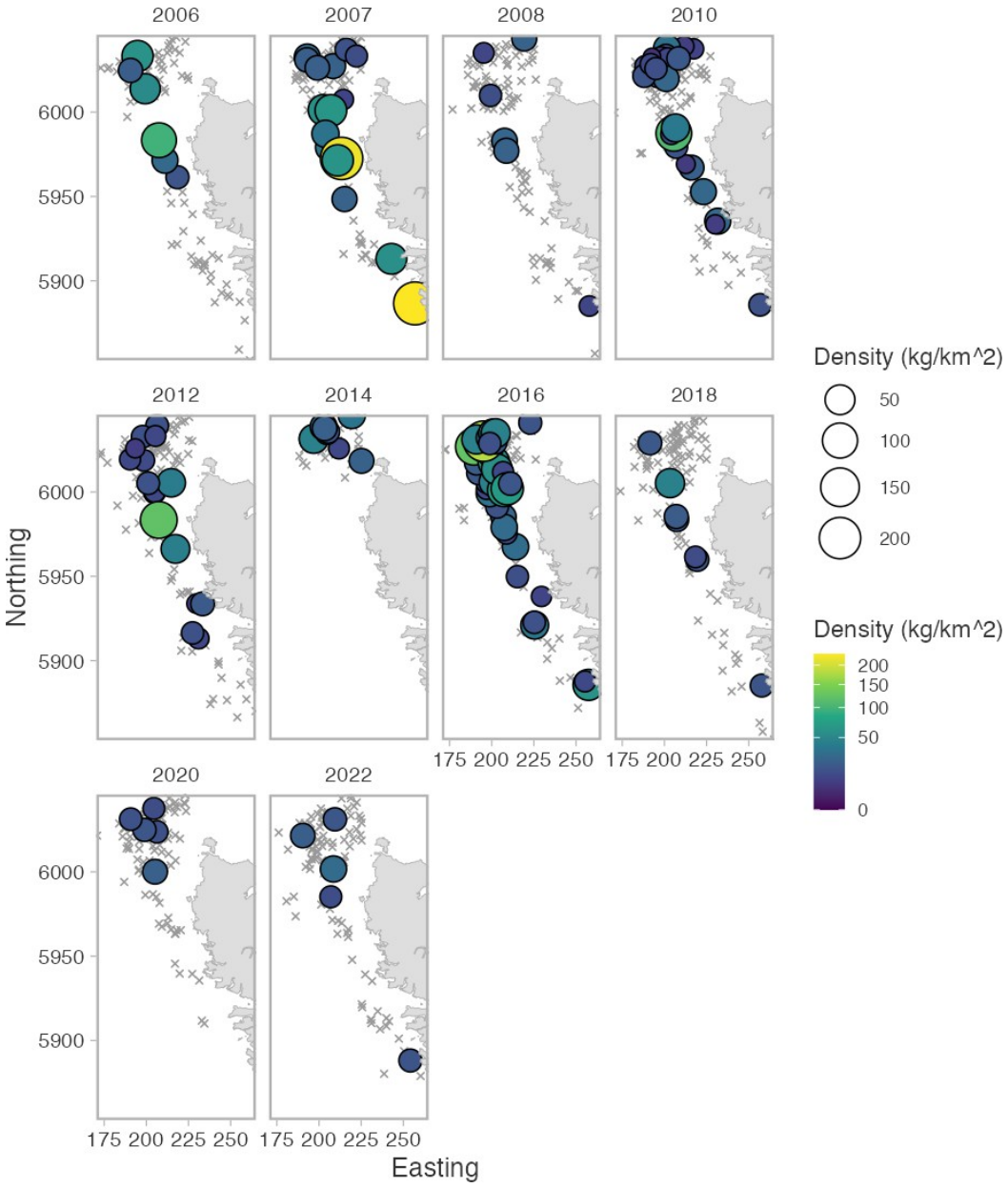

Figure A.13. Dogfish density (kg/km^2) from survey sets on the West Coast Haida Gwaii Synoptic Bottom Trawl Survey (SYN WCHG).

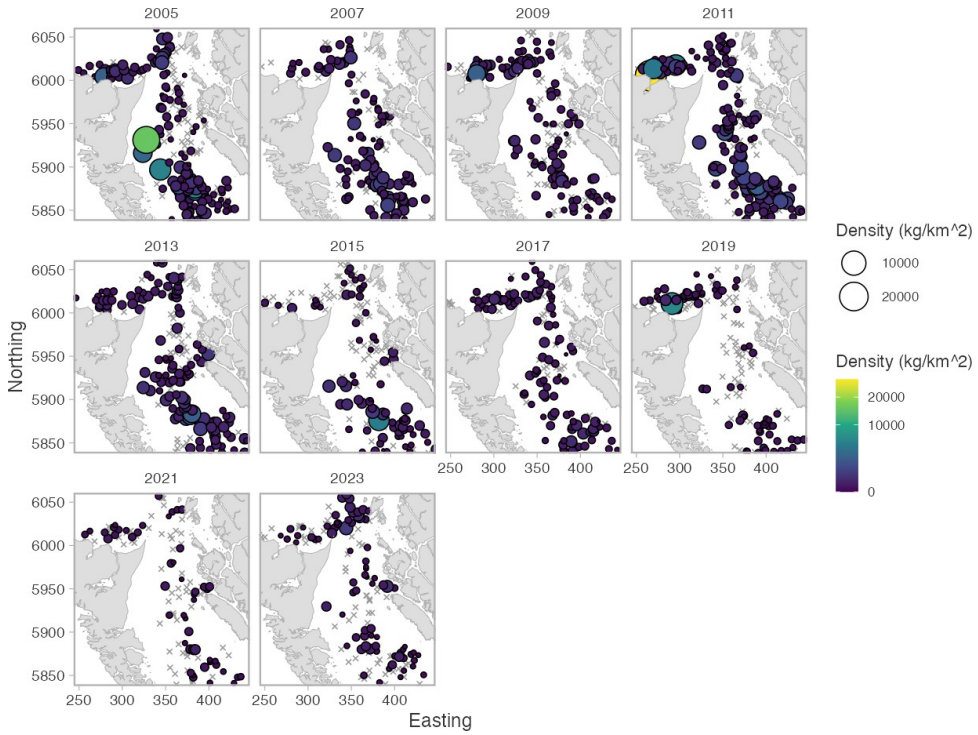

Figure A.14. Dogfish density (kg/km^2) from survey sets on the Hecate Strait Synoptic Bottom Trawl Survey (SYN HS).

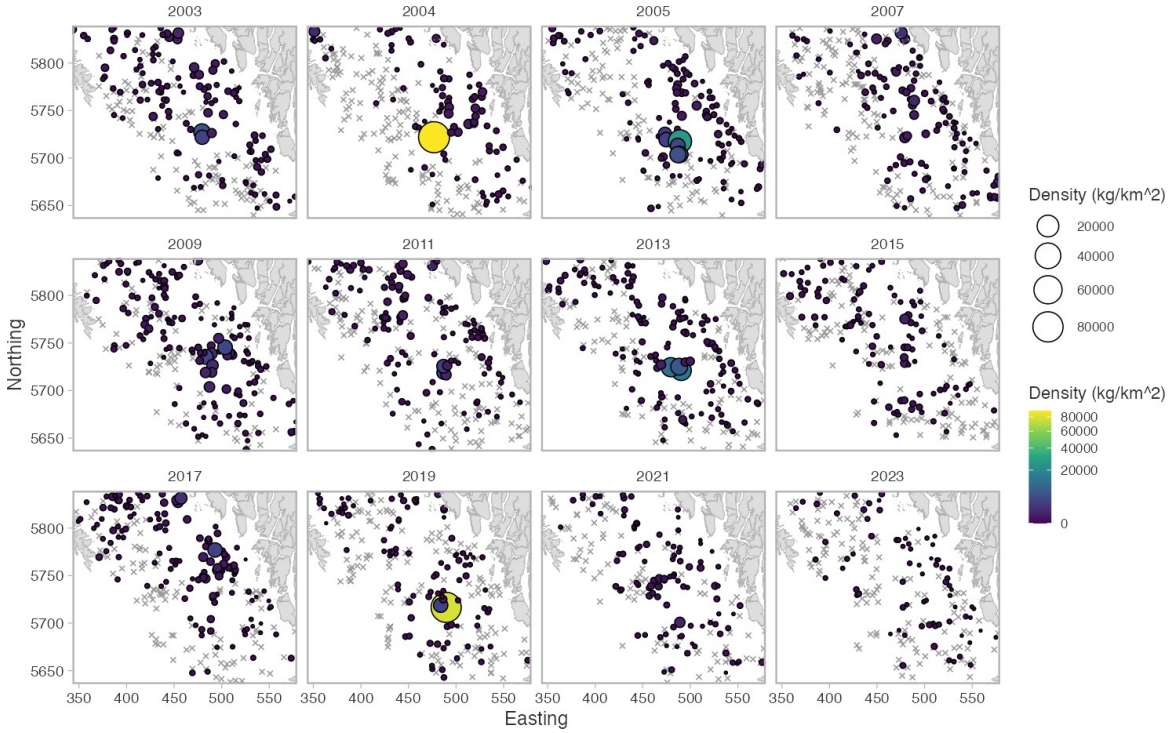

Figure A.15. Dogfish density (kg/km^2) from survey sets on the Queen Charlotte Sound Synoptic Bottom Trawl Survey (SYN QCS).

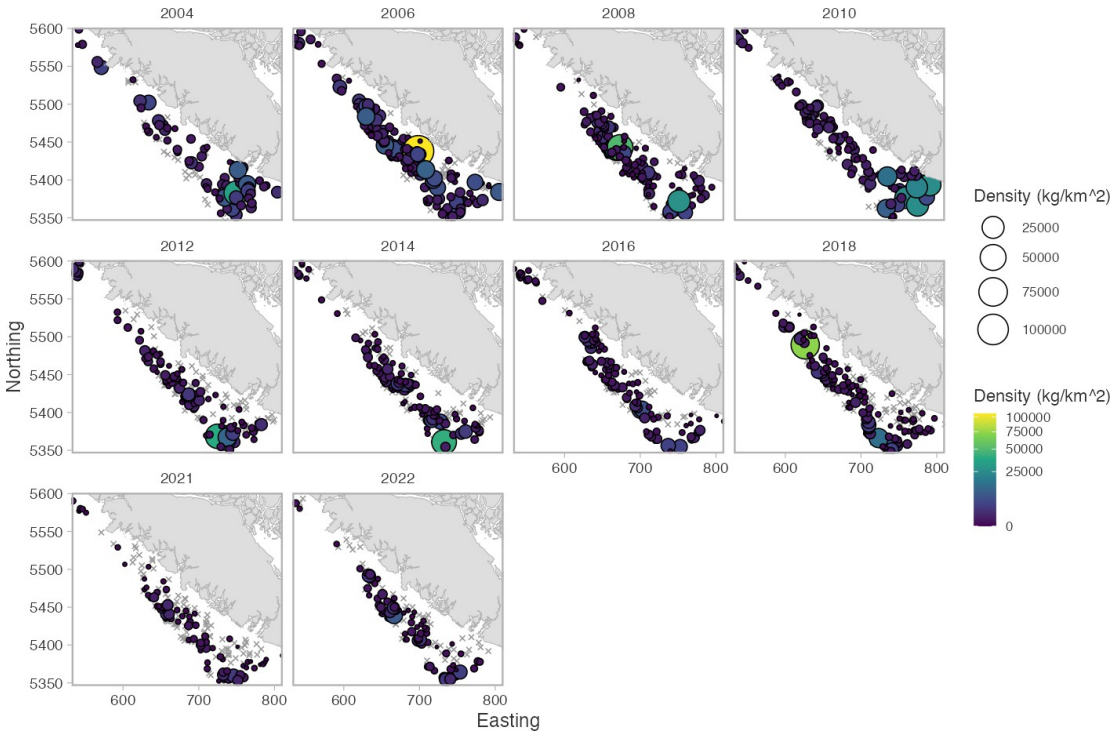

Figure A.16. Dogfish density (kg/km^2) from survey sets on the West Coast Vancouver Island Synoptic Bottom Trawl Survey (SYN WCVI).

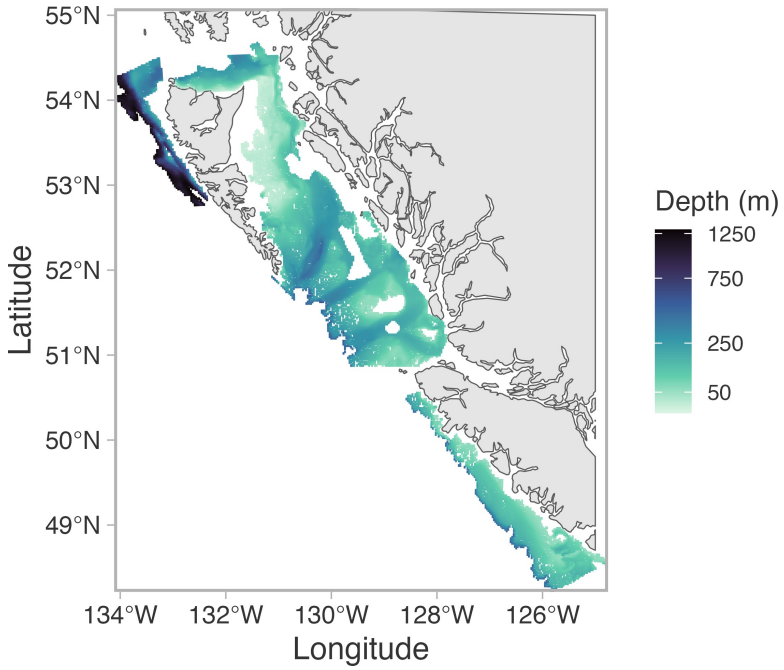

Figure A.17. Bottom depth for the Synoptic bottom trawl survey grid.

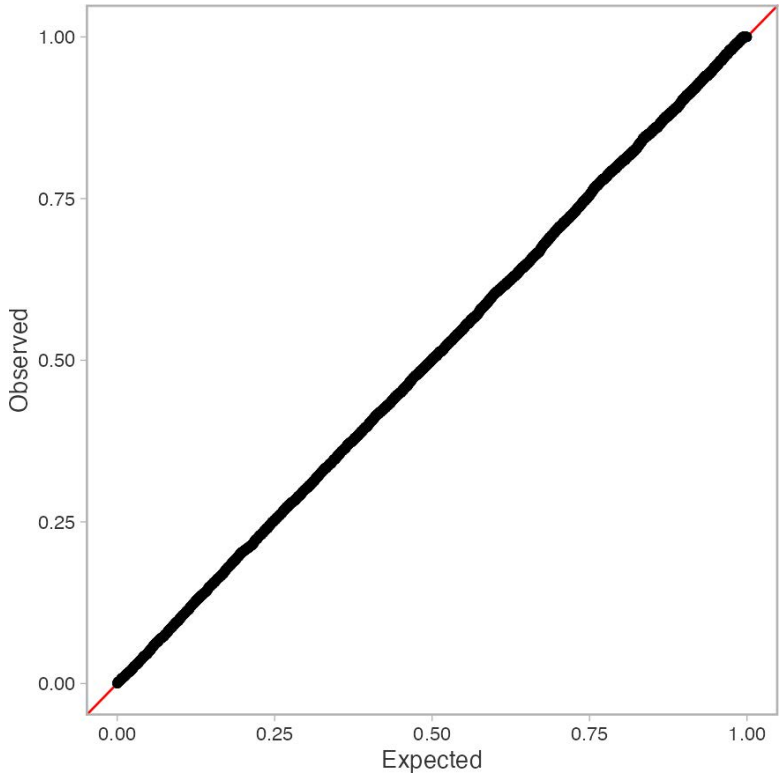

Figure A.18. Simulation-based randomized quantile residuals for the delta-lognormal spatiotemporal model fit to the Synoptic survey catches. The expected distribution in this case is a uniform distribution if the observations are consistent with the model.

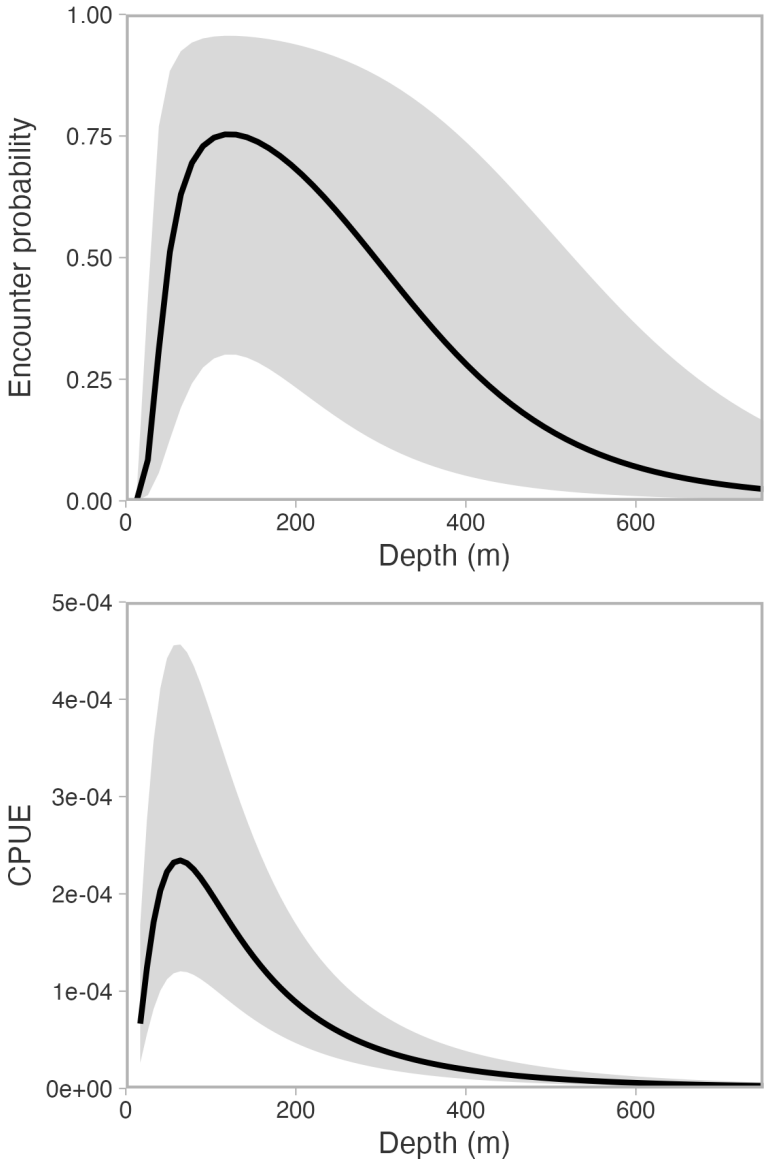

Figure A.19. Conditional depth effects (black line) estimated in the spatiotemporal model for the Synoptic trawl surveys. Top panel is encounter probability and bottom panel is the predicted catch per area swept (kg/m^2) given an encounter. The grey ribbon indicates the 95% confidence interval on the mean.

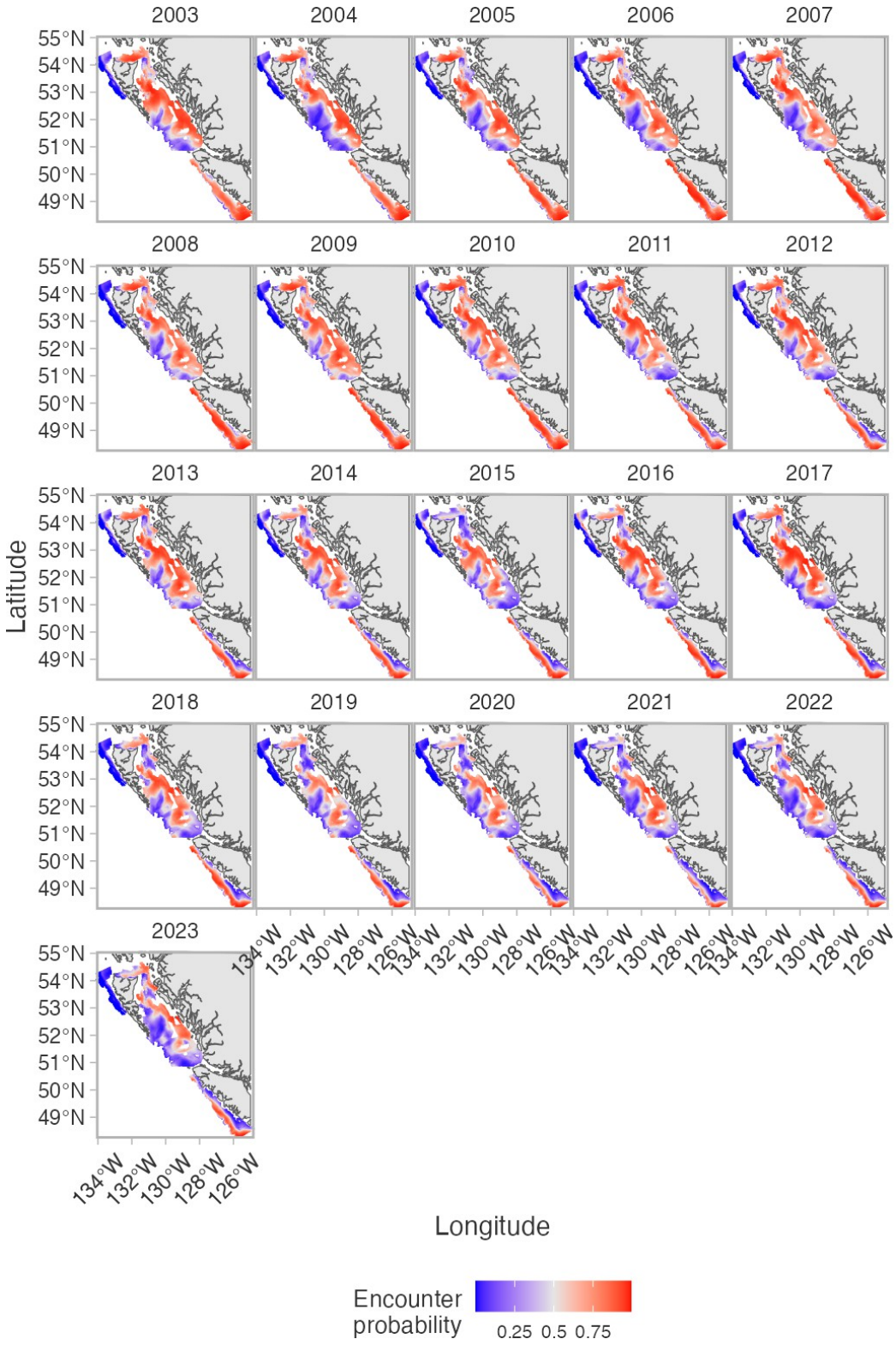

Figure A.20. Predicted encounter probability for Dogfish in the Synoptic bottom trawl survey.

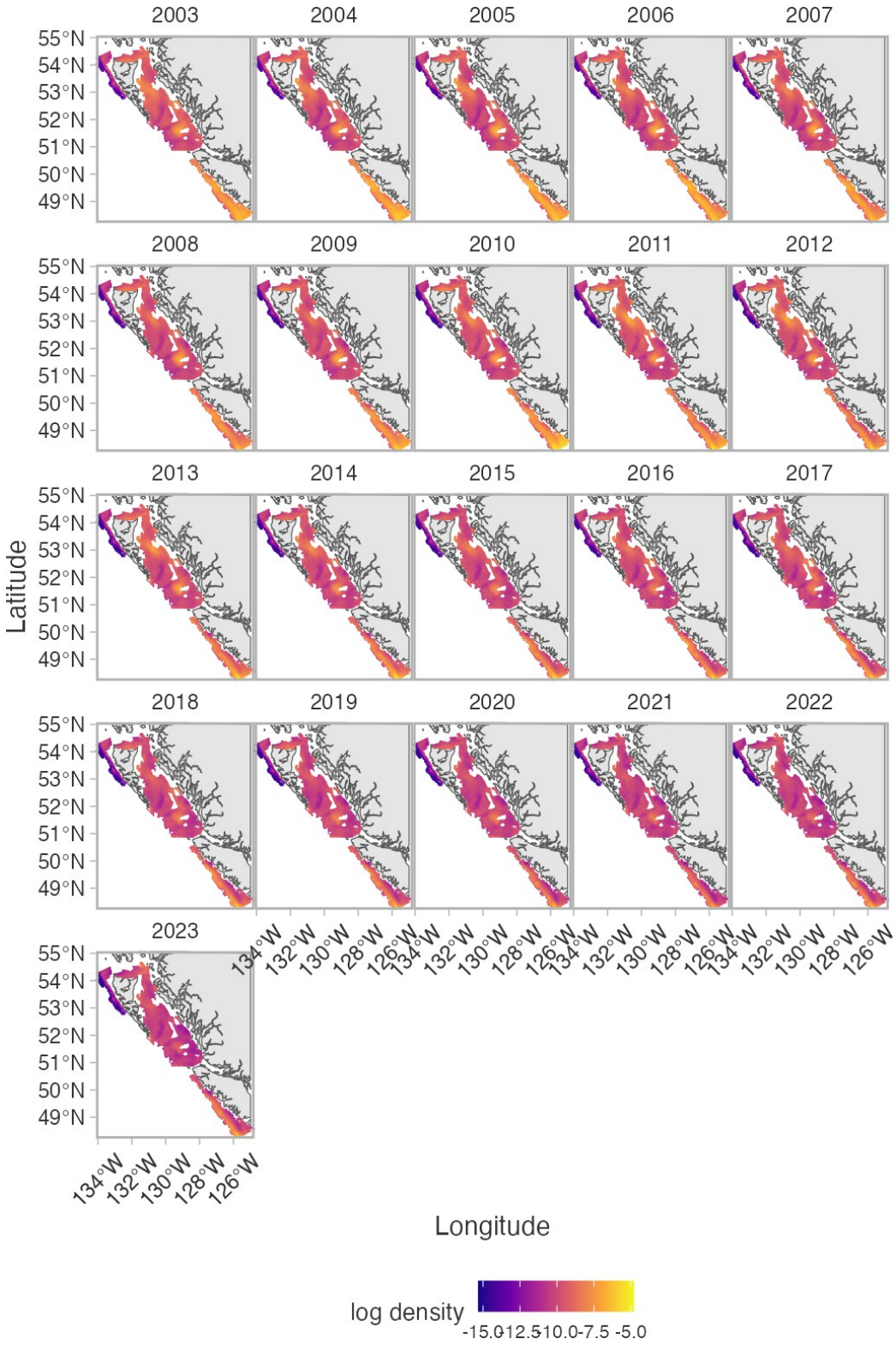

Figure A.21. Predicted log density (log kg/km^2) for Dogfish in the Synoptic bottom trawl survey.

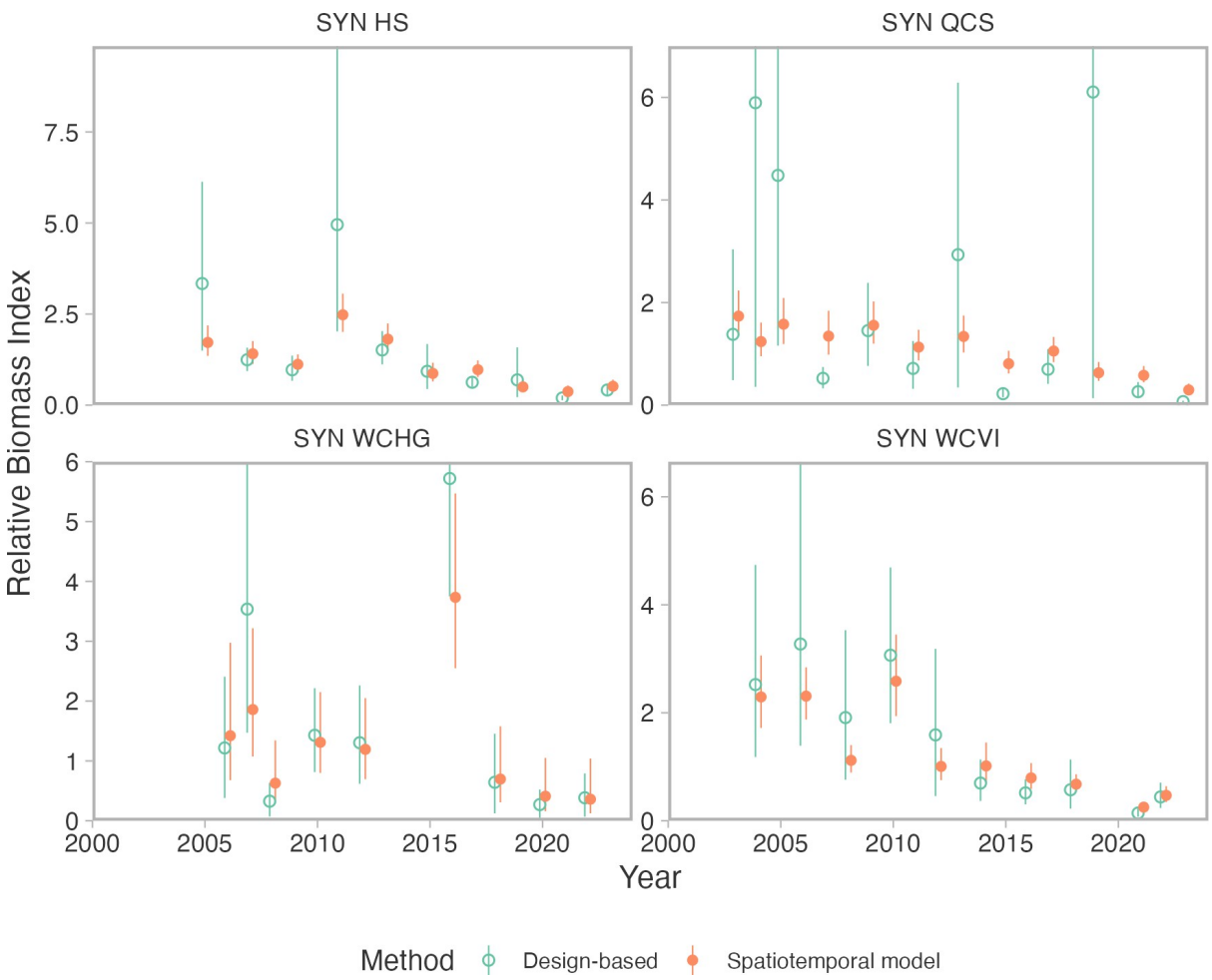

Figure A.22. Comparison of design-based and model-based biomass indices calculated for the subregions of the Synoptic survey. The model-based index is a coastwide model; however, here the predictions from the model have been subdivided by region for comparison. All indices have been centered to have a geometric mean one.

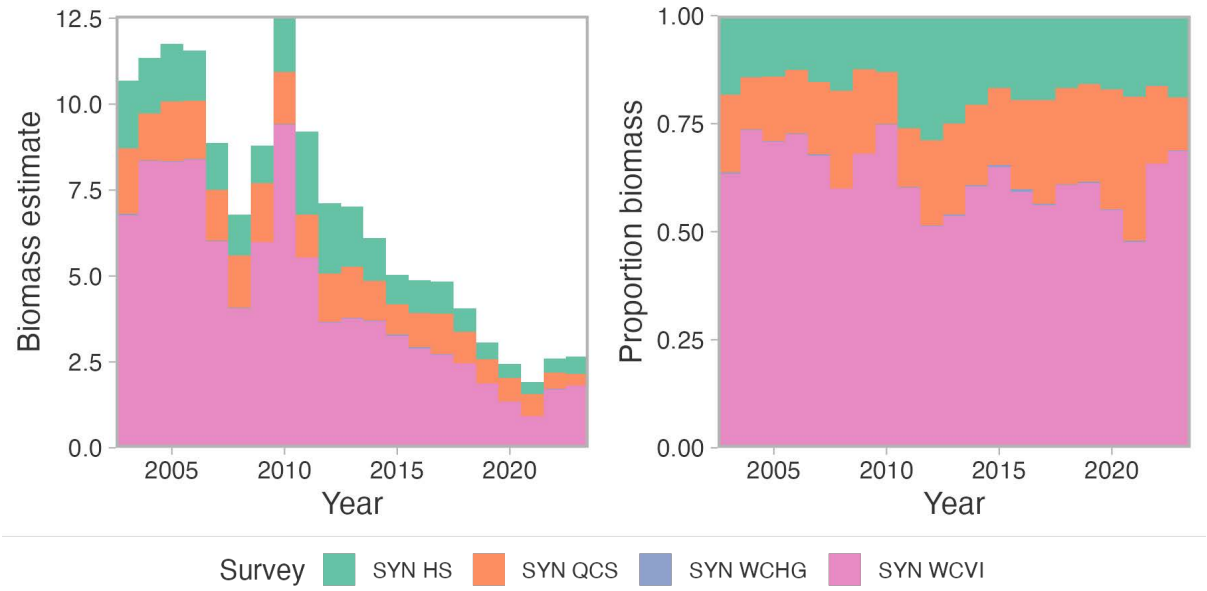

Figure A.23. The estimated Synoptic bottom trawl survey biomass split by survey subregion. The left panel shows survey biomass (1000 t per km^2 not adjusting for survey catchability) and the right panel shows the same data as a proportion by year.

A.5. HECATE STRAIT MULTISPECIES ASSEMBLAGE SURVEY

The Hecate Strait Multispecies Assemblage Bottom Trawl (HS MSA) was conducted from 1984 to 2003 by DFO using a combination of charter vessels and two Canadian Coast Guard Research Vessels (Choromanski et al. 2004). The objective of the survey was to collect catch and biological data on species assemblages in order to develop an ecological basis for mixed species stock assessment in Hecate Strait. A grid of 19 km^2 (10 nm^2) blocks was used to determine set locations. The survey was stratified by area and depth, but the choice of set locations within depth strata was non-random and was left to the discretion of the skipper (Choromanski et al. 2004). This survey is the predecessor to the SYN HS survey. We include the survey here because it is the only fisheries independent survey index we have in this older time period.

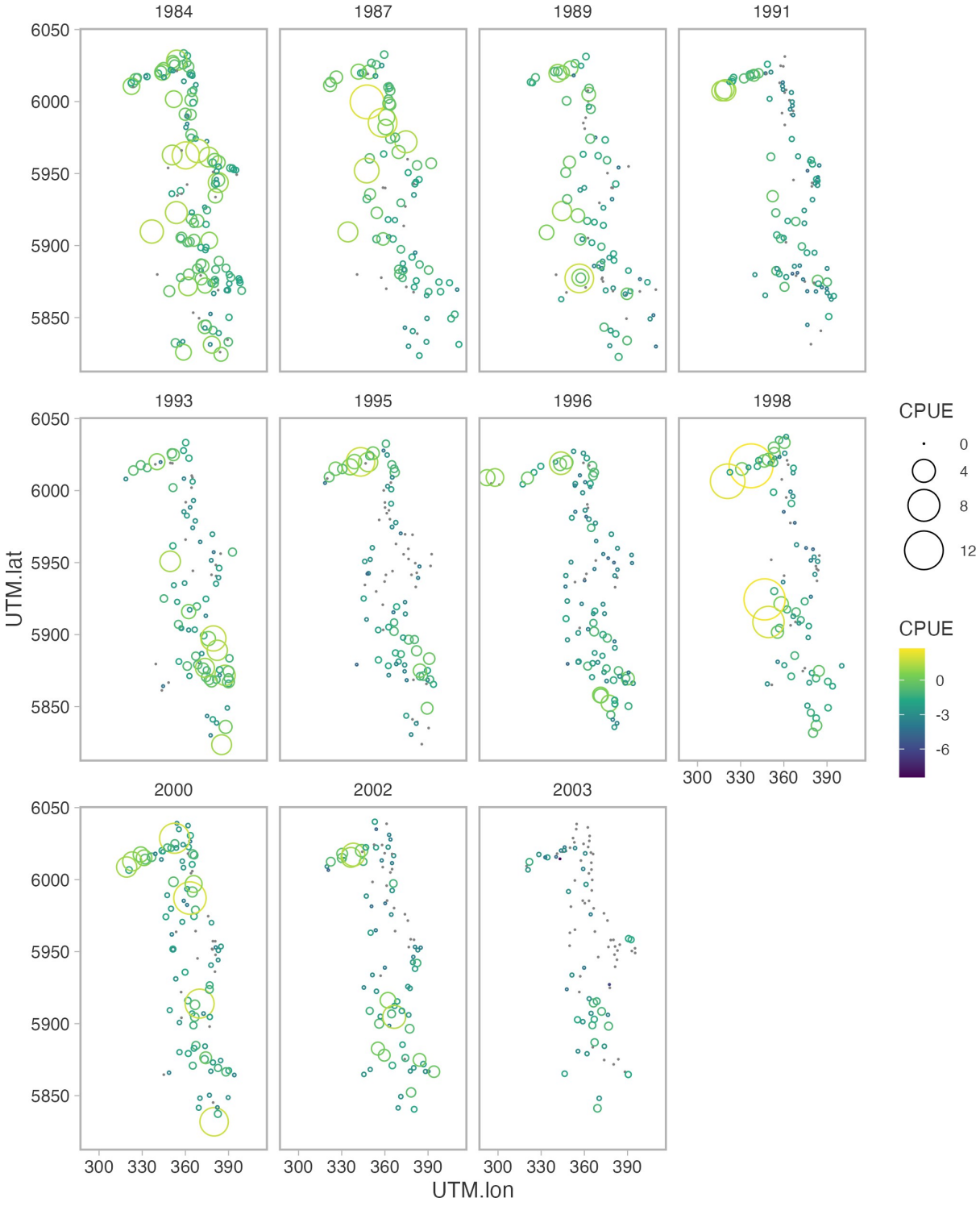

Figure A.24. Catch (weight) per unit effort (area swept) from the HS MSA survey.

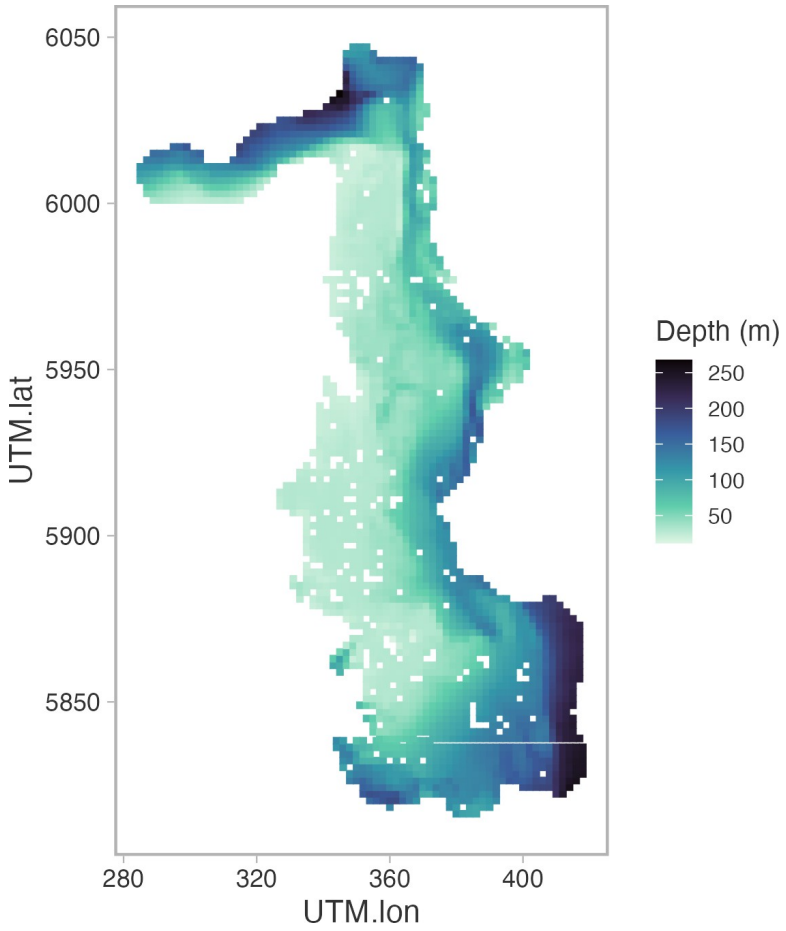

Figure A.25. Bottom depth for the HS MSA survey grid.

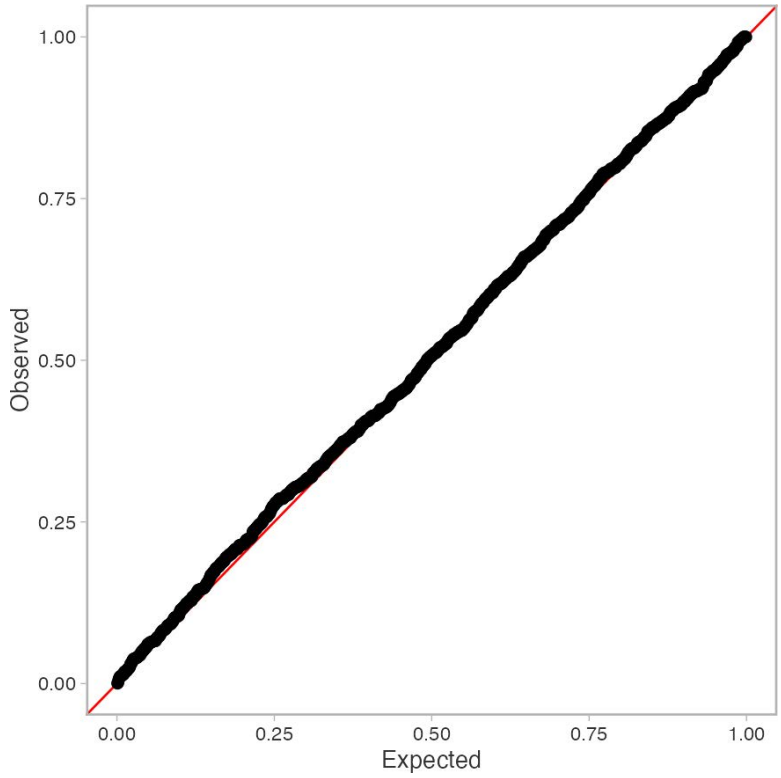

Figure A.26. Simulation-based randomized quantile residuals for the spatiotemporal model fit to the HS MSA survey catches. The expected distribution in this case is a uniform distribution if the observations are consistent with the model.

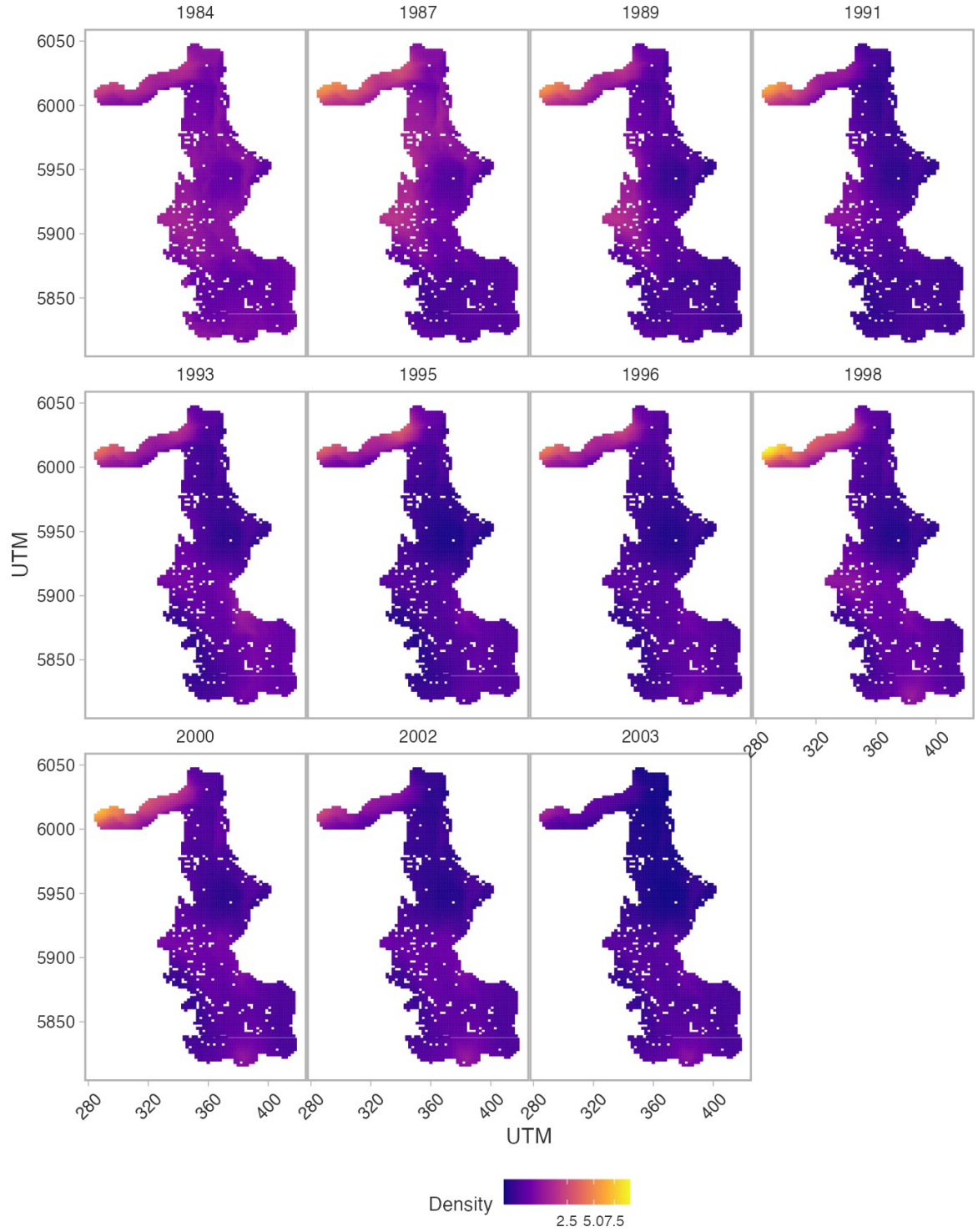

Figure A.27. Predicted biomass density for the HS MSA survey from a spatiotemporal model. Raw data are shown in Figure A.24.

A.6. SABLEFISH OFFSHORE TRAP SURVEY

A longline-trap survey, primarily for the purpose of indexing Sablefish (*Anoplopoma fimbria*), is conducted annually by DFO in collaboration with the Canadian Sablefish Association (CSA) using a stratified random design. The most recent Technical Report describing the survey's activities is available in Hardy et al. (2024). The survey takes place offshore along the BC continental shelf (Figure A.28) from mid-October to mid-November and ranges in depth from approximately 200 m to 1000 m. The longline gear includes 25 baited traps attached to buckets at 150 ft (45.72 m) intervals with 90 pound anchors at each end. The traps are baited with 4.5 kg of Pacific Hake (*Merluccius productus*) and 0.9 kg of squid. Here, we visualize the design-based index of biomass for Dogfish caught in this survey (Figure A.29).

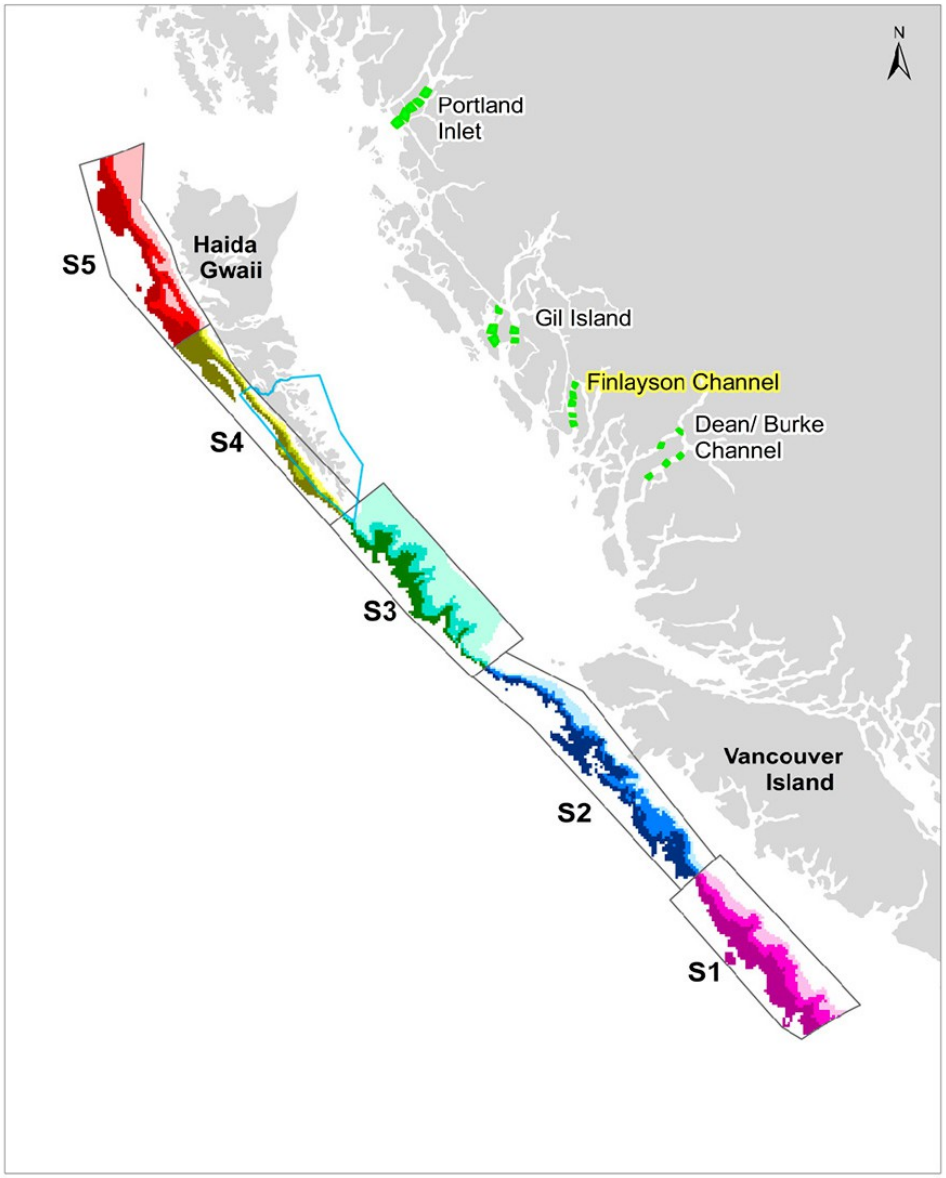

Figure A.28. Sablefish offshore trap survey design for 2003–2022. Reproduced from Figure 1 in Hardy et al. (2024). The colours and "S" labels refer to five spatial strata.

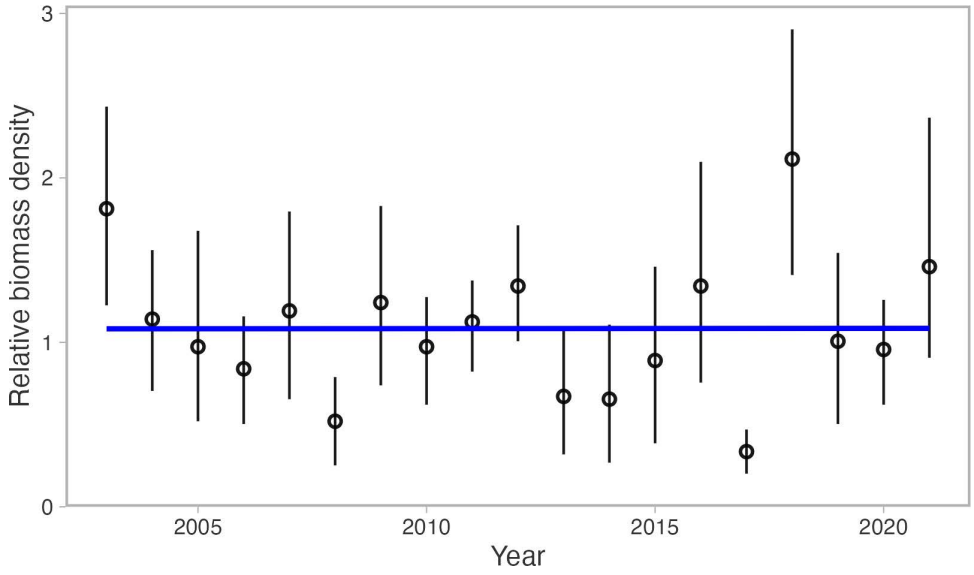

Figure A.29. Design-based index of biomass from the offshore Sablefish trap survey. The index is centered to have a geometric mean of one. Dots and line segments are means and 95% bootstrap-derived confidence intervals. The blue line is the mean fit from a generalized additive model (GAM) with gamma error and a log link. The "wiggliness" in the GAM smoother has been penalized to a straight line.

APPENDIX B. FISHERY DATA

B.1. COMMERCIAL CATCH

This assessment fit population dynamic models to fisheries catch, catch per unit effort, and length composition data. Visualizations of fisheries catch and discards across fleets were provided in the main text (Figures 1, 2, 4) as were visualizations of commercial length composition data (Figure 9, 10, 11). In this appendix, we provide additional visualizations of proportion of catch discarded by year (Figure B.1), number of various types of biological samples from the commercial fleets (Figure B.2) and description of standardizing commercial bottom trawl catch per unit effort (Section B.3). We also include a table of all commercial landings and discards for 1935–2023 (Table B.1).

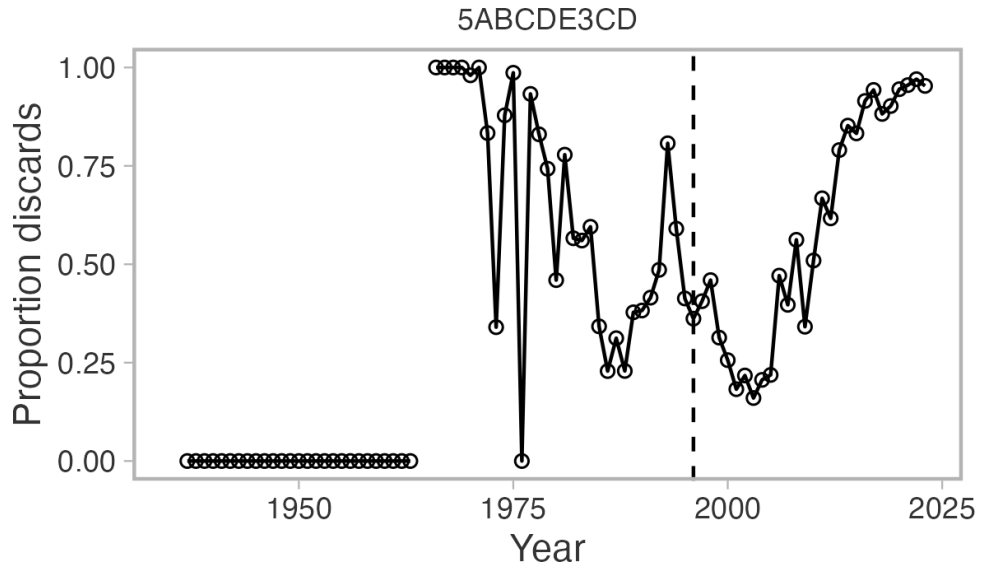

Figure B.1. Proportion of discards to total catch (landings plus discards) of Outside Dogfish. Observer coverage of the trawl fishery started in 1996 (denoted by the vertical dotted line).

*Table B.1. Landings and release data for Dogfish in PFMA 3CD5ABCDE from 1935 to 2023. Longline and trap (combined) discards were entered in the model as counts. The final discard weight column with an * is shown for illustrative purposes assuming an average dogfish weight of 3.07 kg (6.77 lbs; calculated from unsorted longline samples in 2009, 2010, 2012, and 2013), but was not used in model fitting. Years are calendar years. Longline discard data prior to 2006 were not recorded and are therefore not shown.*

Year	Gear	Landed (t)	Released (t)	Released (count)	Released (t)*
1935	Bottom trawl	0.0	0.0		
1936	Bottom trawl	0.0	0.0		
1937	Bottom trawl	410.0	0.0		
1938	Bottom trawl	23.0	0.0		
1939	Bottom trawl	549.0	0.0		
1940	Bottom trawl	1046.0	0.0		
1941	Bottom trawl	2492.0	0.0		
1942	Bottom trawl	6952.0	0.0		
1943	Bottom trawl	7683.0	0.0		
1944	Bottom trawl	27090.0	0.0		
1945	Bottom trawl	22359.0	0.0		
1946	Bottom trawl	10417.0	0.0		
1947	Bottom trawl	13326.0	0.0		
1948	Bottom trawl	10803.0	0.0		
1949	Bottom trawl	13191.0	0.0		
1950	Bottom trawl	1176.0	0.0		
1951	Bottom trawl	2540.0	0.0		
1952	Bottom trawl	1451.0	0.0		
1953	Bottom trawl	1598.0	0.0		
1954	Bottom trawl	673.0	0.0		
1955	Bottom trawl	912.0	0.0		
1956	Bottom trawl	709.0	0.0		
1957	Bottom trawl	1364.0	0.0		
1958	Bottom trawl	620.0	0.0		
1959	Bottom trawl	1407.0	0.0		
1960	Bottom trawl	930.0	0.0		
1961	Bottom trawl	3691.0	0.0		
1962	Bottom trawl	127.0	0.0		
1963	Bottom trawl	68.0	0.0		
1964	Bottom trawl	0.0	0.0		
1965	Bottom trawl	0.0	0.0		
1966	Bottom trawl	0.0	251.0		
1967	Bottom trawl	0.0	337.0		
1968	Bottom trawl	0.0	97.0		
1969	Bottom trawl	0.0	78.0		
1970	Bottom trawl	4.0	197.0		
1971	Bottom trawl	0.0	288.0		
1972	Bottom trawl	8.0	45.0		
1973	Bottom trawl	714.0	368.0		
1974	Bottom trawl	13.0	94.0		
1975	Bottom trawl	19.0	1399.0		
1976	Bottom trawl	3.0	0.0		
1977	Bottom trawl	80.0	1236.0		
1978	Bottom trawl	221.0	1325.0		

1979	Bottom trawl	419.0	1316.0
1980	Bottom trawl	2440.0	2190.0
1981	Bottom trawl	387.0	1472.0
1982	Bottom trawl	1320.0	1834.0
1983	Bottom trawl	641.0	1037.0
1984	Bottom trawl	653.0	1072.0
1985	Bottom trawl	1958.0	1266.0
1986	Bottom trawl	2135.0	687.0
1987	Bottom trawl	1072.0	1239.0
1988	Bottom trawl	1748.0	1310.0
1989	Bottom trawl	875.0	1277.0
1990	Bottom trawl	1282.0	1677.0
1991	Bottom trawl	917.0	1869.0
1992	Bottom trawl	468.0	1898.0
1993	Bottom trawl	68.0	1597.0
1994	Bottom trawl	138.0	1463.0
1995	Bottom trawl	219.0	931.0
1996	Bottom trawl	100.2	1659.9
1997	Bottom trawl	28.4	1090.4
1998	Bottom trawl	98.6	1562.9
1999	Bottom trawl	38.9	941.1
2000	Bottom trawl	91.2	1129.3
2001	Bottom trawl	169.7	800.7
2002	Bottom trawl	199.8	823.5
2003	Bottom trawl	312.2	720.5
2004	Bottom trawl	258.3	1154.1
2005	Bottom trawl	492.2	1054.5
2006	Bottom trawl	456.9	778.8
2007	Bottom trawl	377.8	896.9
2008	Bottom trawl	101.5	827.7
2009	Bottom trawl	442.5	964.6
2010	Bottom trawl	211.4	502.5
2011	Bottom trawl	229.8	709.8
2012	Bottom trawl	21.4	351.4
2013	Bottom trawl	6.3	345.3
2014	Bottom trawl	5.7	178.0
2015	Bottom trawl	6.4	221.1
2016	Bottom trawl	4.3	217.5
2017	Bottom trawl	6.5	312.4
2018	Bottom trawl	4.9	216.3
2019	Bottom trawl	4.5	138.0
2020	Bottom trawl	8.7	94.8
2021	Bottom trawl	5.9	162.0
2022	Bottom trawl	8.2	179.2
2023	Bottom trawl	9.6	261.3
1996	Midwater trawl	1302.6	7.5
1997	Midwater trawl	931.1	8.6
1998	Midwater trawl	615.8	2.2
1999	Midwater trawl	384.3	0.7
2000	Midwater trawl	50.7	0.9
2001	Midwater trawl	797.7	28.4

2002	Midwater trawl	382.3	45.5
2003	Midwater trawl	412.8	67.2
2004	Midwater trawl	759.3	23.7
2005	Midwater trawl	727.3	185.9
2006	Midwater trawl	213.6	29.7
2007	Midwater trawl	62.2	45.0
2008	Midwater trawl	212.6	102.3
2009	Midwater trawl	208.6	54.0
2010	Midwater trawl	168.2	210.7
2011	Midwater trawl	89.2	142.2
2012	Midwater trawl	21.5	82.9
2013	Midwater trawl	43.5	92.6
2014	Midwater trawl	13.7	61.8
2015	Midwater trawl	80.0	167.9
2016	Midwater trawl	61.6	67.7
2017	Midwater trawl	41.8	37.0
2018	Midwater trawl	102.1	93.1
2019	Midwater trawl	87.4	145.2
2020	Midwater trawl	34.3	133.6
2021	Midwater trawl	26.9	109.5
2022	Midwater trawl	17.2	158.5
2023	Midwater trawl	37.0	205.4
1967	Hook and line/longline	0.0	
1968	Hook and line/longline	0.0	
1969	Hook and line/longline	0.0	
1970	Hook and line/longline	0.0	
1971	Hook and line/longline	0.0	
1972	Hook and line/longline	1.0	
1973	Hook and line/longline	0.0	
1974	Hook and line/longline	0.0	
1975	Hook and line/longline	0.0	
1976	Hook and line/longline	0.0	
1977	Hook and line/longline	9.0	
1978	Hook and line/longline	50.0	
1979	Hook and line/longline	37.0	
1980	Hook and line/longline	134.0	
1981	Hook and line/longline	32.0	
1982	Hook and line/longline	86.0	
1983	Hook and line/longline	173.0	
1984	Hook and line/longline	76.0	
1985	Hook and line/longline	476.0	
1986	Hook and line/longline	184.0	
1987	Hook and line/longline	1659.0	
1988	Hook and line/longline	2666.0	
1989	Hook and line/longline	1227.0	
1990	Hook and line/longline	1426.0	
1991	Hook and line/longline	1716.0	
1992	Hook and line/longline	1541.0	
1993	Hook and line/longline	313.0	
1994	Hook and line/longline	877.0	
1995	Hook and line/longline	1104.0	

1996	Hook and line/longline	1539.0		
1997	Hook and line/longline	648.0		
1998	Hook and line/longline	1125.0		
1999	Hook and line/longline	1639.0		
2000	Hook and line/longline	3138.0		
2001	Hook and line/longline	2747.0		
2002	Hook and line/longline	2548.0		
2003	Hook and line/longline	3408.0		
2004	Hook and line/longline	3517.0		
2005	Hook and line/longline	3211.0		
2006	Hook and line/longline	1517.0	369416	1134.1
2007	Hook and line/longline	2863.6	396716	1217.9
2008	Hook and line/longline	1236.4	340234	1044.5
2009	Hook and line/longline	3063.3	291649	895.4
2010	Hook and line/longline	1047.1	249187	765.0
2011	Hook and line/longline	458.3	229968	706.0
2012	Hook and line/longline	602.1	193946	595.4
2013	Hook and line/longline	210.6	174701	536.3
2014	Hook and line/longline	105.3	155974	478.8
2015	Hook and line/longline	80.5	142308	436.9
2016	Hook and line/longline	19.9	206960	635.4
2017	Hook and line/longline	1.5	153237	470.4
2018	Hook and line/longline	0.0	158311	486.0
2019	Hook and line/longline	0.1	183043	561.9
2020	Hook and line/longline	0.0	165077	506.8
2021	Hook and line/longline	0.0	135361	415.6
2022	Hook and line/longline	0.0	155434	477.2
2023	Hook and line/longline	0.0	155914	478.7
2006	Trap	0.0	1830	5.6
2007	Trap	0.0	4689	14.4
2008	Trap	0.0	5247	16.1
2009	Trap	0.0	3428	10.5
2010	Trap	0.0	1286	3.9
2011	Trap	0.0	1119	3.4
2012	Trap	0.0	2448	7.5
2013	Trap	0.0	2012	6.2
2014	Trap	0.0	162	0.5
2015	Trap	0.0	1303	4.0
2016	Trap	0.0	809	2.5
2017	Trap	0.0	1267	3.9
2018	Trap	0.0	1398	4.3
2019	Trap	0.0	909	2.8
2020	Trap	0.0	639	2.0
2021	Trap	0.0	4212	12.9
2022	Trap	0.0	5422	16.6
2023	Trap	0.0	1348	4.1

B.2. COMMERCIAL BIOLOGICAL SAMPLES SUMMARY

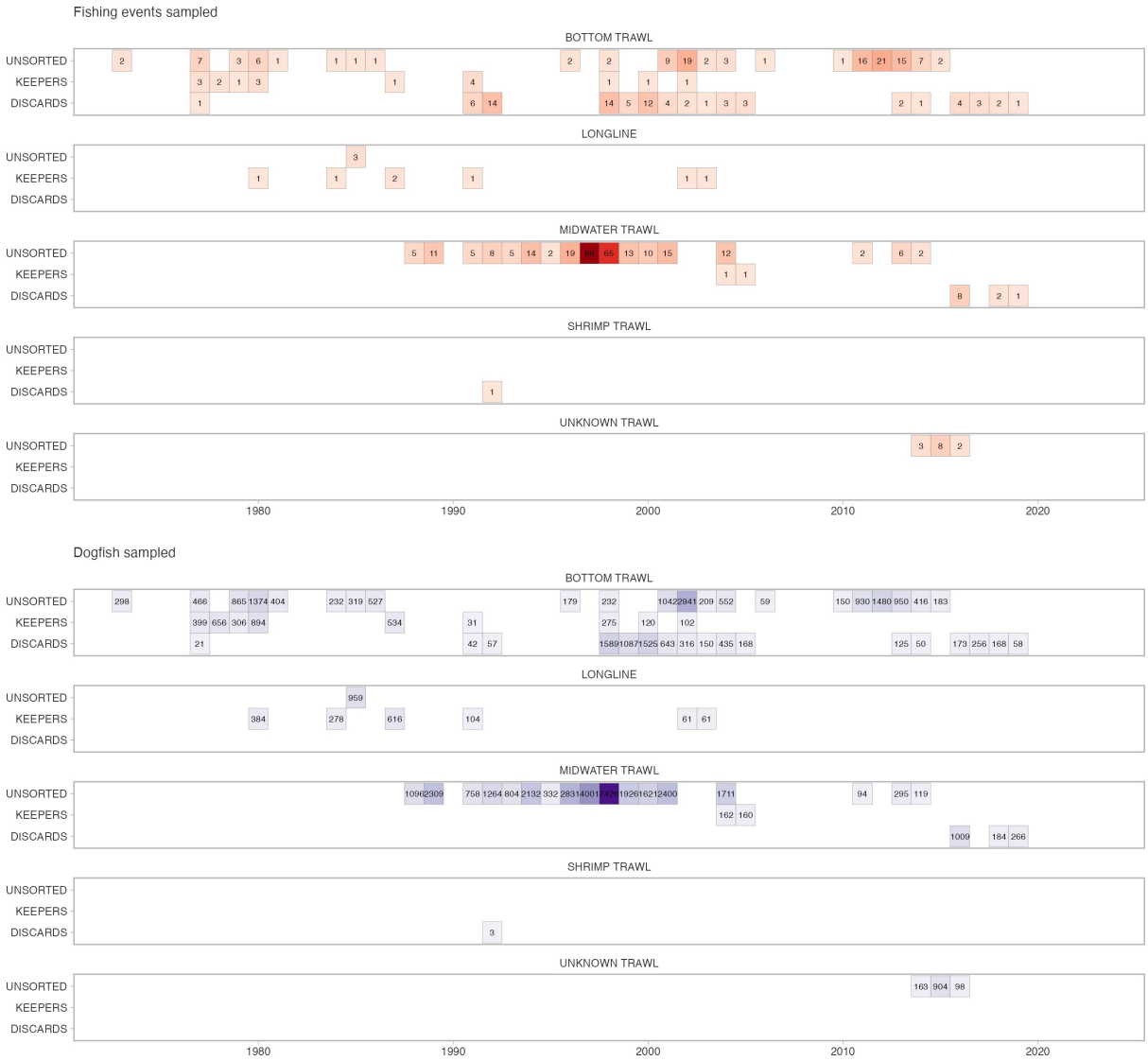

Figure B.2. Biological samples from the commercial fishery. The top panel indicates the number of fishing events sampled and the second number indicates the number of dogfish sampled.

B.3. COMMERCIAL CATCH PER UNIT EFFORT

We applied a spatiotemporal modelling approach to derive an index of commercial CPUE using a similar approach to that described for modelling the scientific surveys (Section A.1). Such an approach has also been shown to perform well for standardizing commercial CPUE and to exceed the performance of other approaches that are not spatially explicit (e.g., Babcock et al. 2023, Grüss et al. 2019).

We defined the "fleet" for our model following a similar protocol used in many recent DFO Pacific groundfish stock assessments. Specifically, we included bottom trawl vessels that had at least 100 positive tows for Dogfish total, and at least 5 years with 5 positive trips per year. For vessels that passed this criteria, we included all of their catch and effort into our CPUE analysis. Future assessments might consider a midwater trawl fleet CPUE standardization as well.

The main difference between the survey models and the commercial models, is how we treated the spatiotemporal variation and the addition of several covariates. For the commercial CPUE spatiotemporal models, we used a more traditional approach (e.g., Thorson et al. 2015) where we assumed the spatiotemporal variation was independent from year to year and the annual means were independent. This is more computationally efficient for this larger dataset. Also, the spatiotemporal random walk approach was not needed given the lack of the biennial data collection in distinct spatial patches. Therefore, our model for either of the two linear predictors in the delta model can be represented as

$$\begin{aligned}
\mathbb{E}[y_{\boldsymbol{s},t}] &= \mu_{\boldsymbol{s},t}, \\
\mu_{\boldsymbol{s},t} &= g^{-1}\left(\alpha_t + \gamma_v + \psi_m + \boldsymbol{X}_{\boldsymbol{s},t}\boldsymbol{\beta} + O_{\boldsymbol{s},t} + \omega_{\boldsymbol{s}} + \epsilon_{\boldsymbol{s},t}\right), \\
\gamma_v &\sim \text{Normal}\left(0, \sigma_v^2\right), \\
\boldsymbol{\omega} &\sim \text{MVNormal}\left(\mathbf{0}, \boldsymbol{\Sigma}_\omega\right), \\
\boldsymbol{\epsilon}_t &\sim \text{MVNormal}(\mathbf{0}, \boldsymbol{\Sigma}_\epsilon).
\end{aligned} \tag{B.1}$$

The symbols are the same as in Equations A.1, A.2, or A.3, but with the addition of α_t, which represents independent means or intercepts for each year, γ_v, which represents vessel (v) catchability effects treated as random intercepts with standard deviation σ_v, ψ_m, which represents factor effects for months (m) relative to January, and $\boldsymbol{\epsilon}_t$, which are assumed independent each year (but drawn from a single multivariate normal distribution).

As in the trawl-survey models, we used a delta-lognormal approach with one linear predictor for the encounter probability and a second linear predictor for the expected catch density given an encounter (Equations A.2, A.3). As before, the likelihoods used were Bernoulli and lognormal with logit and log links, respectively.

To maintain consistency with the Synoptic trawl survey and for simplicity, we used the Synoptic survey grid (Figure A.17) as the prediction grid with the commercial CPUE model. Therefore, we predicted on this grid and summed the expected (relative) biomass density across the grid cells by year (Figures B.5–B.10) to derive an area-weighted index of biomass (Figure B.11).

To investigate potential differences in population trend by depth and time of year as indicated by commercial CPUE, we repeated our modelling with the data subsetted into three depth bins (Figure B.12) and with data subsetted by month (and dropping the month predictor in the model) (Figures B.13–B.15).

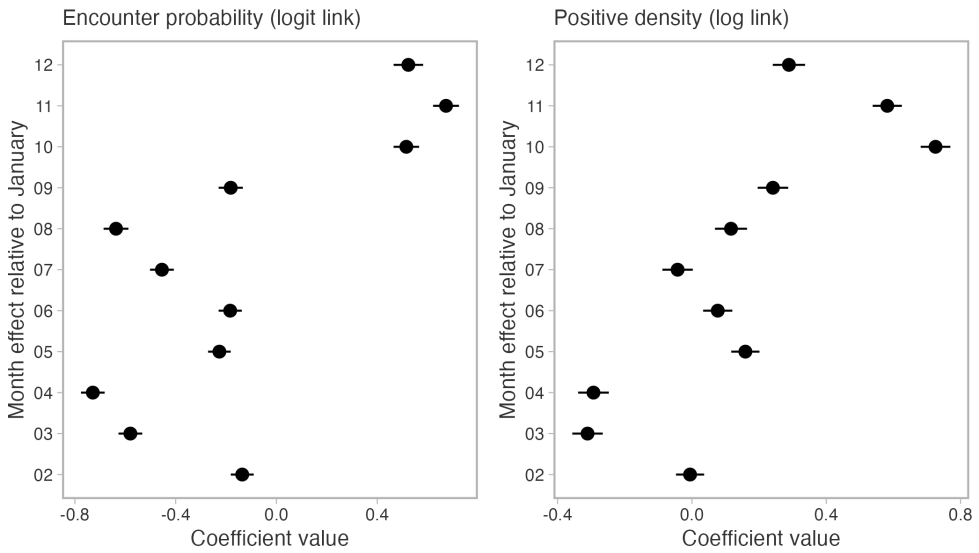

Figure B.3. Month fixed effects (ψ_m) estimated for the encounter probability and positive density linear predictors in the commercial CPUE standardization model. Both are shown in link space. Dots are means and line segments are 95% confidence intervals.

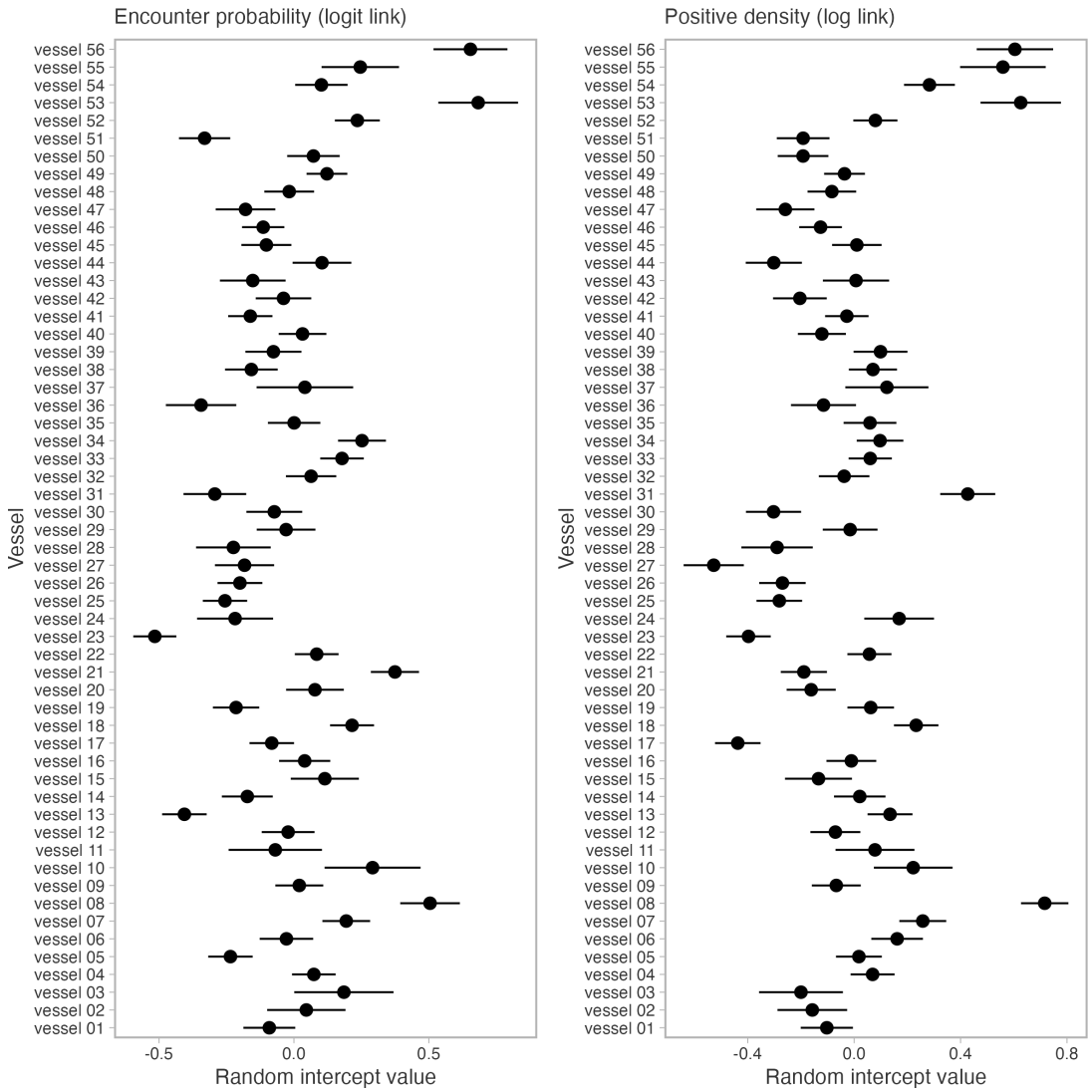

Figure B.4. Encounter probability and positive density random intercept values (γ_v). Both are shown in link space. Dots are means and line segments are 95% confidence intervals.

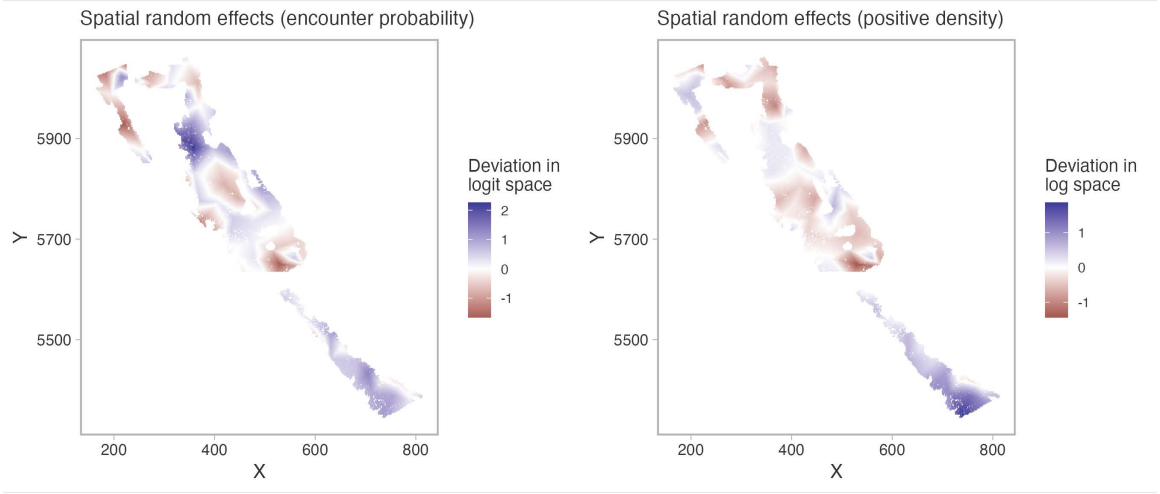

Figure B.5. Spatial random field estimates from the commercial CPUE standardization model.

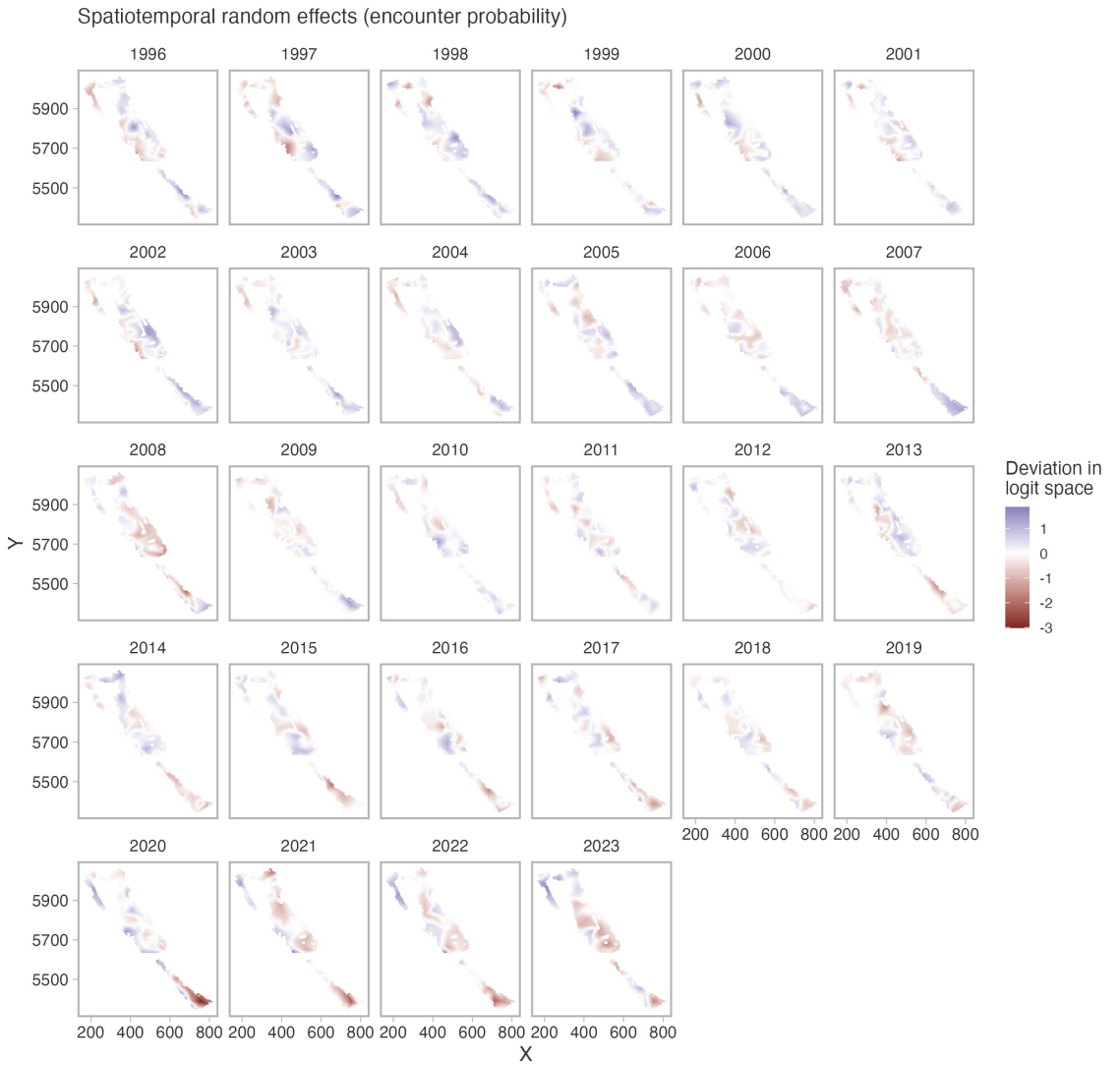

Figure B.6. Spatiotemporal random field estimates for the encounter probability linear predictor in the commercial CPUE standardization model.

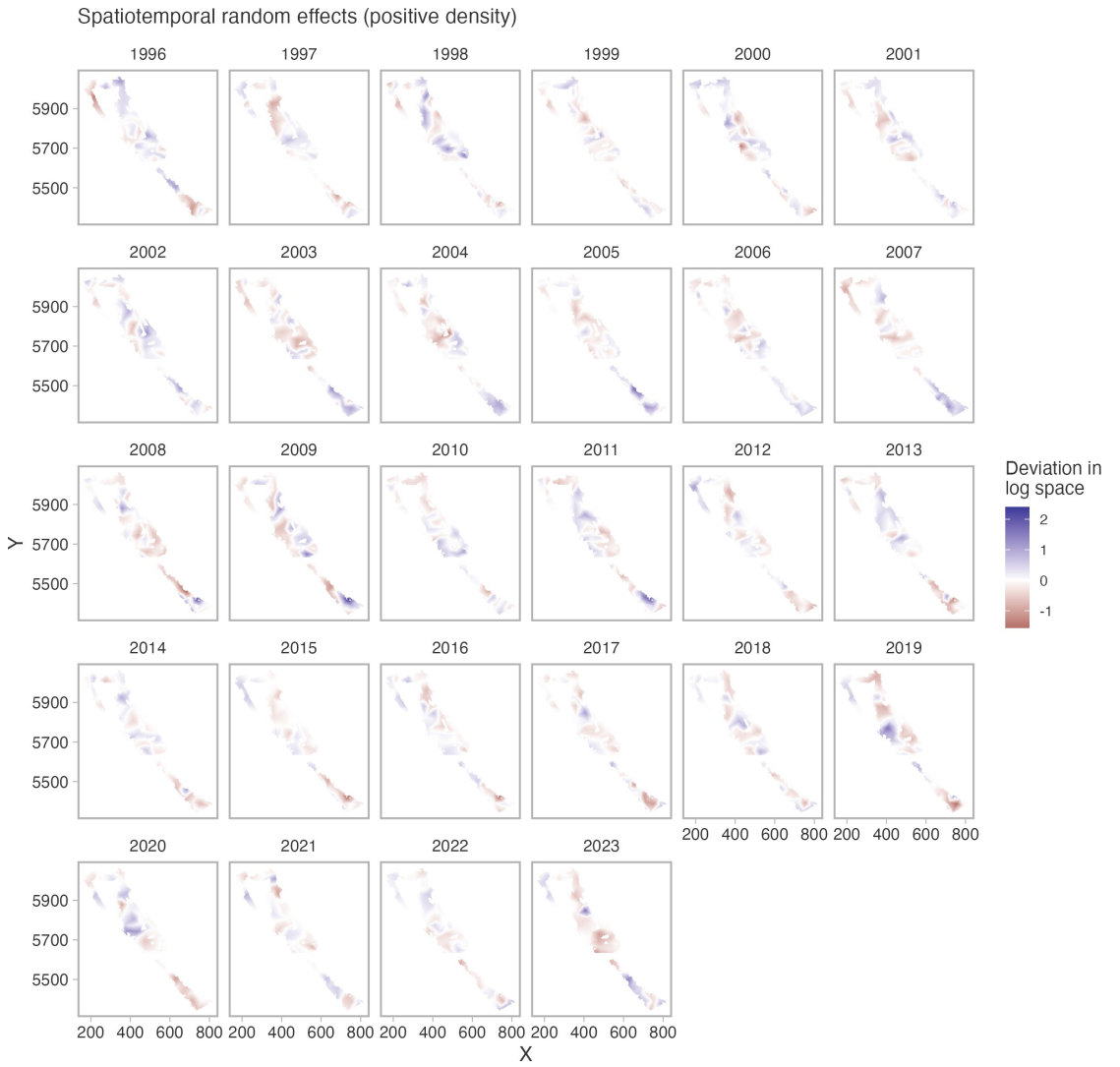

Figure B.7. Spatiotemporal random field estimates for the positive catch density linear predictor in the commercial CPUE standardization model.

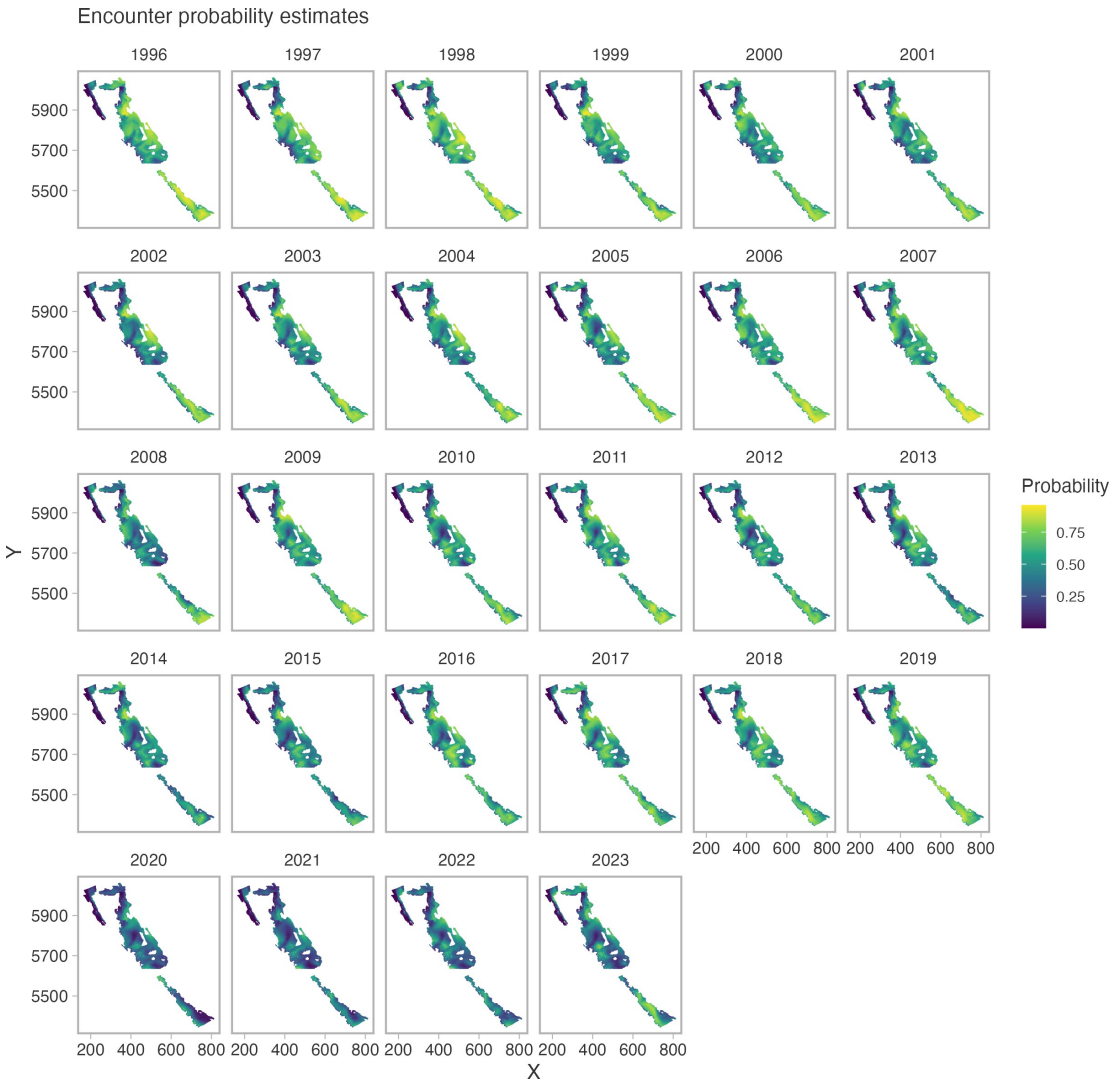

Figure B.8. Encounter probability estimates from the commercial CPUE standardization model.

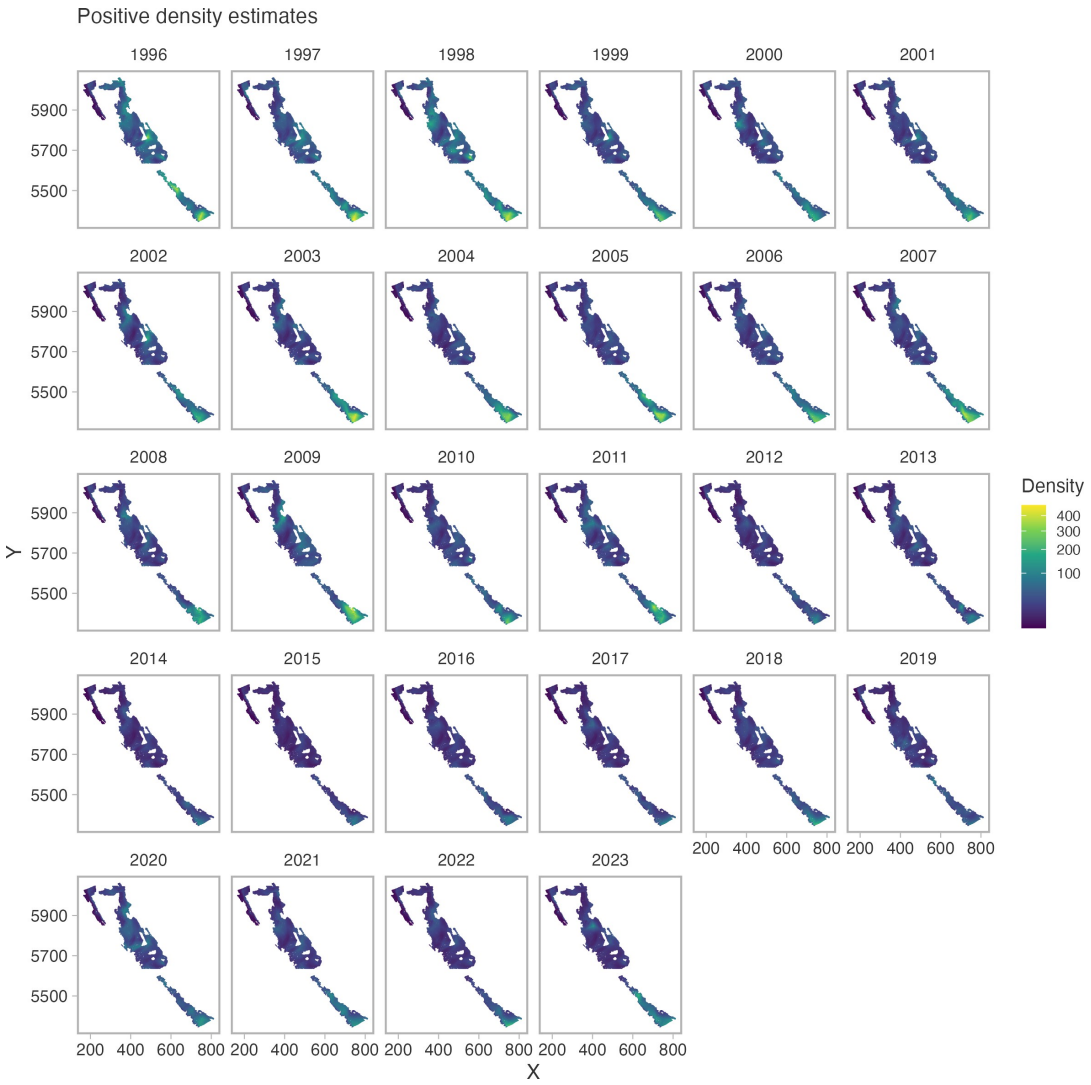

Figure B.9. Positive density estimates from the commercial CPUE standardization model. The units are relative and should not be interpreted but are a measure of catch weight per unit effort given a Dogfish encounter.

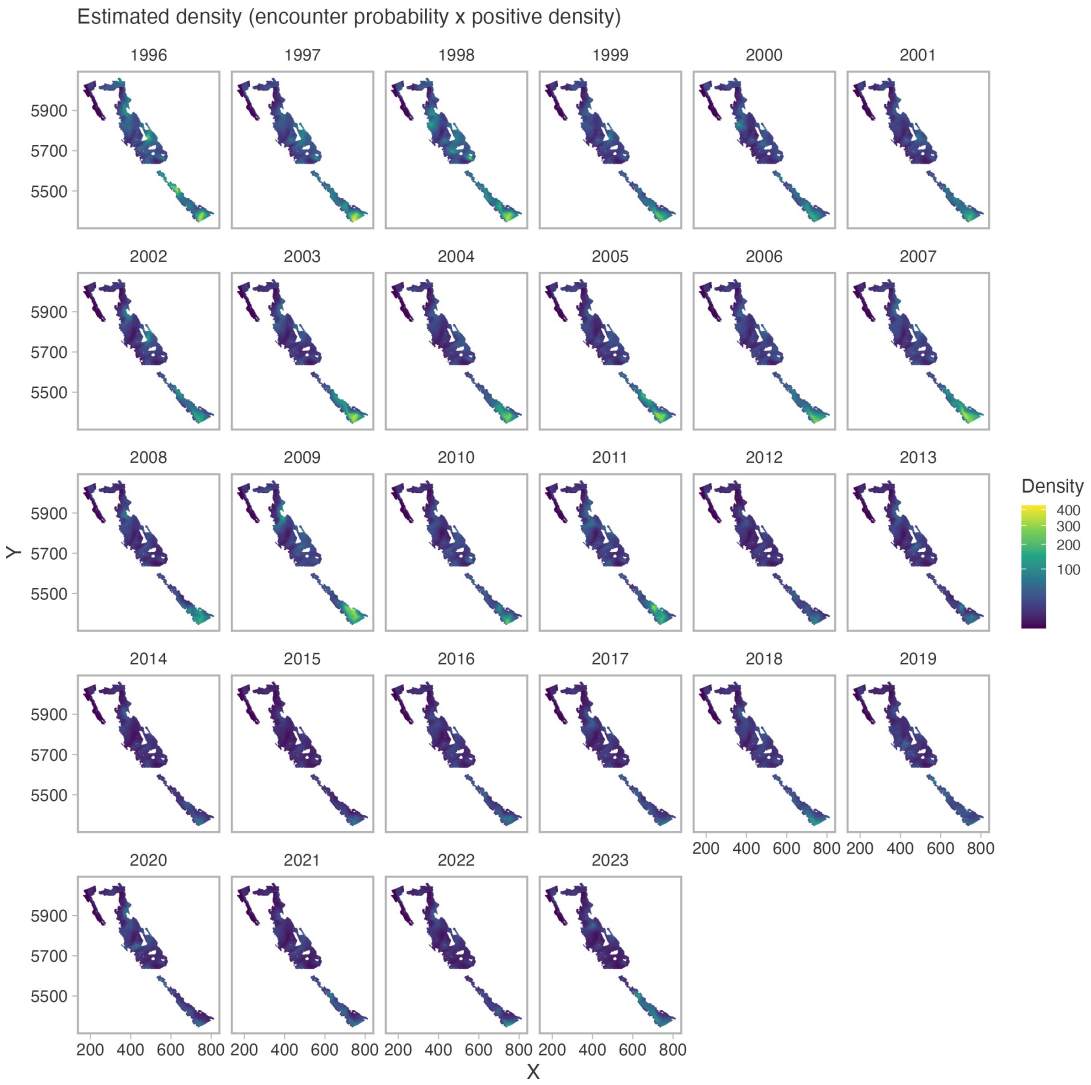

Figure B.10. Estimated catch density from the commercial CPUE standardization model. The units are relative and should not be interpreted but are a measure of catch weight per unit effort.

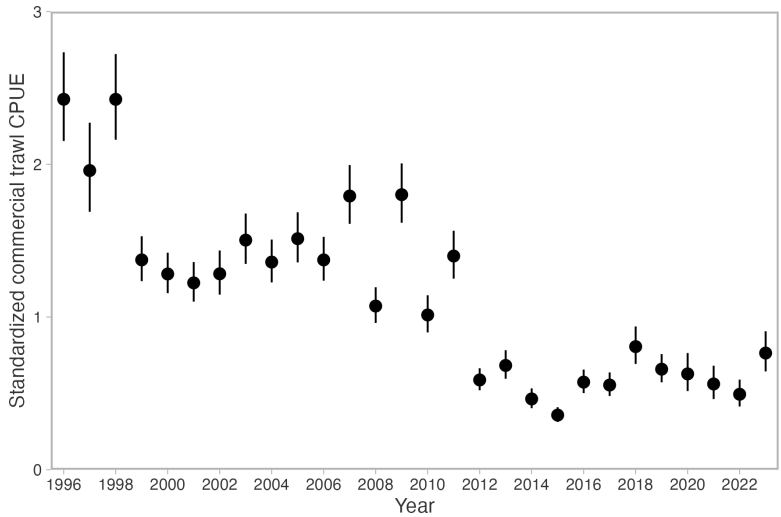

Figure B.11. The resulting index when integrated over space by year. This is repeated from Figure 5 for clarity so it can be compared with subsequent figures. Dots are means and line segments are 95% confidence intervals.

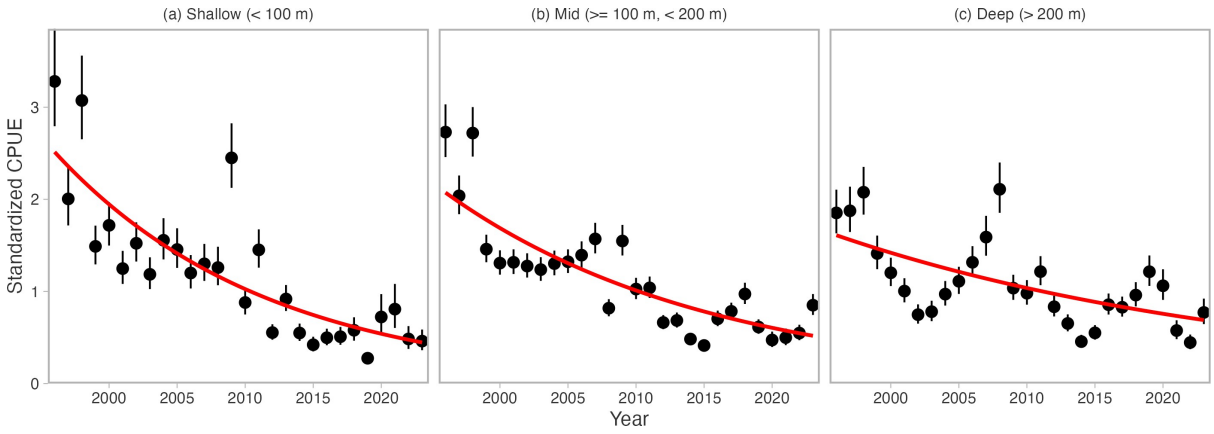

Figure B.12. Standardized commercial CPUE when fit to only data from each month succession. The red lines are gamma log-linked GLMs (generalized linear models) fit for visualization purposes. Dots are means and line segments are 95% confidence intervals.

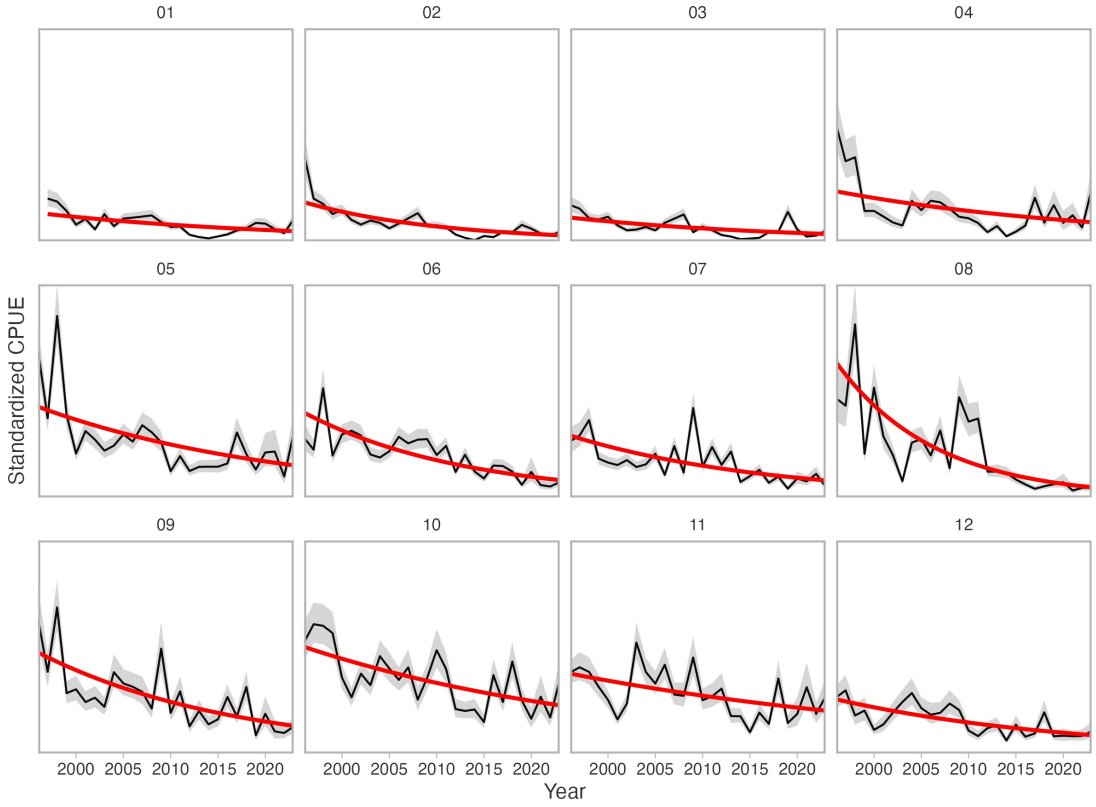

Figure B.13. Standardized commercial CPUE when fit to only data from three depth bins. The red lines are gamma log-linked GLMs (generalized linear models) fit for visualization purposes. The decline is steepest for the shallow data and least steep for the deepest data. Lines are means and ribbons are 95% confidence intervals.

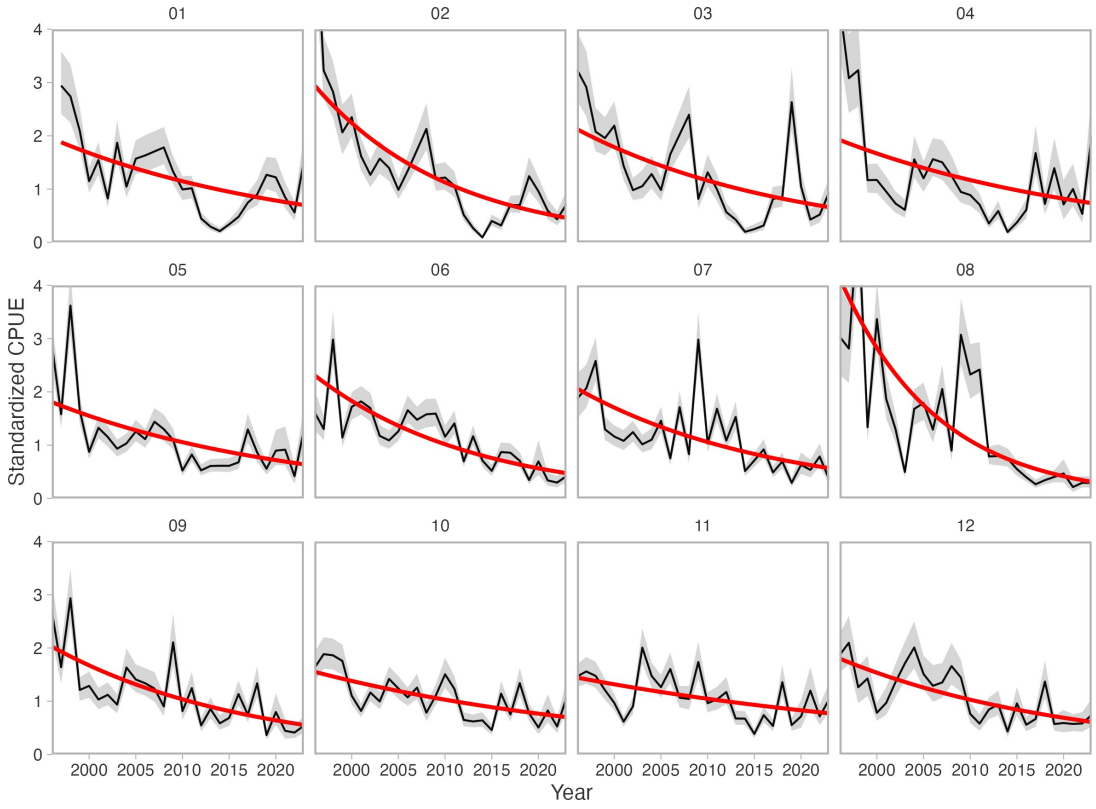

Figure B.14. Same as Figure B.13 but with each panel scaled to have the same geometric mean of one.

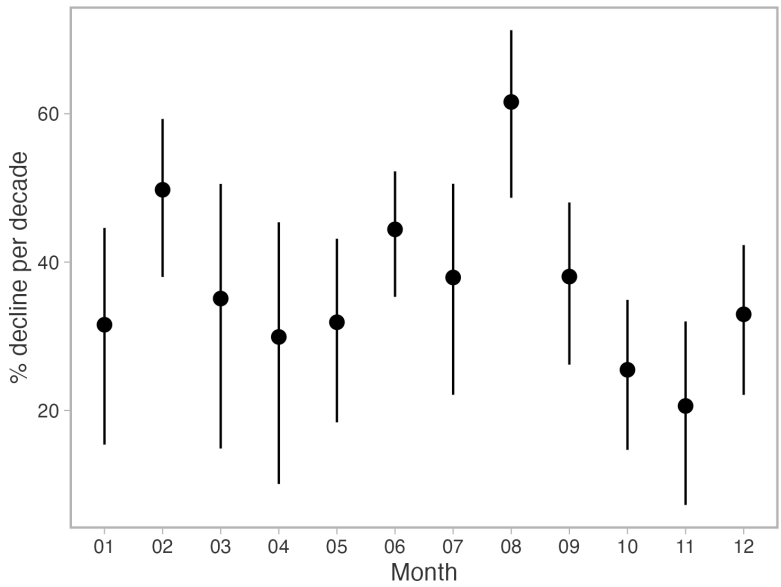

Figure B.15. The slope coefficients from the gamma log-linked GLMs fit in Figures B.13 and B.14. The rates of decline are relatively similar across months with the exception of August, which has a steeper rate of decline. November has the least steep rate of decline. Dots are means and line segments are 95% confidence intervals.

APPENDIX C. GROWTH AND MATURITY

C.1. LENGTH-AGE RELATIONSHIP

Mean length-at-age was modeled as a Schnute function, where the predicted length of sample i is:

$$\hat{L}_i = \left(\hat{L}_1^p + (\hat{L}_2^p - \hat{L}_1^p) \frac{1 - \exp(-\hat{k}[a_i - a_1])}{1 - \exp(-\hat{k}[a_2 - a_1])} \right)^{1/p} \tag{C.1}$$

where a_1 and a_2 are two specified reference ages, L_1 and L_2 are the length corresponding to the reference ages, k is a growth coefficient, and the caret symbol denotes an estimate.

By visual inspection, the data do not indicate that there was an inflection in the growth trajectory (Figure C.1). Therefore, the p parameter was fixed to 1 which reduces the growth equation to the von Bertalanffy model,

$$\hat{L}_i = \hat{L}_\infty (1 - \exp(-\hat{k}[a_i - \hat{a}_0])) \tag{C.2}$$

where

$$L_\infty = \left(\frac{L_2^p \exp(ka_2) - L_1^p \exp(ka_1)}{\exp(ka_2) - \exp(ka_1)} \right)^{1/p} \tag{C.3}$$

$$a_0 = -\frac{1}{k} \log \left(\frac{L_2^p \exp(ka_2) - L_1^p \exp(ka_1)}{L_2^p - L_1^p} \right) + a_1 + a_2 \tag{C.4}$$

Length-at-age were estimated by maximum likelihood with a lognormal distribution. The log-likelihood $\mathcal{L}$ was:

$$\mathcal{L} = \sum_i \left[-\log(\hat{\sigma}_L) - 0.5 \left(\frac{\log(L_i) - \log(\hat{L}_i)}{\hat{\sigma}_L} \right)^2 \right] \tag{C.5}$$

where σ_L is the residual standard deviation.

For Pacific Spiny Dogfish, a_1 and a_2 were set to 0 and 999, respectively. Separate growth curves were fitted for females and males.

Age samples were collected for research projects from various surveys, tag returns, and some fisheries (Table C.1) (McFarlane and King 2009). As such, these data mostly do not reflect any size or age selection in a fishery (Jackie King, DFO, pers. comm. 2023).

Samples collected in Canadian waters do not appear to have samples of smaller dogfish (Figure C.1). Thus, we also considered age samples collected from the U.S. West Coast Groundfish Bottom Trawl (WCGBT) survey in 2010 by the Northwest Fisheries Science Center (NWFSC).

Age determination for Pacific Spiny Dogfish is based on counts of annular rings on dorsal spines (Ketchen 1975). However, ages of older animals are frequently underestimated as the bands wear and become indistinguishable. A correction factor developed by Ketchen (1975) is added based on an exponential relationship between spine size and ring count of younger dogfish whose bands have not degraded. This method of age estimation has been validated (McFarlane and King 2009).

Even then, the ages of older females remains underestimated as it is believed that pregnancy inhibits spine growth (Taylor et al. 2013*a*). For example, the cluster of large (>95 cm) females in 3C are likely to be much older than estimated (Figure C.1).

Four growth models were fitted to evaluate the sensitivity of the various sampling and age determination factors:

1. Fitted with only samples in Canadian waters

2. Same as 1, and added the 2010 NWFSC samples
3. Same as 2, and excluded large females using a threshold of 95 cm for DFO samples (based on the length of 50 percent maturity) and 80 cm for the NWFSC samples (Gertseva et al. 2021).
4. Same as 3, and excluded samples in inside waters (4B) for both sexes.

Inclusion of the NWFSC samples reduced the magnitude of the a_0 parameter and reduced the length at age of the youngest dogfish for both sexes (Table C.2, Figure 12).

There is high variability in length-at-age between individual samples and the estimated relationship. For both sexes, the residual standard deviation around the mean relationship reduces as age increases. The standard deviation appears to stabilize near age 40, where there are fewer samples (Figure C.2).

Excluding the large females in Model 3 reduced the asymptotic length, albeit modestly. When the samples in 4B are excluded, there is a small reduction in asymptotic length and an increase in the k parameter for females. The asymptotic length of males is smaller than of females, while males tend to reach the asymptotic length more quickly with age (based on the k parameter).

Model 2 is believed to be the best descriptor of growth for Outside Spiny Dogfish, after fitting to young dogfish to provide a smaller estimate of a_0. The estimate of the mean length at age 0 is between 20–30 cm, which is consistent with measurements of pup size near the end of the gestation period (Ketchen 1972).

C.2. LENGTH-WEIGHT RELATIONSHIP

The length-weight function is of the form:

$$W_i = aL_i^b, \tag{C.6}$$

where W_i and L_i are the weight and length for fish i, respectively. Parameters a and b are estimated using maximum likelihood using the Student-t distribution in log-space:

$$\log(W_i) \sim \text{Student-t}(df = 3, \log(\hat{a}) + \hat{b}\log(L_i), \hat{\sigma}_W), \tag{C.7}$$

The degrees of freedom of the Student-t distribution was set to 3 to be robust to outliers.

Estimates for Outside Spiny Dogfish are presented in Figure 14.

C.3. MATURITY-LENGTH RELATIONSHIP

The maturity relationship was estimated with respect to size with a binomial generalized linear model. The predicted probability p that sample i is a mature animal is modeled as

$$\hat{p}_i = \frac{1}{1 + \exp(-\hat{y}_i)} \tag{C.8}$$

$$\hat{y}_i = \hat{\beta}_0 + \hat{\beta}_1 L_i + \hat{\beta}_2 F_i \tag{C.9}$$

where L_i is the length of sample i, F_i is a categorical variable for sex, and β are estimated coefficients and intercept terms.

The log-likelihood is

$$\mathcal{L} = \sum_i \begin{cases} \log(\hat{p}_i) & \text{sample } i \text{ is mature} \\ \log(1 - \hat{p}_i) & \text{otherwise} \end{cases} \tag{C.10}$$

Two aspects of female maturity are presented here.

First, maturity on the basis on the presence of mature gonads (ova size 5-10 mm and thickened uterii >10 mm, code 55 in the biological samples) indicated that the size of 50 and 95 percent maturity at 86.3 and 96.2 cm, respectively (Figure 16).

Second, maturity on the basis of bearing pups (code 77 in the biological samples) indicated that the size of 50% and 95% pregnancy at 97.6 and 115.1 cm, respectively. This definition of maturity is relevant for the spawning output of the population and is considered in the population model.

The male maturity ogive, on the basis of mature gonads, was estimated with the size of 50% and 95% maturity at 67.9 and 74.1 cm, respectively.

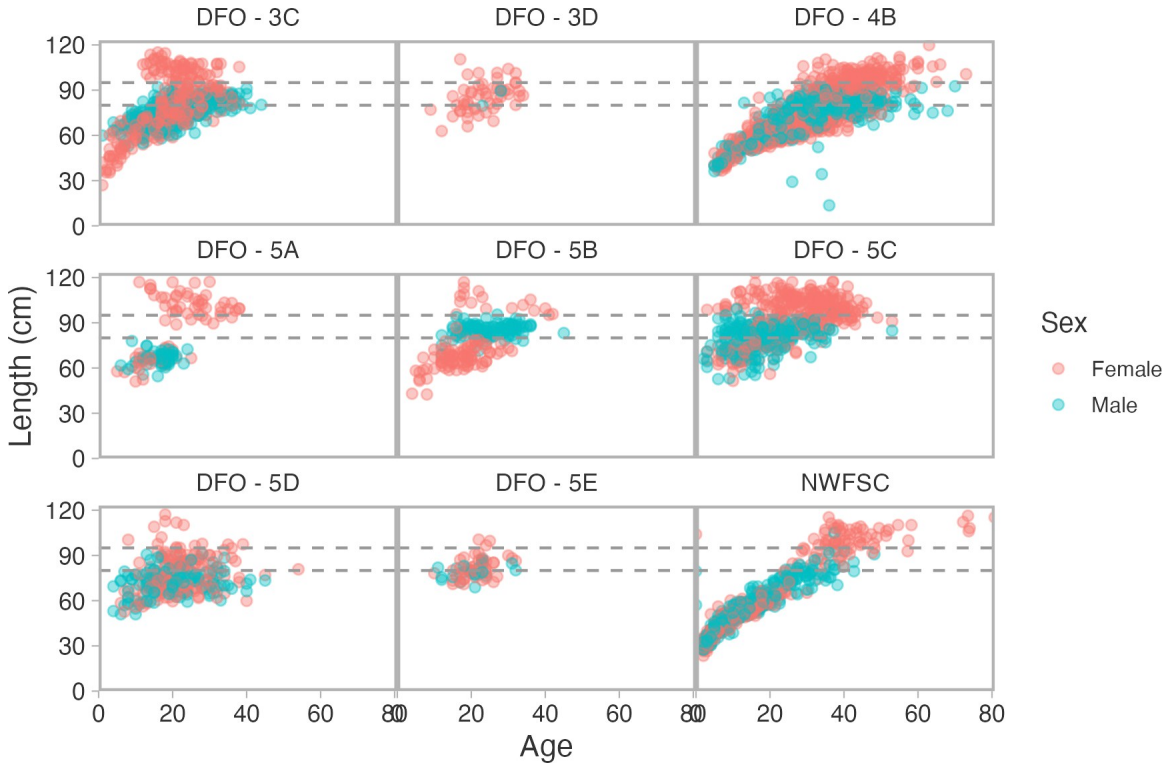

Figure C.1. Length-at-age samples by area and sex. The NWFSC samples were collected from the U.S. West Coast Groundfish Bottom Trawl survey in 2010. Horizontal dotted lines indicate 80 and 95 cm which are the length of 50 percent maturity for females in U.S. and Canadian waters, respectively.

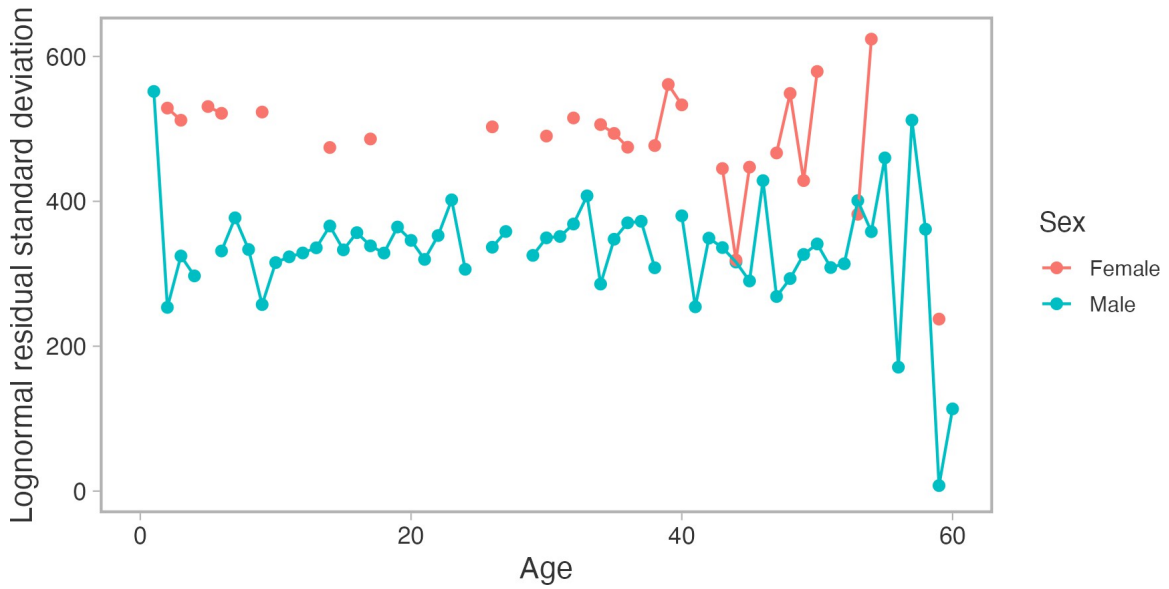

Figure C.2. Standard deviation of the logspace residuals in the fitted von Bertalanffy growth curve (Model 2) by sex and age.

Table C.1. Number of age samples by area and year.

Year	3C	3D	4B	5A	5B	5C	5D	5E	NWFSC	Total
1980	0	0	0	0	79	167	37	0	0	283
1982	0	0	0	0	0	390	150	0	0	540
1984	284	0	0	0	0	0	0	0	0	284
1989	0	0	669	0	0	0	0	0	0	669
1998	52	49	0	119	41	0	55	65	0	381
2000	0	0	0	0	0	0	58	0	0	58
2004	113	0	533	0	0	0	0	0	0	646
2006	40	0	0	0	0	0	0	0	0	40
2007	118	6	0	0	87	0	0	0	0	211
2010	0	0	0	0	0	0	0	0	594	594
Total	566	1080	568	1338	762	116	1292	80	422	1188

Table C.2. Estimates of von Bertalanffy growth parameters by sex.

Model	Parameter	Female Estimate	Male Estimate
(1) DFO samples	L_∞	97.384	83.733
(1) DFO samples	k	0.050	0.077
(1) DFO samples	a_0	-10.635	-11.075
(1) DFO samples	σ	0.184	0.147
(2) DFO + NWFSC	L_∞	97.724	84.368
(2) DFO + NWFSC	k	0.058	0.089
(2) DFO + NWFSC	a_0	-5.726	-4.349
(2) DFO + NWFSC	σ	0.187	0.166
(3) DFO + NWFSC + exclude large female	L_∞	93.227	NA
(3) DFO + NWFSC + exclude large female	k	0.054	NA
(3) DFO + NWFSC + exclude large female	a_0	-6.578	NA
(3) DFO + NWFSC + exclude large female	σ	0.146	NA
(4) DFO + NWFSC + exclude large female + ex4B	L_∞	91.201	85.848
(4) DFO + NWFSC + exclude large female + ex4B	k	0.073	0.090
(4) DFO + NWFSC + exclude large female + ex4B	a_0	-4.052	-4.262
(4) DFO + NWFSC + exclude large female + ex4B	σ	0.141	0.162

APPENDIX D. MARKOV CHAIN MONTE CARLO SIMULATIONS

Here, we present MCMC diagnostics and posteriors from model A1 (with constant natural mortality) and B2 (with stepwise increase in natural mortality in 2010). For both models, adnuts reported sampling behaviour consistent with convergence, as the effective sample size was high ($>$ 200 across all parameters) and the $\hat{R}$ metric was below 1.02 for all parameters. No divergent transitions were detected in the NUTS algorithm.

Trace plots indicated minimal autocorrelation in the posterior (Figures D.1–D.4). Marginal posterior distributions were approximately normally distributed, except for parameters with estimates near their respective bounds, for example, the z_{frac} productivity parameter and the male apical selectivity parameters (all bounded between 0–1, Figures D.5–D.6). These parameters had skewed posteriors.

Correlation plots for the stock recruit parameters are shown in Figures D.7 and D.8. Time series of the spawning output and depletion (S/S_0) are in Figure D.9. In model B2, the unfished recruitment parameter and the recent natural mortality parameter are positively correlated since a larger mortality rate requires a larger population to realize the historical catch.

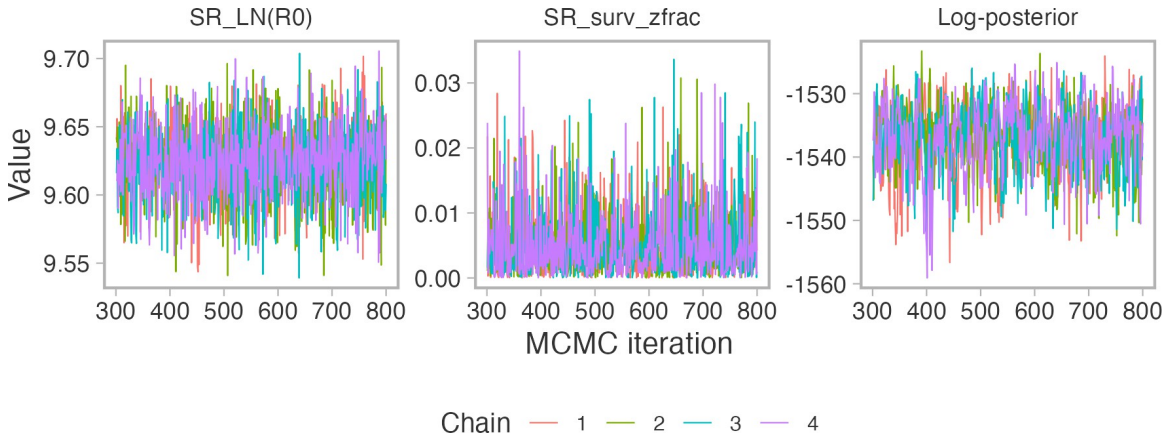

Figure D.1. Trace plots of the MCMC samples in model A1 for the log-posterior and stock-recruit parameters.

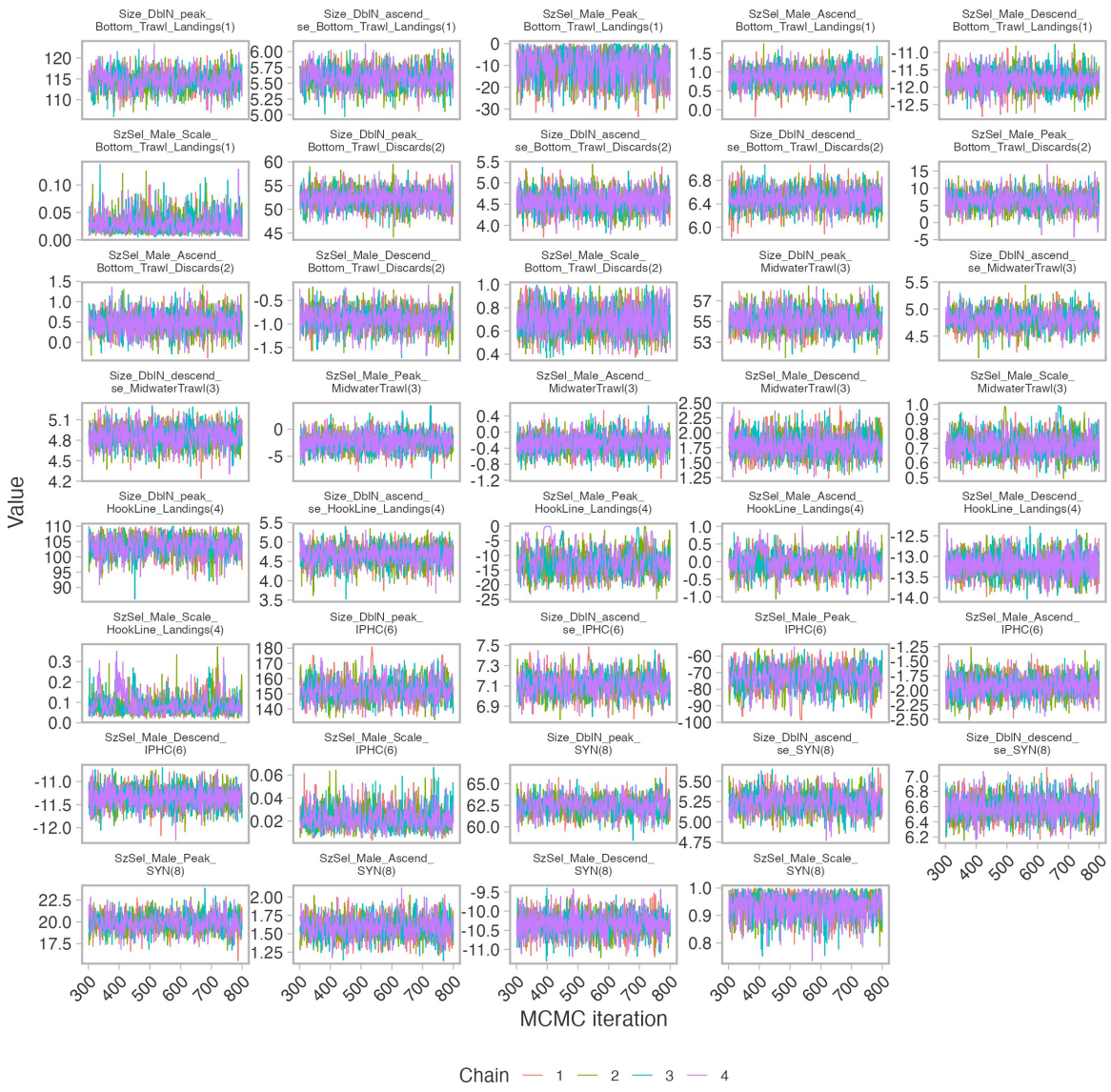

Figure D.2. Trace plots of the MCMC samples in model A1 for the selectivity parameters. Parameter names are defined in Table 3 in the main text.

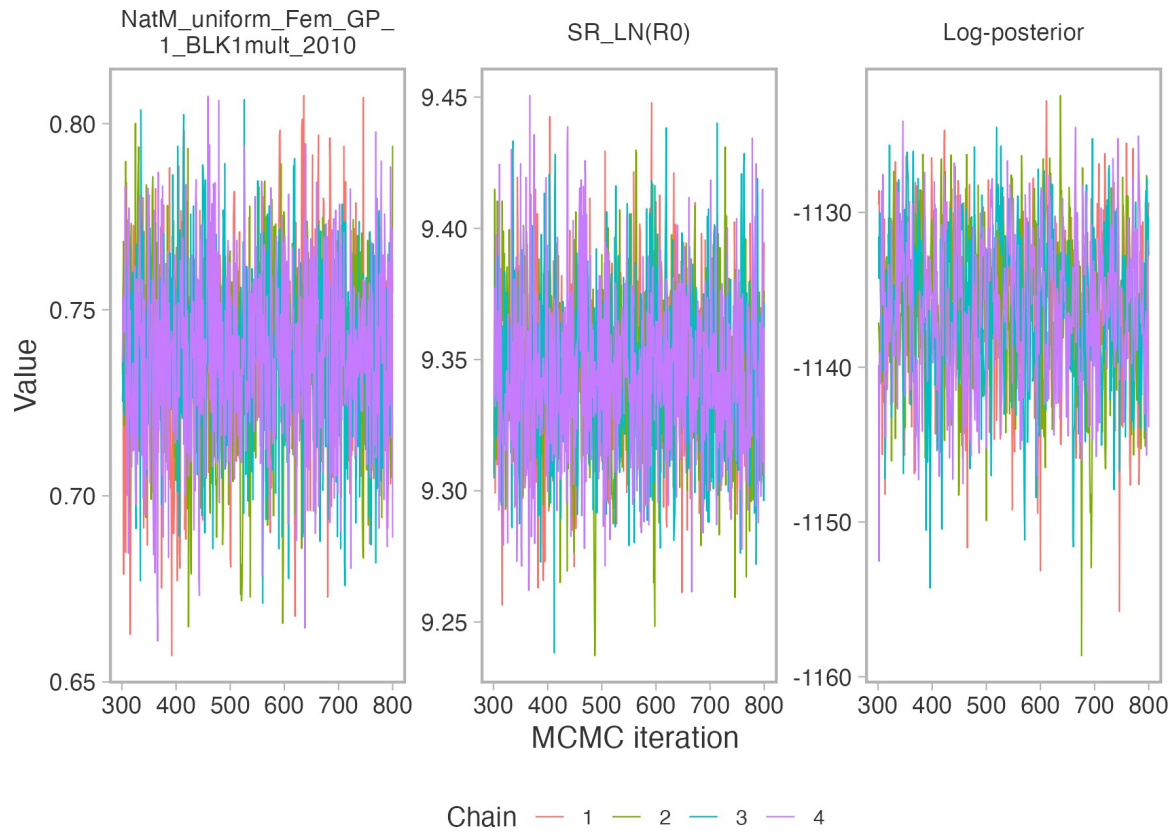

Figure D.3. Trace plots of the MCMC samples in model B2 for the log-posterior and stock-recruit parameters.

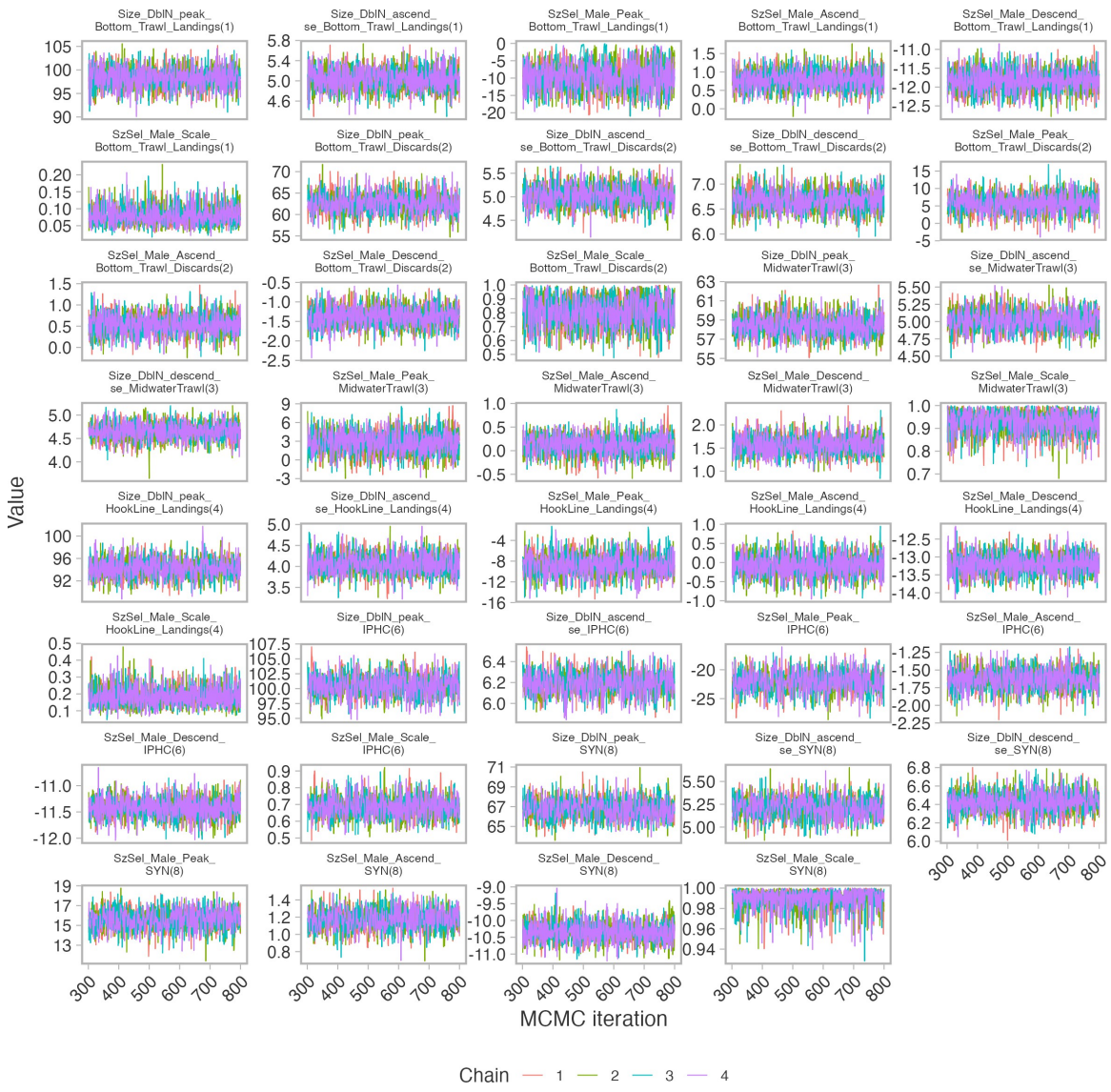

Figure D.4. Trace plots of the MCMC samples in model B2 for the selectivity parameters.

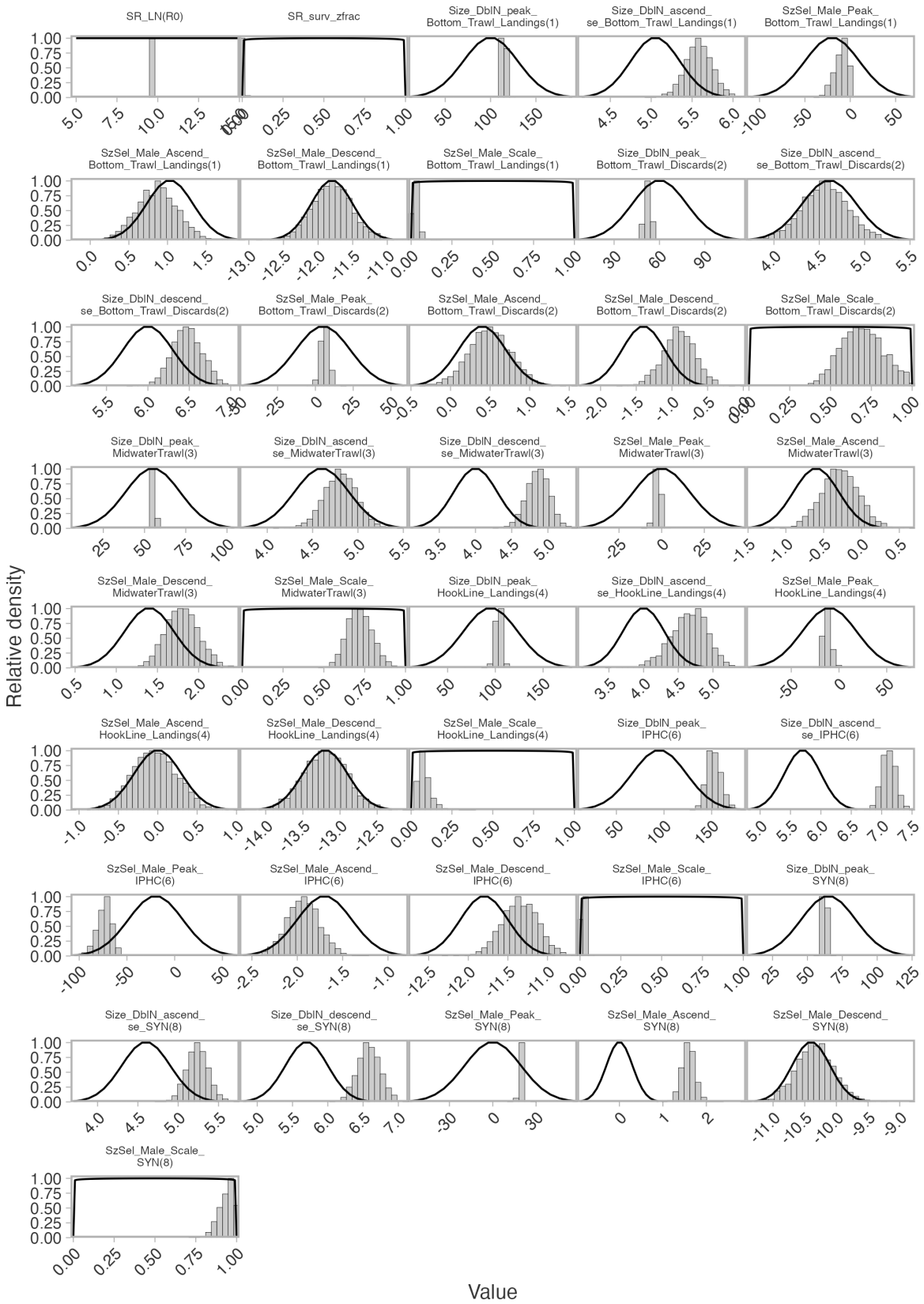

Figure D.5. Prior and posterior distributions for the A1 model. Priors are shown as lines calculated from the probability density function and posteriors are shown as histograms from the MCMC samples. For both, the relative density is shown where the maximum value of the prior and posterior distribution is set to 1. Parameter names are defined in Table 3.

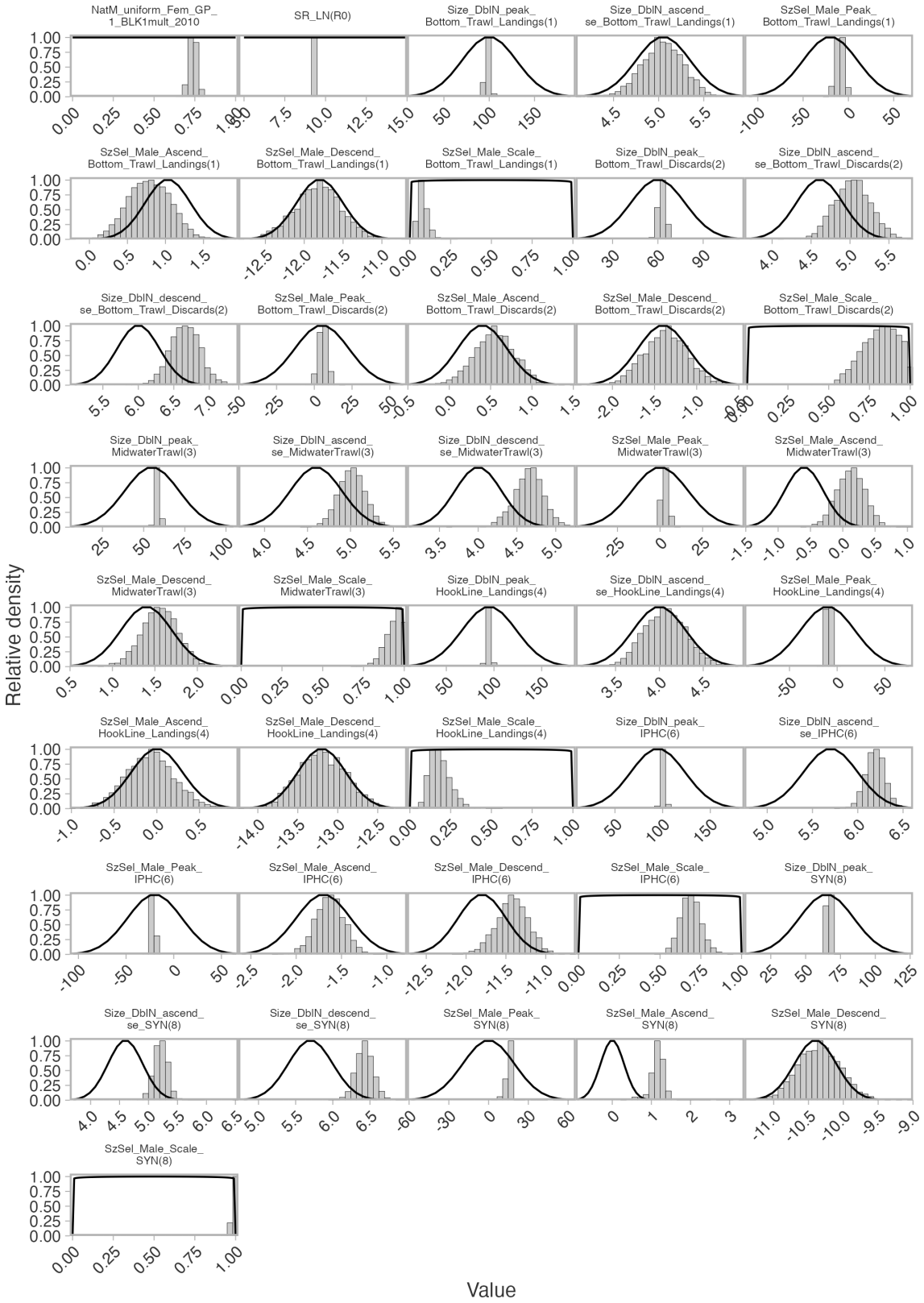

Figure D.6. Prior and posterior distributions for the B2 model. Priors are shown as lines calculated from the probability density function and posteriors are shown as histograms from the MCMC samples. For both, the relative density is shown where the maximum value of the prior and posterior distribution is set to 1.Priors are shown as lines and posteriors as histograms. Parameter names are defined in Table 3. The parameter in the top left corner defines the increase in natural mortality according to the historical M multiplied by the exponential of this parameter.

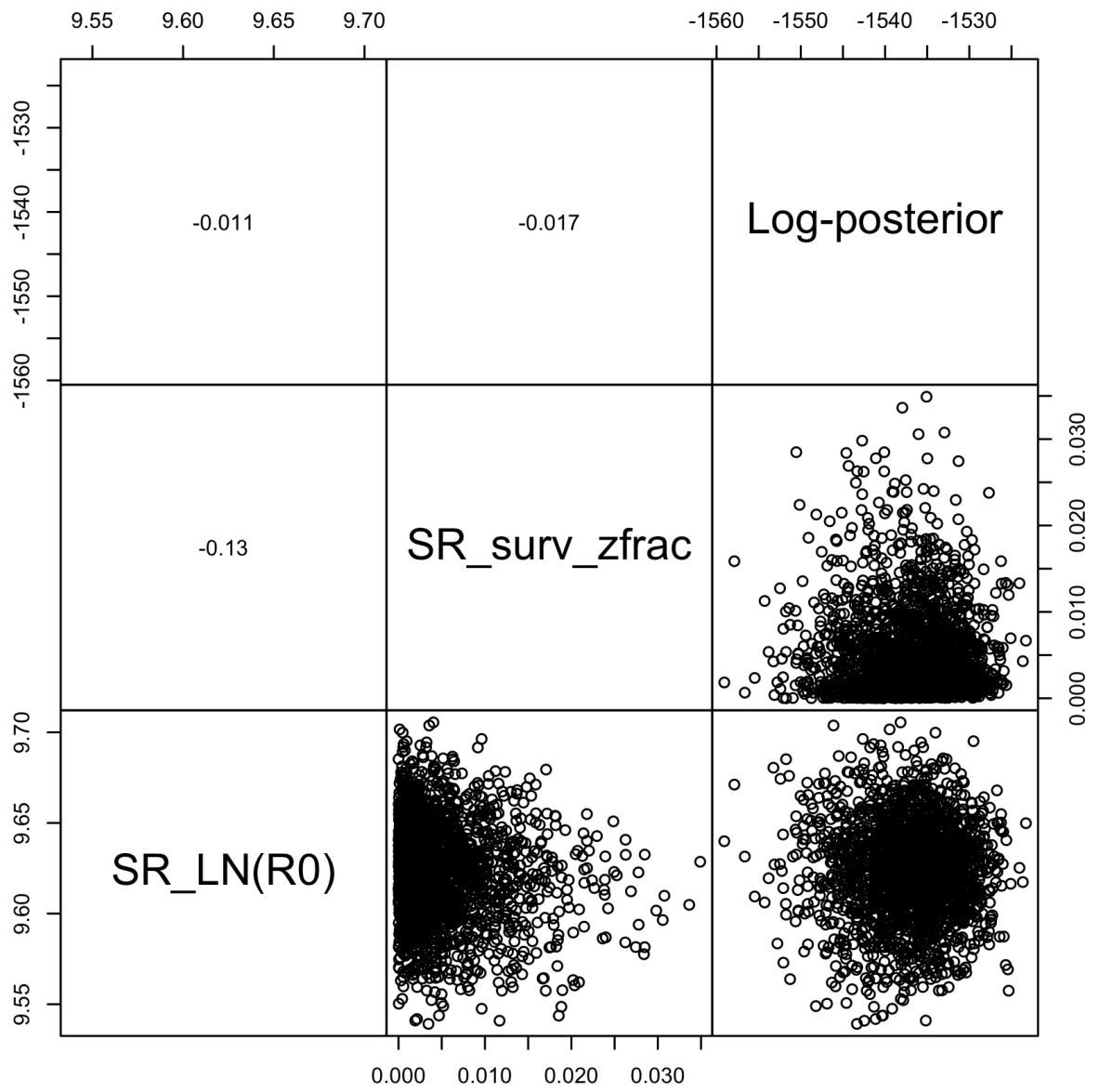

Figure D.7. Pair plots of individual MCMC samples in the log-posterior and stock recruitment parameters in model A1. The reported numbers are the correlation between pairs of parameters.

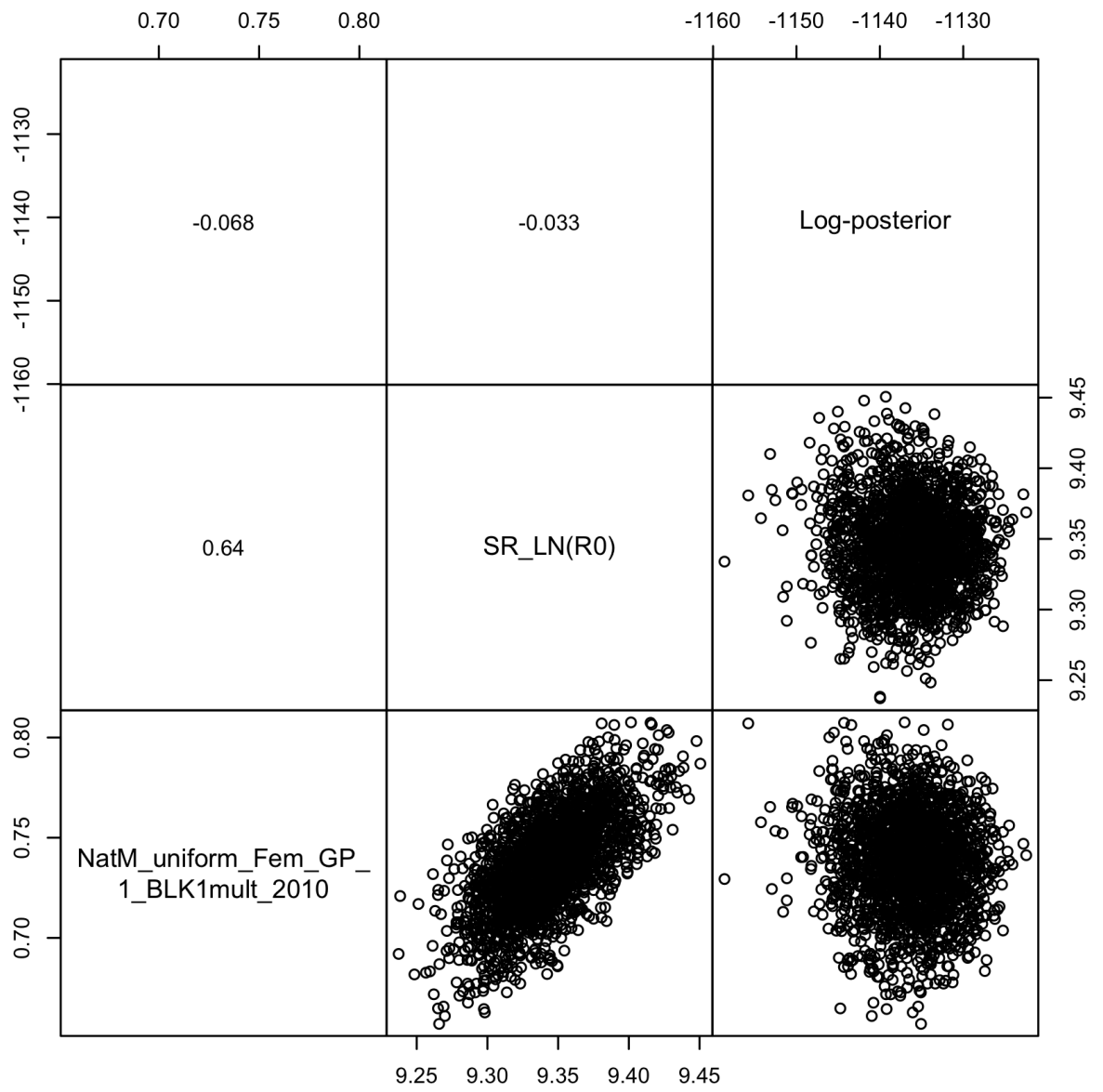

Figure D.8. Pair plots of individual MCMC samples in the log-posterior, stock recruitment parameters, and 2010 change in natural mortality in model B2. The reported numbers are the correlation between pairs of parameters.

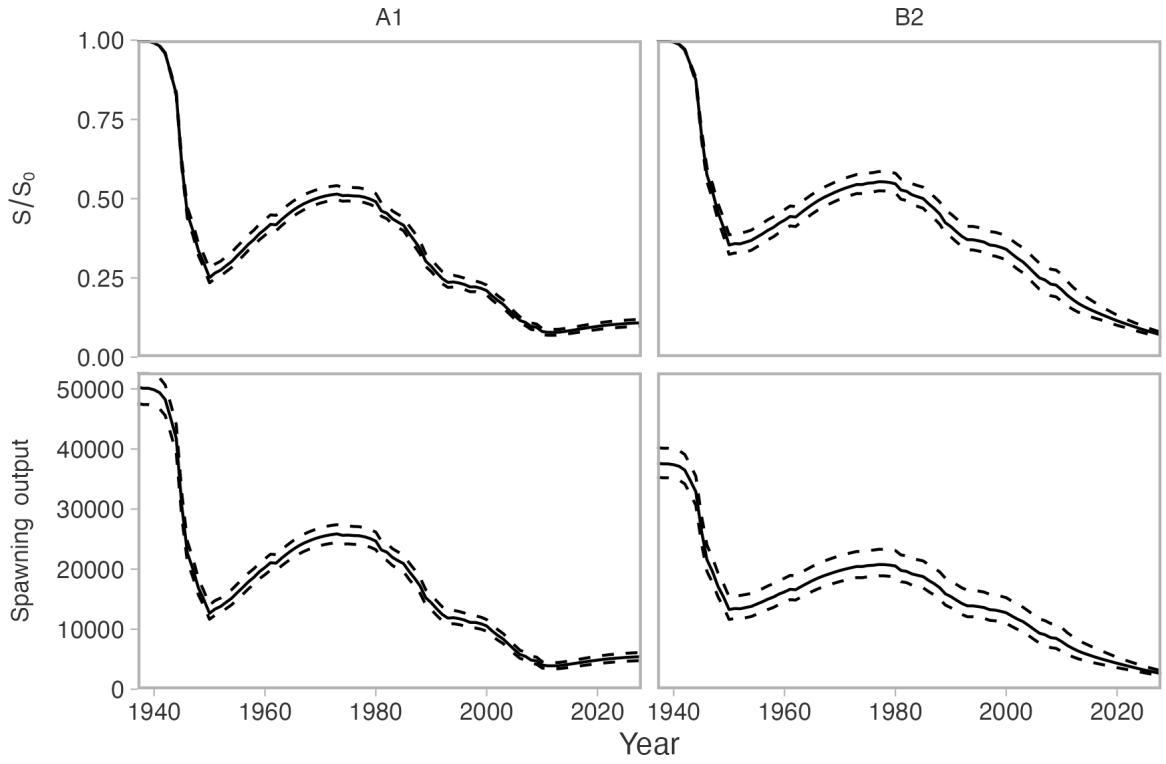

Figure D.9. Time series of depletion (S/S_0) and spawning output by model (columns). Solid lines represent the posterior median and the dotted lines span the 95% credible interval.

APPENDIX E. COSEWIC CONSIDERATIONS

COSEWIC Metric A measures the probability that the stock has declined by 70%, 50% or 30% (COSEWIC 2015). The metric uses a time period of "the last 10 years or 3 generations, whichever is longer" but is also interpreted as a decline over the longest time series available. For Dogfish, we define the generation time as $1/M$ + age at 50% maturity. I.e., 1/0.065 + 33.5 = 49 years; we round this to 50 years. We use 33.5 years as the age at 50% female maturity, which is a midpoint between 31.5 and 35.5 from Taylor and Gallucci (2009) and McFarlane and Beamish (1987). The last COSEWIC assessment assumed a similar generation time of 51 years (COSEWIC 2011). Therefore, the entirety of the time series considered in this assessment (1937–2023, 86 years) spans approximately 1.7 generations. Within this time-span, all assessment models considered estimated a decline in spawning output compared to unfished spawning output in excess of 70% with very high likelihood (Figure 56, 59). Across the models without time-varying M, depletion was estimated at 0.09 (range of 95% CIs: 0.06–0.12), which is equivalent to a 91% (range of 95% CIs: 88%–94%) decline since the beginning of the model in 1937. The models with time-varying M starting in 2010 estimated a similar level of depletion in 2023 but with a steeper rate of recent decline (Figure 59).

A second line of evidence to consider is the trend of the three major fisheries-independent population indices (IPHC, HBLL OUT, and Synoptic trawl surveys) and the standardized commercial CPUE (Figure 5, Appendix A). The Synoptic trawl survey represents a decline in biomass while the HBLL OUT and IPHC surveys represent declines in abundance. If we apply GLMs (generalized linear models) with gamma error and log links to these index means (i.e., ignoring their standard errors), we can obtain a proportional change per decade (Figure E.1). These range from a low of 0.34 (95% CI: 0.24–0.43) for the IPHC survey to a high of 0.71 (95% CI: 0.61–0.79) for the HBLL OUT survey (Figure E.1a). We can adjust these rates to be per 50 years—one generation. If we do this (acknowledging that these indices range in length from 16–27 years), all index trends have a proportional change per generation with a lower 95% CI above 0.7 (Figure E.1b). The COSEWIC Metric A is measured over three generation times, which would result in higher proportion declines than these one-generation values. Finally, we can also calculate these proportional declines for the length of each index (Figure E.1c). These values are from the slope of the fitted GLMs not from the first year compared to the last year.

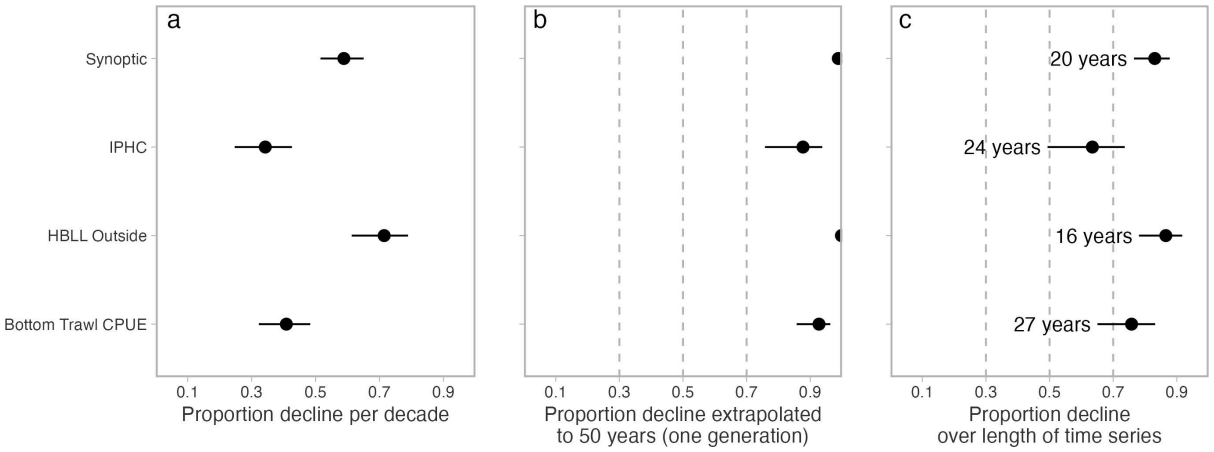

Figure E.1. Proportion decline from the indices of abundance or biomass used in the assessment model (Figure 5). The top three are fisheries independent surveys and the "Bottom Trawl CPUE" is standardized commercial CPUE since 1996. Dots and line segments represent means and 95% CIs from gamma generalized linear models (GLMs) with log links fitted to the index mean values. Dashed lines correspond to the 30%, 50%, and 70% COSEWIC Metric A thresholds, normally applied over three generations or the last 10 years, whichever is greater. Here we show these proportional declines (a) per decade, (b) per generation, and (c) per the length of each time series (with the lengths indicated to the left of each point).

APPENDIX F. REBUILDING CONSIDERATIONS

Although outside Dogfish are not listed as a major stock under the Fish Stocks provisions of the *Fisheries Act*, Dogfish are subject to DFO's Precautionary Approach (PA) Framework (DFO 2009) under the Sustainable Fisheries Framework (SFF). The PA Framework states "when a stock has reached the Critical Zone [below the LRP], a rebuilding plan must be in place with the aim of having a high probability of the stock growing out of the Critical Zone within a reasonable timeframe." The guidelines in DFO (2022*b*) provide the latest advice on implementing rebuilding plans. The guidelines note that "a 'reasonable timeframe' for a stock to grow above its LRP should be between 1.5 to 2 times the generation time. However, for some stocks a longer time may be needed to reach its rebuilding target, for example due to a stock's highly depleted state or its current productivity." Dogfish may fall into this latter category given their low intrinsic growth rate (due to late age at maturity, two-year gestation period, and low litter sizes) and their highly depleted state.

The assessment described in this document places the outside Dogfish stock below the LRP with very high likelihood ($>$ 0.95 probability). Guidance suggests a stock is considered "at or below its LRP if the terminal year stock status indicator is estimated to be at or below the LRP with a greater than 50% probability (DFO 2022*b*). While a full rebuilding plan is outside the scope of the terms of reference of this assessment, here we present information that may be useful to that process. We present projections to illustrate the time-frame that each model would predict the stock to take to recover above the LRP ($0.2S/S_0$) at various fixed catch levels (Figure F.1). We project out to 150 years, which is approximately three generations for Dogfish and thereby aligned with the COSEWIC Metric A timeline (COSEWIC 2015). We then record the number of years before there is at least a 0.95 probability that the spawning output is above the LRP (Figures F.1, F.2). This is different from the lower two-tailed 95% CI crossing the LRP, which implies 0.975 probability of being above the LRP. No one model incorporates a full spectrum of uncertainty, but the ensemble of our models covers a broad range of parametric and structural uncertainty.

A more complete rebuilding plan would include agreed to measurable objectives, a rebuilding target and timeline, socio-economic analysis, a method to track progress towards achieving the objectives, and a plan for periodic review of the rebuilding plan (DFO 2022*b*). From a management measure perspective, a more complete rebuilding analysis might consider management measures that are more complex than constant catch. For example, such an analysis might consider constant fishing mortality rate scenarios or fishing mortality rates combined with a harvest control rule.

When making any projections, and especially projections for such a long time period, it is possible the stock will not respond in ways expected by these models. There could be additional factors responsible for historical and future dynamics. This is particularly likely given our models were unable to capture dynamics from two key population indices over the last two decades. As examples, the stock could experience emigration and immigration north or south with nearby regions. The stock could also move further offshore or inshore out of or into survey and fishery domains.

It is furthermore possible that changes to life-history or environmental conditions will mean that unfished conditions in 1937 are no long a viable unfished state. As noted in Section 1.3, Taylor and Gallucci (2009) observed an increase in growth leading to smaller sizes, along with a decline in age of maturation and an increase in average litter size for Dogfish in the Puget Sound population. The greatest change in these parameters occurred between the 1940 and 1970s, a period of relatively high fishery exploitation and prior to observed increases in sea surface temperature. If these demographic changes are reflective of density dependence, then the rebuilding potential for Dogfish given fishery reductions is low and if recent environmental effects (i.e., temperature increases) further impact the demography, then rebuilding to 1940s

levels is not likely (Taylor and Gallucci 2009). Furthermore, our models explored possible increases in natural mortality in recent decades. If natural mortality levels have increased—for example, due to increased sea lion predation—then rebuilding to 1940s levels is also not likely.

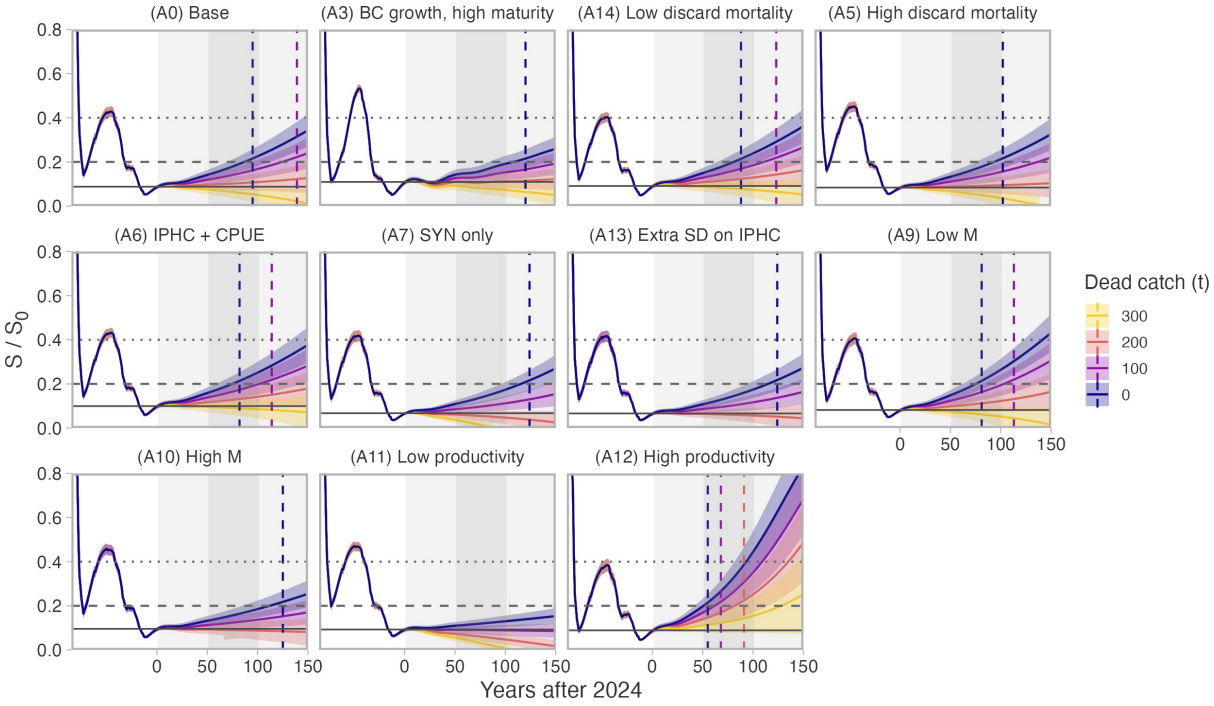

Figure F.1. Timeline to build the stock above 0.2 S/S_0 at fixed dead catch levels conditional on the various models. Solid lines represent means and shaded ribbons represent 95% CIs. Horizontal dashed and dotted lines indicate the LRP and a proposed USR. Vertical dashed lines indicate the year there is ≥ 0.75 probability that $S > 0.2S_0$. Vertical shaded blocks represent 50-year intervals (approximately one generation). These projections assume a closed population and stationary environmental conditions.

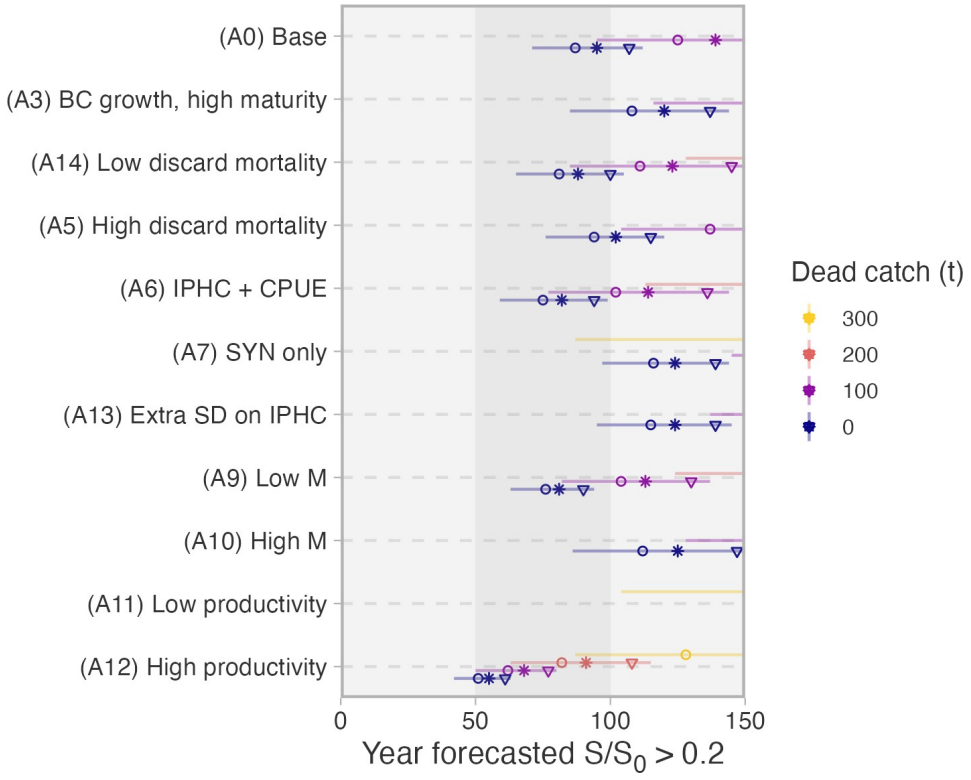

Figure F.2. Timeline to build the stock above 0.2 S/S_0 at fixed dead catch levels conditional on the various models. Open circles represent the year the mean estimated $S > 0.2S_0$. Line segments represent the years the upper and lower 95% CIs cross 0.2 S/S_0. The asterisks and triangles on the right side of the line segments indicate the year that there is $\geq$ 0.75 and $\geq$ 0.95 probability that the stock is above 0.2 S0, respectively. Vertical shaded blocks represent 50-year intervals (approximately one generation). These projections assume a closed population and stationary environmental conditions.